BIOCHEMICAL AND MOLECULAR FACTORS FOR ENHANCED LIPID ACCUMULATION IN MICROALGAE

Ph.D THESIS

by

JYOTI SINGH

DEPARTMENT OF BIOTECHNOLOGY
INDIAN INSTITUTE OF TECHNOLOGY ROORKEE
ROORKEE-247667(INDIA)
JUNE, 2019

BIOCHEMICAL AND MOLECULAR FACTORS FOR ENHANCED LIPID ACCUMULATION IN MICROALGAE

A THESIS

Submitted in partial fulfilment of the requirements for the award of the degree

of

DOCTOR OF PHILOSOPHY

in

BIOTECHNOLOGY

by

JYOTI SINGH

DEPARTMENT OF BIOTECHNOLOGY
INDIAN INSTITUTE OF TECHNOLOGY ROORKEE
ROORKEE-247667(INDIA)
JUNE, 2019

INDIAN INSTITUTE OF TECHNOLOGY ROORKEE
ROORKEE

CANDIDATE'S DECLARATION

I hereby certify that the work which is being presented in the thesis entitled "**BIOCHEMICAL AND MOLECULAR FACTORS FOR ENHANCED LIPID ACCUMULATION IN MICROALGAE**" in partial fulfilment of the requirements for the award of the degree of Doctor of Philosophy and submitted in the Department of Biotechnology of the Indian Institute of Technology Roorkee, Roorkee is an authentic record of my own work carried out during a period from July, 2013 to June, 2019 under the supervision of Dr. R. P. Singh, Professor, Department of Biotechnology, Indian Institute of Technology Roorkee, Roorkee.

The matter presented in the thesis has not been submitted by me for the award of any other degree of this or any other institution.

(JYOTI SINGH)

This is to certify that the above statement made by the candidate is correct to the best of my knowledge.

(R.P. Singh)
Supervisor

Date: June, 2019

ABSTRACT

The rapid increase in global energy demand, the rise of climate change events, and fossil fuel shortages have led humankind to search for alternative greener and sustainable energy resources. With multiple advantages, bioenergy is a promising alternative to conventional energy; however, biofuel production from the first and second-generation sources may add concern mainly the problems in water scarcity and threats to food security. Microalgae have recently emerged as a promising renewable feedstock for biofuel production, mainly due to their rapid growth rate, ability to fix CO2, flexible adaptation, and capability to grow in non-arable lands. However, the real technological challenge is to mass produce microalgae with higher lipid content for the production of a low-value high-volume product to make it economically viable.

To accomplish this, approaches to maximize biomass and lipid production that are crucial for improving the economics of microalgae-based biofuels were employed. This includes the bioprospecting of potential algal strains (preferably from indigenous habitats), derivation of pre-eminent nutritional parameters and exogenous supplementation of phytohormones to direct metabolic flux towards enhanced lipid accumulation. Among the nineteen-microalgal strains screened, *Desmodesmus* sp. JS07 appears to have maximum lipid accumulation (50.01±3.21%) and productivity (36.3±2.06 mg/L/d) in nitrogen-limited conditions. Besides, *Desmodesmus* sp. JS07 had shown improved levels of SFA and MUFA content under the nitrogen-limited condition that is desirable for achieving high-quality biodiesel.

Enhanced biomass and lipid content were observed with exogenous application of *Desmodesmus* sp. JS07 with selected phytohormones. Among auxins, IBA led into improved biomass and lipid content up to 1.46±0.53 g/L and 43.12±3.87%, respectively whereas among cytokinins; BAP increased the biomass and lipid content up to 1.60±0.61 g/L and 38.99±3.11% respectively, in Desmodesmus sp. JS07. Further, the cumulative impact of IBA and BAP was evaluated, which showed their synergistic effect in stimulating biomass and lipid content up to 2.01±0.67 g/L and 45.1±2.11% respectively, in *Desmodesmus* sp. JS07 at $IBA_{7.5mg/l}$+$BAP_{7.5mg/l}$. Therefore, the application of phytohormones, which is an easy and scalable strategy, could be used for significant improvement in microalgal biomass and lipid content for commercial biofuel production.

To reveal the molecular mechanisms of lipid metabolism in response to nitrogen-limited conditions in an isolate *Desmodesmus* sp. JS07, lipidomics, and transcriptomic analysis were performed. Lipidome analysis demonstrated a diverse spectrum of lipids, revealing 8 lipid classes and 87 lipid species consisting of both polar and neutral lipids in *Desmodesmus* sp. JS07. Under N-limitation, TAG levels remarkably increased along with the concomitant decrease in polar lipids. This signifies a significant remodeling in the lipid pools through augmenting de novo fatty acid biosynthesis in chloroplast for enhanced TAG accumulation. Transcriptome profiling of *Desmodesmus* sp. JS07 revealed the up-regulation of potential genes related to fatty acid and TAG biosynthesis. Taken together, this provides a basis for improving our understanding of TAG synthesis and identifying the key enzymes involved in TAG production and for their overexpression in microalgae.

Further, molecular modification of *Desmodesmus* sp. JS07 was taken up by heterologous and homologous expression of BnDGAT2 and CvGPD1 constructs respectively in order to augment the lipid accumulation. An integrated approach involving the overexpression and site-directed mutagenesis of the key regulatory gene CvGPD1 to engineer the microalgae for economic viability for biofuel production was also explored. Therefore, the present work is an endeavor to develop an engineered microalgal strain with enhanced lipid content for sustainable biofuel production.

DEDICATED TO MY PARENTS

ACKNOWLEDGMENT

First of all, I would like to venerate God, the Almighty, without whom this thesis would not have been completed.

I take this rare opportunity to express my earnest gratitude to my supervisor Prof. R. P. Singh, for his inspiring guidance, motivations, constructive suggestions, and continuous involvement throughout these research investigations.

I respectfully acknowledge members of my Doctoral Scrutiny Committee, Prof. A. K. Sharma, Prof. Partha Roy and Prof. M. R. Maurya for their thoughtful, constructive criticisms, generous help.

I wish to express my heartiest thanks to Prof. A.K. Sharma, Head of the Department of Biotechnology and the former Heads Prof. Partha Roy for providing me the necessary facilities for my research work.

Perhaps my most enormous good fortune has been to have my lab-mates who also guided as well as assisted me in my Ph.D. work. I would like to show appreciation and gratefully acknowledge my dear lab-mates, Mukta, Namrata, Shobhit, Dr. Swati Dubey, Dr. Pragati Agarwal, Dr. Samta Saroj, Dr. Arti and Anshu for their unconditional help, care and encouragement. I would also like to thank my dear friends Sonam, Timsy, Akash, Benazir, Ankita, Lipi for the moral support and encouragement throughout this Ph.D. program. I will always cherish the time we spent together in the lab, IITR campus, Sarojini-canteen, hospital-canteen, LBS ground, throughout this Research tenure.

I owe my deep sense of gratitude to my ever-loving parents and my beloved siblings Swati, Amit, and Mayank for their unconditional love, encouragement, affection, and support, without whom this treatise would have remained an ambition.

The financial support is given by MGRD, Govt. of India, New Delhi, India, during my research tenure is gratefully acknowledged.

LIST OF PUBLICATIONS

PUBLICATIONS IN PEER REVIEWED JOURNALS

- **Singh, J.**, Dubey, S. and Singh, R. P. (2017). Lipidomics Profiling: A new approach unravelling the polar and neutral lipids in *Scenedesmus abundans* and *Chlorella* sp. under nitrogen-limited conditions. Journal of Bioremediation & Biodegradation, 8 (5): 37.

- **Singh, J.**, Dubey, S., Chakravarty, N. and Singh, R. P. (2019). Insights into lipidome profiling of *Desmodesmus* sp. JS07 under nitrogen-limited conditions to elucidate major remodeling of intracellular lipid pools towards enhanced TAG accumulation. Biomass and Bioenergy (Submitted)

- **Singh, J.**, Priyanka, P., Jain, D. and Singh, R. P. (2019). Augmented biomass and lipid content in microalgae *Desmodesmus* sp. JS07 by the synergistic influence of auxins and cytokinins: An approach to enhanced biofuel production. Photochemistry (Submitted)

- Dubey S., **Singh J.** and Singh R. P. (2018). Biotransformation of sweet lime pulp waste into high-quality nanocellulose with an excellent productivity using *Komagataeibacter europaeus* SGP37 under static intermittent fed-batch cultivation. Bioresource Technology, 247, 73–80.

- Dubey S., Sharma R. K., Agarwal P., **Singh J.**, Sinha N. and Singh R. P. (2017). From rotten grapes to industrial exploitation: *Komagataeibacter europaeus* SGP37, a micro-factory for macroscale production of bacterial nanocellulose. International Journal of Biological Macromolecules, 96, 52–60.

- Agarwal P., **Singh J.**, Singh R.P. (2016). Molecular cloning and characteristic features of a Novel Extracellular Tyrosinase from *Aspergillus niger* PA2. Applied Biochemistry and Biotechnology.

- Agarwal P., Pareek N., Dubey S., **Singh J.** and Singh R. P. (2016). *Aspergillus niger* PA2: A Novel Strain for Extracellular Biotransformation of L-Tyrosine into L-DOPA, Amino Acids, 48 (5), 1253-1262.

BOOK CHAPTERS

- Mondal P., Kumari P., **Singh J.**, Verma S., Chaurasia A. and Singh R. P. (2017).“Oil from Algae” in Sustainable utilization of natural resources (Mondal P. and Dalai A. K., eds.), CRC press 2017, 213-253.

- Agarwal P., Singh M., **Singh J.** and Singh R. P. (2019). Microbial Tyrosinases: A Novel Enzyme, Structural Features, and Applications. In: Applied Microbiology & Bioengineering: An Interdisciplinary Approach, ed. P. Shukla, pp. 3-20, Acd. Press London, UK

- Agarwal P, Singh M, **Singh J** and Singh R. P. Microbial Tyrosinases: A Novel Enzyme, Structural Features, and Applications. In: Applied Microbiology and Bioengineering, Elsevier publications, 2018.

PROCEEDINS IN NATIONAL AND INTERNATIONAL CONFERENCES

- **Singh, J.**, Jain, D., Dubey, S. and Singh, R. P. (2018). Synergistic effect of phytohormones for enhanced biomass and lipid accumulation in microalgae *Desmodesmus* sp. JS07 and *Scenedesmus* sp. DBT National Workshop on Bioenergy-2018. IIT Roorkee, Roorkee, India, July 6-7, 2018.

- **Singh, J.**, Chakravarty, N., Jain, D. and Singh, R. P. (2018). Auxins: A potential modulator for cell growth and lipid accumulation in *Chlorella emersonii* and *Scenedesmus opoliensis*. 3rd Green & Sustainable Chemistry Conference. Berlin, Germany, May 13-16, 2018.

- **Singh, J.,** Jain, D., Dubey, S. and Singh, R. P. (2018). Engineered microalgae as sustainable cell factories for biodiesel production. International Conference on Sustainable Biofuel 2018. India Habitat Centre, New Delhi, Feb 26-27, 2018.

- **Singh, J.**, Shukla, P., Dubey, S. and Singh, R. P. (2017). Lipidomic analysis towards deciphering the lipid architecture of the oleaginous microalgae in response to the nutrient limited condition. International Conference on Emerging Trends in Biotechnology for Waste Conversion. CSIR-NEERI, Nagpur, India, Oct 8-10, 2017.

- **Singh, J.**, Dubey, S. and Singh, R. P. (2017). Lipidomic Profiling: A new approach unravelling the polar and neutral lipids in *Scenedesmus abundans* and *Chlorella* sp. under nitrogen-limited conditions. Sixth World Congress on Biofuels and Bioenergy (Biofuels Congress 2017). London, UK, Sep 05-06, 2017.

- **Singh, J.**, Dubey, S., Singh M. and Singh, R. P. (2017). Lipidome Analysis: Revealing Polar and Neutral Lipids in *Chlorella* species under Nitrogen Limited Condition for Biodiesel Production. 8th World Renewable Energy Technology Congress & Expo-2017. Delhi, India, Aug 21-23, 2017.

- **Singh J.**, Verma S., Singh A. and Singh, R. P. (2015). Regulation of lipid biosynthesis and fatty acid profiling in microalgae under varying nutrient conditions. New Horizons in Biotechnology, NIIST Trivandrum, India, Nov 22-25.

- **Singh, J.**, Patel, A., Pruthi, P and Singh, R. P. (2014). Nitrogen Starvation: A key regulator of lipid content in microalgae. International Conference on Molecular Signaling: Recent Trends in Biomedical and Translational Research 2014. IIT Roorkee, Dec 17-19.

- Verma, S., **Singh, J.** and Singh, R. P. (2015). Potential of seven fresh water microalgal isolates with prospective of biofuel production. New Horizons in Biotechnology, NIIST Trivandrum, India, Nov 22-25.

- Dubey S., **Singh J.**, Singh M., Bhargava A. and Singh R. P. (2014). Bacterial cellulose as a potential scaffold for bone tissue engineering: production and physicostructural characterization, International conference on Molecular Signalling: Recent Trends in Biomedical and Translational Research, IIT Roorkee, India, Dec 17-19.

CONTENTS

LIST OF FIGURES

LIST OF TABLES

LIST OF ABBREVIATIONS

˚C	Degree Celsius
ACAT	acetyl-CoA-acetyltransferase
ACC	Acetyl-CoA carboxylase
ACOX1	acyl-CoA oxidase
ACS	Acyl-CoA synthetase
AGPase	ADP-glucose pyrophosphorylase
AGPAT	Acyl-sn-glycerol-3-phosphate O-acyltransferase
ASTM	American Society for Testing and Materials
BAP	Benzylaminopurine
BC	Biotin carboxylase
BE	α-1,4-glucan branching enzyme
BME	β-mercaptoethanol
bp	basepair
CCD	Central composite design
CD-HIT	Cluster Database at High Identity with Tolerance
CFPP	Cold filter plugging point
CN	Cetane number
D	Desaturase
DG	Diacylglycerol
DGAT	Diacylglycerol O-acyltransferase
DGE	Differential gene expression
DNA	Deoxyribonucleic acid
DOE	Design of experiment
DU	Degree of unsaturation
EAR	Enoyl-ACP reductase
ECH	Enoyl-CoA hydratase
EDTA	Ethylenediaminetetraacetic acid
EN	European Standards

ER	Endoplasmic Reticulum
FA	Fatty acid
FAME	Fatty acid methyl ester
FFA	Free fatty acid
G3P	Glycerol-3-phosphate
GC-MS	Gas chromatography mass spectroscopy
GK	Glycerol kinase
GO	Gene Ontology
GPAT	Glycerol-3-phosphate O-acyltransferase
HAD	beta-hydroxy acyl-ACP dehydrase
HADH	Hydroxy acyl-CoA dehydrogenase
HXK	hexokinase
IAA	Indole acetic acid
IBA	Indole butyric acid
IPA	Indole propionic acid
IPTG	Isopropyl-ß-thiogalactopyranoside
IV	Iodine value
KAR	beta-ketoacyl-ACP reductase
KAS	beta-ketoacyl-ACP synthase
kb	Kilobase
kDa	Kilodalton
LB broth	Luria Bertani broth
LC-MS	Liquid chromatography mass spectroscopy
LCSF	Long chain saturation factor
LPA	Lysophosphatidic acid
MAT	Malonyl-CoA ACP transacylase
MG	Monoacylglycerol
min	minutes

mL	Millilitre
mM	Millimolar
MS	Mass Spectrometry
MUFA	Monounsaturated fatty acid
MW	molecular weight
NL	Nitrogen limited
NR	Non-redundant
NS	Nitrogen sufficient
OAH	Oleoyl-ACP hydrolase
OD	Optical density
ORF	Open reading frame
PA	Phosphatidic acid
PC	Phosphatidylcholine
PCR	Polymerase Chain Reaction
PDAT	Phospholipid diacylglycerol acyltransferase
PDB	Protein Data Bank
PDC	Pyruvate decarboxylase
pdhD	Dihydrolipoamide dehydrogenase
PE	Phosphatidylethanolamine
PG	Phosphatidylglycerol
PI	Phosphatidylinositol
PP	Phosphatidate phosphatase
PS	Phosphatidylserine
PUFA	Polyunsaturated fatty acid
RNA	Ribonucleic acid
SDS-PAGE	Sodium dodecyl sulphate polyacrylamide gel electrophoresis
SFA	Saturated fatty acid
SPase	Starch phosphorylase

ss	Single-stranded
SS	Starch synthase
SV	Saponification value
TAG	Triacylglycerol
TDZ	Thidiazuron
TF	Transcription factor
T_m	Temperature
α-AMY	α-amylase
β-AMY	β-amylase
µL	Microlitre
µM	Micromolar

CHAPTER 1

Introduction and Review of literature

1.1. Introduction

The continued use of non-renewable fossil fuels for power generation, transportation, and other energy needs are now widely considered as unsustainable because of rapidly depleting resources and their contribution to global warming. The attempts to reduce this dependency on fossil fuels have raised interests in other potential renewable resources, including biofuels (Demirbas, 2011). Biodiesel derived from food crops such as soybean oil, sunflower oil, rapeseed oil, etc. and non-food crops such as *Jatropha curcas*, *Brassica carinata*, etc. have been explored, but their large-scale production is limited due to relatively their slower growth rate and competing with land usually meant for food crops cultivation and economic constraints (Lam and Lee, 2012).

Microbial oil produced by various types of microorganisms like fungus, microalgae, bacteria, yeast have attracted the increasing attention as a viable feedstock for biofuel production owing to its pivotal characteristics, for example, shorter growth cycles, higher lipid content and not competing with agricultural land earmarked for cultivation (Neto et al., 2016). In recent years, microalgae have gained considerable interest as a potential feedstock for the production of biofuel as these have substantial lipid levels and higher biomass yield per unit area due to its relatively higher growth rate (Malcata, 2011). Algae in the presence of light utilize carbon dioxide to convert it into macromolecular constituents, mainly proteins, polysaccharides, and triglycerides through distinct cascades (Demirbas and Fatih Demirbas, 2011). The lipid (triglycerides) content of the algal cell, are the raw material for the biodiesel production that varies among different algal species. Culture conditions such as nutrient (C, N, P, etc.,) concentrations, light intensity, temperature, pH, and CO_2 levels in the medium impact the lipid content in the algal cell. Moreover, the fatty acid profile of algae may also vary along with the culture conditions and depend upon the nutrient employed (Amaro et al., 2011).

Employing microalgae for biofuel production has its advantages and limitations, as the production cost is still not competitive with fossil fuel due to the unavailability of microalga strain with higher lipid content and productivity, technical obstacles regarding harsh microbial culture conditions, tedious and expensive oil extraction etc. that needs to be overcome (Quinn and Davis, 2015; Singh et al., 2011). Therefore, looking for the microalgal strain with higher lipid content is one of the widely explored and desirable requirements for biofuel generation;

besides this, efforts are needed to look into simpler and economical approaches for biomass harvesting, drying, and lipid extraction. The vast indigenous biodiversity enables us to seek out the productive strain with higher lipid content. Furthermore, strain development mainly inculcates employing genetic and metabolic engineering tools to alter the strain characteristics for higher biomass content and increased lipid productivity (De Bhowmick et al., 2015). The recent strategies include manipulating the stress factors, use of chemical additives and phytohormones and co-culturing with other microorganisms for regulating algal metabolism for higher lipid production. However, employing stress factors led to higher lipid accumulation but resulted in decreased biomass. Such stress factors include nutrient depletion, salinity, temperature, and light intensity that affects enhanced lipid productivity under defined conditions (Chiranjeevi and Venkata Mohan, 2016).

Lipid biosynthesis in algae is mainly regulated by two key enzymes: acetyl co-A carboxylase and fatty acid synthase, that leads into the production of malonyl co-A. Fatty acid synthase (FAS) then transfer the malonyl group to the acyl carrier protein. After a few steps of fatty acid synthesis, fatty acids synthesized is transferred to glycerol-3-phosphate by acyltransferases (Gong et al., 2011). It generally leads to an increased synthesis of lipids, resulting in higher TAG (Triacylglycerol) accumulation. Three acyltransferases (DGAT, DGTT, and PDAT) have been observed to be upregulated during nitrogen starvation resulting in more biosynthesis of lipids (Tabatabaei et al., 2011).

The strategies above, such as employing phytohormones and different stresses for enhanced lipid productivity that causes altered metabolic fluxes seem ideal for increased lipid accumulation and biodiesel production (Tate et al., 2013). However, such mechanisms that involve differential gene expression are poorly understood due to lack of desired genomic information and thus partly enabled in exploiting microalgae as a viable feedstock for biodiesel production (Driver et al., 2014). Thus, transcriptome analysis can serve as an effective and prudent approach to obtaining functional genomic information leading to unraveling the misty insights of the lipid metabolic cascades. It would enable in understanding the key regulatory enzymes that may be upregulated or downregulated in response to such alterations. The precise understanding of these key regulatory steps would help in regulating the turn over a number of the desired enzyme for achieving an increased lipid content in microalgal cells.

The recruitment of multidimensional approaches may yield productive strategies to deal with such global concerns. Out of the various resources for biofuel production microalgae appear as a front-runner because of the above-mentioned advantages. The call is to utilize distinct logistic

approaches either alone or in combination to improve the biomass content and lipid productivity. A varied combination of such approaches can lead to desired outputs. Microalgae can be a better and successful alternative for fossil fuels, but to make them economically viable and sustainable, a lot more efforts are needed in this direction to explore this enigmatic renewable resourcefully.

Keeping these in view, the present work is undertaken with the aim to search for potential microalgal strain having considerate amount of lipid and to evaluate the factors for enhanced lipid accumulation, a transcriptome analysis to reveal the key regulatory enzymes of fatty acid biosynthetic pathway and their overexpression in the microalgal strain for augmented lipid accumulation for biodiesel production. Therefore, the present thesis is an endeavor to develop an engineered microalgal strain with enhanced lipid content for sustainable biofuel production, and to achieve this, the major objective of the studies are:

- Bioprospecting of algal strains from various sources and selection of strain(s) with higher lipid content
- Evaluation of the critical physicochemical and biochemical factors and development of a high yielding cultivation system for enhanced accumulation of the neutral lipids.
- Lipidome profiling of selected algal strain under derived conditions.
- Transcriptome analysis to elucidate the differential gene expression under derived conditions
- Molecular modification of the algal strain for achieving higher lipid accumulation

1.2 Review of Literature

1.2.1 Algae for biofuels

Increasing crude oil prices, energy crisis, global warming issues, etc., necessitates the need for exploration renewable energy resources such as biomass, solar, wastes, and wind, etc., around the world to produce sustainable energy. Renewable energy is likely to meet ~50% of the world energy demand by 2050. Amongst various renewable energy sources, the biomass fuel is extensively used to meet the energy requirement in many countries (Soni et al., 2013). Recently it is reported that biomass is used as the main energy resource by about 1.5 billion of the world population (Chisti, 2007). It has been predicted that both European Union and the USA will increase their biomass consumption by ~ 700 % and ~300% respectively by the year 2020 compared to the use in the year 2010 (Kheira et al., 2008).

Various biomass sources like sugar cane, corn, soybeans, jatropha seeds, lignocellulosic biomass, macro, and microalgae, etc., have been used for the production of biofuel/oil. Amongst these, the microalgal feedstock is the most promising as they have higher biomass yield per unit area due to the higher growth rates and productivity (Table 1.1) and no arable land requirement (Singh et al., 2014). In recent years, microalgae have appeared as a promising bioenergy feedstock for the production of biofuel including bioethanol, biodiesel, green gasoline, methanol, biohydrogen, etc., as microalgae can grow rapidly and photoautotrophic, converting solar energy into chemical energy through photosynthesis. (Zhang et al., 2013). Besides this, the biodiesel obtained is non-toxic and biodegradable and leads to lower CO_2 emission.

Table 1.1: Evaluation of microalgae with other feedstocks for biodiesel production.

Source	Seed oil content (% oil by wt in biomass)	Oil yield (L oil/ha year)	Land use (m^2 year/kg biodiesel)	Biodiesel productivity (kg biodiesel/ha year)	References
Soybean (*Glycine max* L.)	18	636	18	562	Antunes et al., 2008
Jatropha (*Jatropha curcas* L.)	28	741	15	656	Kheira et al., 2009
Hemp (*Cannabis sativa* L.)	33	363	31	321	Callaway et al., 2004
Palm oil (*Elaeisguineensis)*	36	5366	2	4747	Eze et al., 2013
Sunflower (*Helianthus annuus*L.)	40	1070	11	946	Nielsen et al., 2008
Canola/Rapeseed (*Brassica napus* L.)	41	974	12	862	Rashid et al., 2008
Physic nut	41–59	741	-	656	Nielsen et al., 2008
Camelina (*Camelinasativa*L.)	42	915	12	809	Vollmann et al., 2007
Corn/Maize (*Zea mays* L.)	44	172	66	152	Chisti et al., 2007
Castor (*Ricinuscommunis*)	48	1307	9	1156	Kulay et al., 2005
Microalgae (low oil content)	30	58,700	0.2	51,927	Trentacoste et al., 2013
Microalgae (medium oil content)	50	97,800	0.1	86,515	Mata et al., 2010
Microalgae (high oil content)	70	136,900	0.1	121,104	Chen et al., 2012

A key consideration for biofuel production is the selection of microalgal strain, as it is important that microalgae should have high lipid content and productivity. Microalgae are the simple photosynthetic microorganisms that present in all existing earth ecosystem, including aquatic as well as terrestrial. It is estimated that more than 50,000 species exist and around 30,000 have been analyzed so far (Mata et al., 2010). Many algal species have been observed to accumulate considerable amounts of lipids under derived conditions. Among the green algae, *Chlorella* species, *Botryococcus braunii*, *Dunaliella salina*, *Nannochloropsis* and *Isochrysis* spp. have been found to contain a notable amount of lipid up to 60% by cell weight (Gong et al., 2011). Table 1.2 shows the lipid content and productivity of selected microalgal strain.

Table 1.2: Biomass productivity, lipid content, and lipid productivity of the microalgae strains (Talebi et al., 2015; Mata, Martins, & Caetano, 2010; Sakthivel, Elumalai, & Arif, 2011)

Algal Group	Microalgal strains	Habitat	Biomass productivity (g/l/day)	Lipid Content (% biomass)	Lipid Productivity (mg/l/day)
Diatoms	*ChaetocerosmuelleriF&M-M43*	Marine	0.07	33.6	21.8
	Chaetoceroscalcitrans CS 178	Marine	0.04	39.8	17.6
	P.tricomuturn F&M-M40	Marine	0.24	18.7	44.8
	Skeletonomacostatum CS181	Marine	0.08	21.0	17.4
	Thakassioriapseudonana CS 173	Marine	0.08	20.6	17.4
	Chlorella sp. F&M-M48	Freshwater	0.23	18.6	42.1
	Chlorella sorokiniana IAM-212	Freshwater	0.23	19.3	44.7
	Chlorella vulgaris CCAP 211/11b	Freshwater	0.17	19.2	32.6
	Chlorella vulgaris F&M-M49	Freshwater	0.20	18.4	36.9
Green Algae	*Chlorococcum sp. UMACC 112*	Freshwater	0.28	19.3	53.7
	Scenedemusquadricauda	Freshwater	0.19	18.4	35.1
	Scenedemus F&M-M19	Freshwater	0.21	19.6	40.8
	Scenedemus sp. DM	Freshwater	0.26	21.1	53.9
	T. suecica F&M-M33	Marine	0.32	8.5	27.0
	Tetraselmis sp. F&M-M34	Marine	0.30	14.7	43.4
	T. suecica F&M-M35	Marine	0.28	12.9	36.4

	Teraselmissuecica	Marine	0.12-0.32	8.5-23.0	27.0-36.4
	Ellipsoidion sp. F&M-M31	Marine	0.17	27.4	47.3
	Monodussubterraneus UTEX 151	Freshwater	0.19	16.1	30.4
	Nannochloropsis sp. CS 246	Marine	0.17	29.2	49.7
	Nannochloropsissp	Freshwater	0.71-1.43	12.0-53.0	37.6-90.0
	Dunaliellasalina	Freshwater	0.05	18.9	10.26
	D. salina (UTEX)	Freshwater	0.15	24.0	36.48
	Chlorella emersonii	Freshwater	0.036-0.041	25.0-63.0	10.3-50.0
	Chlorella vulgaris	Freshwater	0.02-0.2	5.0-58.0	11.2-40.0
Eustigmatophytes	*Nannochloropsis sp. F&M-M26*	Marine	0.21	29.6	61.9
	Isochrysis sp. F&M-M37	Marine	0.14	27.4	37.8
Prymnesiophytes	*Pavlovasalina CS 49*	Marine	0.16	30.9	49.4
	Pavlovalutheri CS 182	Marine	0.14	35.9	50.2
Red algae	*Porphyridiumcruentum*	Marine	0.37	9.5	34.8

1.3 Microalgae lipid biochemistry

Microalgae synthesize fatty acids primarily for the generation of various types of lipids, such as membrane glycerolipids and triacylglycerides that is used for biodiesel production. The most frequently synthesized fatty acid chains in the lipids present in microalgae is ranging from C14 to C20, though the fatty acid constituents may be saturated and unsaturated, as shown in Table 1.3.

To enhance the production of these lipids from the microalgae, it is pertinent to gain insight into the algal lipid biochemistry (Lv et al., 2013). Although there has been considerable progress in the understanding of lipid biochemistry, much has to be learned for in the decoding of metabolic fluxes leading to lipid biosynthesis.

Table 1.3: The major fatty acids present in algal strains (Mondal et al., 2017)

Algal Class	Major Fatty Acids	Major Polyunsaturated fatty acids (PUFAs)
Bacillariophyceae	C14:0,C16:0, C16:1 and C18:1	C20:5 and C22:6
Chlorophyceae	C14:0,C16:0, C18:0 and C18:1	C18:2, C18:3 and C18:4
Euglenophyceae	C16:0 and C18:1	C18:2 and C18:3
Chrysophyceae	C16:0 and C16:1 and C18:1	C20:5, C22:5 and C22:6
Chryotophyceae	C16:0 and C20:1	C18:3, C18:4 and C20:5
Prasinophyceae	C14:0, C16:0 and C18:1	C18:2, C18:3, C20:4 and C20:5
Dinophyceae	C14:0, C16:0	C18:4, C18:5, C20:4 and C22:6
Prymnesiophyceae	C14:0, C16:0, C16:1, C18:0 and C18:1	C18:2, C18:3 C18:4 and C22:6
Phaeophyceae	C14:0,C16:0 and C18:1	C18:2, C18:3 and C20:4
Rhodophyceae	C16:0, C16:1 and C18:1	C18:2, C20:4 and C20:5
Xanthophyceae	C14:0, C16:0 and C16:1	C16:3 and C20:5
Cyanobacteria	C16:0 and C16:1 and C18:1	C16:0, C18:2 and C18:3
Haptophyceae	C14:0, C16:0, C16:1 and C18:1	C20:5 and C22:6
Raphidophyceae	C14:0, C16:0 and C16:1	C18:2, C18:3 C18:4 and C20:5

Photosynthesis in microalgae is the fundamental driving force for biomass production consisting of carbon storage products (e.g., carbohydrates and lipids) and H2 (Beer et al., 2009). Similar to plants, microalgae have subcellular compartments such as cytoplasm, chloroplast, endoplasmic reticulum and mitochondria and. Lipid metabolism in microalgae occurs in the chloroplast, where the light energy is assimilated into the cell in the form of light quanta, which is absorbed by the pigments to drive the photosynthetic electron transport. During electron transport in the outer layers of thylakoids in the chloroplast, NADPH is used to produce ATP via light reactions that are sequentially used in the Calvin cycle; a primary pathway for CO2 fixation as shown in Figure 1.1. The primary step in the Calvin cycle is catalyzed by RubisCO enzyme where ATP and NADPH are used for conversion of CO2 into three carbon molecule glycerol 3-phosphate (G3P). The G3P is then exported to the cytoplasm, where it is being used in sugar synthesis and lipid metabolism (Sarkar and Shimizu, 2015). For lipid metabolism, G3P is converted to pyruvate and then into acetyl-CoA, via a reaction catalyzed by the pyruvate dehydrogenase complex (PDC) that initiates the fatty acid biosynthetic pathway where free fatty acids (FFA) are synthesized. Afterwards, FFA is exported to ER where they converted into triacylglycerols (TAG) by the action of ER enzymes. These TAG molecules are accumulated into lipid bodies in the cytoplasm of microalgal cells that can be utilized for biofuel production (Bellou et al., 2014).

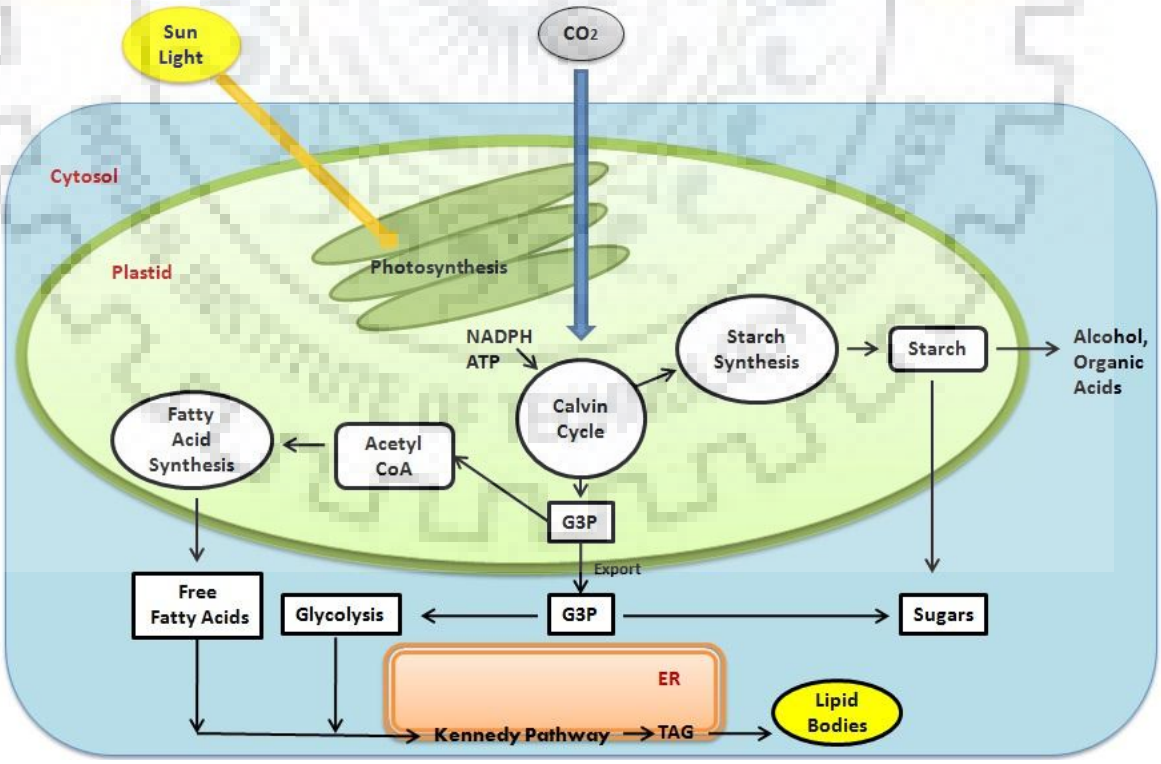

Figure 1.1 Schematics of metabolic pathways of algae leading to for biofuel production

1.3.1 Lipid biosynthesis

In microalgae, the lipids are classified into polar lipids such as phospholipids and neutral lipids like triglycerides. Polar lipids from the structural component, whereas the triglycerides are the main precursor for the production of biodiesel. The triglycerides biosynthesis in microalgae consist of the following steps: (i) the formation of acetyl coenzyme A; (ii) the desaturation and elongation of fatty acids; and (iii) the triglycerides production in microalgae (Huang et al., 2010). Acetyl-CoA being provided by photosynthetic reactions acts as a precursor for fatty acid synthesis. Acetyl CoA Carboxylase (ACCase) catalyzes the first committed step in fatty acid biosynthesis by converting acetyl CoA to malonyl CoA. Further, the malonyl CoA is transferred to the acyl carrier protein (ACP) by malonyl–CoA: ACP transacetylase, which then get introduced in fatty acid synthesis cycle through the 3-ketoacyl-ACP synthase (KAS) (Bellou et al., 2014). The formation of 16 or 18 carbon chain of fatty acids relies on the acetyl-CoA carboxylic and fatty acid synthase (FAS) enzymes.

Fatty acid elongation occurs in the ER, and their synthesis requires specific classes of desaturases and enolases enzymes. The fatty acid elongation system elongates the precursors in two- carbon increments where the desaturase enzymes insert double bonds at specific carbon atoms in the fatty acid chain (Gong et al., 2011). TAG (triacylglycerol) biosynthesis and assembly is a complex process in microalgae, and this may occur via the direct glycerol pathway, i.e. Kennedy pathway where the acyltransferases residing in the ER catalyze a sequential transfer of acyl group from the acetyl-COA to glycerol-3-phosphate backbone determining the final content of TAG as shown in Figure 1.2. TAG is then accumulated into the cytosol as ER-derived lipid droplets (De Bhowmick et al., 2015).

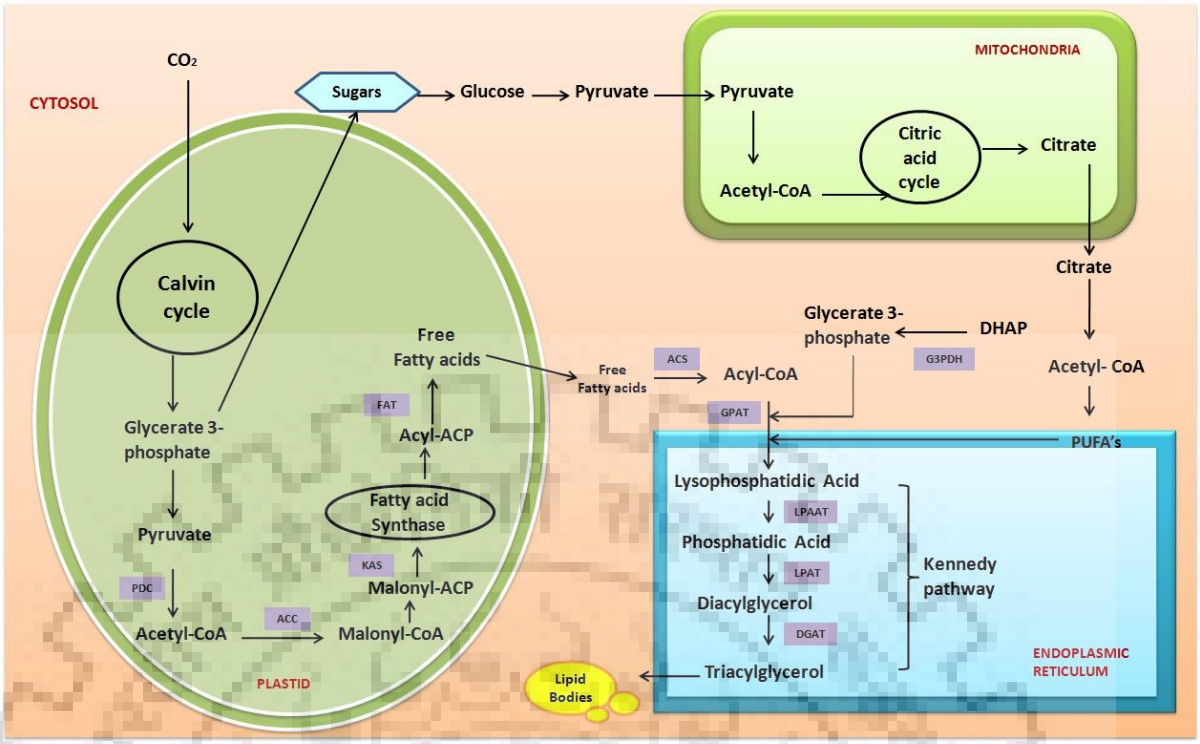

Figure 1.2 Representation of lipid biosynthesis in microalgae. Where, ACC, acetyl-CoA carboxylase; ACP, acyl-carrier protein;ACS, acyl-CoA synthetase; CoA, coenzyme A; DGAT, diacylglycerolacyltransferase; FAT, fatty acyl-ACP thioesterase; GPAT, glycerol-3-phosphate acyltransferase; G3PDH, glycerol-3-phosphate dehydrogenase; KAS, 3-ketoacyl-ACP synthase; LPAAT, lysophosphatidic acid acyltransferase; LPAT, lyso-phosphatidylcholineacyltransferase; PDC, pyruvate dehydrogenase complex.

1.4 Lipidomics: Unravelling the lipid profile of microalgae

Fatty acids are the crucial component of microalgal lipids. The fatty acid profile of microalgal lipids are directly related to the properties of biofuels and have been used to evaluate the feasibility of using microalgal feedstock for biodiesel production. The analysis of the lipidome profile of microalgae is an emerging field that revealed the various lipid classes as well as their fatty acids constituents in microalgae to determine their suitability for biodiesel (Li et al., 2014). Relatively higher proportions of SFA and MUFAs found in the oils of algal species such as *Scenedesmus obliquus* and *Chlamydomonas sp*., results in the production of biodiesel with the high cetane number, high oxidation stability and low iodine values (IV), the desirable feature for high-grade biodiesel (Nascimento et al., 2013). Moreover, lipid classes and their constituents have been used as 'biomarkers' to differentiate the closely related microalgal species at generic levels. For instance, Chlorophyta contains predominantly saturated fatty acids (SFA) and monounsaturated fatty acids (MUFA) and trace amounts of polyunsaturated fatty acids (PUFAs).

On the other hand, certain other classes of algae, such as Chromal veolate contain significant amounts of PUFAs (Lang et al., 2011). Lipidome profiling of microalgae thus is a vital bio-prospecting tool for evaluating the potential of a particular algal species for producing high-quality biodiesel.

1.5 Approaches for enhanced lipid accumulation in microalgae

Many of the algal species with ideal growth parameters generate large amounts of biomass but with relatively lower lipid content, which is around 5–30% of dry mass. Although the production cost of microalgal based diesel is as high as fossils derived diesel. To tackle this, it is desirable to screen the microalgae that have significant lipid content and productivity through varying environmental conditions (Rawat et al., 2013). Faced with unfavorable environmental conditions, many microalgae shift their lipid biosynthetic pathway towards the formation of neutral lipids primarily in the form of triacylglycerols (Sibi et al., 2015). Employing nutrient stress conditions mainly nitrogen and phosphorus starvation; varied light irradiation, changes in temperature and pH; as well as the presence of heavy metals and other chemicals, etc. have been observed to regulate the lipid yield (Kwak et al., 2016). Further, genetic engineering approaches can also be used to enhance the lipid accumulation in the microalgae (Sharma et al., 2012). Several key genes of fatty acid metabolism such as G3PDH, ACCase, DAGAT, etc. have been involved in the lipid accumulation in the microalgal cells when exposed to stress or certain stimuli (Fan et al., 2014). Transforming microalgae with extra copies of such genes participating in the TAG biosynthesis or inhibiting the expression of the genes of other metabolic routes such as citric acid cycle have been found to enhance the neutral lipid content in microalgae (Yao et al., 2014). Fig 1.3 depicts the important approaches for augmenting lipid accumulation in microalgae.

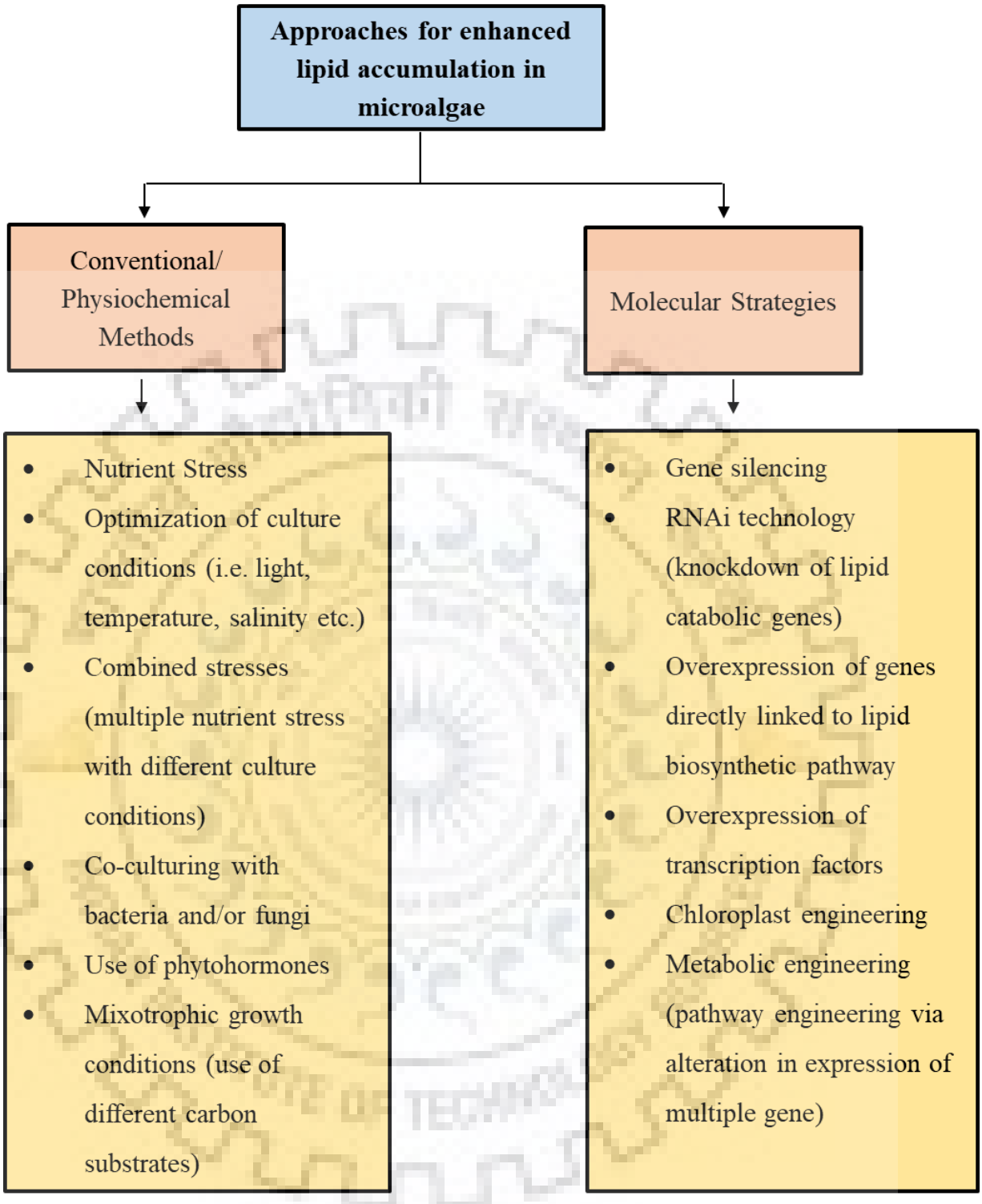

Figure 1.3 Strategies for enhanced lipid accumulation in microalgae

1.4.1 Enhancing microalgal lipid: Conventional approaches

The levels of lipid accumulation in microalgae are influenced by the microenvironment around the cells. Microenvironment can be derived through the various parameters including light intensity, photo-oxidative stress, temperature, nutrient limitation, and high saline conditions.

Conventional approaches to enhance lipid production involve understanding the role of each of these physical and chemical parameters in microalgal growth and lipid biosynthesis. These parameters can then be altered or modified in a specific manner to achieve the desired biomass and lipid content. Among these, nutrient deprivation, mainly nitrogen and phosphorous have been widely analyzed. Owing to the limitations of nutrient stress on arresting algal growth at an early stage, other approaches such as supplementation of additives, which exerts a positive effect on both biomass and lipid accumulation are also being investigated. Some important observations on the lipid accumulation through conventional routes are summarized in Table 1.4

1.4.1.1 Physiological stress and nutrient deprivation

Nutrient deprivation leads to restricted cell growth through channeling metabolic fluxes to the fatty acid synthesis led to storage lipids accumulation in the forms of TAGs. Nutrient starvation leading into Enhanced lipid accumulation has been observed for a number of microalgal species under nutrient starvation condition such as *Botryococcus braunii* (Dayananda et al., 2005), *Chlamydomonas reinhardtii* (Miller et al., 2010), *Phaeodactylum tricornutum* (Yang et al., 2014) and *Chlorella vulgaris* (Ikaran et al., 2015). Some important observations on the lipid accumulation through conventional routes are summarized in Table 1.4. Among nutrient stress conditions, nitrogen deprivation has been found to augment the lipid content significantly in microalgal strains (Fan et al., 2014). However, the biomass production was not satisfactory due to the nitrogen insufficiency.

Conventional strategies like nutrient deprivation and physiological stresses might seem to be useful for improving lipid content in microalgae, but they frequently failed to enhance the volumetric lipid productivity significantly, as the increase in lipid content happens led to decrease biomass. Thus, it is imperative to develop strategies for attaining higher lipid content with uncompromised biomass.

Table 1.4 Effects of various physiochemical factors on lipid accumulation in different species of microalgae

Species	Factors	Effect	References
Chlamydomonas reinhardtii,	Nitrogen starvation	Nearly fivefold increase in neutral lipid content in low N condition in comparison with high N condition.	Dean *et al.,* 2010
Anacystisnidulans	Nitrogen starvation	Accumulation of saturated, longer-chain (C18) fatty acids	Gombos et al., 1987
Nannochloropsis oculata	Nitrogen starvation	Total lipid increased by 15.31%	Converti et al., 2009
Chlorella vulgaris	Nitrogen starvation	Total lipid increased by 16.41%	Converti et al., 2009
Chlorella vulgaris	Nitrogen starvation	Lipid productivity of 78 mg/L/d achieved, nearly 1.5 fold of normal productivity	Yeh et al., 2011
Scenedesmus sp.	Nitrogen & Phosphorous starvation	~30 % lipid content at N 2.5 mg/L compared with ~24 % at N 25 mg/L	Xin et al., 2010
Chlorella sp.	Phosphate, Potassium, Iron starvation	Lipid productivity in N limitation went from 40.27 to 53.97 mg/L/d & in combined stress to 49.16 mg/L/d	Praveenkumar et al., 2012
Phaeodactylum tricornutum	Phosphorus starvation	Increase in total lipids with higher relative content of 16:0 and 18:1	Reitan et al., 1994
Chlamydomonas reinhardtii	Sulphur starvation	2-fold increased PG	Sato et al., 2000
Chlorella vulgaris	Iron starvation	High levels of chelated Fe^{3+} results in high levels of lipid accumulation(3-7 fold increase)	Liu et al., 2008
Cyclotellacryptica	Silica starvation	Increased in total lipids from 27.6% to 54.1%	Roessler et al., 1998

Nannochloropsisgaditana	Nitrogen starvation	5.7 fold increase in NgMCAT expression	Tian et al., 2013
Isochrysisgalbana	Nitrogen starvation	Desaturation of fatty acids	Heurlimann et al., 2014
Chlorella vulgaris	Nitrogen starvation	Increased lipid accumulation in shorter time period	Mujtaba et al., 2012
Micractiniumpusillum	Nitrogen starvation	Genes linked to pyruvate and acetyl-CoA synthesis were radically increased over 100 times after nitrogen starvation	Li et al., 2012
Dunaliella sp.	High Salinity	high intracellular lipid content and a high percentage of triacylglyceride in the lipid	(Takagi and Yoshida, 2006)
Chlorella vulgaris	CO2 concentration	maximum lipid productivity of 29.5 $mg.l^{-1}.day^{-1}$ at 8% (v/v) CO2 in which higher saturated fatty acids were obtained	(Sibi et al., 2015).
	Light intensity	High light intensity decreases total polar lipid content with a simultaneous increase for lipids, mainly TAGs.	Harwood et al.,1998

1.4.1.2 Exogenous application of natural additives/phytohormones

There is an urgent need to devise strategies through which the biomass levels can be stabilized or even increased with high lipid content. One such strategy that is recently being investigated is the effect of exogenous application growth regulators and natural additives on microalgal growth and lipid production. Among the regulators, phytohormones were found to have to regulate effect on the growth and metabolite production, for instance carbohydrates, proteins, and lipids. Phytohormones are a class of stimulants that have been observed to regulate cell growth and metabolism in plants (Voβ et al., 2014). Considering the evolutionary relationship between plant and algae, they are expected to play the same role in microalgae (Hunt et al., 2010). Although their physiological functions remain largely unknown, many of these phytohormones such as auxins, cytokinins abscisic acid and gibberellic acids have been detected in the wide range of algal extracts. Auxins, cytokinins, abscisic acid, and gibberellins are the major classes of phytohormones, among these, auxins and cytokinins are the essential ones that regulate plant cell growth and division respectively (Bajguz and Piotrowska-Niczyporuk, 2013), (Liu et al., 2016).

1.4.2 Enhancing microalgal lipid: Molecular Approaches

Modifications in nutrients and culture conditions can work towards increasing lipid accumulation but only up to a certain limit. Attempts have been made to decipher the mechanism involved in the lipid biosynthesis at the molecular level to uncover possible ways to alter/enhance it. They have identified several key genes, responsible for changes in lipid accumulation and any correlation between changes in their expression levels with changing microenvironment. Previous studies have reported that, in nitrogen-limited condition, microalgal strains accumulate a higher proportion of lipid compared to normal growth condition. Although the relative alteration in lipid metabolic pathways in both these conditions is identified, many global changes, such as differential genes expression remain poorly understood. The lack of this genomic information generally hinders the genetic modification in these microalgae to enhance the lipid accumulation and other bioproducts. Consequently, the lipid production from microalgal strains is significantly lower than the theoretical maximum led to the cost of biodiesel excessively high.

1.4.2.1 Transcriptomics as a molecular approach

So far, many algal genomes have been sequenced, including green algae *Chlamydomonas reinhardtii*, *Coccomyxa sp.* C-169, *Micromonas CCMP 1545*, *Ostreococcuslucimarinus* CCE9901, *Ostreococcustauri* and *Volvoxcarteri*, red alga: *Cyanidioschyzonmerolae*, brown alga: *Ectocarpussiliculosus* (De Bhowmick et al., 2015). These genome sequences have provided us

the tools to unravel the molecular and genetic mechanism behind lipid biosynthesis, but the task is very difficult as these genome sequences are voluminous and it requires huge cost, time and effort to infer them in detail.

Transcriptomic could be a resourceful and cost-effective strategy deciphering the broad view of different metabolic pathways associated with biofuel production in microalgae without the complete genomic information (Rai and Saito, 2016). Recently, to inspect the regulatory mechanism of lipid accumulation in oleaginous microalgae, a larger number of transcriptomes were observed to be *de novo* sequenced and annotated (Fan et al., 2014).

The transcriptome analysis can provide insights into the regulation of lipid metabolism by revealing the upregulation and downregulation of the genes that are mainly associated with fatty acid biosynthetic pathway such as Acetyl CoA carboxylase (ACCase), Glyceraldehyde 3-phosphate dehydrogenase (G3PDH), Ketoacyl synthase (KAS), Diacylglycerol acyltransferase (DAGAT) etc in microalgae under nitrogen stress conditions (Goncalves et al., 2016). It will further result in accurately altering the key enzymes of the fatty acid biosynthetic pathway through genetic modification in microalgae to improve lipid productivity.

The use of molecular techniques over conventional methods offers several advantages such as providing molecular insights of lipid metabolism, a better understanding of strategies to increase the lipid productivity, targeted alteration at the genetic level that can be stably transmitted across generation. Further, targeted molecular intervention can alter lipid metabolism without affecting cellular growth, resulting in stable biomass yield, and desired quality and quantity of oil. Moreover, it provides diversified methods for increasing lipid content in a specific strain that can be promising on the industrial front.

Two conventional approaches to enhance the lipid accumulation in the microalgae are, up-regulation of the genes participating in the biosynthesis of lipid and down-regulation or blocking of genes participating in the catabolism of lipids. Both the strategies focus on turning the metabolic flux towards fatty acid biosynthesis.

1.4.2.1 Overexpression/upregulation of key enzymes

Overexpression of specific genes produces a higher amount of the corresponding enzyme that competitively blocks other enzymes of the same substrate, eventually increasing the metabolic flux towards the reaction catalyzed by the overexpressed enzyme. The same phenomenon can be used to enhance the lipid accumulation in the microalgal cells by overexpressing the genes

involved in the fatty acid biosynthesis. Several studies have been performed to investigate the effect of upregulation of different genes on lipid accumulation in microalgae, few of which are mentioned in Table 1.6. In some instances, instead of overexpression of essential genes of the lipid biosynthetic pathway, up-regulation of transcription factors associated with those genes have also been found to enhance the lipid content in the microalgal cells.

Table 1.6 Enhancement of lipids in microalgae via molecular approaches.

Species	Gene	Approach	Effect	References
Chlamydomonas reinhardtii	Dof-type Transcription factor	Over-Expression	A two-fold increase in total lipid	Salazar et al., 2014.
Phaeodactylumtricornutum	G3PDH	Over-Expression	60% increase in neutral lipid content, reaching up to 39.70% of total dry cell weight.	Yao et al., 2014.
Chlamydomonas reinhardtii	Citrate synthase	Downregulation	TAG levels increased by 169.5% in response to a 37.7% decrease in CrCIS activities	Deng et al., 2013.
Schizochytrium sp.	Acetyl-CoA Synthetase	Over-Expression	The biomass and fatty acid proportion increased by 29.9 and 11.3 %, respectively	Yan et al., 2013
Thalassiosirapseudonana	Lipase (Thaps3-264297)	Downregulation	Strains 1A6 and 1B1, respectively, contained 2.4- and 3.3-fold higher lipid content than wild-type during exponential growth	Trentacoste et al., 2013
Phaeodactylumtricornutum	The malic enzyme (PtME)	Over-Expression	Total lipid content in transgenic cells markedly increased by 2.5-fold and reached a record 57.8% of dry cell weight.	Xue et al., 2014.
Chlamydomonas reinhardtii	DGTT4	Over-Expression	Enhanced TAG accumulation.	Iwai et al., 2014
Nannochloropsissalina	bHLH transcription factor	Over-Expression	Increase in biomass production by 36% and FAME productivity by 33% under Nitrogen stress	Kang et al., 2015

Synechocystis sp.	*maqu_2220* (acyl-CoA reductase), aldehyde-deformylatingoxygenase gene (*sll0208*)	Combinatorial Approach	Overexpression of *maqu_2220* and knockout of *sll0208* resulted in higher production of Fatty alcohols	Yao et al., 2014
Chlorella ellipsoidea	*GmDof4* (Transcription factor)	Over-Expression	Heterologous-expression of GmDof4 gene from soybean can significantly increase the lipid content but does not affect the growth rate.	Zhang et al., 2014

1.4.2.2 Downregulation of key enzymes/Thwarting accessory pathways

There are several key metabolites, which are common for different metabolic pathways such as Pyruvate, a glycolysis product, which can be utilized either for the energy generation through TCA cycle or used for fatty acid biosynthesis. To increase the flux of pyruvate towards Fatty acid biosynthesis, enzymes of TCA can be blocked or down-regulated. It would enhance the fatty acid biosynthesis, leading to an enhanced level of lipids in the microalgal cell. Also, downregulating the enzymes of lipid catabolic pathways such as lipases can augment the lipid accumulation. Therefore, recent studies have focussed on the downregulation of certain genes as an approach for enhanced lipid production in microalgae. (Deng et al., 2013); (Trentacoste et al., 2013).

For selecting any of the two-abovementioned approaches, the motive behind every metabolic manipulation has to be the increased metabolic flux towards fatty acid biosynthesis in microalgal cells. Combinatorial methods utilizing both these approaches simultaneously by genetic engineering of the microalgae have also been employed for maximizing the lipid content. (Yao et al. 2014).

CHAPTER 2

Bioprospecting for Microalgal strains for Biofuel Production: Evaluation of Biomass content and Lipid productivity under Standard and Nutrient Limited Cultivation

2.1. Introduction

The Conventional resources of fuel generation are depleting at an alarming rate due to multifaceted applications of the limited reserves for energy generation. The growing trend of the rising greenhouse gas emissions leading to global warming demands restricted use of conventional fuel resources. Consequently, there is an upsurge in the fuel prices and their uses, leading to disastrous climatic changes, which need immediate attention as a global concern (Chisti, 2007). Therefore, it is imperative to search for alternative resources to meet the increasing demands. The alternatives should be feasible, environment-friendly, and economical (Lang et al., 2011). Biofuels offer many advantages like decreased emissions of greenhouse gases, sustainability, assurance of their uninterrupted supply with desired fuel characteristics, and many more. Hence, these match the prerequisites for alternative fuels and exhibit potential for meeting the demands of future generations.

Earlier, vegetable oils, e.g. soybean, sunflower, rapeseed oil, etc. have been considered as potential sources for biodiesel production. This shift of food production to fuel production from the agricultural land is quite controversial, especially with the primary aim of fuel generation. Thus, many efforts were made to explore non-edible crops like *Jatropha curcas*, *Brassica carinata*, etc. for biofuel production (Pinzi et al., 2009). The requirements for large stretches of land for crop production turns out to be a big hurdle for their success as potential resources for biofuels. Keeping in mind with these drawbacks, microalgae appear to be a promising resource for biofuels.

Microalgae serve as a potential candidate for biofuel because of various advantages like higher growth rates, higher photosynthetic efficiency, higher lipid accumulation, and biomass production (Huang et al., 2010). Microalgae with potential to accumulate vast amounts of lipids along with high biomass are desirable for biofuel production. In addition to that, microalgae have been observed to convert carbon-dioxide to a variety of other valuable constituents and biologically active compounds (Mata et al., 2010). Besides their inherent advantageous qualities, microalgae can be pioneered into mini-lipid factories when grown under defined conditions.

Thus, they would be a potential resource for regulating carbon dioxide levels and thus dealing with global warming concerns.

Moreover, orchestrated efforts are needed to explore microalgae as a potential feedstock for biofuels. Therefore, to utilize these as a potential resource for biofuels, it is imperative to select the promising and viable algal strain with higher lipid content and desired fatty acid profiles for biofuels (Abou-Shanab et al., 2011). Thus, it would be desirable to explore the robust microalgal strains from distinct sources with higher biomass and lipid contents. Therefore, the objectives of the present study are (i) to procure the microalgal strains from repositories in India and also to isolate the microalgal strain from and around the Garhwal region, Uttarakhand, India, (ii) Analyse the strains for their biomass and lipid content and select the potential strains with higher lipid productivity, and (iii) to evaluate the fatty acid profiles of the selected strains.

2.2. Methods

2.2.1. Isolation and procurement of microalgal strains

The microalgae used in this study, *Scenedesmus abundans* was obtained from NCIM - National Chemical Laboratory Pune; *Scenedesmus opoliensis*, *Senedesmus sp.*, *Chlorococcum* sp. *Chlorococcum infusionum*, *Pediastrum sp.*, *Chlorella sp.*1, *Chlorella sp.*2, *Chlorella sp.*3, *Chlorella sp.*4, *Neochloris sp.*, and *Chlamydomonas sp.* were provided by the Institute of Bioresources And Sustainable Development (IBSD), Imphal, India. The microalgal Strains JS01 to JS07 were isolated from the Garhwal region of Uttarakhand, India by single-cell isolation technique.

2.2.2 Cultivation of strains

2.2.2.1. Standard nutrient cultivation of microalgal strains (phase I)

The microalgal strains were grown using standard BG11 medium with the following composition: 1500 mg/L $NaNO_3$, 40mg/L $K_2HPO_4 \cdot 3H_2O$, 75 mg/L $MgSO_4 \cdot 7H_2O$, 20mg/L Na_2CO_3, 27mg/L $CaCl_2$, 6mg/L citric acid monohydrate, 6mg/L ammonium ferric citrate, and 1 mg/L Na_2EDTA, with 1 mL trace metal solution (2.86mg/L H_3BO_3, 1.81 mg/L $MnCl_2 \cdot 4H_2O$, 0.222 mg/L $ZnSO_4 \cdot 7H2O$, 0.079 mg/L $CuSO_4 \cdot 5H2O$, 0.050 mg/L $CoCl_2 \cdot 6H_2O$, 0.39 mg/L $Na_2MoO_4 \cdot 2H_2O$) (Aravantinou et al., 2013). Each strain was grown in a 500 mL Erlenmeyer conical flask containing 150 mL of the BG-11 growth medium. Experiments were conducted under controlled laboratory conditions; the temperature of 25 ^{0}C, continuous illumination from daylight fluorescent lamps of 200 µEm-2 s-1 and at 150 rpm for 20 days. Samples were taken

for cell growth determination, every 5th day for up to 20 days and total lipid and fatty acid profiling at the stationary phase (20th day).

2.2.2.2 Nutrient limited cultivation of microalgal strains (phase II)

In the second phase (phase II), four potential microalgal strains (*Chlorella* sp. 3, *Scenedesmus* sp. *Chlorella emersonii* JS04 and *Desmodesmus* sp. JS07) were selected for further study. Pure cultures of microalgal strains at exponential phase (OD~0.6) were inoculated into fresh BG11 medium for microalgae growth assay. Before the inoculation of microalgal cells, different concentrations, i.e., 0, 25, 50, 75, and 100% (control) of N and P, were added separately into the BG-11growth media. The effect of 0, 4.4, 8.8, 13.2 and 17.6 mM N (using $NaNO_3$ as nitrogen source) and 0, 0.058, 0.115, 0.172 and 0.23 mM P (KH_2PO4 as phosphorus source) were determined independently in the modified BG-11 media. Other conditions were similar, as defined in Section 2.2.1. Samples for cell growth determination were taken every 5th day for 15 days and total lipid and fatty acid profiling during the early stationary phase (at 15th day).

2.2.3. Analytical methods

2.2.3.1 Measurement of growth

The growth was measured as dry biomass (g/L, dry weight, DW). For dry biomass estimation, 5mL aliquots of the microalgal cultures were filtered through preweighed Whatman GF/C filters with pore size 1.2 μm. The filters containing the microalgae were rinsed twice with deionized water and dried at 70°C for 18-24 h until the constant weights were achieved. Afterwards, cooling to room temperature using vacuum desiccator, the weights were measured using an analytical balance (Mettler Toledo, USA).

2.2.3.2 Nile Red fluorescence for visualization of lipid globules

The distribution of lipid globules in microalgal stained cells was studied by confocal microscopy. Nile Red was prepared as a stock solution of (0.1 mg/ml) in acetone. The Nile Red staining procedure was followed as described by Govender et al., 2012, with slight modifications. Concisely, 1 ml of microalgal cultures (1×10^5 cells/ml) were suspended in 25% dimethyl sulfoxide and stained using Nile red (1.5 μg/ml) followed by 15 min of incubation in the dark at room temperature. Following staining, the slides were prepared using 10% glycerine (v/v) and analyzed under Confocal Laser Scanning Microscope (LSM 780, Carl Zeiss, Germany) equipped with 490-530 nm excitation and 575-610 nm emission using 60X objective.

2.2.3.3 Lipid extraction and quantification

The cultures were harvested by centrifugation at 6000 rpm for 30 min. Subsequently, the pellet obtained was lyophilized using vacuum freeze-dryer (ALPHA1-2LD, Osterode am Harz, Germany) for 12-24 h until constant weights were achieved. Lipids were extracted using a modified Bligh and Dyer procedure (Bligh and Dyer, 1959). Briefly, the lipid extraction from the dry biomass (100 mg) was performed by using chloroform: methanol (1:2 v/v). The mixtures were sonicated at 50 Hz (Transonic model 460/H, Elma, Germany) in an ice bath followed by shaking for 2 hr using a magnetic stirrer and then centrifuged at 5000 rpm for 10 min. Then, the chloroform phase was collected, and samples were oven dried at 50^{o}C for gravimetric analyses of lipid content and expressed as % dry weight.

2.2.3.4 Identification of microalgae

Microalgae samples JS03, JS04, and JS07, were harvested in the mid-exponential growth phase, and genomic DNA was extracted using a modified CTAB method. A 700-bp of 18S rRNA gene was amplified by using the universal forward (5'- GTCAGAGGTGAAATTCTTGGATTTA-3') and reverse (5'- AGGGCAGGGACGTAATCAACG-3') primers. Based on multiple alignments phylogenetic analysis was performed through MEGA software v.6.0 using the neighbor-joining (NJ) algorithm. The BLASTn algorithm at the NCBI server had generated sequence identities, and the sequences were submitted in the GenBank database.

2.2.3.5 Fatty acid methyl esters (FAMEs) profiling

For fatty acid methyl esters (FAMEs) analysis, transesterification of the total lipids (10mg) was performed using 1 mL of 2% (v/v) sulphuric acid in methanol. Afterwards, the samples were incubated at 60^{o}C for 3hr and FAMEs were extracted using hexane (1 mL) and vortexing for 5 min. 1µl of this hexane containing FAMEs was then used for GC-MS analysis (Tai and Stephanopoulos, 2013).

FAMEs were analyzed employing gas chromatography-mass spectrometry (GC-MS) (Agilent 7890A-5975C, Agilent Technologies Ltd. Santa Clara, CA, USA) equipped with a flame ionization detector (FID). 1µl of the sample was introduced straight onto the GC-MS system and separation of FAMEs was performed using a DB5 column (30 m×250 µm×1 µm; Agilent Technologies, USA) with helium as a carrier gas at a flow rate of 1ml/min. The column program was set as: an oven temperature gradient of 50-180 °C at 25 °C/min and held for 1 min, then with an oven temperature gradient of 180 °C-220°C at 10°C/min and held for 1 min; lastly the gradient

of 220-250 °C at 15°C/min and held for 15 min. FAMEs were identified using retention times of the peaks of known FAME standards mix (FAME Mix, C8:0–C240) in the reference solution.

2.2.4. Statistical analysis

All cultivations were carried out in triplicate, and the final values were expressed as mean ± standard deviation.

2.3. Result and Discussions

2.3.1. Standard nutrient cultivation (phase I)

2.3.1.1 Isolation and identification of microalgal strains

In the present study, fifteen microalgal cultures were isolated from the freshwater streams near Dehradun, Garhwal region of Uttarakhand, India. Seven promising isolates (JS01, JS02, JS03, JS04, JS05, JS06, and JS07) were selected based on their purity and were further explored for biomass and lipid content. Microscopic observation od isolates displayed their colonial existence and indicated that the cells are solitary, 2–10 µm in diameter and are spherical or globular (Fig 2.1). The morphological heterogeneity of the microalga makes the microscopic examination difficult. Thus, further, phylogenetic analysis was performed by isolating the total DNA of the promising isolates following PCR amplification of the 18S rRNA as potential markers for species identification.

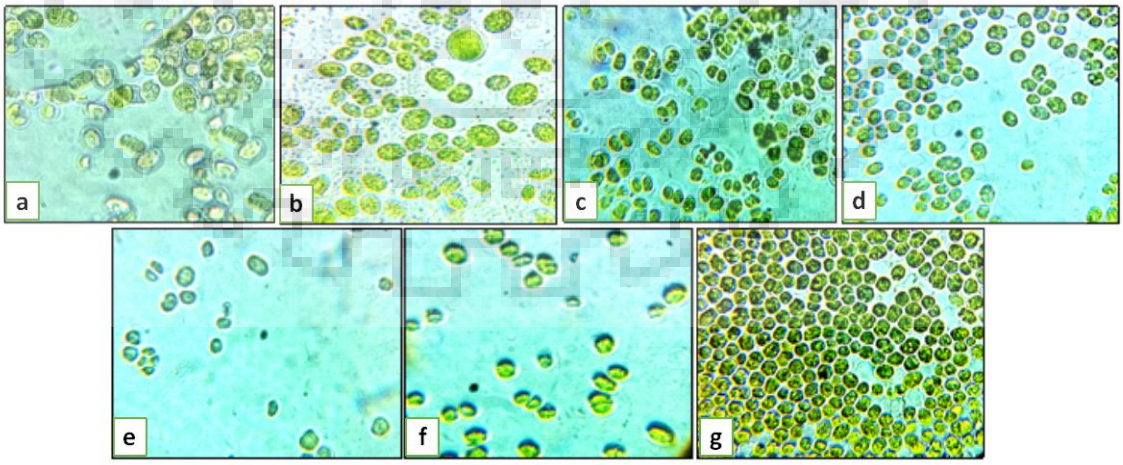

Fig. 2.1 Light microscopy (40x) of the microalgal isolates. (a), JS01; (b), JS02; (c), JS03; (d), JS04; (e), JS05; (f), JS06 and (g), JS07.

2.3.1.2 Biomass, lipid content, and productivity of the microalgal strains

Under standard nutrient cultivation for 20 days, the growth profile of all the nineteen-microalgal strains in terms of biomass content is shown in Fig. 2.2. Among isolated microalgal strains, JS01, JS02, and JS07 had the higher biomass content of 2.11±0.05, 2.29±0.07 and 1.67±0.08 g/L respectively. While among procured strains, *Chlamydomonas sp., Chlorella sp. 4 and Secnedesmus abundans* had higher biomass levels of 2.01±0.07, 1.812±0.08 and 1.68±0.04 g/L respectively at 20th day.

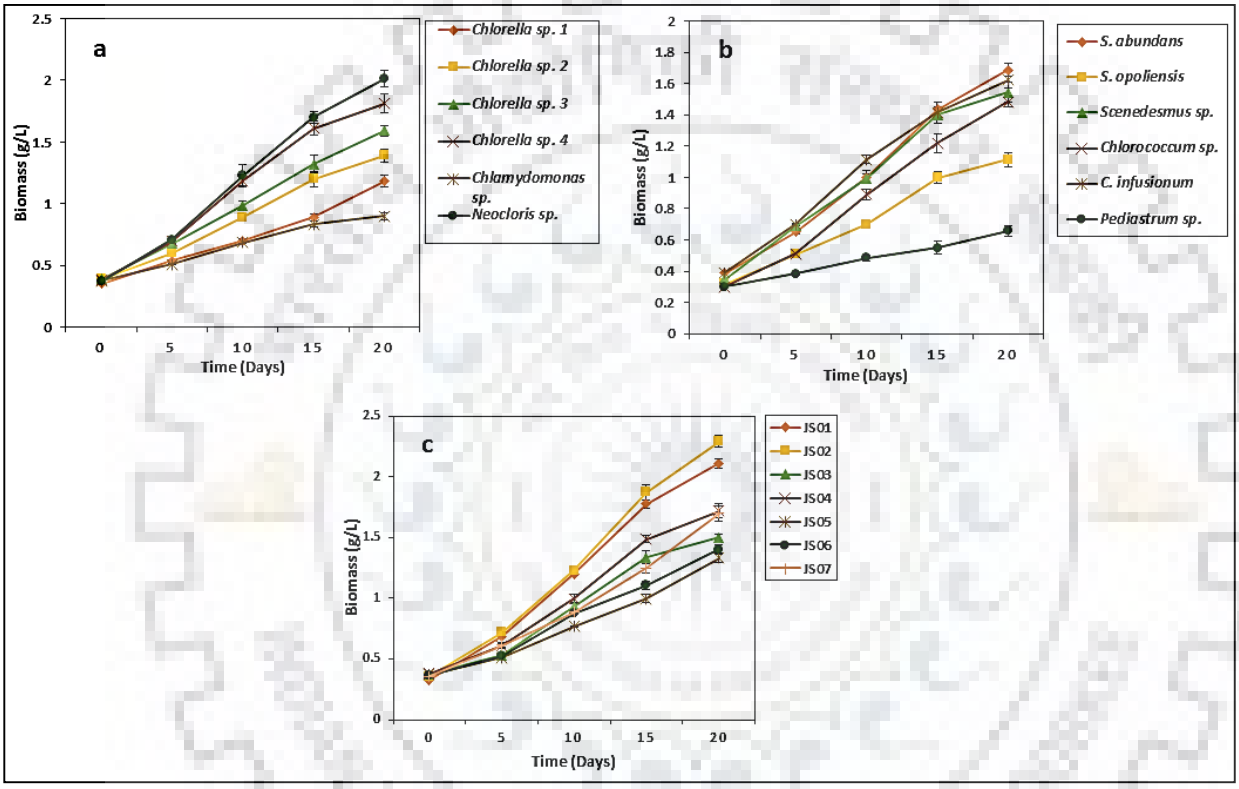

Fig. 2.2. Biomass content of the procured (a), (b) and isolated (c) microalgal strains. Data are represented as Mean ± SD; error bars represent the standard deviation of triplicate experiments.

Further, the isolated and procured strains were screened for their biomass, lipid content, and productivity (Table 2.1). The total lipid content for the microalgal strains enumerated ranged from 10.45 % to 27.04 % of the dry weight. Isolate JS07 had the maximum lipid content (27.55±1.42 %), followed by isolate JS04 (24.11±2.49 %) at the 20th day. In addition, *Scenedesmus* sp. and *Scenedesmus abundans* and *Chlorella* sp. 3 also had higher levels of lipids (25.98±2.88, 20.32±3.14 and 24.98±4.42 % respectively) that was comparable with lipid content observed for similar strains (Bohutskyi et al., 2015; C and S, 2013).

Higher lipid content is often offset by lower growth rates, which in turn resulted in lower lipid productivity (Huerlimann et al., 2010). Thus, lipid content, along with productivity, could be determined for selecting a suitable microalgal strain for scale-up production. Notably, isolate JS07 had maximum lipid productivity (23.40±1.88 mg/l/d) followed by JS04 (20.74±0.87 mg/l/d), thus marking these two strains for further evaluation. Further, *Scenedesmus sp.* and *Chlorella sp.* 3 were also promising candidates owing to their higher growth rates and lipid content. It is worth noting that among all the strains evaluated, isolated strains appeared superior in terms of both biomass and lipid content under defined conditions compared to the procured strains.

Table 2.1. Biomass, lipid content, and productivity of microalgal strains grown in BG-11 medium. Data represented as Mean ± SD; error bars represent the standard deviation of triplicate experiments.

Microalgal strain	**Biomass**		**Lipid**	
	Content (g/L)	Productivity (mg/L/ D)	Content (%)	Productivity (mg/L/D)
Isolates				
JS01	2.11±0.05	105.50±1.49	17.57±1.78	18.53±1.23
JS02	2.29±0.07	114.50±1.46	13.09±2.63	14.98±1.01
JS03	1.50±0.06	78.25±0.97	23.91±1.32	18.71±0.97
JS04	1.72±0.06	86.05±1.93	24.11±2.49	20.74±0.87
JS05	1.33±0.04	66.55±1.06	23.39±2.59	15.57±1.13
JS06	1.40±0.03	70.20±1.88	18.47±0.13	12.97±1.03
JS07	1.67±0.08	84.95±2.69	27.55±1.42	23.40±1.88
Procured				
Chlorella sp.1	1.180±0.02	59.00±1.21	14.83±2.54	8.75±0.08
Chlorella sp.2	1.390±0.06	69.50±1.04	17.30±1.76	12.02±0.04
Chlorella sp.3	1.590±0.03	79.55±0.78	24.98±4.42	19.87±0.89
Chlorella sp.4	1.812±0.08	90.60±2.07	21.30±5.32	19.03±1.02
Chlamydomonas sp.	2.01±0.07	100.50±1.76	20.01±1.86	10.50±0.88

Chlorococcum sp.	1.48±0.06	74.15±1.00	19.63±1.82	14.56±0.76
Chlorococcum infusionum	1.62±0.03	81.10±0.92	12.12±2.35	9.82±0.99
Neochloris sp.	0.901±0.01	45.05±0.98	10.45±2.77	9.01±0.76
Pediastrum sp.	0.66±0.01	32.95±0.43	11.11±3.83	3.66±0.05
Scenedesmus abundans	1.68±0.04	84.35±2.88	20.32±3.14	17.14±1.87
Scenedesmus opoliensis	1.11±0.05	55.60±1.03	14.26±1.24	7.9±0.04
Senedesmus sp.	1.54±0.02	77.15±1.44	25.98±2.88	20.04±1.22

2.3.1.3 Confocal microscopy to visualize lipid bodies in microalgal strains

Lipophilic fluorescent dye Nile red that is commonly used as a vital stain for lipid bodies was used to ascertain microalgae species with high lipid content (Storms et al., 2014). The observations following staining are shown in Fig. 2.3, and 2.4. The accumulation of lipid bodies was examined under a fluorescent microscope, which showed the yellow fluorescence in microalgal cells, while the red emission is due to characteristic autofluorescence peak of chlorophyll A. The maximum accumulation of lipid bodies was observed in isolate JS07 and JS04 followed by the Scenedesmus sp. whereas *Chlorella* sp. 3 and isolate JS03 had also shown a moderate extent of lipid bodies. These results are consistent with that of the lipid content of microalgal isolates, thus denoting isolate JS07, JS04, and JS03, the potential strains for lipid content.

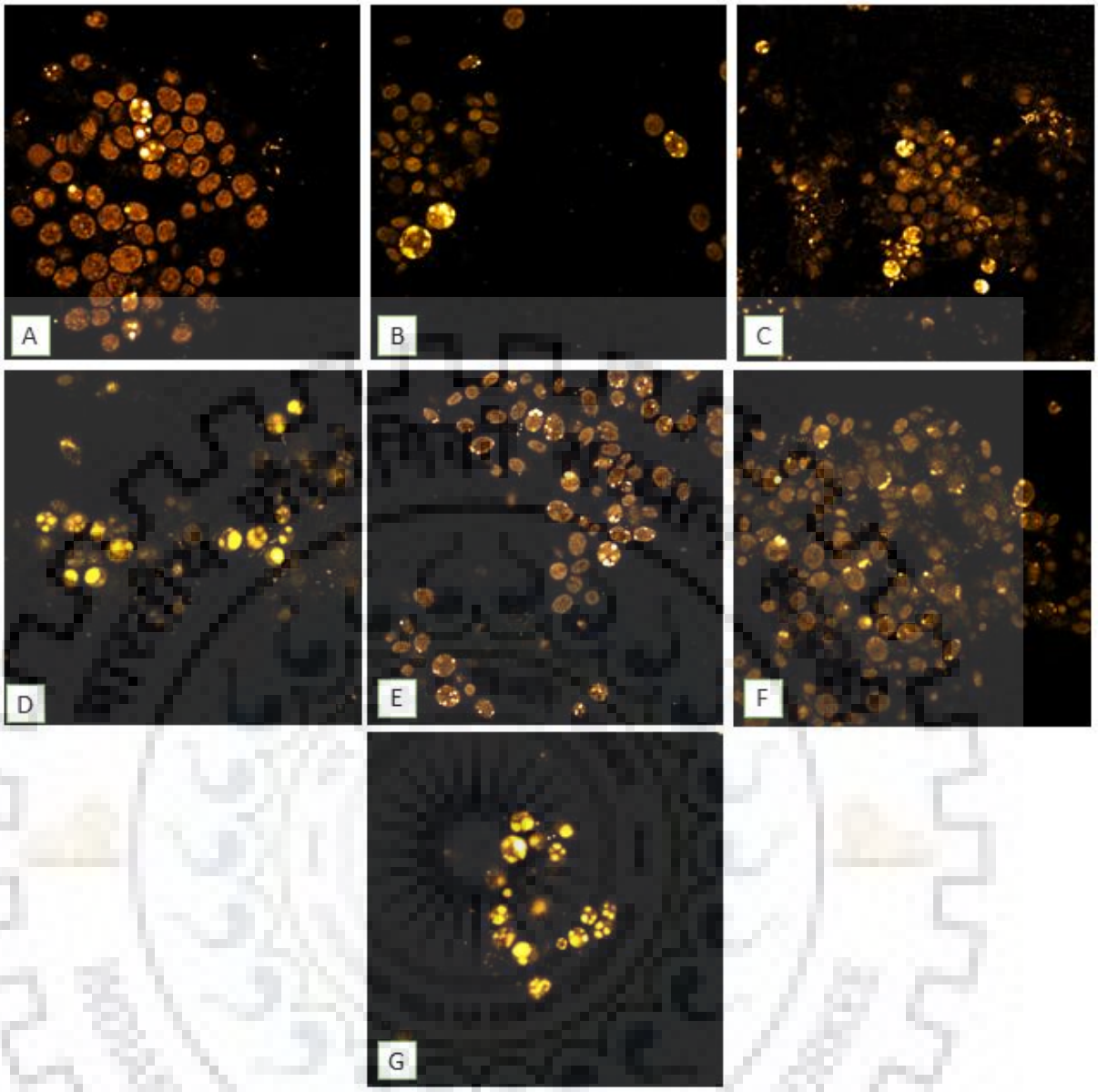

Fig. 2.3. Fluorescence images of microalgal isolates at 60X (A, JS01; B, JS02; C, JS03; D, JS04; E, JS05; F, JS06 and G, JS07) bright yellow spots represent lipid droplets.

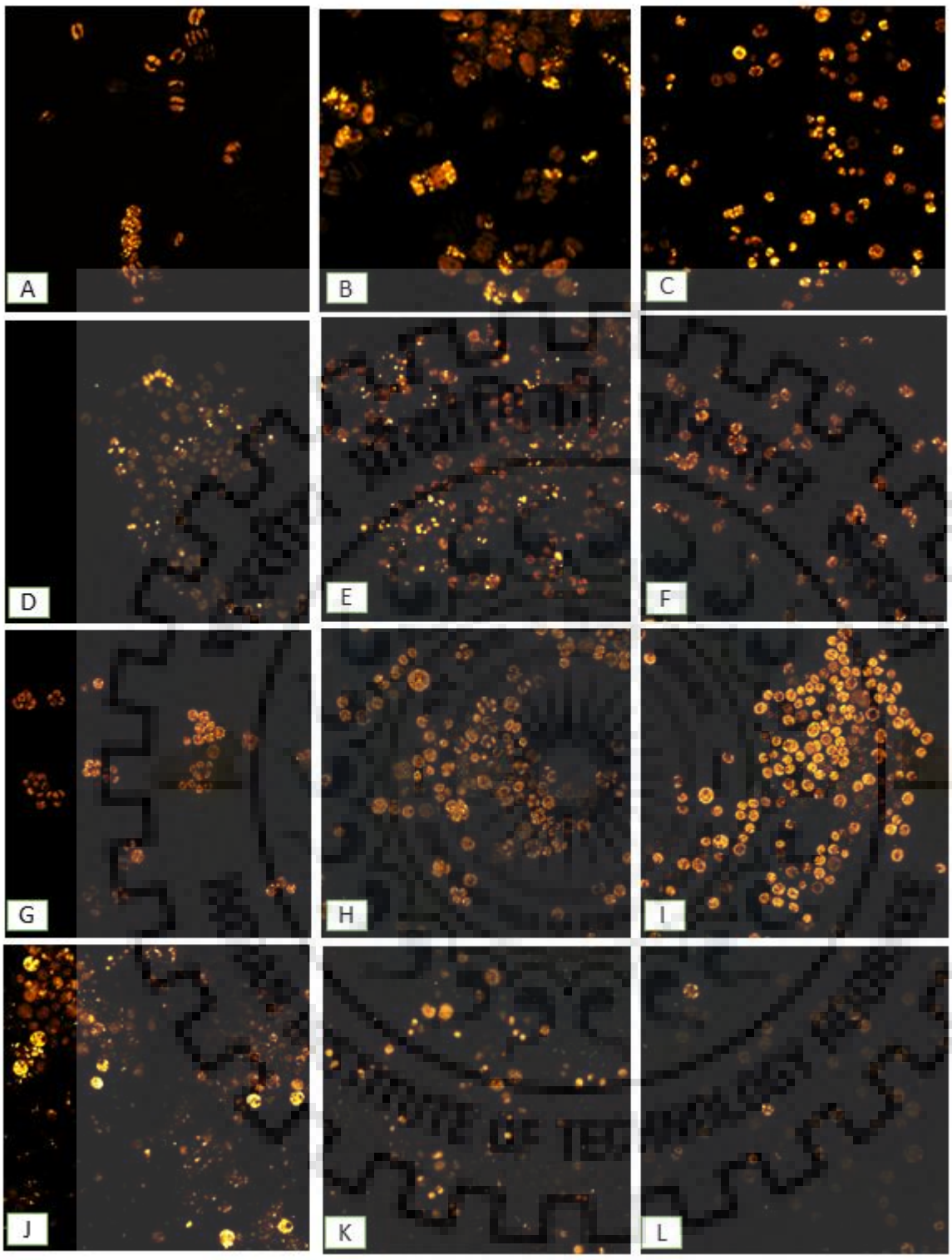

Fig. 2.4. Fluorescence images of the procured microalgal strains at 60X (A, *Scenedesmus opoliensis*; B, *Scenedesmus sp*.; C, *Scenedesmus abundans*; D, *Chlorococcum infusionum*; E, *Chlorococcum* sp.; F, *Pediastrum sp*; G, C*hlorella sp.* 1; H, *Chlorella sp*. 2; I, *Chlorella sp*. 3; J, *Chlorella sp.* 4; K, *Neochloris sp*.; L, *Chlamydomonas sp*.) bright yellow spots represent lipid droplets.

2.3.1.4 PCR amplification, sequencing of partial 18S gene and phylogenetic analysis

Based on the maximum lipid productivity among microalgal isolates, we selected three isolates (JS03, JS04, and JS07) for characterization. The phylogenetic relationships of these isolates were ascertained based on the 18S rRNA gene sequence using BLAST sequence similarity search. Partial 18S rRNA regions (700 bp) of these potential microalgal isolates were PCR amplified, sequenced and submitted in Gene bank under accession numbers of MK530223, MK530225, and MH128320 for strains JS03, JS04, and JS07 respectively. The 18S rRNA gene sequences of the isolates were subjected to BLASTN sequence similarity search to identify the nearest taxa. JS03 showed 92.6% sequence identity with *Desmodesmus opoliensis* while JS07 was 99.3% similar to *Desmodesmus* sp. F18, both belonging to the family of Scenedesmaceae. Isolate JS04 showed 99.54% sequence similarity with *Graesiella emersonii* (also known as *Chlorella emersonii*) isolate CCAP, which belongs to the Chlorellaceae family. The phylogenetic tree was constructed using the MEGA6 software (Fig. 2.5).

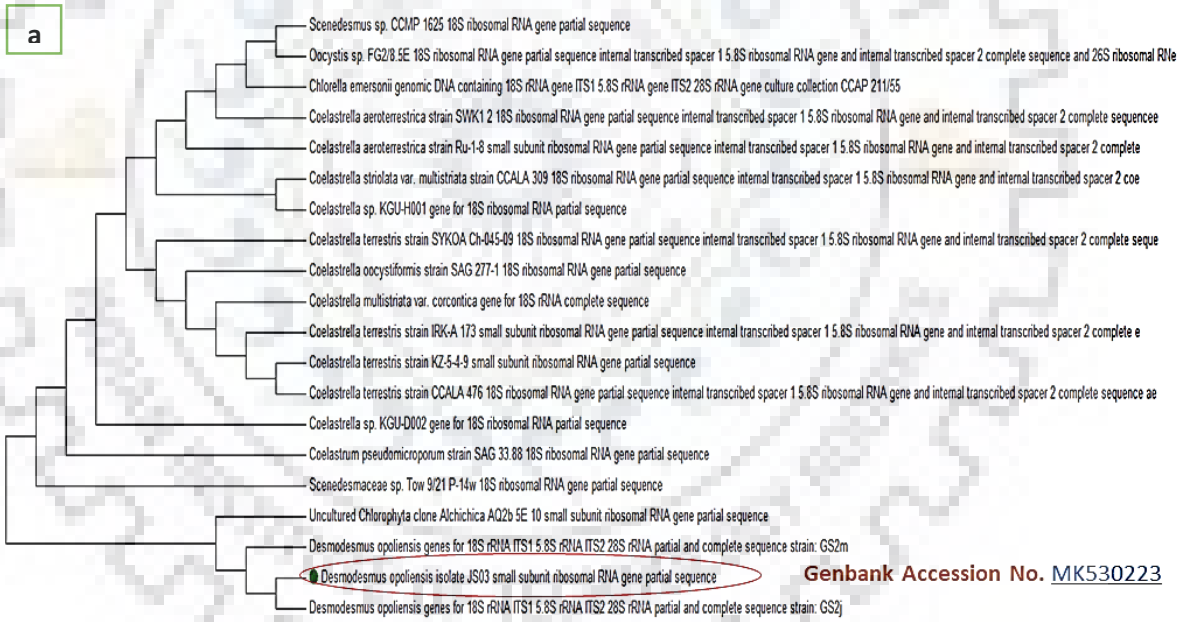

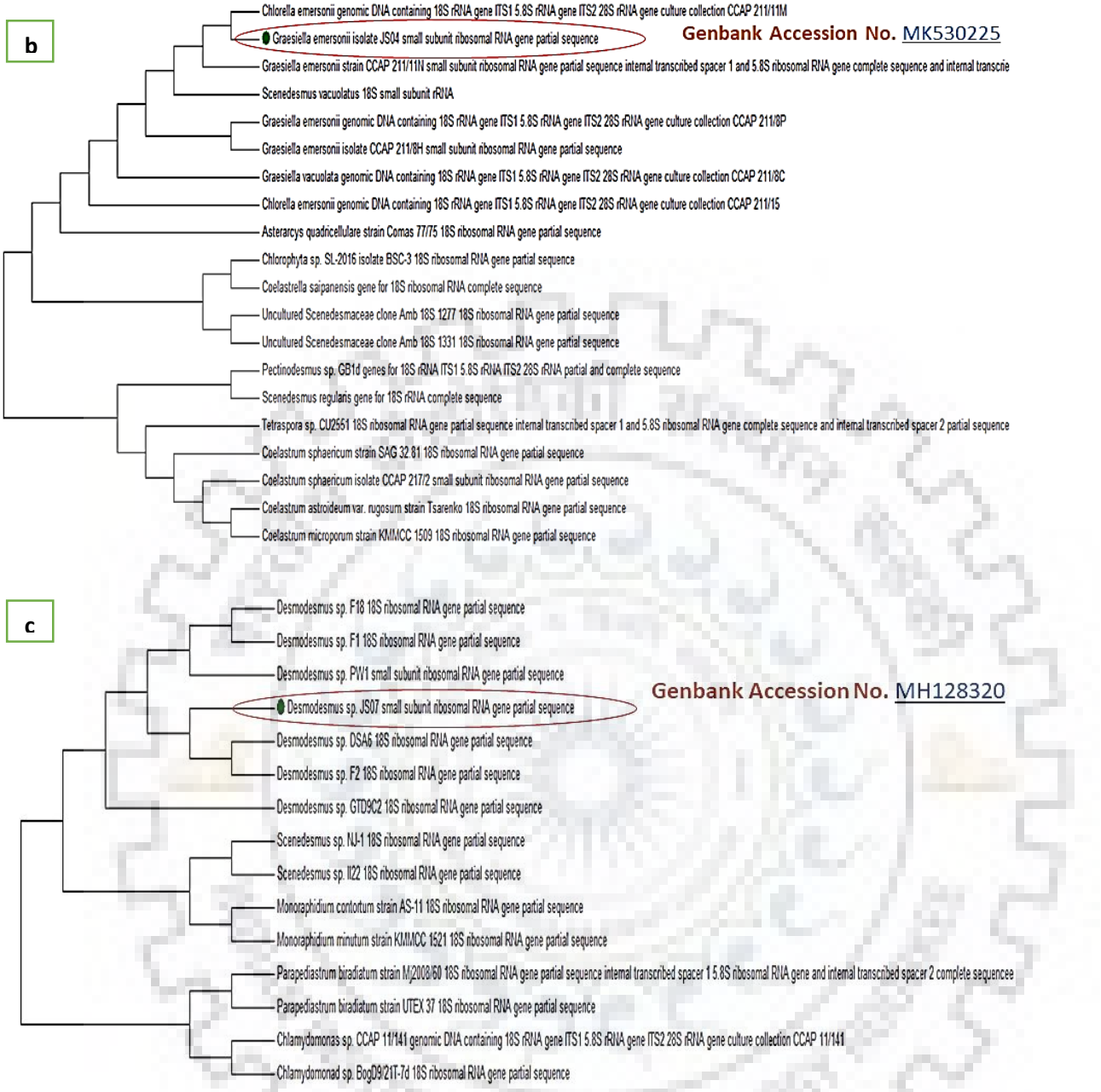

Fig. 2.5. Phylogenetic tree denoting the relationships among 18s rRNA sequences of isolates JS03 (a), JS04 (b) and JS07 (c) with the most similar sequences retrieved from the NCBI nucleotide database

2.3.1.5. Fatty acid profiling of microalgal strains

The fatty acid composition of lipids varied noticeably among microalgal strains and their cultivation conditions. Enumeration of the fatty acid profile of microalgal strains is pivotal for determining their suitability for biodiesel quality. The fatty acid composition of three potential microalgal isolates and twelve procured strains were analyzed and are detailed in Table 2. In the microalgal isolates, palmitic acid (C16:0), oleic acid (C18:1) and linoleic acid (C18:2) were

commonly dominant, which ranged from 20%-54%, 8%-43%, and 8%-20% respectively, whereas the palmitoleic acid (C16:1), stearic acid (C18:0) and linolenic acid (C18:3) existed as minor fatty acids. Monounsaturated fatty acid especially oleic acid (C18:1) that is considered as an ideal component of biodiesel accounted for 24.66%, 38.65%, and 34.89% of the total fatty acids for *Desmodesmus opoliensis* JS03, *Chlorella emesonii* JS04, and *Desmodesmus* sp. JS07 respectively. These proportions were comparable to the oleic acid content, as observed earlier by Zhang et al., 2014.

Further, among the procured microalgal strains, palmitic acid (C16:0) was the predominant fatty acid in most of the microalgal lipid extracts. The maximum content was obtained with *Chlorella* species and *Scenedesmus* species. Nonetheless, the highest amount of C18:1 was detected in *Chlorella* sp. 3 (42.48%) and *Scenedesmus* sp. (27.1 %). Microalgae oils rich in MUFAs (C18:1) and SFAs (C16:0) have been reported to have a reasonable balance of biofuel properties comprising oxidative stability, combustion heat, viscosity, lubricity and cold filter plugging point (CFPP) which are determined by the structure of its component fatty acid methyl esters (Knothe, 2012). Therefore, between the analyzed microalgal strains *Chlorella emesonii* JS04 and *Desmodesmus* sp. JS07, *Chlorella* sp. 3 and *Scenedesmus sp.* had denoted the maximum content for SFA and MUFA, enumerating it pertinent for obtaining the high-quality biodiesel.

Table 2.2 Fatty acid profile of microalgal strains grown in BG-11 media.

Microalgal strain	Fatty acids composition (%)										
	Palmitic acid (C16:0)	**Palmitoleic acid (C16:1)**	**Hexadecadienoic acid (C16:2)**	**Hexadecatrienoic acid (C16:3)**	**Stearic acid (C18:0)**	**Oleic acid (C18:1)**	**Linoleic acid (C18:2)**	**Linolenic acid (C18:3)**	**SFAs**	**MUFAs**	**PUFAs**
Isolates											
Chlorella emersonii JS04	28.08	9.76	-	4.27	1.11	38.65	5.03	-	29.19	48.41	9.3
Desmodesmus opoliensis JS03	19.37	2.08	-	-	4.48	24.66	20.05	6.06	23.85	26.74	27.91
Desmodesmus sp. JS07	34.98	3.78	2.1	7.3	1.57	34.89	8.03	-	36.55	38.67	8.03
Procured Strains											
Chlorella sp.1	53.9	3	-	-	1.01	15	3.91	9	54.91	18	12.91
Chlorella sp.2	27.85	7.29	-	-	2.89	16.13	8.35	7.28	30.74	23.42	15.63
Chlorella sp.3	38.98	7.48	2.94	-	2.94	42.48	1.89	4.18	41.92	49.96	6.07
Chlorella sp.4	39.33	2	-	-	5	26.5	3.88	3.2	44.33	28.5	8.58
Chlamydomonas sp.	30.89	3.11	-	2.74	18.45	8.32	20.09	-	49.34	11.43	22.82
Chlorococcum sp.	38.4	-	7.2	4.2	9	27.78	5.1	-	47.4	27.78	16.5

Chlorococcum infusionum	41.37	-	5.95	3.45	8.87	8.79	15.65	14.95	50.24	8.79	36.55
Neochloris sp.	26.05	1.11	-	11.04	1.81	17	12.49	-	27.86	18.11	23.53
Pediastrum sp.	39.48	2.56	2.65	-	10.56	19.08	12.4	7.2	50.04	21.64	22.25
Scenedesmus abundans	20.19	10.53	-	-	3.21	20.65	14.87	3.91	23.4	31.18	23.99
Scenedesmus opoliensis	52.81	-	1.04	14.98	-	22.68	3.8	-	52.81	22.68	19.82
Senedesmus sp.	35.56	9.66	-	-	7.84	27.1	14.84	-	43.4	36.76	14.84

2.3.2 Nutrient limited cultivation of selected microalgal strains (phase II)

2.3.2.1 Variations in biomass content of the microalgal strains

The growth was determined as biomass concentration and was observed to be notably affected in all four microalgal cultures by limiting the nitrogen concentration in the media (Fig 2.6). In N-deprived microalgal cultures, growth was restricted after the 5th day, whereas cells grown under N-limited conditions (70, 50, and 25%N) had displayed decreased growth during the cultivation of the strains. The biomass content decreased noticeably up to 1.38 fold and 1.5 fold in *Desmodesmus* sp. JS07 and *Chlorella sp.* 3 respectively with 25%N in the media on the 15th day. These findings corroborate the earlier observations of Cobos et al., 2017 who have revealed that the nitrate concentration in the medium affect the growth rate, as it is a vital nutrient for protein and nucleic acids *de novo* biosynthesis. Thus, under nitrogen limited conditions, cessation of microalgae cell division occurred that instigated substantial reduction in the growth rate. Breuer et al. 2012 had also shown that the biomass content of the nine microalgal strains had decreased significantly during nitrogen starvation.

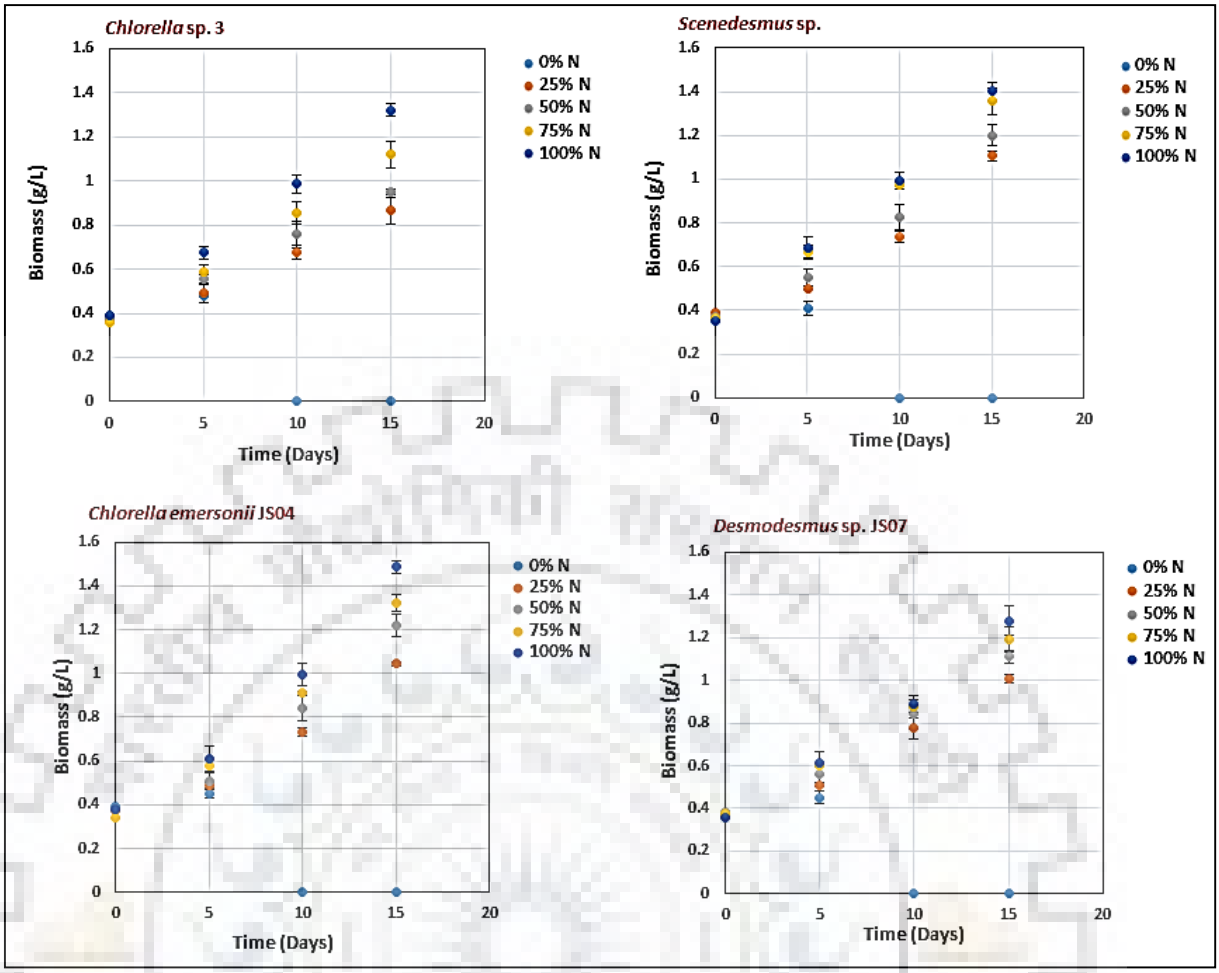

Fig. 2.6 Biomass content of microalgal strains under nitrogen limited conditions

Phosphorous limitation had also demonstrated a marked difference in the growth characteristics of the four-microalgal strains. Fig. 2.7 shows the growth profiles of microalgal strains under P-limited conditions. On the 10th day, the cultures in the flask with 0% P turned brown and settled at the bottom of the flask, and the treatments were then discontinued. The cultures cultivated in phosphate-deprived medium utilized their internally stored phosphate and able to grow up to five days as was observed with cultures growing with normal medium. In phosphorous-limited media, the biomass content had decreased significantly on the days 10th and 15th with 25 and 50% P levels compared to control. These results are consistent with the previous observations on *Microcystis aeruginosa*, and *Phaeodactylum tricornutum* that shown a decreased growth rate under phosphate-limited conditions (Yewalkar-Kulkarni et al., 2017). Thus, it was observed that 25% phosphorus concentration in the growth media led to 1.1-1.2 fold decrease in biomass content of the four-microalgal strains used throughout the cultivation period of 15 days.

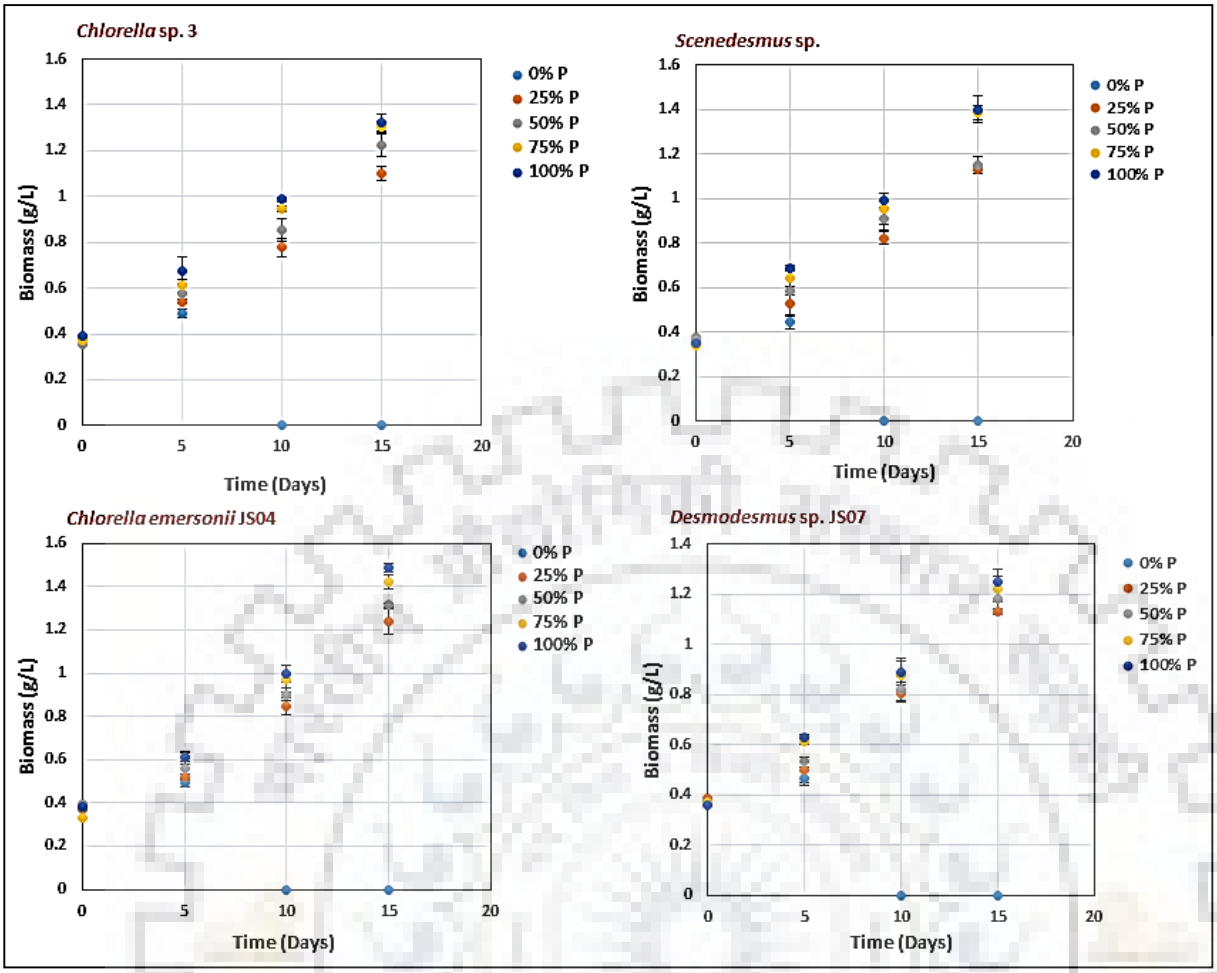

Fig. 2.7 Biomass content of microalgal strains under phosphorous limited conditions

2.3.2.2 Variations in lipid content and productivity of the microalgal strains

A considerable variation in lipid content was observed in the microalgal cultures with varying nutrient conditions. Limiting the nitrogen concentration from 100% to 25%, led to a 2.2-fold increase in lipid content of *Desmodesmus* sp. JS07 and 2-fold in *Scenedesmus* sp. (Fig. 2.8), These results are in agreement with the earlier observations where the lipid content of *Nannochloropsis sp*. grown under nitrogen-limited condition (0.9mM KNO_3) had enhanced by 2.2 fold. Similarly, Griffiths et al., 2012 had explored the impact of nitrogen limitation on lipid production in 11 microalgal strain. Apart from *Spirulina platensis*, the lipid content of the strains was enhanced to several levels. It was enunciated that under nitrogen-limited conditions, microalgal cells often accumulate the surplus of carbon metabolite as lipids (Ahlgren and Hyenstrand, 2003). Dayananda et al., 2005 had also stated that microalgae retort to nitrogen stress by accumulating carbon reserve compounds like lipids and degrading nitrogen-containing macromolecules.

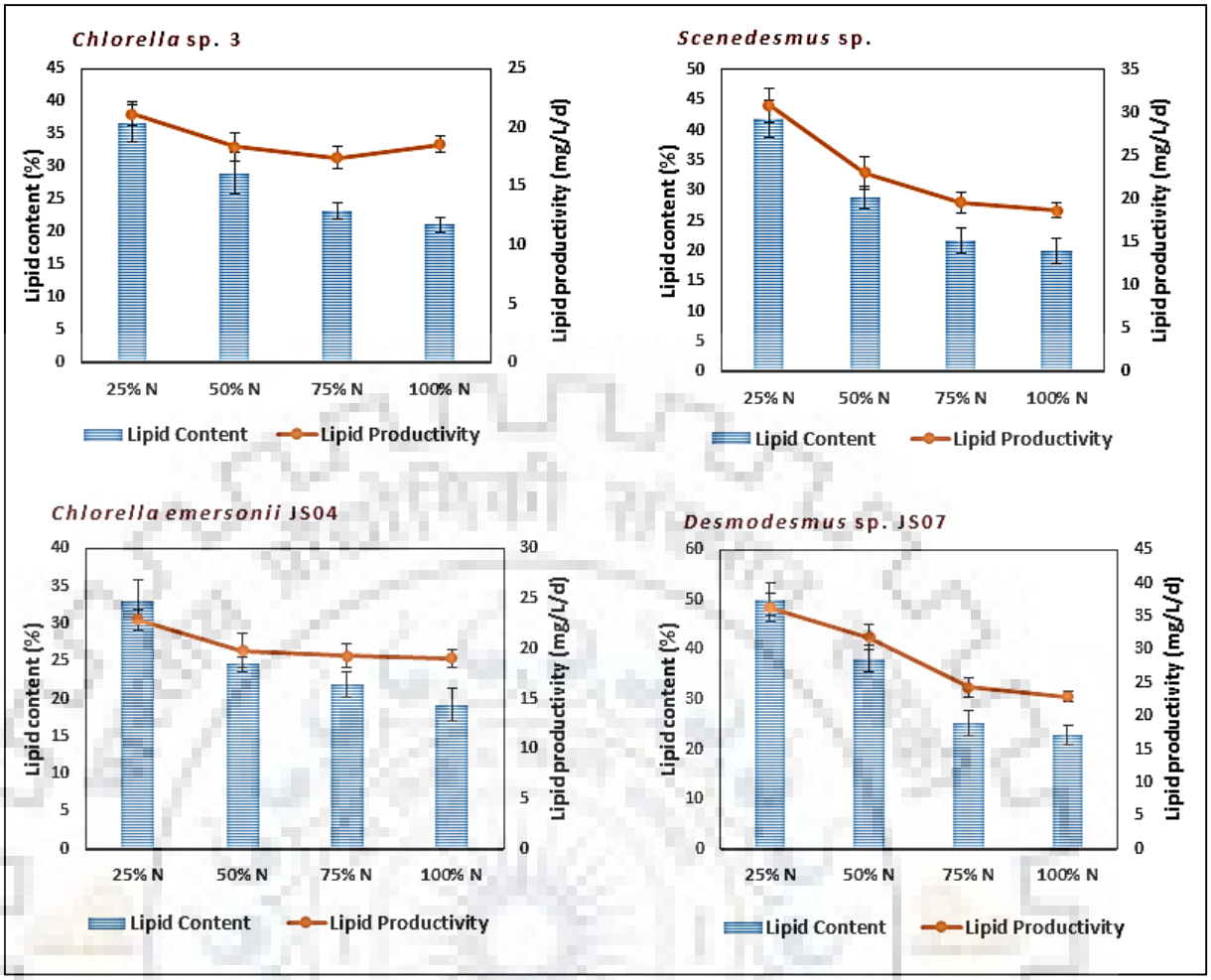

Fig. 2.8. Effect of nitrogen limitation on lipid content and lipid productivity of microalgal strains. Data are represented as Mean ± SD; error bars represent the standard deviation of triplicate experiments.

Similarly, the lipid content of all four microalgal strains had notably increased under phosphorus limitation (Fig 2.8). Maximum lipid content of 37.93 ± 2.11% for *Desmodesmus* sp. JS07 followed by *Scenedesmus* sp. (33.22±2.66 %) was obtained by cultivating with 25%P. Similar to our results, it had been shown that the phosphorous limitation triggers the lipid accumulation in *N. oleoabundans.*

Both lipid content and growth profiles enumerate lipid productivity. The lipid productivity had increased when microalgal strains were grown under nitrogen-limitations due to the notable increase in the lipid content. The highest lipid productivity on day 15th was observed for *Desmodesmus sp.* JS07 up to 36.3±2.06 mg/L/d whereas the lowest was found for *Chlorella* sp. up to 21.16±1.02 mg/L/d at 25% N. Lipid productivity, in contrast to biomass productivity, is normally higher when strains were cultivated under nitrogen limitation (Huerlimann et al., 2010). Nonetheless, Li et al., 2008 had observed maximal lipid productivity

in *Neochloris oleoabundans* at optimal nitrogen level, and concentrations below or above optimal value led into decreased lipid productivity.

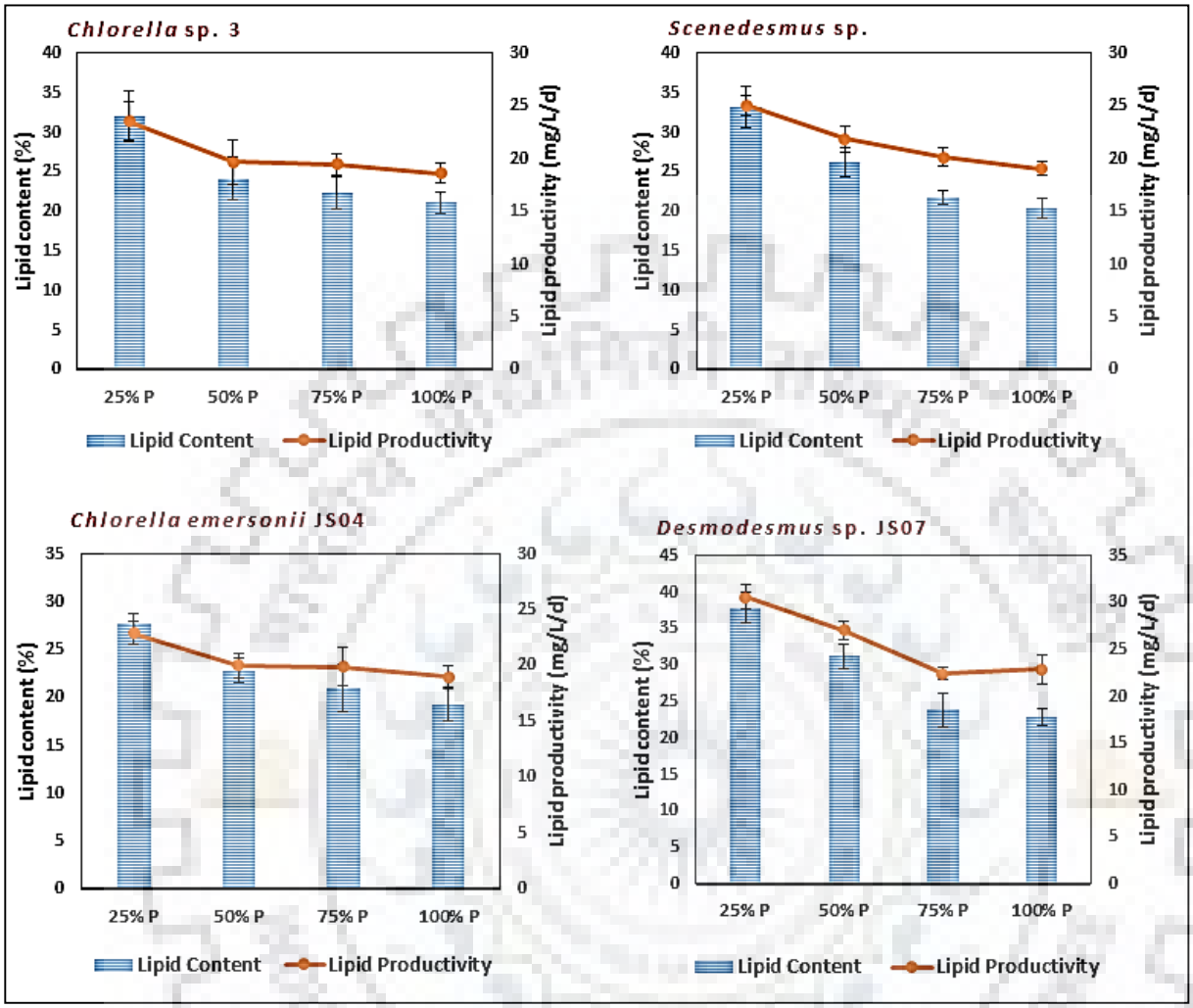

Fig. 2.9. Effect of phosphorous limitation on lipid content and lipid productivity of microalgal strains. Data are represented as Mean ± SD; error bars represent the standard deviation of triplicate experiments.

The limitation of phosphorus in the medium increases the lipid content of microalgal cells moderately with decreased biomass; therefore, the overall lipid productivity remains the same. Thus, no significant variations in the lipid productivity were observed due to phosphorous limitation for microalgal strains (Fig 2.9).

2.3.2.3 Analysis of fatty acid composition under nutrient-limited conditions

Fatty acid composition of the total lipids in all four strains was enumerated with nutrient limitation consisting of 25%N, 25%P and control (Fig. 2.10). In nitrogen-limited condition (25% N) *Desmodesmus* sp., JS07 had higher C18:1 than C16:0. In *Chlorella* sp., the major fatty acids

(FAs) of *Chlorella* sp. 3 and *Chlorella emersonii* were C18:1, specifically *Chlorella* sp. 3 produced more C18:1 whereas *Chlorella emersonii* produced both C16:0 and C18:1 with 25%N. In contrast, *Scenedesmus* sp. had produced increased levels of C16:1 under similar conditions. Lipid composition owing to nitrogen-limitation resulted in FAME profile with higher levels of SFA and MUFAs and lowered PUFA levels and similar findings were reported by Pasquet et al., 2014.

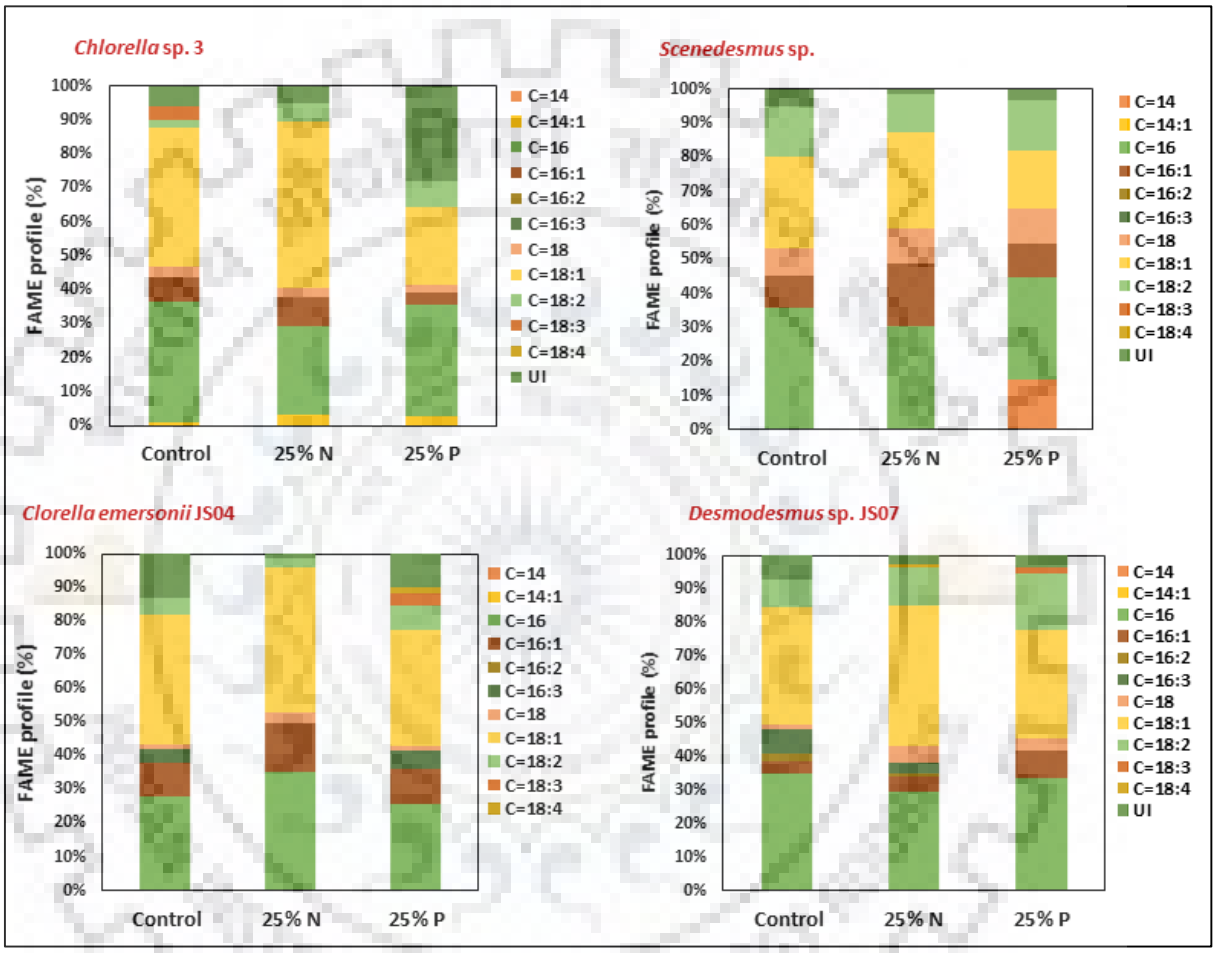

Fig. 2.10. Effect of nutrient limitation on FAME profile of microalgal strains.

Limitations with phosphorous had resulted in increased levels of C16:1 and C18:2 in *Desmodesmus* sp. JS07, while C18:1 decreased considerably. In the case of *Scenedesmus* sp. the saturated FAs, C16:0 and C18:0 and polyunsaturated FA C18:2 increased, while the unsaturated FAs, C18:1 had decreased. *Chlorella* sp. had also shown the increased levels C18:2 fatty acids with 25%P. Therefore, it is evident that there was an increase in the polyunsaturated fatty acids in all microalgal strains with phosphorous limited conditions (25% P) (Fig. 2.11).

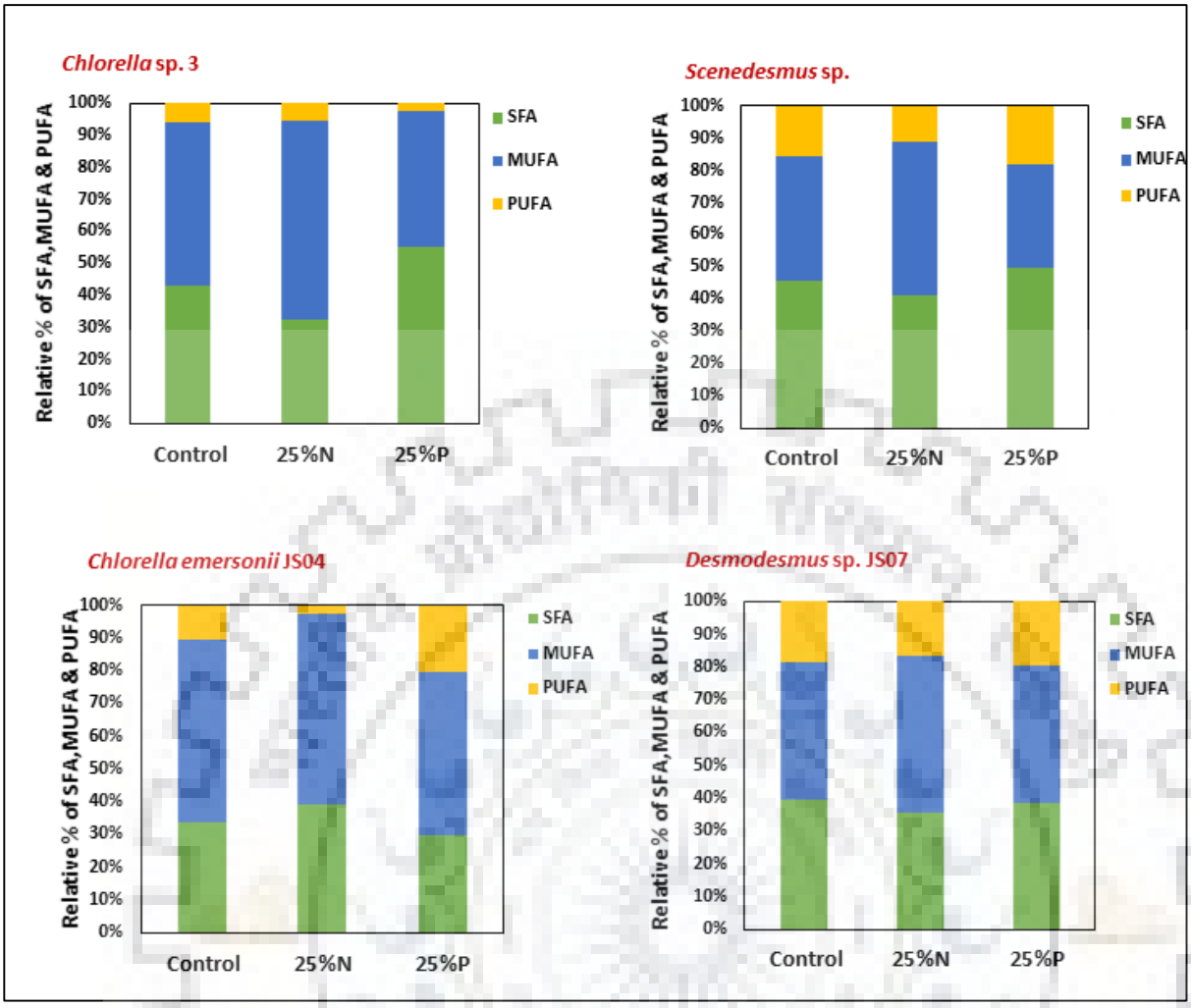

Fig. 2.11. Effect of nutrient limitation on SFA, MUFA, and PUFA content of microalgal strains.

2.4. Conclusion

Increasing global demands for renewable liquid fuels necessitate the need for exploring the alternative resources for fuel. Comparative evaluation of oil from algae and crop-based biomass denote former to be advantageous. Thus, it would be desirable to explore the strains with convincingly higher lipid content and can be accounted for as a benchmark for designing a viable technology for biofuel production. Exploring microalgal strains shows that biomass and lipid content displays notable variations. Among the seven microalgal isolates *Desmodesmus sp*. JS07 and *Chlorella emersonii* JS04 were selected owing to their high lipid content and productivity. Further, among the procured strain, *Scenedesmus* sp. and *Chlorella* sp.3 exhibited notable levels of biomass and moderate lipid productivity. Enumeration of fatty acid in these strains had shown the presence of palmitic, oleic, stearic and palmitoleic acids as the major constituents and thus indicating these as the potential strains for biodiesel production. Besides, the impact of nutrient limitation, particularly nitrogen and phosphorous limitation on the biomass, lipid content, and

productivity of *Desmodesmus sp*. JS07, *Chlorella emersonuu* JS04, *Chlorella* sp.3, and *Scenedesmus* sp. were analyzed. Among the microalgal strains, *Desmodesmus* sp. JS07 appears to have maximum lipid accumulation and productivity in nitrogen-limited conditions. In addition, *Desmodesmus* sp. JS07 had shown improved levels of SFA and MUFA content under the nitrogen-limited condition that is desirable for achieving high-quality biodiesel. The present work, therefore, denotes *Desmodesmus* sp. JS07 as a potential strain for biofuel production and when cultivated under defined conditions could affect into an enhanced lipid content and productivity.

CHAPTER 3

Synergistic Influence of Auxins and Cytokinins: An Approach for Enhanced Biofuel Production

3.1. Introduction

The post-industrialization era has improved the quality of life, but on the other hand, with cascading consumerism, life has become dependent on the use of energy like never before. This has led to worldwide problems relating to exhaustion of non-renewable resources of energy, that form a major chunk of the current energy reserves and this ultimately also leading to global warming. Therefore, to tackle the energy crisis and environmental issues, microalgae could serve as a renewable, sustainable, and eco-friendly substitute to fossils. These appear to be a promising and viable energy source owing to their unique advantages such as non-arable cultivation, ability to withstand severe culture conditions, rapid growth, and with higher lipid production (Chisti, 2007; Yilancioglu et al., 2014). However, the existing approaches for the cultivation of microalgae and biodiesel production are expensive, that is one of the significant limitations for sustainable production of biofuels (Salama et al., 2014). Thus, challenges, mainly approach for large-scale cultivation of microalgae and enhancing the lipid productivity, need to be addressed before exploiting microalgae for commercial production of biofuels.

In the last decade, various groups were involved in finding out high yielding microalgal strains, cultivating microalgae with wastewater, enhancing microalgal growth and lipid productivity by modulating biochemical or environmental factors and developing a high yielding (Challagulla et al., 2015; Valdez-ojeda et al., 2015) approaches had resulted into moderately enhanced biomass and lipid content of microalgae. Nevertheless, there is still a need to look for alternative strategies for achieving a higher rate of biomass production for economic considerations. Hence, it is imperative to explore biochemical and molecular modulators for further attaining an improved rate biomass production of microalgae.

Phytohormones are chemical messengers which are involved in various physiological and biochemical processes mainly for growth and development of higher plants (Salama et al., 2017). Keeping in mind the evolutionary relationships between the plants and algae, studies have demonstrated that phytohormones exert stimulatory effects on biomass, carbohydrates, lipids and protein content in some microalgal species (Hunt et al., 2010; Lu and Xu, 2015) Nevertheless, their physiological role in these microorganisms has been barely quantified. Auxins, cytokinins,

abscisic acid, and gibberellins are the major classes of phytohormones, among these, auxins and cytokinins are the essential ones that regulate plant cell growth and division respectively (Bajguz and Piotrowska-Niczyporuk, 2013; Liu et al., 2016). Phytohormones mediated modulation could be recruited to devise rational approaches for enhanced microalgal biomass through regulated biochemical cascades. Auxins have been observed to stimulate cell division affecting into an increased number of daughter cells in *Chlorella pyrenoidosa* (Vance, 1987) and facilitate the cell enlargement in *Chlorella vulgaris* (Yin, 1937). Recently, it was found that auxin together with gibberellin is capable of stimulating the cell size as well as the number of daughter cells generated through successive cell divisions in *Chlamydomonas reinhardtii* (J. Park et al., 2013).

Auxins and cytokinins act as a stimulant when administered exogenously to microalgal cells by augmenting an increase in biomass and lipid contents (Yu et al., 2018). Park et al., 2013 had shown that *Chlamydomonas reinhardtii* growth had increased up to 54–69%, when cultured in a medium consisting of indole-3-acetic acid, abscisic acid, gibberellic acid, 1-triacontanol, and kinetin. Similar changes were observed with indole-3-butyric acid, indole-3-propionic, and naphthalene acetic acid, stimulating cell growth by 3-4 fold in *Scenedesmus quadricauda* and *Chlorella pyrenoidosa* (Liu et al., 2016). The exogenous supplementation of cytokinin, kinetin, and zeatin had been used to induce lipid accumulation and biomass in *Acutodesmus obliquus* (Renuka et al., 2017). Thus, auxins and cytokinins appear to be potential stimulators for growth and lipid production in microalgae. The work undertaken so far have focused on to the regulatory role of the individual phytohormones on biomass and lipid content of different microalgae; however, the cumulative impact of the phytohormones on biomass, lipid content and fatty acid profile has yet not been elucidated in detail.

Desmodesmus sp. JS07 has been isolated and analyzed that exhibited spectral advantages like rapid growth and notable levels of lipid content up to 26% of the dry biomass during normal growth conditions. To the best of our knowledge, the influence of phytohormones on the biomass and lipid content of this promising strain has not been studied so far. Thus, the prime objective of the present study has been elucidating insights leading to enhanced biomass and lipid content in microalgae *Desmodesmus* sp. JS07 following treatments with varying concentrations of auxins (IAA, IPA, and IBA) and cytokinins (BAP and TDZ). Further, the synergistic effect of phytohormones (IBA and BAP) on biomass and lipid content was also analyzed. Consequently, we had attempted to find out the optimal concentrations of IBA+BAP for achieving maximal biomass and lipid accumulation. Besides, their impact on cell morphology mainly elucidating the lipid bodies and fatty acid profiles was also analyzed. The results obtained may be promising for

achieving enhanced lipid yields along with higher biomass for realizing large-scale biofuel production.

3.2. Materials and methods

3.2.1. Chemicals

Molecular grade phytohormones Indole-3-acetic acid, Indole-3-butyric acid, Indole -3-propionic acid, Benzyl amino purine, and Thidiazuron (purity,>99.0%) were purchased from Himedia. HPLC grade methanol and hexane were procured from Merck. Nile red dye and FAME Mix (C8:0–C24:0) were purchased from Sigma-Aldrich. BG-11 media and other chemicals used in this study, e.g., acetone, ethanol, glutaraldehyde, methanol, and sulphuric acid were purchased from Himedia and were of analytical grade.

3.2.2. Microalgae strain and culture conditions

The microalgae *Desmodesmus* sp. JS07 was used in this study. The strain was maintained in BG11 media at 25 ± 2^0C under continuous illumination from white fluorescent lamps at 200 μEm^{-2} s^{-1} at 150 rpm. 10% (v/v) of fresh microalgal cells (OD~0.6 at 750 nm) was used as an inoculum.

3.2.3. Experimental design

Impact of phytohormones on the biomass and lipid content of microalgae strains *Desmodesmus* sp. JS07 were analyzed by applying auxins and cytokinins exogenously. Auxins *viz.* IAA, IPA and IBA and Cytokinin *viz.* BAP and TDZ were employed at a dosage of 5, 10, 15, and 20 mg/L into BG-11 medium following inoculation with cultures. The microalgal cells cultured in BG-11 (without phytohormones) were used as a control group. The cultivation was performed at 27 °C under constant illumination from white fluorescent lamps at 200 μEm^{-2} s^{-1} for 25 days.

Further, individual treatment and observations, the cumulative effects of auxin, IBA and cytokinin, BAP on the biomass and lipid content of *Desmodesmus* sp. JS07 were evaluated. For optimization studies, central composite design (CCD) was used considering BAP (X_1) and IBA (X_2) as independent variables to study effects on responses, i.e., biomass (g/L) and lipid content (%). The concentration of both variables was varied from 0 to 7.5 mg/L. Full-face CCD design (three level-two factors) consisting of 13 experimental runs at three coded levels (-1, 0, +1) corresponding to BAP and IBA 0, 3.75 and 7.5 mg/L was followed. Experimental runs were designed as four factorials, four axials, and five center points, which were carried out in

triplicates. Trial version 11 of Design-Expert software (Stat-Ease, USA) was used to perform optimization and RSM regression analysis. Responses, i.e., biomass and lipid content, are represented as Y_1 and Y_2, respectively, whereas statistical analysis was performed by a second order polynomial equation given as follows:

$$Y = \beta_0 + \sum \beta_i X_i + \sum \beta_{ii} X_i^2 + \sum \beta_{ij} X_i X_j + \varepsilon$$

where Y - response, β_0 - intercept term, β_i - linear effect, β_{ii} -squared effect, and β_{ij} - interaction effect, X_i, X_j - independent variables and ε - error.

Table 3.1 Coded and real levels of input parameters

Factors	Name	Low level (-1)	Mid-level (0)	High level (+1)
X_1	BAP	0	3.75	7.5
X_2	IBA	0	3.75	7.5

The statistical testing of the model was performed through ANOVA analysis, where F-test was carried out to establish a mathematical correlation between input and responses. For this, experimental data were fitted into three different models such as linear, 2FI, and quadratic, while the goodness of fit of each model, and each term of the model was also predicted. The p-values should be less than 0.05 for each model as well as each term to be significant. The correlation coefficients such as R^2, adjusted R^2, predicted R^2, and lack of fit and adequate precision of models were also estimated to predict the well-fitted polynomial. To visualize the dependency of responses on variable parameters, the effect of individual parameters as well as interaction parameters on the responses were also studied.

3.2.4. Analytical methods

3.2.4.1. Measurement of growth

The growth of microalgae was analyzed spectrophotometrically at 750 nm. Biomass was estimated gravimetrically in terms of dry biomass (g/L, dry weight, DW) as described in section 2.2.3.1.

3.2.4.2. Field-emission scanning electron microscope (Fe-SEM) analysis

For Fe-SEM analysis, microalgae *Desmodesmus* sp. JS07 samples were harvested from the three-week-old culture in BG-11 medium (control) and with phytohormones supplemented BG-11 media. The cells were rinsed with deionized water followed by centrifugation at 6000 rpm, and

consequently, the pellet was carefully fixed using 2.5% glutaraldehyde in a BG-11 medium at 4^0C overnight. After fixation, the microalgal cells were dehydrated in gradually increasing ethanol concentrations (up to 100% ethanol), critical point dried, sputter coated with gold particles and analyzed under a field-emission scanning electron microscope (FE-SEM) (Carl Zeiss, Germany) (Patel et al., 2015).

3.2.4.3 Visualization of lipid globules using Nile Red fluorescence

The distribution of lipid globules in microalgal stained cells was studied by confocal microscopy as described in section 2.2.3.2.

3.2.4.4 Lipid extraction and quantification

The microalgal biomass was harvested after 15 days of cultivation (late log phase) by centrifugation and lyophilized using vacuum freeze-dryer. The extraction of lipids from the lyophilized biomass (100mg) was performed by using Bligh and Dyer's method, as described in section 2.2.3.3.

3.2.4.5 Fatty acid methyl esters (FAMEs) profiling

For fatty acid methyl esters (FAMEs) analysis, transesterification of the total lipids (~100mg) was performed using 1 mL of 2% (v/v) sulphuric acid in methanol. Afterwards, the samples were incubated at 60^{o}C for 3hr and FAMEs were extracted using hexane (1 mL) and then vortexing for 5 min. 1µL of this hexane containing FAMEs was then used for GC-MS analysis as described in section 2.2.3.5.

3.3. Results and discussion

3.3.1. Effect of phytohormones on biomass and lipid content of *Desmodesmus* sp. JS07

The cultivation of microalgae is considered as a critical step, as the cultivation conditions will not only decide in harvesting the maximum biomass levels but also ensure the quality and quantity of lipids. It has been well documented that phytohormones are potential 'cultivation additives' for stimulating microalgal growth and lipid content (Cho et al., 2015; Park et al., 2013). Therefore, the present study has endeavored to maximize the biomass and lipid content in *Desmodesmus* sp. JS07 by exogenous application of auxins (IAA, IPA, and IBA) and cytokinins (BAP and TDZ). For initial screening, four different concentrations: 5, 10, 15, and 20 mg/L were assessed for each phytohormone in *Desmodesmus* sp. JS07 for 25 days.

3.3.1.1 Effect of auxins on biomass and lipid content of Desmodesmus sp. JS07

The improved biomass content with exogenous application of auxins was evident in microalgae *Desmodesmus* sp. JS07 cultures, where the cells had exhibited a faster growth rate (Fig. 1). However, it was observed to be reliant on the concentrations and auxins employed. The results indicate that with IBA and IPA at 10 mg/L, microalgal cells had 1.62 and 1.6 fold increase in the biomass respectively, whereas, IAA supplemented medium showed 1.1 fold increase in biomass. The increased concentration of IBA and IPA beyond 10 mg/L led into declined growth was observed, similar to the observations of Bajguz and Piotrowska-Niczyporuk, 2013 where IAA and IBA had resulted into an increased number of cells by 52–83%. Similarly, IBA had notably maximized the biomass levels of *C. protothecoides* to 29.15 ± 2.02 g/m^2/day; however, higher concentrations appeared inhibitory (Parsaeimehr et al., 2017). Thus, auxins at a lower concentration appear promoting microalgal growth by regulating the cellular redox levels (Piotrowska-Niczyporuk and Bajguz, 2014) and stimulating the chlorophyll contents which led into the enhanced rate of photosynthesis (Dao et al., 2018), however higher concentrations denoted adverse impact that was similar to the higher plants.

In agreement with the previous studies (Cho et al., 2015; Lu and Xu, 2015), the supplementation of phytohormones, in addition to increasing the biomass levels, had also triggered lipid accumulation. This can be corroborated from our present study upon analyzing the lipid content; it was observed that IBA and IPA supplementation at 10mg/L had resulted in higher lipid yield up to 38.17±2.43 % and 37.81±1.87 %, respectively in *Desmodesmus* sp. JS07 at their stationary phase (20th day). After that, the lipid content remained unchanged or reduced after raising the IPA and IBA concentrations. However, no substantial increase in lipid content was observed at varying levels of IAA. Our results had also revealed that IBA, among auxins, was more effective in lipid accumulation, however as noted earlier in *Scenedesmus quadricauda* and *Chlorella pyrenoidosa* (Liu et al., 2016) IPA had led into comparatively higher growth and lipid productivity.

Although some of these auxins were earlier observed to augment the lipid accumulation in photosynthetic microorganisms, the effects auxins had so far not been analyzed in *Desmodesmus* sp. JS07. For example, ethanolamine (ETA) has been found to improve the lipid content by 22% in *Scenedesmus obliquus*; thereby acknowledged as 'potential modulator' for increasing lipid content in such photosynthetic microorganisms (Cheng et al., 2012). Likewise, earlier observation had also demonstrated that exogenous application of auxins had a stimulatory effect on cell division and lipids accumulation (Tarakhovskaya et al., 2007). The regulatory

mechanisms of auxins, i.e. IBA and IPA, have not been elaborated. However, IAA among auxins was observed to have a stimulatory impact on pentose phosphate pathway (PPP) by inhibiting Embden Meyerhof pathway (EMP), thus resulting into an increased flux of ATP for the fatty acid biosynthesis in *Schizochytrium* (Lian et al., 2010). Thus, our observation denotes that auxins function as the key regulator in modulating growth and lipid accumulation in microalgae. However, the regulatory role of auxins is dependent on the auxin type and the concentrations of these regulators used for the microalgae.

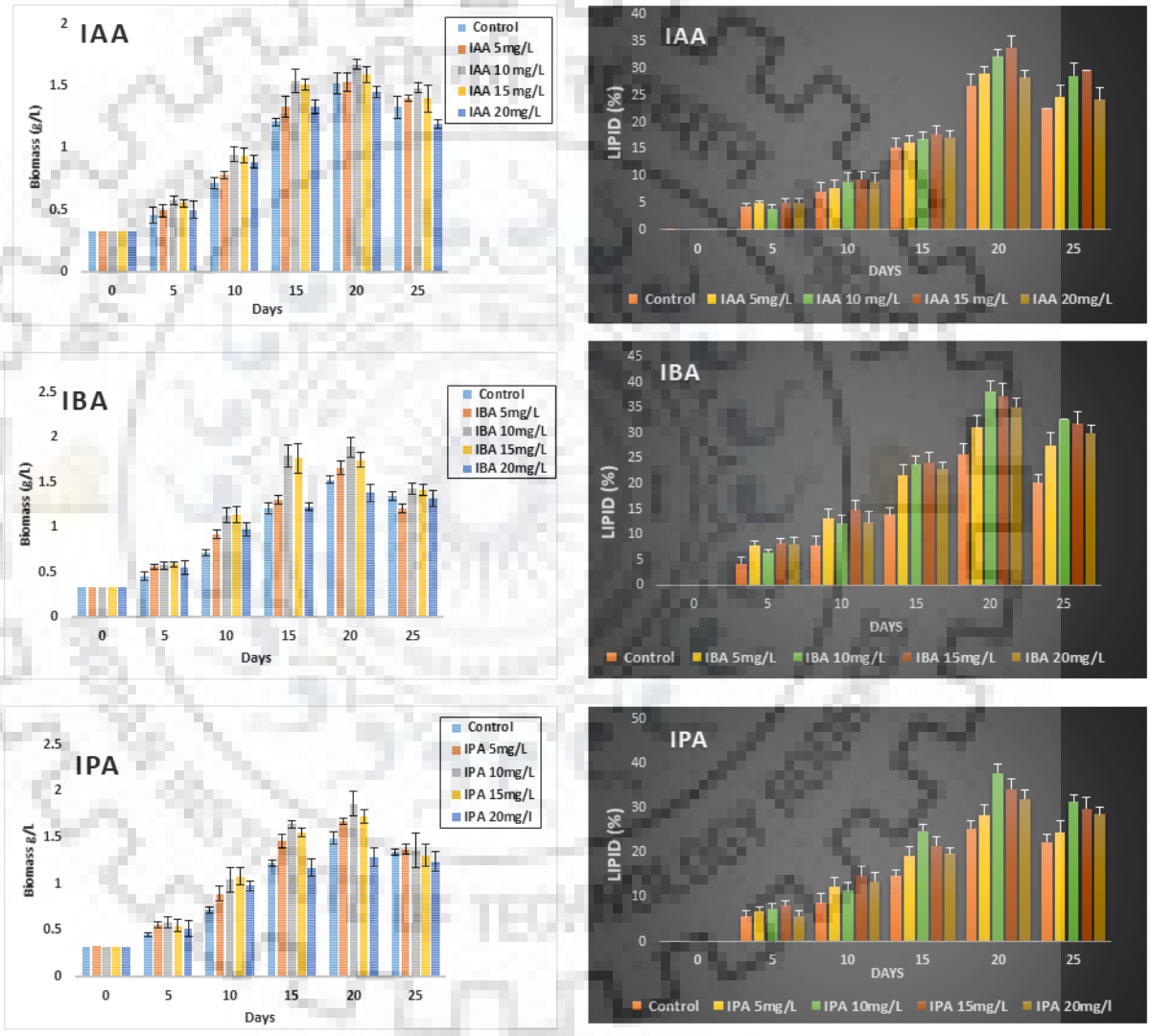

Fig. 3.1 Effect of phytohormones, IAA, IPA, and IBA, on biomass and lipid content of *Desmodesmus* sp. JS07. Error bars indicate standard deviations of the means (n = 3).

3.3.1.2 Effect of cytokinins on the biomass of Desmodesmus sp. JS07

The stimulatory effects of cytokinins *viz* BAP and TDZ on the biomass of *Desmodesmus* sp. JS07 are shown in Fig. 3.2. In the present study, both the Adenine-type (BAP) and Phenylurea-type

(TDZ) cytokinins were used, the former one is naturally occurring cytokinin and has been identified in microalgal extracts, whereas the phenylurea-type cytokinins are present at lower levels. Among cytokinins, a remarkable influence on microalgal biomass was detected with BAP while TDZ had a moderate impact. Increased biomass content (1.92g/L) was obtained with BAP supplementation (10mg/L) on the 20th day; however, higher concentrations were ineffective. Furthermore, increased lipid yields (1.5 fold) were observed with BAP supplementation (10mg/L). However, lipid yields had decreased with higher concentrations of BAP, whereas biomass continued to increase (Fig. 3.2). However, TDZ did not influence lipid content. Thus, BAP appears to have a regulatory role towards cellular processes leading into enhanced biomass production in microalgae. So far, there are only limited reports for the stimulatory role of cytokinins in microalgae, and these are mainly restricted to biomass content and microalgal morphology. Exogenous supplementation of cytokinins has been observed to regulate cell by augmenting the enzymes responsible for nitrogen assimilation (Tian et al., 2006). As nitrogen get assimilated via conversion to nitrite from nitrate and then into amino acids via ammonium, it has been interpreted that the internal pools of amino acids within microalgae may contribute to the majority of cell mass. Thus, our results further add to the stimulatory role of cytokinin BAP on microalgal growth.

Likewise, cytokinin application conceivably induces the lipid biosynthesis, which may eventually affect the permeability and fluidity of the cell membrane that facilitates enhanced absorption of phytohormones (Jusoh et al., 2015). This study substantiates BAP as a potential cytokinin in improving the biomass and lipid content of *Desmodesmus* sp. JS07, whereas earlier studies observed no significant difference in lipid content with BAP supplementation (Parsaeimehr et al., 2017; Piotrowska and Czerpak, 2009). Also, BAP supplementation above 10mg/L led into decreased lipid content of *Desmodesmus* sp. JS07. Exogenous supplementation of microalgal culture with cytokinins beyond the optimum levels may affect into an imbalanced ratio of intracellular and extracellular cytokinin homeostasis and therefore may affect into decreased lipid content.

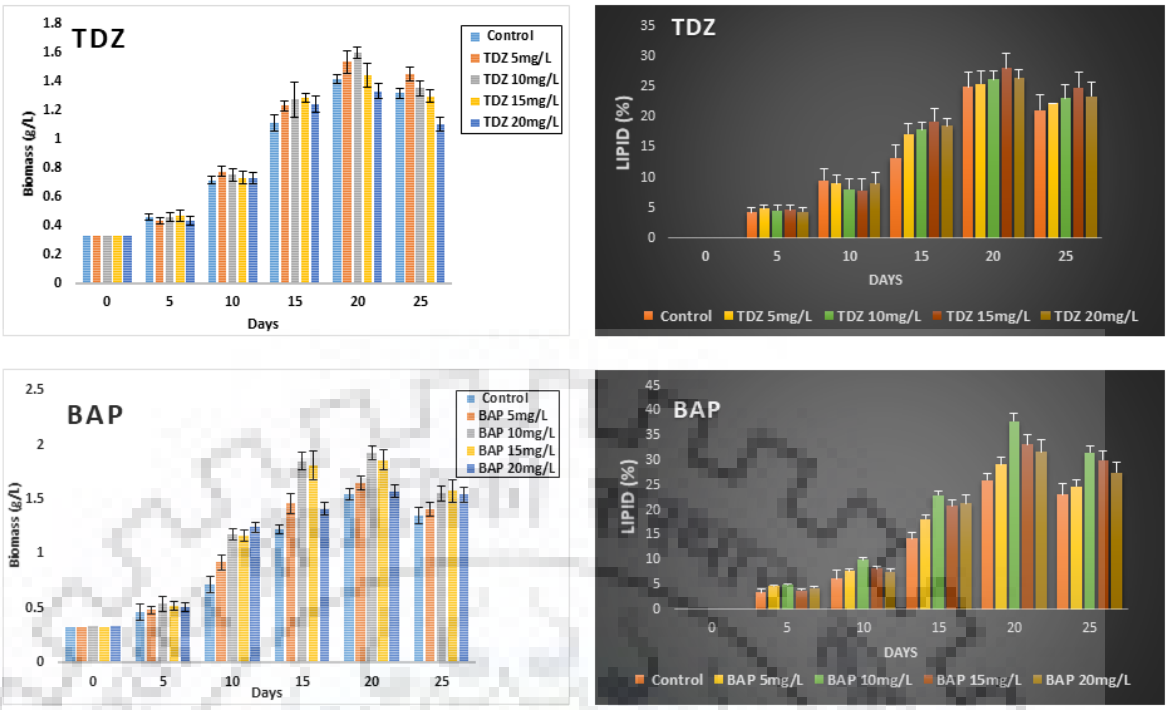

Fig. 3.2 Effect of phytohormones, TDZ, and BAP on biomass and lipid content of *Desmodesmus* sp. JS07. Error bars indicate standard deviations of the means (n = 3).

3.3.2 Cumulative effect of phytohormones on biomass and lipid production

As required, microalgae with high lipid content are desirable for biodiesel production, which in the present study, was attempted with exogenous supplementation of phytohormones. Based on the initial observations in *Desmodesmus* sp. JA07, among auxins and cytokinin, IBA and BAP respectively had resulted in a marked increase in the biomass and lipid contents (Fig. 3.1 and 3.2). Therefore, a combination consisting of IBA and BAP were further evaluated to achieve maximum biomass and lipid production in *Desmodesmus* sp. JS07. Bradley and Cheney (Bradley and Cheney, 1990) had also suggested that phenylacetic acid, zeatin, and naphthalene acetic could stimulate cell growth of seaweed cells alone as well as in combinations.

Table 3.2 Optimization of phytohormones concentration for biomass and lipid content through central composite design (CCD)

Run	Independent variable		Responses (Experimental)		Responses (Predicted)	
	IBA (mg/L): X_1	BAP (mg/L): X_2	Biomass (g/L): Y_1	Lipid content (%):Y_2	Biomass (g/L): Y_1	Lipid content (%):Y_2
1	7.5	3.75	1.783	38.44	1.887	39.47
2	7.5	7.5	2.412	42.1	2.274	41.25
3	3.75	3.75	1.501	36.54	1.54	34.87
4	3.75	7.5	1.653	35.02	1.756	37.29
5	0	0	1.136	21.33	1.149	20.58
6	3.75	0	1.378	28.98	1.325	29.91
7	0	3.75	1.235	24.01	1.193	26.18
8	3.75	3.75	1.501	35.01	1.54	34.87
9	3.75	3.75	1.52	35.54	1.54	34.87
10	3.75	3.75	1.541	35.24	1.54	34.87
11	3.75	3.75	1.501	35.22	1.54	34.87
12	7.5	0	1.56	35.34	1.5	35.16
13	0	7.5	1.302	30.67	1.237	29.25

The optimal concentrations of IBA and BAP were derived through CCD, and their impact biomass and lipid content were studied. As shown in Table 3.3 and 3.4, regression results indicated that 2FI model is best fitted for both responses in comparison to the other models, i.e., linear, quadratic and cubic as the goodness of fit (R^2) for 2FI model approach to unity. Considering the 2FI model, ANOVA analysis is carried out to establish the relative significance of the individual terms based on p-values < 0.0001. For biomass, X_1, X_2, and X_1X_2 were observed significant over X_1^2 and X_2^2 while X_1 and X_2 were found significant terms over X_1X_2 X_1^2 and X_2^2 for lipid content as given in Table 3.4.

The 2FI model also provided a correlation between variables (biomass and lipid content) and responses based on model fitting, given as Eqs. (i) And (ii). Hence, the highest values of biomass and lipid content can be assessed by altering the concentrations of the IBA (mg/L) and BAP (mg/L) in the Eqs. (i) and (ii) where a positive symbol signifies more interaction with the

response, however negative symbol denotes lesser interaction. Based on the 2FI model, predicted values of biomass and lipid content are shown in Table 3.2. The parity plots were also observed to compare experimental values with predicted values of biomass and lipid content that shows that values show no deviation; hence, model, as predicted, is acceptable.

Table 3.3 ANOVA results of biomass for the 2FI model

Source	Sum of Squares	df	Mean Square	F Value	p-value Prob > F
Model	1.118745	3	0.372915	57.9162146	3.30821E-06
X1-IBA	0.722454	1	0.722454	112.202029	2.21162E-06
X2-BAP	0.278642	1	0.278642	43.2749236	0.000101781
X1X2	0.117649	1	0.117649	18.2716914	0.002066472
Residual	0.05795	9	0.006439		
Lack of Fit	0.056685	5	0.011337	35.8538948	0.002038796
Pure Error	0.001265	4	0.000316		
Cor Total	1.176694	12			

Table 3.4 ANOVA results of lipid for the 2FI model

Source	Sum of Squares	df	Mean Square	F Value	p-value Prob > F
Model	373.34055	5	74.6681104	27.99521645	0.000172903
X1-IBA	264.93615	1	264.93615	99.33216234	2.18719E-05
X2-BAP	81.6966	1	81.6966	30.63039881	0.0008741
X1X2	1.6641	1	1.6641	0.623918825	0.455514411
X1^2	11.523104	1	11.52310419	4.320342301	0.076248947
X2^2	4.4377589	1	4.437758949	1.663843127	0.238061808
Residual	18.670217	7	2.667173892		
Lack of Fit	17.201417	3	5.733805747	15.6149394	0.011295589
Cor Total	392.01077	12			

$$Y_1 = 1.5 + 0.047 * X_1 + 0.011 * X_2 + 0.012 * X_1 X_2 \quad \text{(i)}$$

$$Y_2 = 20.57 + 3.033 * X_1 + 1.832 * X_2 - 0.045 * X_1 X_2 - 0.145 * X_1^2 - 0.090 * X_2^2 \quad \text{(ii)}$$

3.3.2.1 Effect of variables

To find out the individual and interactive effects of variables on the response, the perturbation plots and 3D surface plots are shown in Fig. 3.3, 3.4. Fig. 3.3(a) depicts that biomass content is increasing with increasing the concentrations of BAP and IBA up to 7.5 mg/L. Similarly, lipid content also increases with BAP and IBA, as shown in Fig. 3.4 (a). The effect on responses, i.e., biomass and lipid content due to the interaction of BAP and IBA can be studied using 3D surface plots as shown in figure 3.3 (b) and 3.4 (b), respectively. Interaction plots also support the trend being demonstrated by the individual effect of variables. It can be noticed that the interaction of both variables is leading to enhanced biomass and lipid contents.

Based on the optimization study, DOE predicted the optimal values of BAP and IBA as 7.5 mg/L each, that maximized the biomass and lipid content to 2.27 g/L and 41.25% respectively. However, it can be seen from Table 3.2 that experimental run-2 of CCD experiment yielded the highest biomass and lipid content to 2.41 g/L and 42.1% respectively, at BAP and IBA concentration of 7.5 mg/L each. Hence, the optimal values predicted through CCD are in good accordance with those of experimental data.

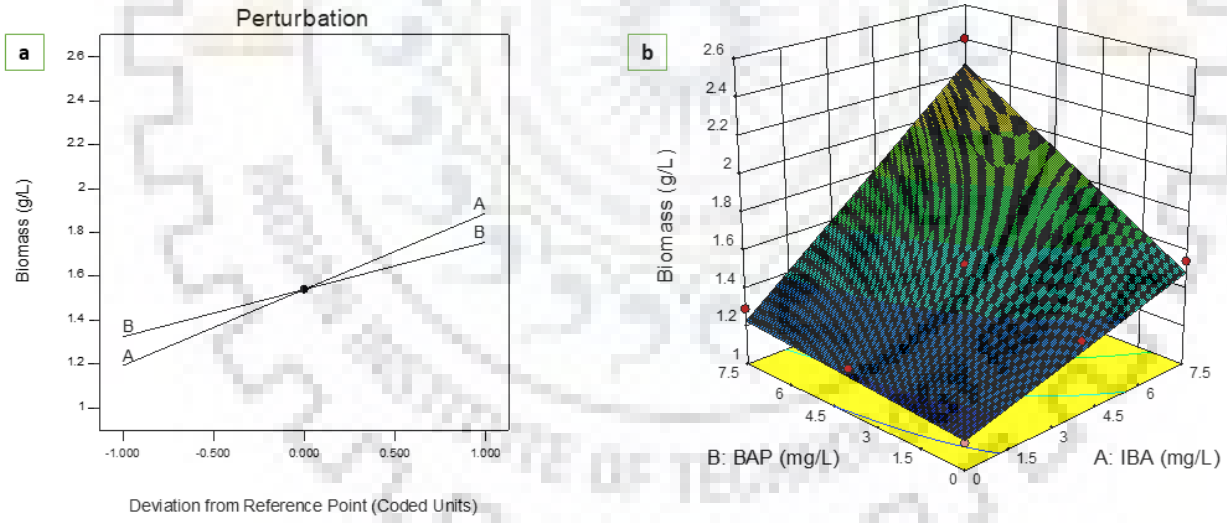

Fig. 3.3 Effect of variables on the Biomass (g/L)- (a) individual, (b) interaction.

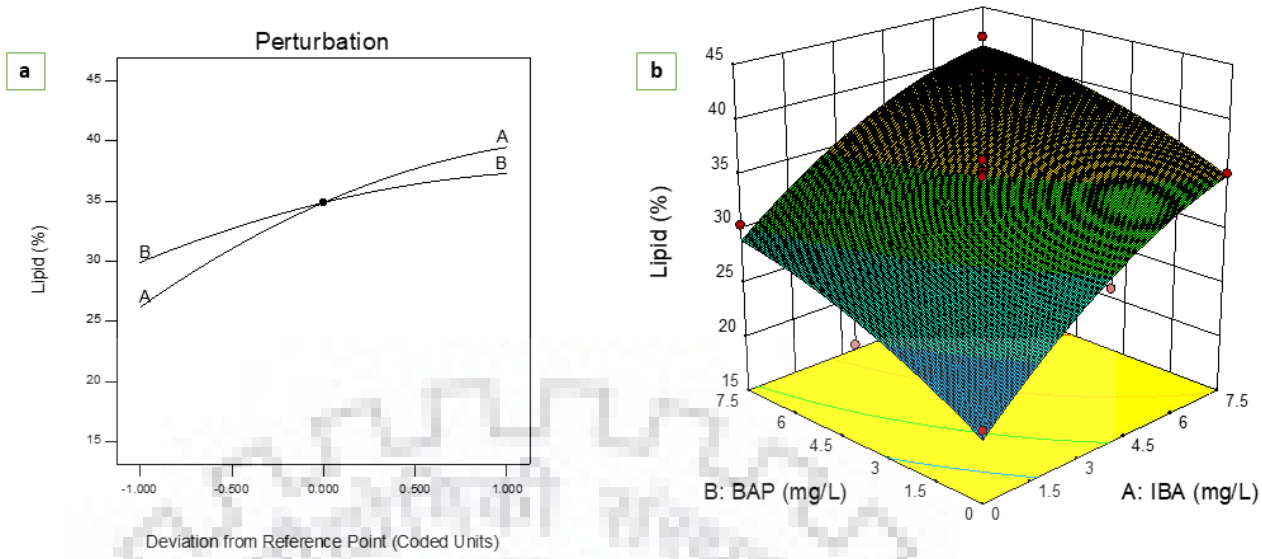

Fig.3.4 Effect of variables on the Lipid content (%)-(a) individual, (b) interaction

Thus, co-application treatments propose a novel relationship between auxins and cytokinin in microalgae. Besides, BAP and IBA in combination are found to be an effective biochemical modulator that can serve as an alternative to genetic modification strategy for improving microalgal biomass and lipid content in microalgae. Recently, the combined influence of biochemical stimulants ethanolamine (152.7 mg/L) and salicylic acid (1.0 mg/L) had increased the lipid levels by 22.4% as compared to salicylic acid, and ethanolamine added alone by 19.7% and 11.7% respectively in *Crypthecodinium cohnii* (Li et al., 2015). Likewise, Hunt et al. (Hunt et al., 2010) observed that treatment with a combination of zeatin (1 mg/L), gibberellic acid (310 mg/L) and naphthalene acetic acid (5 mg/L) improved the biomass productivity to 0.14 g/L/day in *Chlorella sorokiniana*. The present work is the first attempt to report the synergistic effect of IBA and BAP treatment on *Desmodesmus* sp. JS07. This co-application is synergistic as the outcome of two phytohormones applied concomitantly surpasses the sum of individual effect on microalgal biomass and lipid production.

3.3.3 Effect of phytohormones on cell morphology and lipid bodies

Phytohormones, such as auxins and cytokinins, have been observed to play significant roles in various metabolic pathways in microalgae. Auxins stimulate cell division, cell enlargement, bud formation, and root development (Park et al., 2013; Rubio et al., 2009), while cytokinins have profound effects on growth promotion and cell division in plants (Werner et al., 2001). To decipher the effect of phytohormones on growth promotion and lipid accumulation, the treated microalgal cells of *Desmodesmus* sp. JS07 were analyzed using Fe-SEM and confocal laser scanning microscopy (Fig. 3.5).

The observations revealed that phytohormones had a remarkable influence on microalgal growth. The microalgae under normal growth conditions showed a typical cell division where the average cell size was maintained, normally less than 10μm in diameter. However, the cells supplemented with auxins mainly IBA and IPA had resulted in a marked increase up to ~2μm in diameter on the 21st day. The treatment with phytohormones possibly alters the cellular metabolic pathways leading to elongation of microalgal cells, in agreement with the earlier finding of cell enlargement in *C. sorokiniana* SDEC-18 following treatment with phytohormones (Yu et al., 2017).

The enhanced accumulation of lipid bodies, as shown in Fig. 3.5 were also observed with IBA and IPA supplementation at 10 mg/L. Interestingly, BAP among cytokinins induced cell division having more number of dividing cells with moderate lipid accumulation; however, the cell size remained the same as that of untreated cells. Thus, the biological impact of phytohormones in microalgae appears equitable with that of higher plants. The co-treatment of IBA and BAP had shown a remarkable impact of microalgal cell enlargement and cell division. Thus, the synergistic action of auxin and cytokinins seems to be more productive compared to their unitary application for biomass and lipid accumulation.

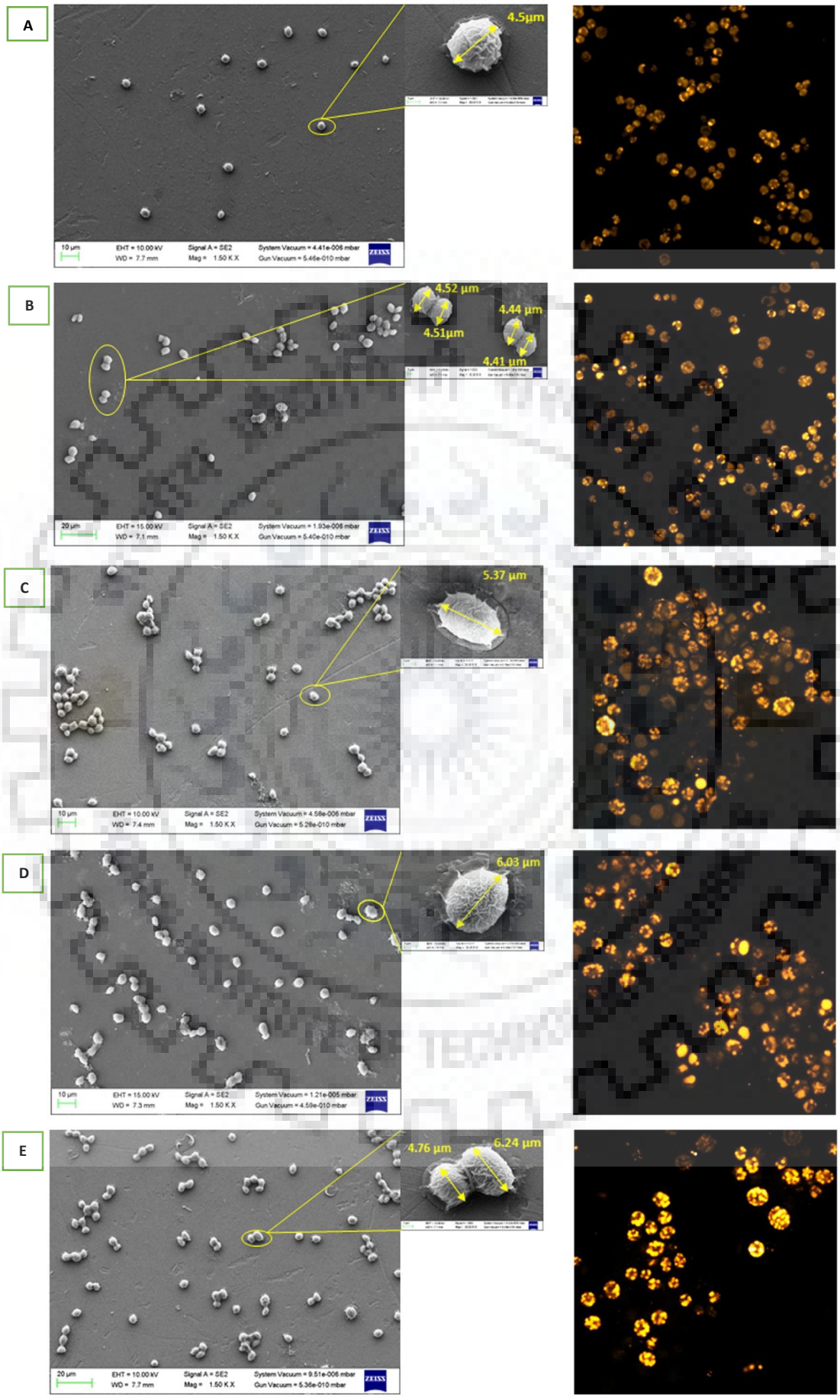
A
4.5µm
B
4.52 µm
4.44 µm
4.51µm
4.41 µm
C
5.37 µm
D
6.03 µm
E
4.76 µm
6.24 µm

Fig. 3.5 SEM and fluorescence microscopic images of Nile red-stained *Desmodesmus* sp. JS07 in BG11 media. A, control; B, BAP at 10mg/L; C, IPA at 10mg/L; D, IBA at 10mg/L and E, IBA at 7.5 mg/L and BAP at 7.5 mg/L.

3.3.4 Effect of phytohormones on fatty acid methyl esters profiling

Fatty acids are the pivotal component of microalgal lipids. The fatty acid profile of microalgal lipids are directly related to the properties of biofuels and have been taken into account for assessing the feasibility of using microalgae as a feedstock for biodiesel production. Fatty acid methyl esters (FAMEs) of microalgae under the influence of salinity (Salama et al., 2014), light intensity (Xu and Beardall, 1997), and nutrients (Ruangsomboon, 2015) have been earlier studied. However, the impacts of phytohormones on microalgal FAME profile have not been elaborated comprehensively. The enumeration of the fatty acid profile of *Desmodesmus* JS07 consisted of C14-C22 fatty acids; among these, C16-C18 (C16:0, C16:1, C16:2, C18:0, C18:1, C18:2 and C18:3) desirable for producing high-quality biodiesel accounted for more than 80% (Table 3.5). The treatment with increased concentrations of auxin up to 15 mg/L led to enhanced levels of C16:0 further higher concentration of auxins resulted into decreased levels of C16:0, in contrast, levels of C18:1 had increased with increasing concentration of auxins mainly with IBA and IPA, that is considered as a significant determinant of biodiesel quality (Table 3.5). Nevertheless, cytokinins had resulted in increased levels of C18:2 and C18:3 fatty acids. Furthermore, the synergistic effect of auxin and cytokinin, i.e., $IBA_{7.5mg/L}$+$BAP_{7.5mg/L}$ had led to increased levels of C16-C18 fatty acid profile.

GC-MS analysis had denoted Palmitic (C16:0) and stearic acid (C18:0) among SFA, palmitoleic (16:1) and oleic acids (18:1) as MUFAs and linoleic (18:2) and linolenic acids (18:3) among PUFAs as the major constituents of fatty acids profile of *Desmodesmus* sp. JS07. Among the auxins, mainly IBA and IPA (10 mg/L) induced the accumulation of SFA in *Desmodesmus* sp. JS07, IBA performed better than IPA, as shown in Table 3.5. The enhanced levels obtained may be due to the breakdown of monogalactosyldiacylglycerol (MGDG), a key intermediate for triacylglycerol (TAG) production to generate oleic acid possibly for building TAG (Lei et al., 2012). Nevertheless, irrespective of the auxins, PUFAs (mainly linolenic acid; C18:3) levels decreased following auxin treatments.

In contrast, cytokinins had significantly improved the production of PUFA in *Desmodesmus* sp. JS07; meanwhile, SFA levels had declined. BAP among cytokinin elevated MUFA content, whereas TDZ did not affect. The levels of PUFA (primarily linolenic acid; C18:3) were observed

elevated with increasing the concentrations of BAP and TDZ in the BG11 culture media. These results are in agreement with the earlier observations, where Kinetin had led into enhanced levels of a-linolenic acid in *Acutodesmus obliquus* (Renuka et al., 2017). Thus, possibly cytokinins at higher concentrations may impact into senescence of microalgal cells and consequently modulate the flux towards biosynthesis of PUFAs, along with linolenic acid, a precursor for jasmonic acid biosynthesis a crucial constituent for the generation of senescence response.

Table 3.5 Effect of phytohormones on fatty acid compositions of *Desmodesmus* sp. JS07.

Treatment (mg/L)	Fatty acids composition (%)										
	Palmitic acid (C16:0)	Palmitoleic acid (C16:1)	Hexadecadienoic acid (C16:2)	Hexadecatrienoic acid (C16:3)	Stearic acid (C18:0)	Oleic acid (C18:1)	Linoleic acid (C18:2)	Linolenic acid (C18:3)	SFAs	MUFAs	PUFAs
Control	34.98	3.78	2.1	7.3	1.57	34.89	8.03	-	36.55	38.67	17.43
IAA5	35.01	3.81	1.98	2.21	1.66	35.22	7.81	4.53	36.67	39.03	16.53
IAA10	35.82	5.22	2.16	-	1.97	36.74	6.3	6.12	37.79	41.96	14.58
IAA15	37.12	5.04	2.04	2.21	2.19	36.89	7.12	6.44	39.31	41.93	15.6
IAA20	32.1	4.48	2.43	3.45	2.34	37.02	6.54	6.07	34.44	41.5	18.49
IPA5	36.87	4.28	0.98	1.67	1.87	35.67	6.92	0.92	38.74	39.95	10.49
IPA10	42.01	5.93	1.36	0.72	2.82	40.01	5.16	-	44.83	45.94	7.24
IPA15	42.19	6.12	1.12	1.02	1.23	41.03	5.08	-	43.42	47.15	7.22
IPA20	37.21	7.02	1.03	1.88	2.35	41.76	5.11	0.54	39.56	48.78	8.56
IBA5	35.45	4.22	1.03	2.08	2.1	40.11	7.81	-	37.55	44.33	10.92
IBA10	36.32	7.4	-	-	3.67	42.18	8	-	39.99	49.58	8
IBA15	36.28	7.89	-	-	3.69	42.43	7.43	-	39.97	50.32	7.43
IBA20	35.81	5.23	0.92	1.43	3.92	43.79	6.22	-	39.73	49.02	8.57
BAP5	30.23	3.79	-	-	1.45	37.91	7.89	10.21	31.68	41.7	18.81
BAP10	25.12	4.02	-	-	1.58	41.12	12.02	13.01	26.7	45.14	25.03
BAP15	27.18	4.11	-	-	1.22	40.22	11.34	13.27	28.4	44.33	24.61

BAP20	25.22	3.54	-	-	0.98	38.17	12.78	13.58	26.2	41.71	26.36
TDZ5	29.54	3.67	--		1.65	34.82	10.21	9.87	31.19	38.49	20.08
TDZ10	29.12	3.33	-	-	1.82	35.22	14.56	11.34	30.94	38.55	25.9
TDZ15	29.16	3.21			1.88	35.01	15.21	12.76	31.04	38.22	27.97
TDZ20	30.21	3.19			1.91	34.98	16.34	12.78	32.12	38.17	29.12
IBA7.5+BAP7.5	30.87	10.11	-	-	4.54	42.19	9.37	2.5	35.41	52.3	11.87

Furthermore, the cumulative impact of auxin and cytokinin, mainly, $BAP_{7.5mg/L}$+$IBA_{7.5mg/L}$ had resulted in higher MUFA and moderate SFA levels while the PUFAs remained mostly unaffected. The abundance of MUFA (particularly C18:1) as compared to SFAs or PUFAs is essentially a desirable feature as these maintain a balance between ignition quality, oxidative stability and cold flow properties (Kwak et al., 2016) of the fuel. Overall, the observations demonstrate that auxins and cytokinin, particularly IBA and BAP, are the key modulators of the fatty acid accumulation in *Desmodesmus* sp. JS07. Particularly the cumulative impact of phytohormones on fatty acid composition and accumulation is relatively a promising and unexplored area and denote that *Desmodesmus* sp. JS07 could be a potential feedstock for biodiesel production. However, more efforts are needed to fully understand the orchestrated mechanisms and possibly a cross-talk involving auxins and cytokinin regulating biomass and lipid content in microalgae.

3.4. Conclusion

The work illustrates the impact of phytohormones *viz* auxins and cytokinins in stimulating the biomass and lipid content in the microalgae *Desmodesmus* sp. JS07. Exogenous application of phytohormones IBA and BAP exerted a stimulatory effect on biomass and lipid content in *Desmodesmus* sp. JS07. Further, the optimal levels of IBA and BAP were determined by the design of experiment (DOE) approach. The cumulative effect of IBA and BAP had resulted in a remarkable increase in the biomass and lipid contents. This is the first evidence demonstrating a synergistic relationship between auxins and cytokinin in enhancing microalgal growth and lipid content. Additionally, their cumulative exposure had modulated the fatty acid composition of *Desmodesmus* sp. JS07 specifically thereby increasing palmitic (C16:0) and oleic acids (C18:1) that are preferable constituents for achieving high-quality biofuel. The present work can significantly contribute to designing strategies utilizing phytohormones treated microalgal culture as a sustainable feedstock for the production of biofuel.

CHAPTER 4

Insights into lipidome profiling of Desmodesmus sp. JS07 under nitrogen-limited conditions

4.1. Introduction

The current global issues of climatic changes and rising prices of fossil fuels necessitate looking for alternative renewable sources for fuels. Microalgae would be a promising resource since they have been observed to accumulate higher levels of TAGs (key substrates for biodiesel production). Lipid accumulation can further be enhanced (Wijffels and Barbosa, 2010) due to abiotic stresses like temperature (Ördög et al., 2016), salinity (Lawton et al., 2015) and nutrient stress (nitrogen, iron, sulfur and phosphorous) (Fan et al., 2014; Lei et al., 2012). However, with conditions having limited nitrogen stress TAG along with biomass have been found to increase (Tevatia et al., 2014). Thus, it is of great relevance to gain a detailed insight into metabolic modulation, ultimately leading to TAG biosynthesis along with other value products.

Lipid metabolism in microalgae encompasses majorly *de novo* synthetic pathways in the chloroplast (prokaryotic) and endoplasmic reticulum (eukaryotic), lipid trafficking among sub-cellular compartments and recycling pathways (Joyard et al., 2010; Mühlroth et al., 2013). Such pathways must be in balanced co-ordination with each other to achieve productive lipid homeostasis and ensure that their composition is maintained or altered as required in each sub-cellular membrane during the various environmental conditions. Besides TAGs, microalgae produce a variety of other lipids including polar lipids (membrane) and neutral lipids (storage). The polar lipids in microalgae mainly include glycolipids such as monogalactosyldiacylglycerol (MGDG) and digalactosyldiacylglycerol (DGDG); phosphoglycerolipids such as phosphatidylglycerol (PG); phospholipids such as phosphatidylinositol (PI), phosphatidylethanolamine (PE), phosphatidylcholine (PC), and phosphatidylserine (PS) with diacylglycerol (DG) and monoacylglycerol (MG) as neutral lipids (Vítová et al., 2016). Polar lipids, apart from as the major constituent of membrane lipids, display essential roles in cell signaling (Guschina and Harwood, 2009). Hence, they are vitally important in regulating the metabolic network in microalgae. Thus, it would also be imminently significant to evaluate these lipid molecules in microalgae through lipidomics research. While plenty of information is available for mechanistic pathways regulating TAG accumulation in *Chlamydomonas reinhardtii*

(Work et al., 2010), not much has been deciphered for other algae, and there is successive development in this area over the years.

Currently, *Desmodesmus* sp. JS07 has been isolated and analyzed by our group that exhibited notable levels of lipids up to 50% of dry biomass in nitrogen-limited conditions. To depict the variations in *Desmodesmus* sp. JS07 under the nitrogen-limited condition, it is imperative to have precise information about lipid classes and its composition. The present work elucidates the variations in lipid and fatty acyl compositions across lipid classes in microalgae *Desmodesmus* sp. JS07 by lipidomics profiling through mass spectrometry under normal and nitrogen-limited conditions. To the best of our knowledge, it is the first study with *Desmodesmus* sp. JS07 for lipidomic profiling, enabling to widen our understanding of intracellular lipid trafficking in response to nitrogen-limited conditions for enhancing TAG accumulation. Consequently, it would add to our understanding concerning to insights of metabolic and regulatory mechanisms of TAG biosynthesis and in designing strategies for enhanced lipid accumulation for biofuel production.

4.2. Materials and Methods

4.2.1 Microalgal strain and culture conditions

The microalgae *Desmodesmus* sp. JS07 was used in this study. The strain was maintained in BG11 media at 25 ± 2^0C under continuous illumination from white fluorescent lamps at 200 μEm^{-2} s^{-1} at 150 rpm.

4.2.2 Experimental design

The microalgae species were grown in 150 mL of BG11 medium in 500 mL conical flasks containing different concentrations (0, 4.4, 8.8, 13.2 and 17.6 mM (control)) of sodium nitrate. The cultures were grown at temperature 25 ± 2 ^{0}C under illumination from fluorescent tubes (200 μEm^{-2} s^{-1}) continuously on a shaker rotated at 150 rpm for 15 days. The nitrogen limiting concentration of 4.4mM was selected based on lipid content and productivity. Microalgal cells (10%, v/v) growing in the log phase (OD~0.6 at 750 nm) used as an inoculum.

4.2.3 Growth and biomass analysis

The growth of microalgae was analyzed spectrophotometrically at 750 nm. Biomass was estimated gravimetrically in terms of dry biomass (g/L, dry weight, DW) as described in section 2.2.3.1.

4.2.4 Lipid Extraction

The microalgal biomass was harvested after 15 days of cultivation (late log phase) by centrifugation and lyophilized. The extraction of lipids from the lyophilized biomass (100mg) was performed by using Bligh and Dyer's method, as described in section 2.2.3.3.

4.2.5 LC-MS analysis

Before injection, 1 mg of the dried lipid sample was re-suspended in methanol/chloroform (9:1). 5µl injection volume was used for mass spectrometric analysis of lipids by using UPLC system (Thermo Scientific LTQ Orbitrap XL) equipped with C30 reversed phase column (100 mm×2.1 mm×3 µm particles, Acclaim ^{TM}) coupled to a high-resolution mass spectrometer (Q-Exactive Thermo- Fisher, Germany).

Acetonitrile and water (60:40, v/v; AcN: H_2O) was used as mobile phase A, and acetonitrile with isopropyl alcohol (10:90; v/v; AcN: IPA) was used as mobile phase B. 10 mM Ammonium formate and 0.1 % of formic acid were added to the mobile phases as electrolyte. The MS analysis was performed with both positive and negative mode, and corresponding data set was attained in the centroid mode from 70 to 1,200 m/z in MS scanning. Resolution for the full scan was set to 1,40,000 for precursor ion and 35,000 for product ion.

The data analysis was achieved in a targeted way; Xcalibur.RAW files from each of the two experiments were processed individually by Lipid search software (Thermo Scientific). For each MS spectrum, search results were summarized, along with a score indicating the fit, for lipid species matching the predicted fragmentation pattern from the database of the lipid search software. For the qualitative and quantitative analysis a combined deuterated lipid internal standard of 20µl consisting of PC (15:0/18:1) d(7) of 0.1607 µg/µl, PE (15:0/18:1) d(7) of 0.0057 µg/µl, PS (15:0/18:1) d(7) of 0.0042 µg/µl, PI (15:0-18:1) d(7) of 0.0091 µg/µl, PG (15:0/)18:1 d(7) of 0.0291 µg/µl, MG (18:1) (d7) of 0.002 µg/µl, DG (15:0/18:1) d(7) of 0.0094 µg/µl and TAG (15:0/18:1/15:0) of 0.0573 µg/µl was used. A single point calibration was employed to quantify each lipid class using the standards, and the final concentrations were determined in the extracted lipid mass. The concentration of each lipid class and lipid species were measured as relative abundance as a percent of total abundance and is shown in the form of bar graphs.

4.2.6 Determination of fuel properties

Biofuel properties of *Desmodesmus* sp. JS07 biodiesel such as density was evaluated by using standard method ASTM D941 and viscosity by ASTM D445 (Alptekin and Canakci, 2008).

Further properties including cetane number (CN), saponification value (SV), degree of unsaturation (DU), iodine value (IV), long chain saturation factor (LCSF) and cold filter plugging point (CFPP) were determined from the fatty acid profile of *Desmodesmus* sp. JS07 for both the conditions using the following empirical formula (1)-(6) (Kwak et al., 2016; Parsaeimehr et al., 2015)

$$SV = \sum(560 \times FA)/MM \quad (1)$$

$$IV = \sum(254 \times D \times FA)/MM \quad (2)$$

$$CN = 46.3 + \left(\frac{5458}{SV}\right) - (0.225 - IV) \quad (3)$$

$$DU = MUFA + (2 \times PUFA) \quad (4)$$

$$LCSF = (0.1 \times C16) + (0.5 \times C18) + (1 \times C20) + (1.5 \times C22) + (2 \times C24) \quad (5)$$

$$CFPP = (3.1417 \times LCSF) - 16.477 \quad (6)$$

where FA denotes fatty acid percentage in biodiesel, MM signifies the molecular mass of each fatty acid, D is the number of double bonds, MUFA and PUFA represent monounsaturated fatty acids and polyunsaturated fatty acid respectively in wt %.

4.3. Results and Discussion

4.3.1 Lipidome profiling of *Desmodesmus* sp. JS07

LC-MS was carried out for analysing both polar and nonpolar lipids in microalgae *Desmodesmus* sp. JS07 under nitrogen sufficient and limited conditions. The LC-MS could precisely elucidate the spectra of single lipid class (targeted analysis) based on total acyl chain concentration, profiles of the combined acyl content of each lipid class and the entire lipid species (untargeted analysis) in the microalgae. In addition, to find out the cumulative fatty acid composition of the lipid classes, LC-MS analysis was performed for *Desmodesmus* sp. JS07 under nitrogen sufficient and nitrogen-limited condition to ascertain the fatty acids for the respective lipid species. The lipidome profiling exhibited varying lipid patterns consisting of 8 lipid classes including DG, MG, PC, PG, PI, PE, PS, and TAG and 87 lipid species (Table 4.1-4.8). Lipid classes i.e. TAG, DG, MG, PC, PE, and PS were identified in positive mode while PG and PI were detected in negative mode. The total lipid samples were collected from the column up to 13 min following sample injection; MGs had eluted earlier between 3 to 5 min, followed by polar lipids between 1 to 10 min and neutral lipids eluted within 7 to 13 min. This pattern was similar

for both the conditions. The accumulation of total lipids as detected earlier had increased notably during N-limited conditions; however, the polar lipids had decreased, suggesting that many complex lipids mainly the polar ones may undergo remodeling thereby to enhance TAG accumulation and thus affecting the lipid composition during nitrogen-limited conditions.

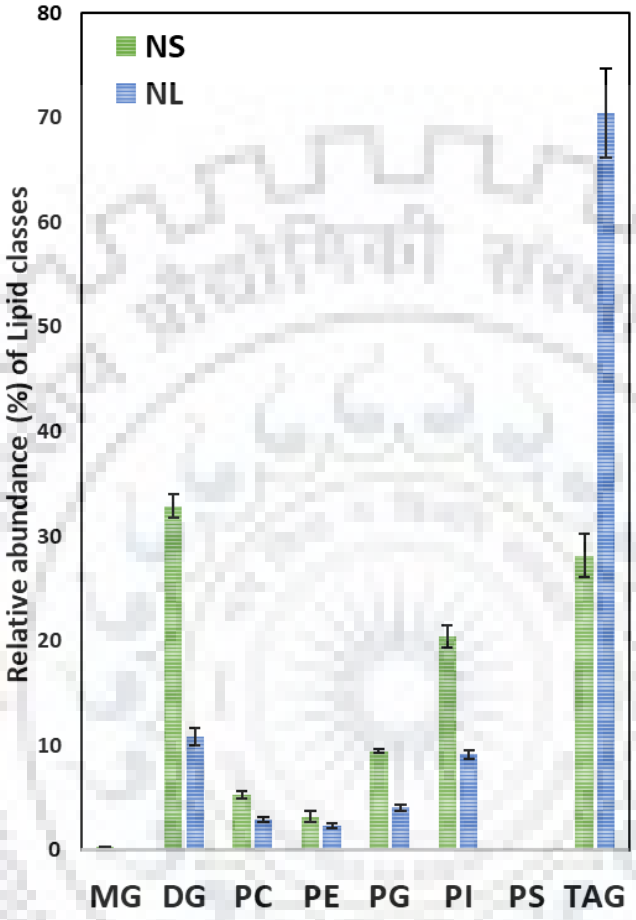

Fig. 4.1 Lipid classes in *Desmodesmus* sp. JS07 under nitrogen sufficient (NS) and nitrogen-limited conditions (NL). Data are represented as Mean ± SD; error bars represent the standard deviation of triplicate experiments.

4.3.3 Analysis of neutral lipids

LC-MS analysis revealed a remarkable increase, i.e. 2.5 fold in the quantity of TAG under nitrogen-limited conditions that are consistent with earlier studies that had displayed the enhanced TAG levels during nitrogen starvation (Fan et al., 2011). The TAG profiling of *Desmodesmus* sp. JS07 had shown 57 TAG lipid species where the carbon number of TAGs varied from 34 to 64, consisting of 1-10 unsaturations (Table 4.1; Fig 4.2). This had marginally differed to the earlier observations whereby carbon number of TAGs ranged from 48 to 54, and unsaturations were from 1–9 (Sharma et al., 2015). While, 64 TAG species consisting of 1-12

unsaturation's were observed for *Chloromonas* (Nedbalová et al., 2014) and 32 TAG species were found in crude algal oil from *Nannochloropsis salina* (Lee et al., 2013) through LC-MS analysis. Further, elucidation of TAG composition revealed relatively greater fraction of TAG 50:1 (16:0/16:0/18:1), TAG 52:2 (16:0/18:1/18:1), TAG 52:3 (16:1/18:1/18:1) and TAG 54:3 (18:1/18:1/18:1) under N-limitation. Similar findings were observed in previous studies depicting TAG accumulation in *Coccomyxa subellipsoidea* under nitrogen stress (Allen et al., 2015). In contrast, saturated TAGs specifically, TAG 46:0 (16:0/14:0/16:0) and TAG 44:0 (16:0/14:0/14:0) remained essentially unchanged under nitrogen-limited conditions.

Thus, as observed in contrast to the previous studies denoting decreased levels of unsaturated TAG under complete nitrogen depletion (Breuer et al., 2012), considerate levels of unsaturated TAGs mainly TAG 52:4 (16:0/18:2/18:2) and TAG 52:6 (16:0/18:3/18:3) were detected in the present study. The level of unsaturation observed in *Desmodesmus* sp. JS07 could be due to the differential levels of lipid desaturases localized in ER for the generation of polyunsaturated fatty acids (Li-Beisson et al., 2015).

Table 4.1 Fatty acid composition, retention time, and calculated mass of TAG lipid species in *Desmodesmus* sp. JS07

S No.	TAG	Fatty Acid Composition	Base Retention time (min)	Calculate mass m/z
1.	TAG(34:0)	TAG(10:0/12:0/12:0)	9.22	610.5172
2.	TAG(36:0)	TAG(12:0/12:0/12:0)	11.52	638.5485
3.	TAG(38:0)	TAG(12:0/12:0/14:0)	12.44	666.5798
4.	TAG(40:0)	TAG(12:0/14:0/14:0)	10.60	694.6111
5.	TAG(40:0)	TAG(16:0/12:0/12:0)	11.48	694.6111
6.	TAG(42:0)	TAG(16:0/12:0/14:0)	10.96	722.6424
7.	TAG(44:0)	TAG(16:0/14:0/14:0)	11.28	750.6737
8.	TAG(46:0)	TAG(16:0/14:0/16:0)	11.58	778.7050
9.	TAG(46:1)	TAG(16:0/14:0/16:1)	11.29	776.6894
10.	TAG(54:0)	TAG(16:0/14:0/24:0)	12.64	890.8302
11.	TAG(48:0)	TAG(16:0/16:0/16:0)	11.86	806.7363
12.	TAG(48:1)	TAG(16:0/16:0/16:1)	11.58	804.7207
13.	TAG(50:1)	TAG(16:0/16:0/18:1)	11.84	832.7520
14.	TAG(48:2)	TAG(16:0/16:1/16:1)	11.32	802.7050
15.	TAG(50:2)	TAG(16:0/16:1/18:1)	11.57	830.7363

16.	TAG(50:4)	TAG(16:0/16:1/18:3)	11.09	826.7050
17.	TAG(52:2)	TAG(16:0/18:1/18:1)	11.81	858.7676
18.	TAG(56:1)	TAG(16:0/18:1/22:0)	12.62	916.8459
19.	TAG(58:1)	TAG(16:0/18:1/24:0)	12.90	944.8772
20.	TAG(52:4)	TAG(16:0/18:2/18:2)	11.36	854.7363
21.	TAG(52:6)	TAG(16:0/18:3/18:3)	10.95	850.7050
22.	TAG(36:0)	TAG(16:0/8:0/12:0)	12.05	638.5485
23.	TAG(44:1)	TAG(16:1/14:0/14:0)	10.96	748.6581
24.	TAG(46:2)	TAG(16:1/14:0/16:1)	11.00	774.6737
25.	TAG(48:3)	TAG(16:1/16:1/16:1)	11.03	800.6894
26.	TAG(50:3)	TAG(16:1/16:1/18:1)	11.35	828.7207
27.	TAG(52:3)	TAG(16:1/18:1/18:1)	11.56	856.7520
28.	TAG(50:0)	TAG(18:0/16:0/16:0)	12.13	834.7676
29.	TAG(52:0)	TAG(18:0/16:0/18:0)	12.39	862.7989
30.	TAG(52:1)	TAG(18:0/16:0/18:1)	12.10	860.7833
31.	TAG(54:2)	TAG(18:0/18:1/18:1)	12.08	886.7989
32.	TAG(54:4)	TAG(18:0/18:1/18:3)	11.56	882.7676
33.	TAG(42:1)	TAG(18:1/12:0/12:0)	10.61	720.6268
34.	TAG(52:8)	TAG(18:1/12:1/22:6)	10.40	846.6737
35.	TAG(50:5)	TAG(18:1/14:3/18:1)	10.98	824.6894
36.	TAG(54:3)	TAG(18:1/18:1/18:1)	11.79	884.7833
37.	TAG(54:5)	TAG(18:1/18:1/18:3)	11.34	880.7520
38.	TAG(58:2)	TAG(18:1/18:1/22:0)	12.59	942.8615
39.	TAG(60:2)	TAG(18:1/18:1/24:0)	12.87	970.8928
40.	TAG(54:6)	TAG(18:2/18:2/18:2)	11.07	878.7363
41.	TAG(50:7)	TAG(18:3/14:1/18:3)	10.41	820.6581
42.	TAG(54:7)	TAG(18:3/18:2/18:2)	11.15	876.7207
43.	TAG(54:9)	TAG(18:3/18:3/18:3)	10.26	872.6894
44.	TAG(52:5)	TAG(18:4/16:0/18:1)	11.07	852.7207
45.	TAG(54:3)	TAG(18:4/18:0/18:3)	10.85	876.7207
46.	TAG(54:8)	TAG(18:4/18:1/18:3)	10.62	874.7050
47.	TAG(54:1)	TAG(20:0/16:0/18:1)	12.37	888.8146
48.	TAG(56:2)	TAG(20:0/18:1/18:1)	12.33	914.8302
49.	TAG(56:4)	TAG(20:0/18:1/18:3)	11.93	910.7989
50.	TAG(56:3)	TAG(20:1/18:1/18:1)	12.04	912.8146

51.	TAG(56:0)	TAG(26:0/14:0/16:0)	12.92	918.8615
52.	TAG(64:4)	TG(28:0/18:1/18:3)	12.99	1022.9241
53.	TAG(38:1)	TAG(4:0/16:0/18:1)	9.97	664.5642
54.	TAG(32:0)	TAG(8:0/12:0/12:0)	10.62	582.4859
55.	TAG(34:0)	TAG(8:0/12:0/14:0)	9.73	610.5172
56.	TG(50:6)	Not identified	8.59	822.6737
57.	TG(52:10)	Not identified	11.72	842.6424

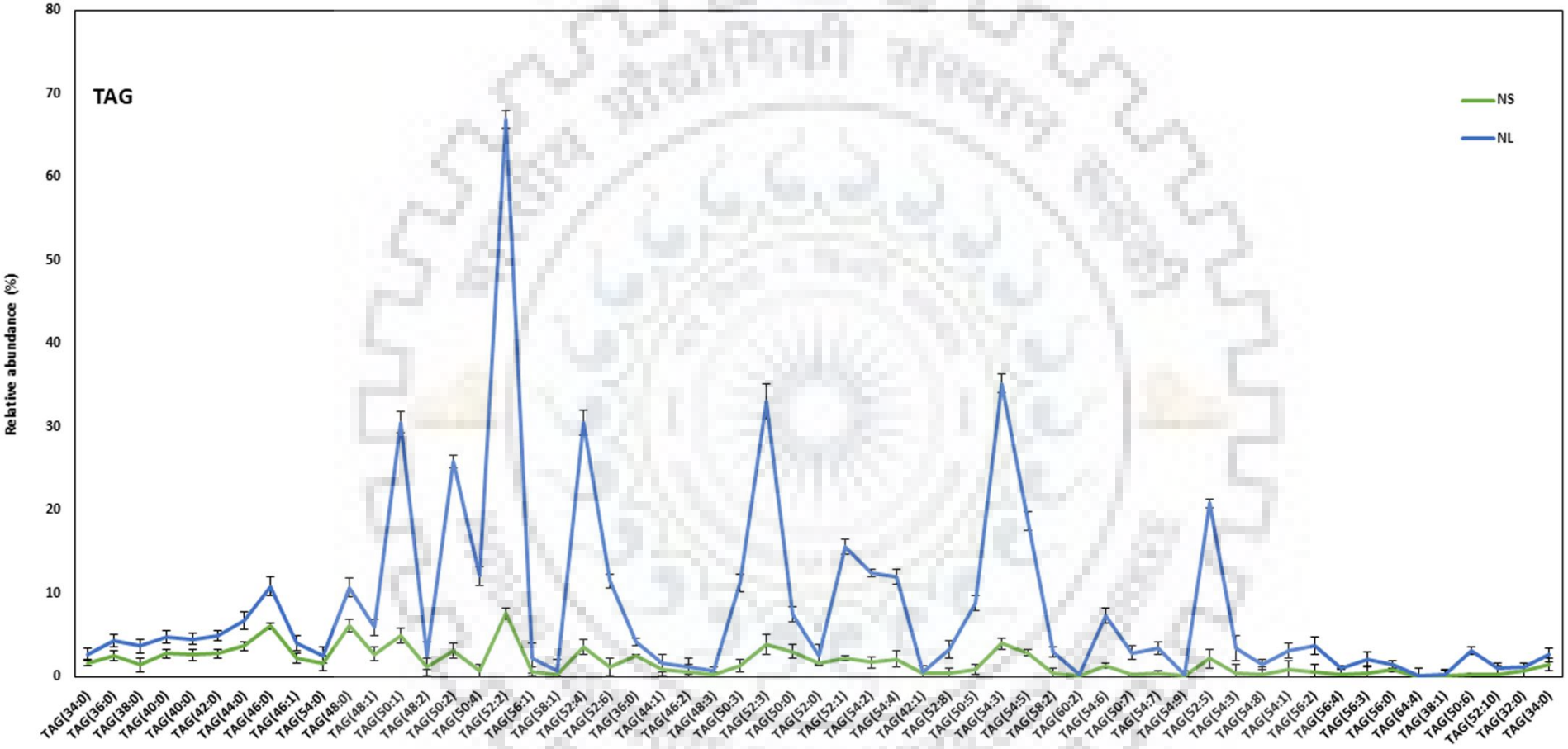

Fig. 4.2 TAG profiling of *Desmodesmus* sp. JS07 under nitrogen sufficient (NS) and nitrogen-limited conditions (NL). Data are represented as Mean ± SD; error bars represent the standard deviation of triplicate experiments.

Besides TAG, the lipid profiles of *Desmodesmus* sp. JS07 under both conditions had shown 5 lipid species of DG (Diacylglycerol) (Fig. 4.3; Table 4.2), eluted between 6 to 10 min. However, 10 DG species were identified in *Nannochloropsis salina* under normal nitrogen condition (Lee et al., 2013). Remarkably, DGs were observed to decrease 3 fold under nitrogen-limited conditions. As reported, DGs generated in chloroplasts primarily serve as a precursor for membrane lipids of the photosynthetic system (De Bhowmick et al., 2015) whereas DGs produced in ER can be used for both structural and storage lipids (TAG). The decreased membrane lipids synthesis in chloroplast and ER following N-limitation denotes that DGs were predominantly been utilized for TAGs production in the chloroplast as well as in ER.

Table 4.2 Fatty acid composition, retention time and calculated mass of DG lipid species in *Desmodesmus* sp. JS07

S No.	DG	Fatty Acid Composition	Base Retention time (min)	Calculate mass m/z
1.	DG(32:0)	DG(16:0/16:0)	9.17	568.5067
2.	DG(34:0)	DG(18:0/16:0)	9.74	596.5380
3.	DG(38:0)	DG(18:0/18:0)	10.22	624.5693
4.	DG(38:2)	DG(18:1/18:1)	9.21	620.5380
5.	DG(38:6)	DG(18:3/18:3)	7.21	612.4754

Interestingly, lower levels of MG (Monoacylglycerol) with C16:0 and C18:0 fatty acyl chain were detected in *Desmodesmus* sp. JS07 under nitrogen sufficient conditions (Table 3) which further reduced 30 fold under nitrogen-limited conditions; indicating possibly its plausible diversion towards TAG formation.

Table 4.3 Fatty acid composition, retention time and calculated mass of MG lipid species in *Desmodesmus* sp. JS07

SL No.	DG	Fatty Acid Composition	Base Retention time (min)	Calculate mass m/z
1.	MG(16:0)	3.73	330.2770	MG(16:0)
2.	MG(18:0)	4.79	358.3083	MG(18:0)

3.2.2 Analysis of polar lipids

The polar fraction of the lipids revealed mainly PG, PI, PC, PE and PS phospholipids under both the conditions (Fig. 4.3). The results obtained were comparable with recent reports where major polar lipids characterized were PI, PG, together with PC, and fewer amounts of PE and PS in

microalgae species through LC-MS analysis (Guschina and Harwood, 2009; Lu et al., 2013). Nevertheless, the significant differences in the composition of polar lipids of microalgae had also been observed in different species. For example, same observations had indicated that PC, PE, and PG were predominant in *Chlorella sorokiniana* (Lu et al., 2013) and PC, PG, PE and PI in *Nannochloropsis oculata* (He et al., 2011).

Further, under nitrogen limitation PG levels decreased by 2.3 fold, similar was the observation in *Chlamydomonas reinhardti* (Fan et al., 2011). PGs were within 6 and 7 min and consisted of 6 lipid species including 32:0, 34:0, 34:2, 34:3, 36:2 and 38:2 (Fig. 3; Table 4). PG is the major phosphoglycerolipid present in the photosynthetic membranes of chloroplasts and works as a cofactor for photosystems and the light-harvesting complex II (Darwish et al., 2009). Therefore, decreased PG levels under nitrogen-limited condition may adversely affect the photosynthetic system of the microalgae, thereby reducing the cell growth under nitrogen-limited conditions. Likewise, microalgae *Haematococcus pluvialis* grown under nitrogen starvation, had displayed smaller chloroplasts containing fewer thylakoids and decreased level of electron transport chain that led to the declined growth rate (Scibilia et al., 2015).

Table 4.4 Fatty acid composition, retention time, and calculated the mass of PG lipid species in *Desmodesmus* sp. JS07

SL No.	PG	Fatty Acid Composition	Base Retention time (min)	Calculate mass m/z
1.	PG(32:0)	PG(16:0/16:0)	7.67	722.5098
2.	PG(34:0)	PG(16:0/18:1	7.71	722.5098
3.	PG(34:2)	PG(16:0/18:2)	7.14	722.5098
4.	PG(34:3)	PG(16:0/18:3)	6.66	744.4941
5.	PG(36:2)	PG(18:1/18:1)	7.72	774.5411
6.	PG(38:2)	PG(19:1/19:1)	8.54	802.5724

Likewise, PI with 3 lipid species C32:0, C34:1 and C34:2 had eluted between 6-8 min (Table 5). PI constitute a minor component on the cytosolic side of cell membranes of chloroplast in microalgae (Li-Beisson et al., 2015) and 2.2 fold decreased the level of PI possibly denote its consequent trafficking towards TAG accumulation by *de novo* synthesis.

Table 4.5 Fatty acid composition, retention time and calculated mass of PI lipid species in *Desmodesmus* sp. JS07

SL No.	PI	Fatty Acid Composition	Base Retention time (min)	Calculate mass m/z
1.	PI(32:0)	PI(16:0/16:0)	7.48	810.5258
2.	PI(34:1)	PI(16:0/18:1)	7.55	836.5415
3.	PI(34:2)	PI(16:0/18:2)	6.99	834.5258

Similarly, nitrogen limitation had resulted in decreased levels of PC, PE, and PS in *Desmodesmus* sp. JS07. PCs were eluted from the column in between 9-11 min and consisted of C18:0, C18:3, C18:4, C36:2, C36:4 C36:6 and C38:2 lipid species (Fig. 4.4; Table 4.6). The five lipid species of PE *i.e.* C18:0, C18:3, C18:4, C36:2, C36:3 and C36:4 had eluted from column between 8 to 10 min and the PS eluted from the column between 8 to 9 min with two lipid species of C38:4 and C48:3 (Table 4.7 and 4.8). PC is one of the main constituents in cellular membranes specifically in the endoplasmic reticulum (ER), mitochondria and a minor constituent of chloroplast membranes (Barelli and Antonny, 2016; Benning, 2008). However, PE and PS are largely excluded from the chloroplast membranes and mainly present on the other endomembranes, as reported in plants (Jouhet et al., 2007). The *de novo* biosynthesis of PC, PE and PS are localized in the ER. Thus, the notable decrease of 1.8 fold, 1.4 and 0.8 fold in PC, PE, and PS respectively during nitrogen limitation may indicate the remodeling of membrane lipids towards TAG production in ER under nitrogen-limited conditions.

Table 4.6 Fatty acid composition, retention time and calculated mass of PC lipid species in *Desmodesmus* sp. JS07

SL No.	PC	Fatty Acid Composition	Base Retention time (min)	Calculate mass m/z
1.	PC(18:0)	PC(18:0)	2.82	521.3481
2.	PC(18:3)	PC(18:3)	1.99	517.3168
3.	PC(18:4)	PC(18:4)	1.74	515.3012
4.	PC(36:2)	PC(18:1/18:1)	8.69	785.5935
5.	PC(36:4)	PC(18:1/18:3)	7.50	781.5622
6.	PC(36:6)	PC(18:2/18:4)	6.28	777.5309
7.	PC(38:2)	PC(20:1/18:1)	9.54	813.6248

Table 4.7 Fatty acid composition, retention time and calculated mass of PE lipid species in *Desmodesmus* sp. JS07

SL No.	PE	Fatty Acid Composition	Base Retention time (min)	Calculate mass m/z
1.	PE(18:0)	PE(18:0)	2.78	479.3012
2.	PE(36:2)	PE(18:1/18:1)	8.31	743.5465
3.	PE(36:3)	PE(18:1/18:2)	7.80	741.5309
4.	PE(36:4)	PE(18:1/18:3)	7.32	739.5152
5.	PE(18:3)	PE(18:3)	1.94	475.2699

Table 4.8 Fatty acid composition, retention time and calculated mass of PS lipid species in *Desmodesmus* sp. JS07

SL No.	PS	Fatty Acid Composition	Base Retention time (min)	Calculate mass m/z
1.	PS(38:4)	Not identified	8.31	811.5363
2.	PS(48:3)	Not identified	5.85	953.7085

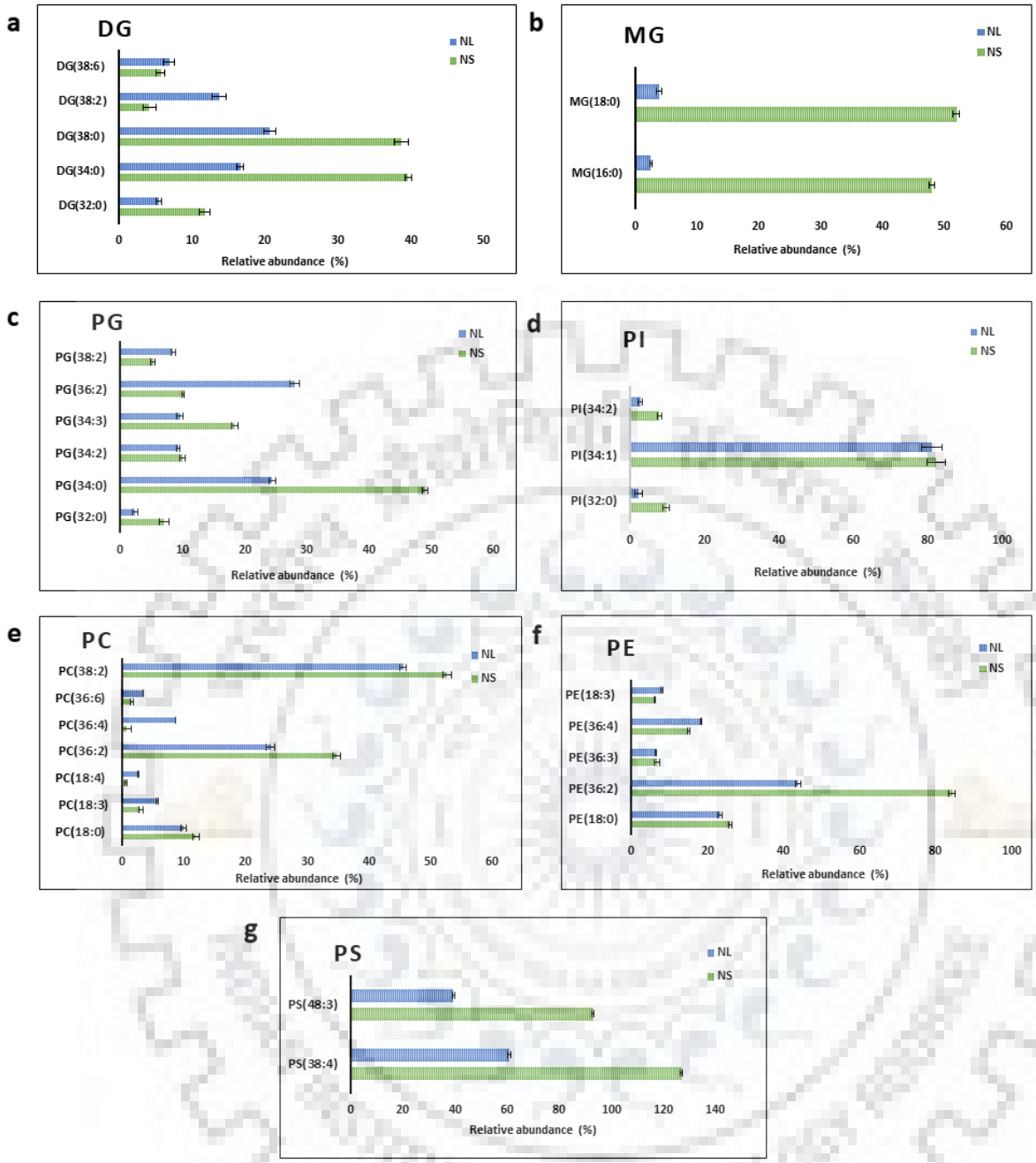

Fig. 4.3 Profile of lipid species in varying lipid classes, DG (a), MG (b), PG (c), PI (d), PC (e), PE (f) and PS (g) in *Desmodesmus* sp. JS07 under nitrogen sufficient (NS) and nitrogen-limited conditions (NL). Data are represented as Mean ± SD; error bars represent the standard deviation of triplicate experiments.

4.3.3 Comparison of fatty acids composition of different lipid classes

LC-MS analysis was performed to identify and quantify the fatty acid composition of each lipid species. As stated earlier, the noticeable TAG species observed in *Desmodesmus* sp. JS07 under both the conditions were 50:1, 52:2 and 54:3 (Fig. 4.2), consisting of C16:0 and C18:1 fatty acid.

While the major TAGs reported in microalgae *Nannochloropsis sp.* during both nitrogen replete and depleted conditions were 48:1 and 48:2 and consisted of 16:0 and 16:1 fatty acyl chains (Martin et al., 2014). There was also a demarcated increase of C52:2, C52:3, C54:3 and C52:5 TAG species, comprising of (18:1/18:1/16:0), (18:1/18:1/16:1), (18:1/18:1/18:1) and (18:4/18:1/16:0) fatty acids respectively (Fig. 4.2) in nitrogen-limited conditions. Thus, indicating an overall increase in fatty acyl chain moieties comprising of C16:0, C16:1, C18:1 and C18:3 (with a maximum surge of C16:0 and C18:1) in TAG under N-limitation. Similar results were observed for the green algae *Coccomyxa subellipsoidea* under nitrogen depletion, were C18:1 fatty acid was the predominant acyl chains in the newly synthesized TAG (Allen et al., 2015). Thus, the LC-MS analysis has denoted higher accumulation of monounsaturated fatty acids and moderate levels of saturated fatty acids in TAG of *Desmodesmus* sp. JS07, and that is a desirable feature for achieving the high-value biodiesel (Guschina et al., 2014; Ohlrogge and Browse, 1995).

The C16:0 and C18:1 fatty acid in TAGs as demonstrated earlier suggests the *de novo* fatty acid synthesis under nitrogen sufficient (normal) conditions. Thus, the increased levels of C16:0 and C18:1 under nitrogen-limited condition suggest that newly synthesized fatty acids may get incorporated into TAGs without undergoing any desaturation and may be an energy saving mechanism under stress, which in turn could direct the resulting flux towards enhanced TAGs accumulation through *de novo* fatty acid synthesis in chloroplast. However, the presence of a significant amount of elongated and polyunsaturated fatty acids in TAGs proposes the recycling of membrane polar lipids (Simionato et al., 2013).

Additionally, the detectable levels of long chain fatty acids comprising of C20:0, C22:0, C22:6 and C24:0 (Fig. 4.4) detected in the polar lipid and TAGs, suggest that these contribute to fluidity, flexibility and selective permeability of cellular membranes in stress conditions.

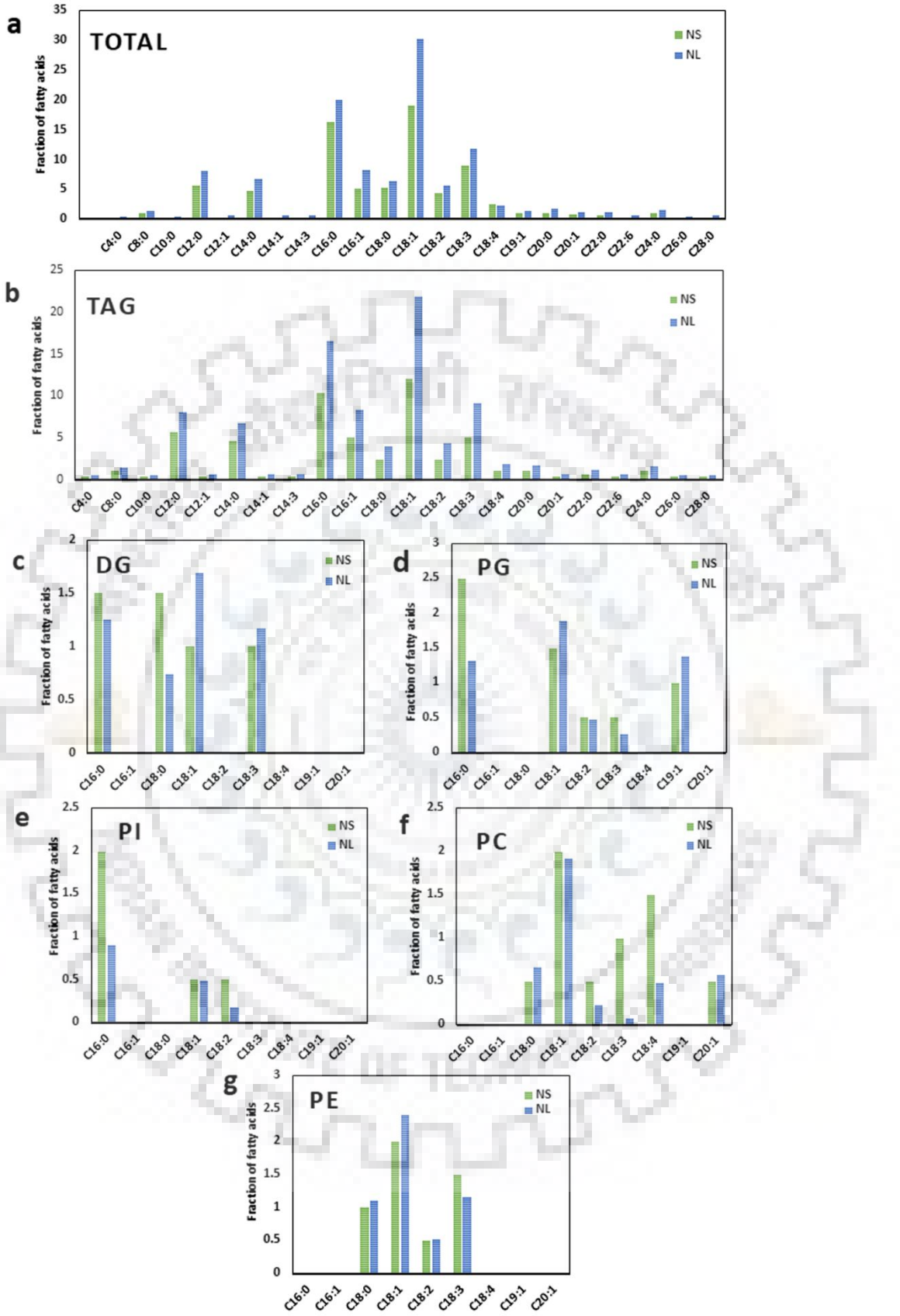

Fig. 4.4 Fatty acid composition of total lipids (a), TAG (b), DG (c), PG (d), PI (e), PC (f) and PE (f) under nitrogen sufficient (NS) and nitrogen-limited (NL) conditions.

As observed earlier, DGs that is a precursor for membrane lipids and storage lipid TAG had decreased under nitrogen-limited conditions (Fan et al., 2011; Ohlrogge and Browse, 1995). The C16:0 fatty acid, a major constituent in DG under normal conditions indicate their synthesis primarily in the chloroplast. However, the decreased levels of DG and C16:0 under nitrogen limited conditions possibly indicate that DGs generated in chloroplast may get channelized for TAG production during nitrogen limitation. However, the augmented C18:1 concentration in DG suggests possibly their generation in ER, that eventually results into both membrane lipids and TAG (Guschina et al., 2014; Li et al., 2012).

The fatty acyl chain moieties of the polar lipids primarily did not show high diversity as nonpolar lipids. Both PI and PG consisted of short-chain fatty acids (C32–C38), with increased levels of C16:0 and C18:1 under nitrogen sufficient conditions thus indicating their generation in chloroplast *via* PA (phosphatidic acid) (Klok et al., 2014); thus, their decreased levels under nitrogen-limited conditions eventually suggest that PG and PI are metabolized to TAG accumulation. Moreover, the occurrence of C18:2, C18:3, C18:4 and C20:1 in PC and C18:1, C18:2 and C18:3 in PE during normal growth conditions denote their generation in ER as stated above. Subsequently, their decreased levels under nitrogen-limited condition suggest an increase in the TAG biosynthesis in the ER through the Kennedy pathway (Fig. 4.6).

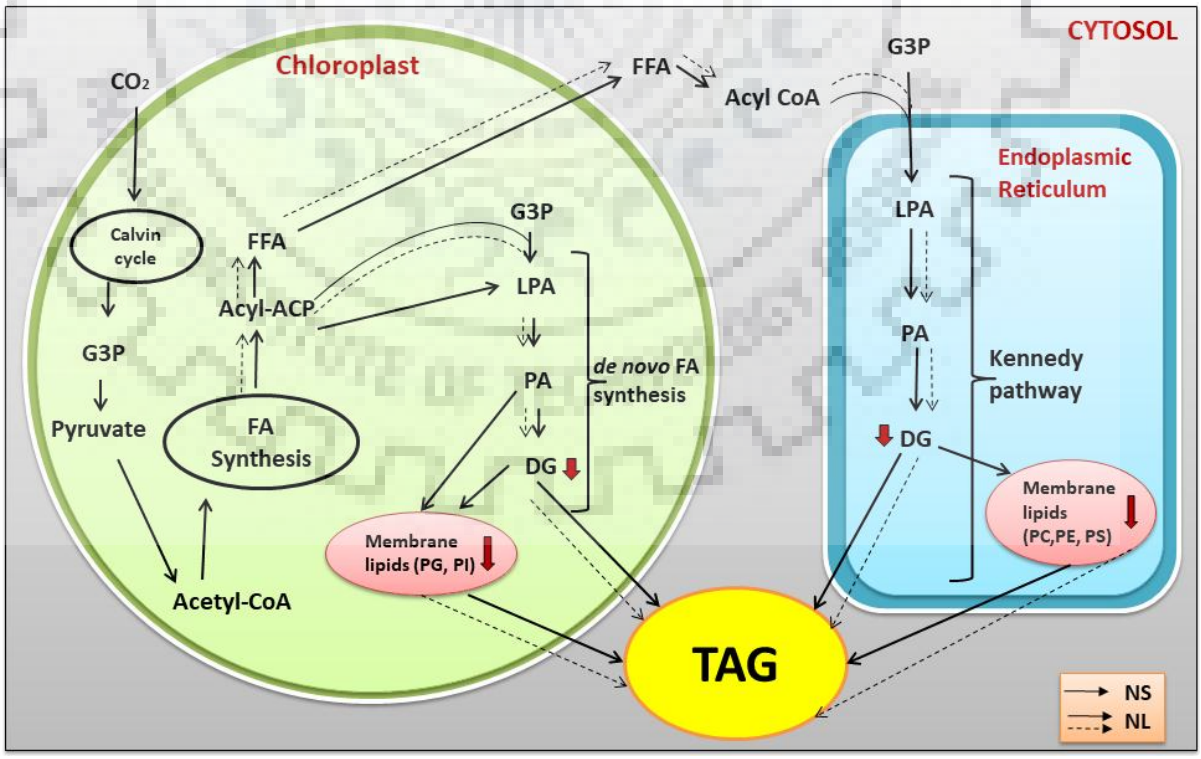

Fig. 4.6 Schematic representation of lipid biosynthesis in microalgae under nitrogen sufficient (NS) and nitrogen-limited conditions (NL). The figure depicts the TAG biosynthesis in

microalgae *via* Kennedy and *de novo* fatty acid synthesis pathway. The dotted lines represent the augmented pathways under nitrogen limited conditions. "Where DG, diacylglycerol; FFA, free fatty acids; G3P, glycerol-3-phosphate; LPA, lysophosphatidic acid; PA, phosphatidic acid; PC, phosphatidylcholine; PE, phosphatidylethanolamine; PG, phosphatidylglycerol; PI, phosphatidylinositol; PS, phosphatidylserine".

4.3.4 Fuel Properties of Biodiesel from *Desmodesmus* sp. JS07

The fuel properties of biodiesel from *Desmodesmus* sp. JS07 was enumerated and compared with the American (ASTM D6751) and European (EN 14214) biodiesel standards (Table 9). The microalgal biodiesel density elucidated in the present study was 879 and 868 kg/m^3 under normal and nitrogen limited condition respectively and was observed to be similar with bio-diesel (863 kg/m^3) from *Spirulina platensis* (Mostafa and El-Gendy, 2017) and lower in comparison to the density of biodiesel from Karanja (884 kg/m3) and waste cooking oil (883.5 kg/m3) (An et al., 2013; Chauhan et al., 2013). The viscosity of biodiesel from *Desmodesmus* sp. JS07 under nitrogen sufficient and nitrogen limited conditions was detected to be 3.63 mm^2/s and 3.85 mm^2/s, respectively, that was equivalent to *Nannochloropsis gaditana, i.e.*, 3.8 mm^2/s under normal conditions (Knothe, 2012). Higher values of density and viscosity will affect into a higher mass of fuel that can be injected, thereby with enhanced brake specific fuel consumption features. However, the greater values may also lead to poor air-fuel mixing that will further lower the efficiency of the engine (Alptekin and Canakci, 2008). In the present study, the density and viscosity were found ideal and comparable with the international biodiesel standards ASTM D6751 and EN 14214.

Moreover, the FAME profiling can provide expedient data such as cetane number (CN), saponification value (SV), cold filter plug point (CFPP), iodine value (IV) and degree of unsaturation (DU) to define the quality of biodiesel from microalgae. Amongst them, CN is used to measure the ignition quality of fuels and primarily depend on the SFA content and chain length in the biodiesel. The CN was estimated to 53.76 and 56.51 under nitrogen sufficient and nitrogen limited conditions, respectively, which was found to be higher than EN 14214, and ASTM D6751 biodiesel standards (Table 9). Still, a high proportion of SFA in biodiesel has a limitation in CFPP. The CFPP, denoting the flow performance of biodiesel at lower temperatures, is related to degree of unsaturation in the fatty acids of biodiesel that was found to be 9.70 and 12.71 under nitrogen sufficient and nitrogen limited conditions that are comparable with earlier observation, where the CFPP detected for different microalgal oils varied from 0.55-12.23 (Nascimento et al., 2013).

Iodine value (IV) is a measure of the oil unsaturation that increases with the increase in the degree of unsaturation (Knothe, 2012). The calculated IV in the present study under both conditions were within the acceptable standards. In particular, IV under nitrogen-limited condition exhibited the lowest value of 72. Likewise, DU is also related to the fuel properties such as IV, CFPP and CN, increase in DU affects into reduced of CFPP and enhancement of IV in biodiesel (Kwak et al., 2016). DU is the sum of the masses of MUFA and PUFA, thereby stimulating the oxidative stability of biodiesel (Mandotra et al., 2016). Therefore, reduced DU as found in the present study under the nitrogen-limited condition is desirable for ideal biodiesel characteristics.

Table 4.9 Comparative evaluation of biodiesel properties of *Desmodesmus* sp. JS07 under nitrogen sufficient (NS) and nitrogen-limited (NL) conditions.

Biodiesel Properties	**NS**	**NL**	**EN 14214 standard**	**US ASTM D6751 standard**
Density (kg/m^3)	879	868	-	860–900
Viscosity (mm^2/s)	3.63	3.85	3.5–5.0	1.9–6.0
SV	182.13	205.93	-	-
IV	99.91	72.4	≤120	
CN	53.76	56.51	≥51	≥47
CFPP	9.70	12.71	-	-

Thus, *Desmodesmus* sp. JS07 appears to be a potential candidate for the production of biodiesel; since the biodiesel characteristics were in close agreement with European (EN 14214) and American (ASTM D 6751) biodiesel standards. Furthermore, nitrogen-limited conditions led into the enhanced quality of by elevating MUFA levels (mainly C18:1) that impart higher CN compared to normal conditions.

4. Conclusion

The present study outlines a detailed lipid profiling of *Desmodesmus* sp. JS07 under nitrogen sufficient and nitrogen limited conditions to understand the intracellular cascades of lipid pools for enhanced TAG accumulation. The major Conclusion derived from the study under N-limitation are as below:

- A notable increase in lipid content up to 50% were found in the nitrogen-limited condition with average biomass production.

- Lipidome profiling deciphered a notable rise in the levels of TAGs concurrently with decreased levels of polar lipids PG and PI, denoting a significant remodeling of the intracellular lipid pools by augmenting *de novo* fatty acid biosynthesis in the chloroplast for enhanced TAG accumulation.

- The decreased levels of PC, PE, and PS during to N-limitation signifies the enhanced TAG accumulation through the Kennedy pathway in ER.

- A number of the newly synthesized TAGs had relatively higher levels of C16:0, C18:0 and C18:1 fatty acid that eventually affect the biofuel properties and thus demonstrating *Desmodesmus sp*. JS07 as a pivotal strain for biofuel production.

This study therefore not only enables in understanding the intricacies of the complex mechanistic lipid profiling of microalgae in response to nitrogen limitation but also delineates avenues for further insights into TAG cascade as a possible target for achieving enhanced neutral lipids intended for biofuel production.

CHAPTER 5

Unfolding the transcriptome of Desmodesmus sp. JS07 in response to nitrogen-limited condition to elucidate TAG metabolism

5.1. Introduction

Microalgae are considered as one of the potential feedstocks for biofuels. Microalgae accumulate a substantial amount of triglycerides, a precursor for biofuel during stress conditions such as nutrient limitation (Mutanda et al., 2011). The relatively higher growth rate, lipid content and possibility to improve strains for the production of neutral lipid and other valuable bio-products without competing for arable land, demarcate microalgae as an imperative addition to the sustainable resource for biofuel generation (Subramaniam et al., 2010). In spite of this, exploiting microalgae as a potential resource for biofuel production has not become a reality due to the higher cost of microalgal biofuels compared to conventional fuels (Demirbas, 2011). Thus looking for a novel or designing the strains for achieving the faster growth rate along with increased oil content are the viable options for economizing the biofuel obtained from microalgal resources.

In recent years, attempts have been made to transform microalgal strains, offering a great prospect to genetically modify the anabolic and catabolic pathways comprising lipid and starch metabolic pathways. So far, some of the algal genome sequences are available for instance *Phaeodactylum tricornutum*, *Thalassiosira pseudonana* and *Chlamydomonas reinhardtii* that provide the prospects to ascertain the key regulatory gene by comparative genomics coupled with transcriptomic and metabolomics study (Armbrust et al., 2004; Bowler et al., 2008; Merchant et al., 2007). However, still, several potential strains having higher lipid content have not been sequenced genome not annotated. In microalgae, primarily the transcriptomic analysis instead have focused on model organisms that are not oleaginous but with their genome sequenced (López García de Lomana et al., 2015).

Transcriptome sequencing is a powerful tool for obtaining functional genomic information without genomic information. It has been observed not only in enabling for identifying the key regulatory enzymes of TAG biosynthetic cascade under nitrogen-limited conditions but also facilitate in understanding the orchestrated metabolic cascades (Huang et al., 2017; Koid et al., 2014; Schwarz et al., 2013). Recently, an increasing number of the transcriptome of microalgae were *de novo* sequenced, assembled and annotated to understand the mechanism of lipid

biosynthesis, that has led into identifying potential targets and strategies for molecular manipulation (Rismani-Yazdi et al., 2012; Zheng et al., 2013).

Desmodesmus sp. JS07, a green microalga with moderately high lipid content can synthesize and accumulate large amounts of neutral lipids (up to 50% by dry weight) under nitrogen-limited conditions. Thus to unravel the regulatory mechanism of lipid accumulation in *Desmodesmus* sp. JS07 in response to normal and nitrogen-limited conditions, the transcriptome was sequenced, and *de novo* assembled. Furthermore, differential gene expression (DGEs) and Gene Ontology (GO) enrichment analysis identified several biological processes and pathways related to lipid accumulation. The present study would aid as a blueprint for the gene expression profile in microalgae that led to unraveling the network of differentially expressed genes and suggest potential targets for improving lipid content in microalgae by genetic manipulation approaches.

5.2 Materials and Methods

5.2.1 Culture conditions

Desmodesmus sp. JS07 was used in this study. For the transcriptome analysis study (Fig.1), the organism was grown in nitrogen limited (4.4mM), and nitrogen sufficient (17.6mM) BG-11 medium in 150 mL volumes in 500 ml conical flasks at temperature 25^{o}C under continuous illumination (200µEm-2 s-1) on a shaker rotated at 150 rpm. Fig 5.1 represents the overall workflow of *de novo* transcriptome analysis.

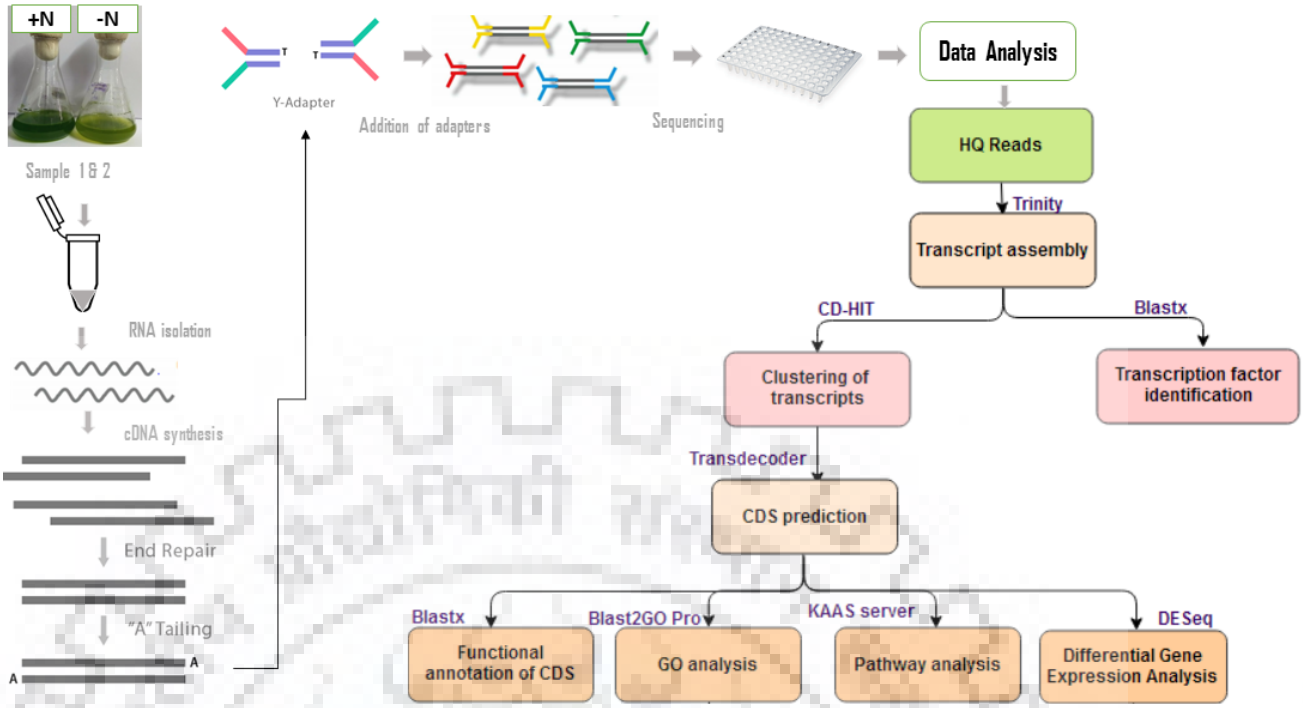

Fig. 5.1. The overall workflow for the *de novo* transcriptome analysis

5.2.2 RNA Isolation

All cultures were harvested during mid-exponential growth phase by centrifugation in a centrifuge (Thermo Scientific) at 5000 rpm for 15 min at 15°C. The supernatant was carefully decanted, and RNA was extracted from the pellet of the samples using Trizol reagent according to the manufacturer's instruction (Invitrogen, USA) (Ren et al., 2017). The RNA was quantified using Nanodrop 8000 spectrophotometer, and the quality was checked using 1% formaldehyde denaturing agarose gel.

5.2.3 Library Preparation and sequencing

The libraries were prepared with input total RNA ~1µg using Illumina TruSeq RNA Library Preparation Kit as per the manufacturer's instructions. Briefly, total RNA was Ribo depleted using plant rRNA removal mix and rRNA removal beads, then subjected to purification, fragmentation, and priming for cDNA synthesis. The Ribo depleted fragmented RNA was converted into cDNA followed by A-tailing, adapter-index ligation, and finally amplified by the recommended number of PCR cycles. Bioanalyzer 2100 (Agilent Technologies) was employed to analyze the quality and quantity of the sample library using High Sensitivity (HS) DNA chip as per manufacturer's instructions. After qualified, the cDNA library was sequenced with the Illumina Hiseq2000 platform.

5.2.4 Transcriptome assembly and function annotation

The 150 bp paired-end raw reeds data were produced on the Illumina Hiseq2000 platform and were analyzed for quality assessment by FastQC tool (v0.10.1). Following this, *de novo* assembly of high-quality reads was performed with **Trinity (v2.1.**1) which is a de Bruijn graph-based assembler. Further, transcripts were clustered using CD-HIT (Cluster Database at High Identity with Tolerance) package. CD-HIT-EST (v4.6.1) was used to remove the shorter redundant transcripts when they were 100% covered by other transcripts with more than 90% identity. The non-redundant clustered transcripts were then named as unigenes used for the following analysis. Candidate coding regions or sequence (CDS) were identified within unigenes using TransDecoder (v2.0).

The functional annotation of the transcripts was based on homology search between the transcripts and known sequence databases. The predicted CDS were annotated evaluating the homology by BLASTX search against NCBI's NR (Non-redundant) database with an E-value cut-off of 10−5. Blast2GO pro was used for Gene Ontology (GO) analysis to identify the cluster of orthologous groups (COG). Further, for the mapping of biological pathways, nonredundant contigs were submitted to KEGG automatic annotation server (KAAS). All the CDS were compared against the KEGG database for KEGG ortholog assignment and corresponding enzyme commission number (EC number) using BLASTX with threshold bit-score value of 60.

5.2.5 Differential gene expression (DGE) analysis

Differential gene expression was identified between the culture grown under nitrogen-limited conditions as ‘Sample 1’ and control as ‘Sample 2’ by using FKPM (fragments per kilobase of transcript per million mapped reads) algorithm using the RSEM (v1.2.7). For obtaining differentially expressed genes, reads were mapped to their respective CDS sequences using bwa v0.7.12-r10 and read counts were obtained using samtools v0.1.18. A read count matrix was prepared programmatically where columns represent samples; rows represent CDS each cell represents read count corresponding to the sample and the CDS id. The count matrix was given as input to the R package DESeq which in turn provides normalized values in terms of “basemean” which is further used for log2FC (log2 fold change) and p-value evaluation. The criterion used to identify up-regulated, and down-regulated genes, along with the significance, are provided in Table 1.

5.2.6 Transcription Factor Analysis

To identify the putative transcription factor (TF) families in the assembly of *Desmodesmus* sp. JS07, the plant transcription factor database PlantTFDB was selected using BLASTX algorithm with an E-value cut-off of < 1e-05.

5.3 Results and Discussion

5.3.1 Sequencing and *denovo* transcriptome assembly

To infer the effect of nitrogen limitation on lipid accumulation in *Desmodesmus* sp. JS07, two libraries were constructed from samples with different nitrogen treatments (Control: 17.6mM of N and Treated: 4.4mM of N), and approximately 88 million raw reads have been generated by Illumina HiSeq™2000 sequencing device. After subjected to length based trimming and quality score; a total of 85.76 million high quality (HQ) reads and 12.67 Gb data were obtained.

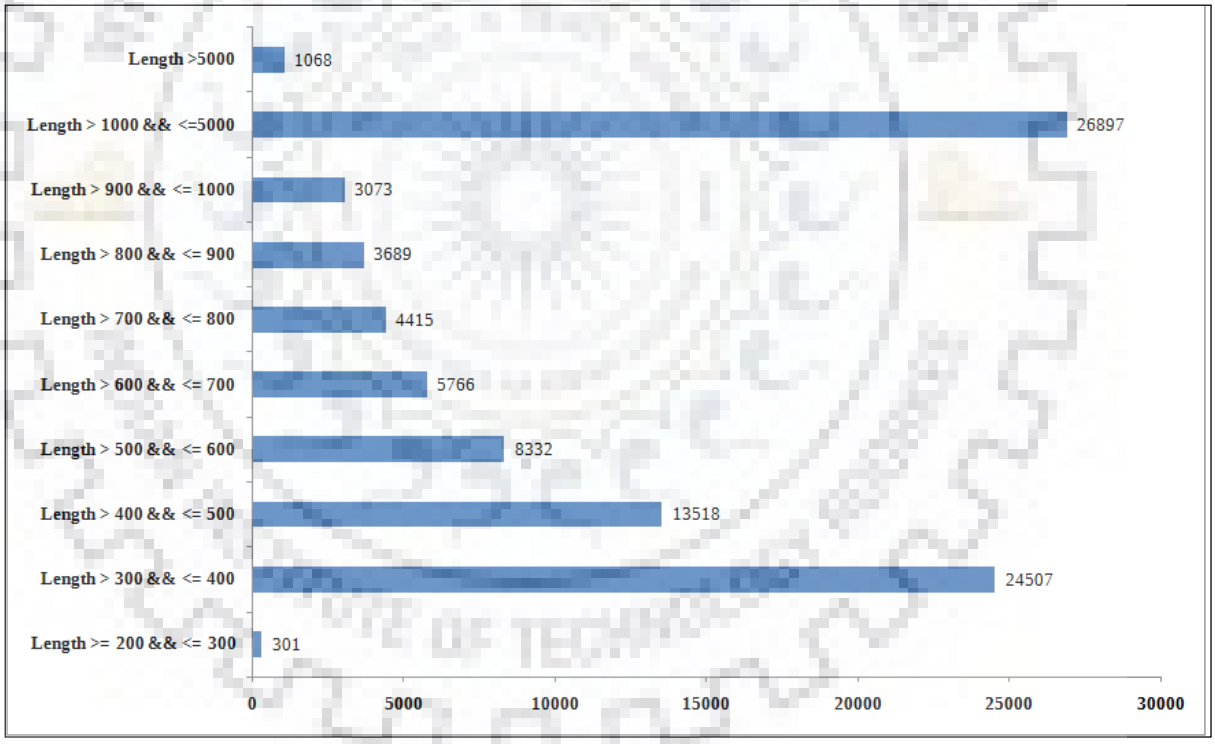

Fig. 5.2. Length distribution of assembled transcripts.

The high-quality reads were *de novo* assembled into 91,566 transcripts with an average length of 1008 bases and N50 of 1538 bases (Fig. 5.2). After clustered, 69,785 unigenes (non-redundant transcripts) ranging from 300bp to 13,214bp were generated with an average length of 921bp and N50 of 1349bp (Fig. 5.3).

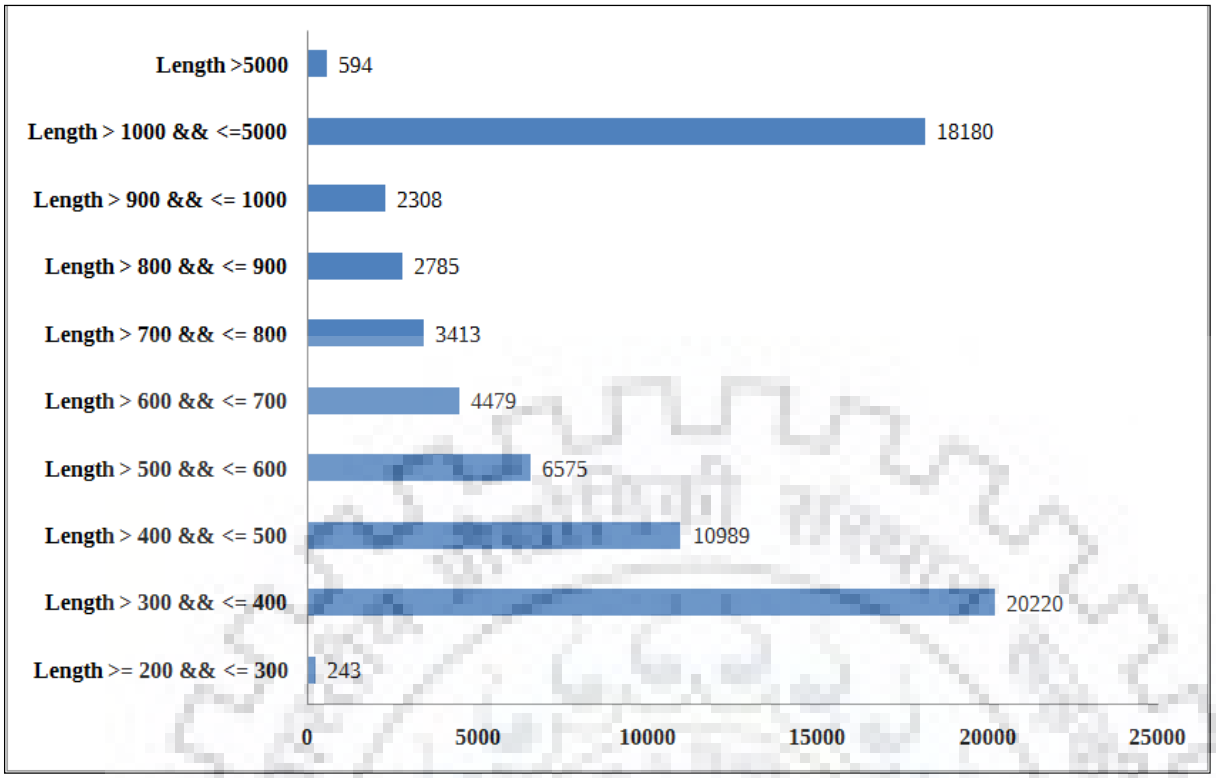

Fig. 5.3. Length distribution of unigenes.

5.3.2 Annotation and expression of Unigenes

For functional analysis of the unigenes, initially, the coding regions or sequence (CDS) prediction was performed using transdecoder. A total of 47,543 CDS regions were identified with an average length of 678bp and N50 of 804bp (Fig. 5.4). Functional annotation of the CDS was carried out using BLASTX search against NCBI's NR (Non-redundant) database. Out of 47,543 CDS, hits were obtained for 22, 471 and no hits were found for 25, 072 CDS. Top hit species distribution shows a close homology with *Monoraphidium neglectum* followed by *Chlamydomonas reinhardtii* (Fig. 5.5). About more than half of the CDS (25,072) could not be annotated to any existing genes, and this may be due to the presence of short ORFs and short of relevant genes.

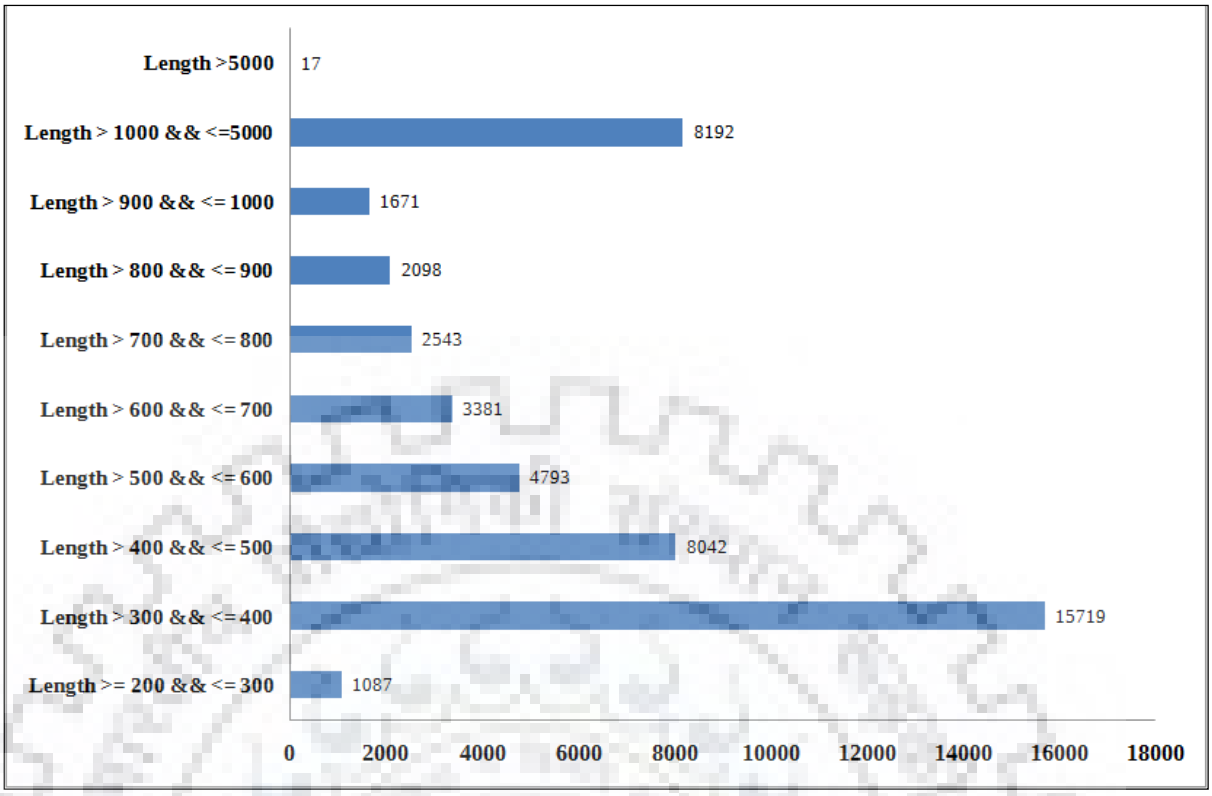

Fig. 5.4. Length distribution of predicted CDS

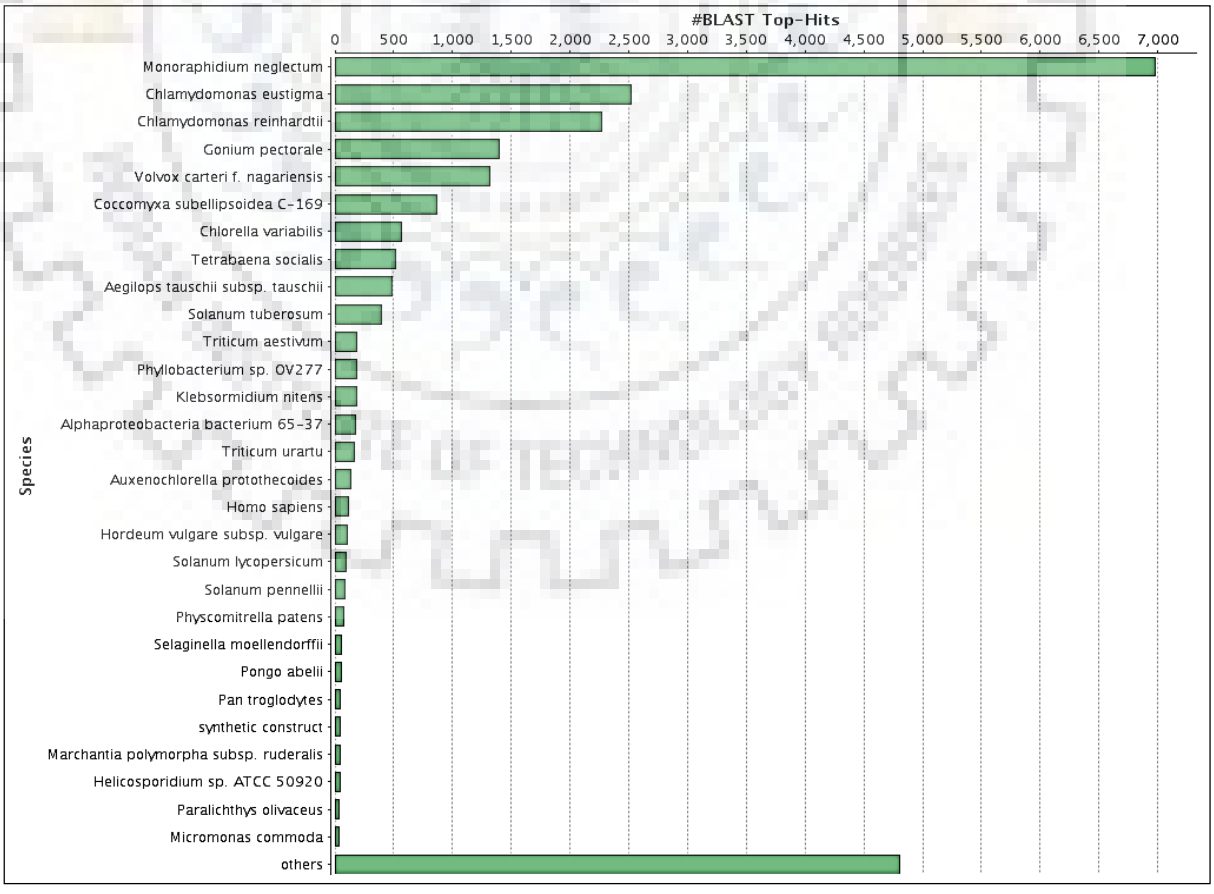

Fig. 5.5. The top-hit species distribution based on the blastx hits

The CDS sequences were subjected to GO analysis using Blast2GO Pro that categorized them into three domains. These cover: biological process (BP) consisting sets of molecular events pertinent to the functioning of the cell, tissues or organs; molecular function (MF) comprising the activities of a gene product at the molecular level; and cellular component (CC) which is mainly consisted the parts of the cell. A single CDS could fall to more than one category. A total of 9,788 assigned to GO, classes, with 7821 belonging to molecular functions followed by 6438 and 5003 to the biological process and cellular component. Bar chart representation of all the three GO domains was plotted using Blast2GO pro v4.1.5 at level 2 is shown in Fig. 5.6.

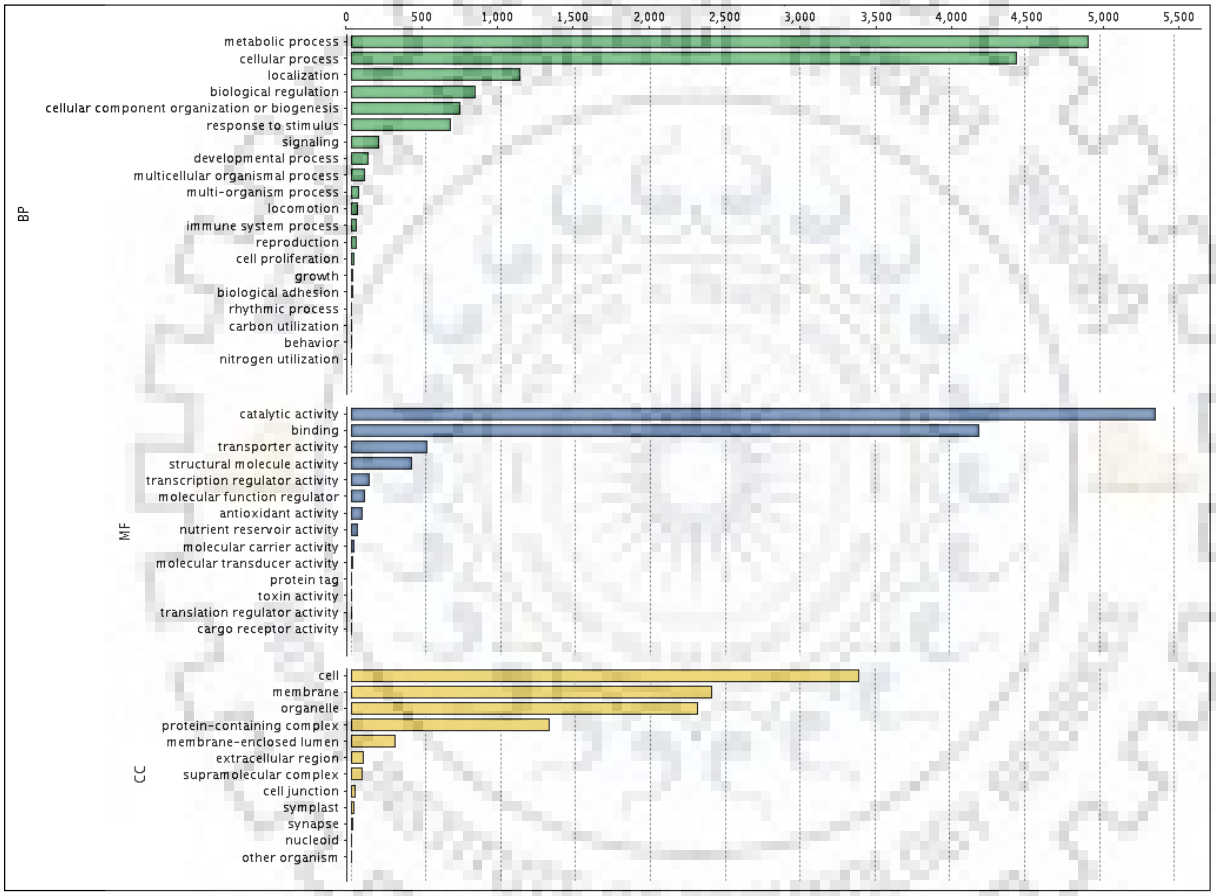

Fig.5.6. GO domain distribution in *Desmodesmus* sp. JS07

To perform the mapping of the CDS to the biological pathway in *Desmodesmus* sp. JS07, the unigenes were searched against the KEGG automatic annotation server (KAAS). The mapped unigenes represented the major metabolic pathways including lipid metabolic pathway, carbohydrate metabolism, terpenoid biosynthesis and amino acid synthesis. The mapped CDS also signified the genes related to the cellular processes, genetic information processing, membrane, and metabolism. Category wise CDS distribution is shown in Fig. 5.7.

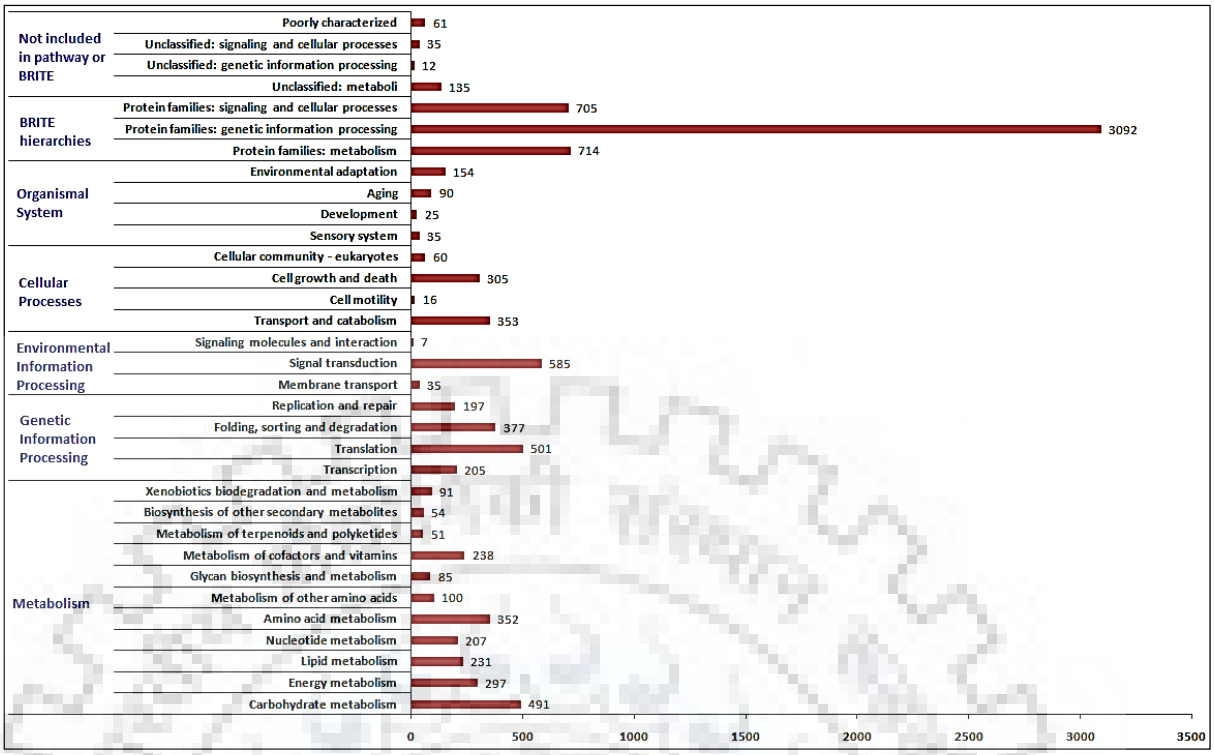

Fig. 5.7. KEGG pathway distribution in *Desmodesmus* sp. JS07

5.3.3 Differential gene expression analysis

Differential gene expression between the control and treated samples were quantified based on the FPKM approach. Based on the comparison between genes expression abundance of Sample 1 (nitrogen-limited condition) with that of Sample 2 (control) a total of 19,345 unigenes (CDS) were differentially expressed (Fig. 8) where 9337 unigenes were upregulated, and 10,008 were downregulated based on the log2fold change in nitrogen-limited condition. Venn diagram was made to categorize commonly and exclusively regulated genes in both the treatments under normal and nitrogen-limited conditions. Further, based on p-value (p-value <0.05), 425 unigenes were significantly up regulated, and 360 unigenes were significantly down regulated. Top 50 significantly expressed genes (i.e., highly up and highly down-regulated genes) were represented in the form of heat map using pheatmap package from R software. The color-coding ranges from red to green, where shades of red represent lowly expressed genes and shades of green represent highly expressed genes (Fig. 5.9).

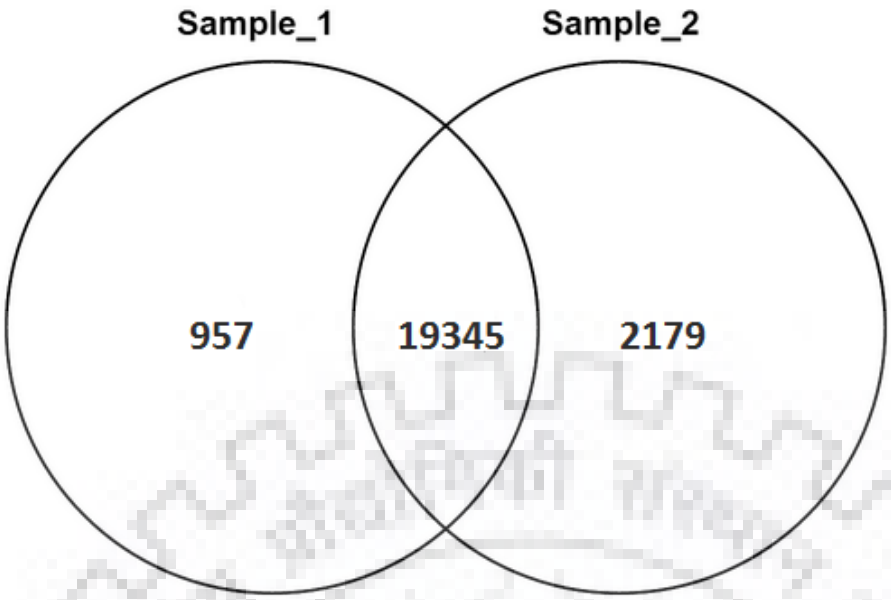

Fig. 5.8. Venn diagram representing sets of exclusively and differentially expressed CDS. The left circle represents the no of CDS expressed exclusively in sample1 (nitrogen limited), and the right circle represents the no of CDS expressed exclusively in sample2 (control).

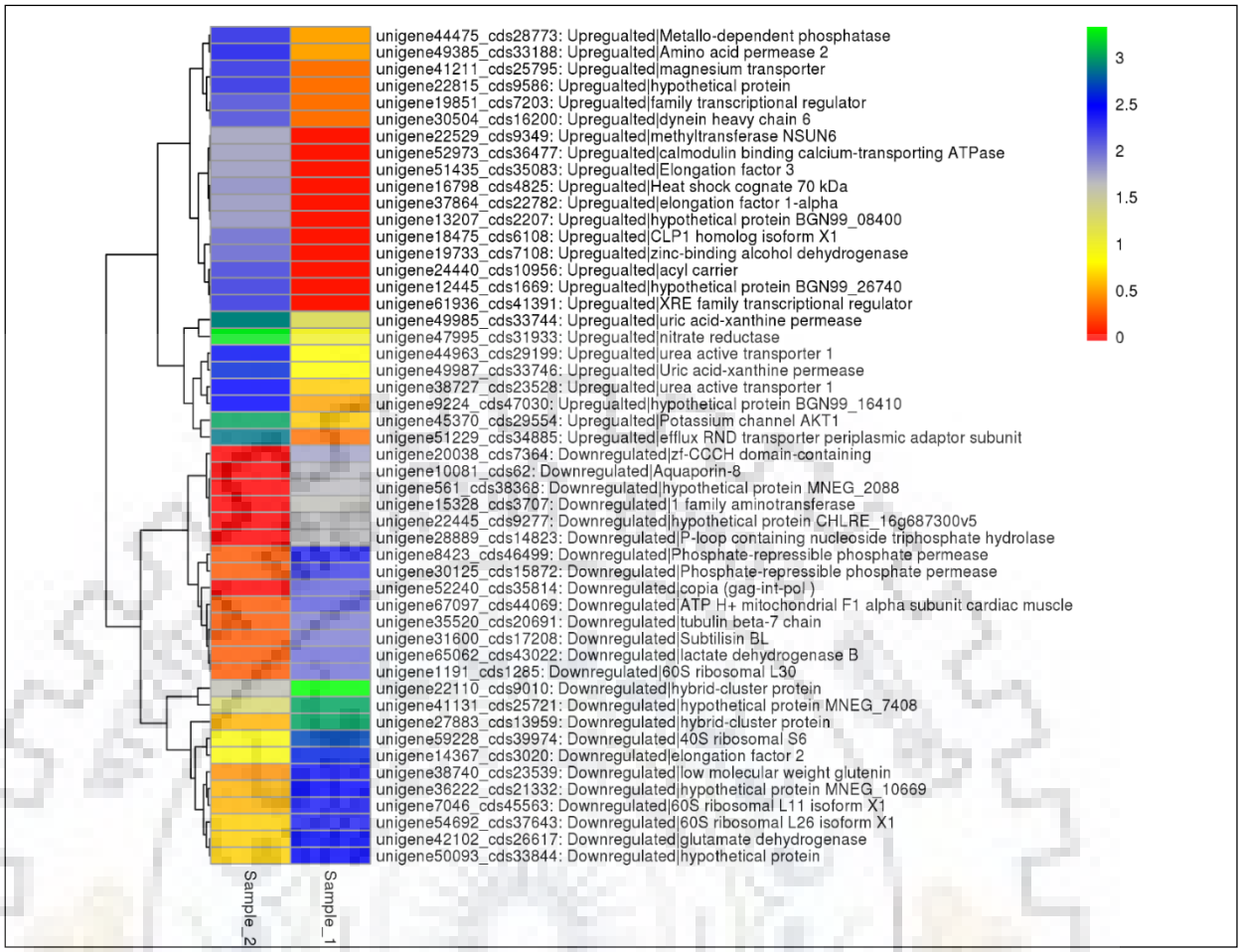

Fig. 5.9. Heat map representing top 50 highly up-regulated and highly down-regulated genes were plotted using log10 transformed basemean values. The CDS id appears at the immediate right of the heatmap followed by the hit description. Where sample 1, nitrogen limited, and sample 2, control.

5.3.3.1 Differential gene expression related to lipid accumulation

To depict the differential expression of genes involved in lipid biosynthesis, the lipid-related metabolic pathways encompassing fatty acid biosynthesis and triacylglycerol biosynthesis pathway were mainly focussed. Further, starch metabolism and other catabolic pathways were also analyzed in response to nitrogen-limited condition. The majority of the genes associated with the fatty acid biosynthesis were observed to be upregulated in nitrogen-limited conditions (Fig. 5.10).

The first committed step in fatty acid biosynthesis is the carboxylation of acetyl-CoA to form malonyl-CoA by the action of Acetyl-CoA Carboxylase (ACCase) and the gene encoding

ACCase was observed to upregulated under N-limited conditions. Subsequently, the initiation of fatty acid elongation occurs, which requires malonyl-CoA ACP transacylase (MAT) to transfer malonyl group to an acyl carrier protein (ACP) giving rise to malonyl ACP. The expression of MAT gene was observed to be upregulated under nitrogen limitation. This step is followed by the successive round of condensation reaction catalyzed by beta-ketoacyl-ACP synthase (KAS), reduction reaction catalyzed by beta-ketoacyl-ACP reductase (KAR), dehydration reaction by beta-hydroxy acyl-ACP dehydrase (HAD) and again reduction step catalyzed by enoyl-ACP reductase (EAR) (Huang et al., 2016). The expressions of gene encoding KAS (III), KAR, HAD, and EAR upregulated while KAS (II) is downregulated under N-limited conditions (Fig. 11). This cycle repeats six or seven more times to form C16:0-ACP and C18:0-ACP. These mature fatty acids either retained in the plastid where acyl transferase (AT) transferred it to glycerol-3-phosphate for the generation of membrane lipids; or exported to the cytosol where it is hydrolyzed by Oleoyl-ACP thioesterase (OAT) generating palmitic and stearic acids, the end product of fatty acid synthesis. The gene encoding thioesterase was observed to upregulated under N-limited conditions, which is involved in reducing the feedback inhibition that partially regulates the production of fatty acid biosynthesis and led to the overproduction of fatty acids; as also previously reported in microalga *P. tricornutum* (Rismani-Yazdi et al., 2012). Furthermore, the upregulation of gene encoding acyl-ACP desaturase (AAD) and down-regulation of delta-12 desaturase and delta-15 desaturase were observed denoting the enrichment of C18:1 during nitrogen-limited condition.

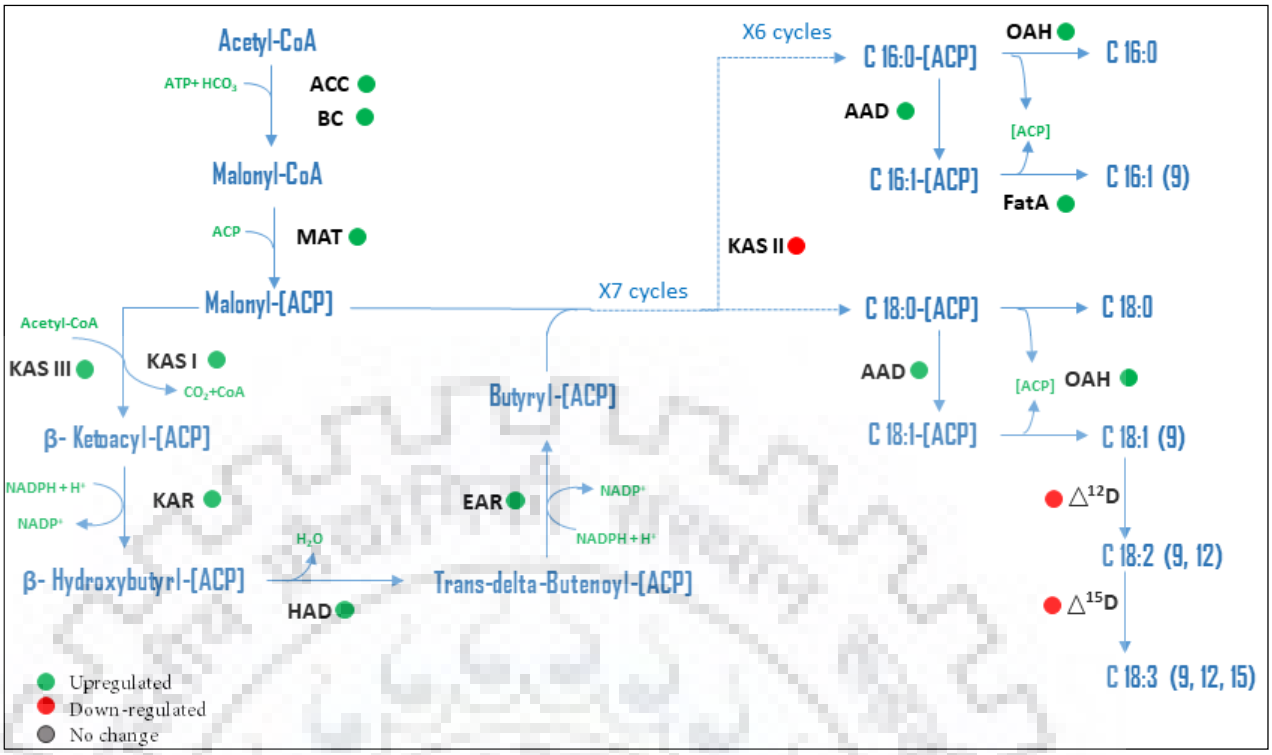

Fig. 5.10. Expression profile of genes related to fatty acid biosynthesis. "ACC, acetyl-CoA carboxylase; AAD, acyl-ACP desaturase; BC, Biotin carboxylase; Δ12D, Δ12(ω6)-desaturase; Δ15D, Δ15(ω3)-desaturase; EAR, enoyl-ACP reductase; FatA, Acyl-ACP thioesterase A; HAD, beta-hydroxy acyl-ACP dehydrase; KAS, beta-ketoacyl-ACP synthase; KAR, beta-ketoacyl-ACP reductase; MAT, malonyl-CoA ACP transacylase and OAH, oleoyl-ACP hydrolase".

TAG biosynthesis in algae is mediated by two pathways: an acyl-CoA dependant pathway, the acyl-CoA independent pathway, and the Kennedy pathway (Ohlrogge and Browse, 1995). The necessary genes involved in TAG biosynthesis were identified in the transcriptome data and displayed changes in their expression in response to nitrogen limitation (Fig 11).

Biosynthesis of TAG begins by using two building blocks, the one is acyl CoA, and other is glycerol-3-phosphate. For Kennedy pathway, acyl-CoA transfers the two consecutive acyl moieties to glycerol-3-phosphate at position 1 and 2 to form lysophosphatidic acid and phosphatidic acid respectively, which is Afterwards dephosphorylated to form 1,2-diacylglycerol and then converted to TAG. These enzymes included in the respective steps of the Kennedy pathway are glycerol-3-phosphate acyltransferase (GPAT), acyl-glycerol-3-phosphate acyltransferase (AGPAT), phosphatidate phosphatase (PP), and diacylglycerol acyltransferase (DGAT). The expression of genes encoding GPAT, AGPAT, and DGAT, were observed to be upregulated under nitrogen-limited condition. Whereas, the expression of gene encoding PP and PDAT remained unchanged. The last step of the Kennedy pathway which is catalysed by DGAT,

plays a crucial role in determining the carbon flux towards TAG production (Liu et al., 2012). DGAT was also observed to be upregulated in micrpalgal strains in response to varying conditions accompanied by TAG accumulation (Boyle et al., 2012; Gwak et al., 2014). Overexpression of DGAT was found to remarkably enhanced the TAG accumulation in plant and microalgae (Iwai et al., 2014; Sanjaya et al., 2013).

Besides, Glycerol-3-phosphate dehydrogenase (GPD) and glycerol kinase (GK) which diverted the glycolytic flux towards TAG biosynthesis by providing glycerol-3-phosphate, a precursor for TAG and were significantly upregulated under nitrogen-limited conditions. Overexpression of GPD was reported to strongly enhanced the TAG content in plants and microalgae (Lu et al., 2017; Vigeolas et al., 2007)

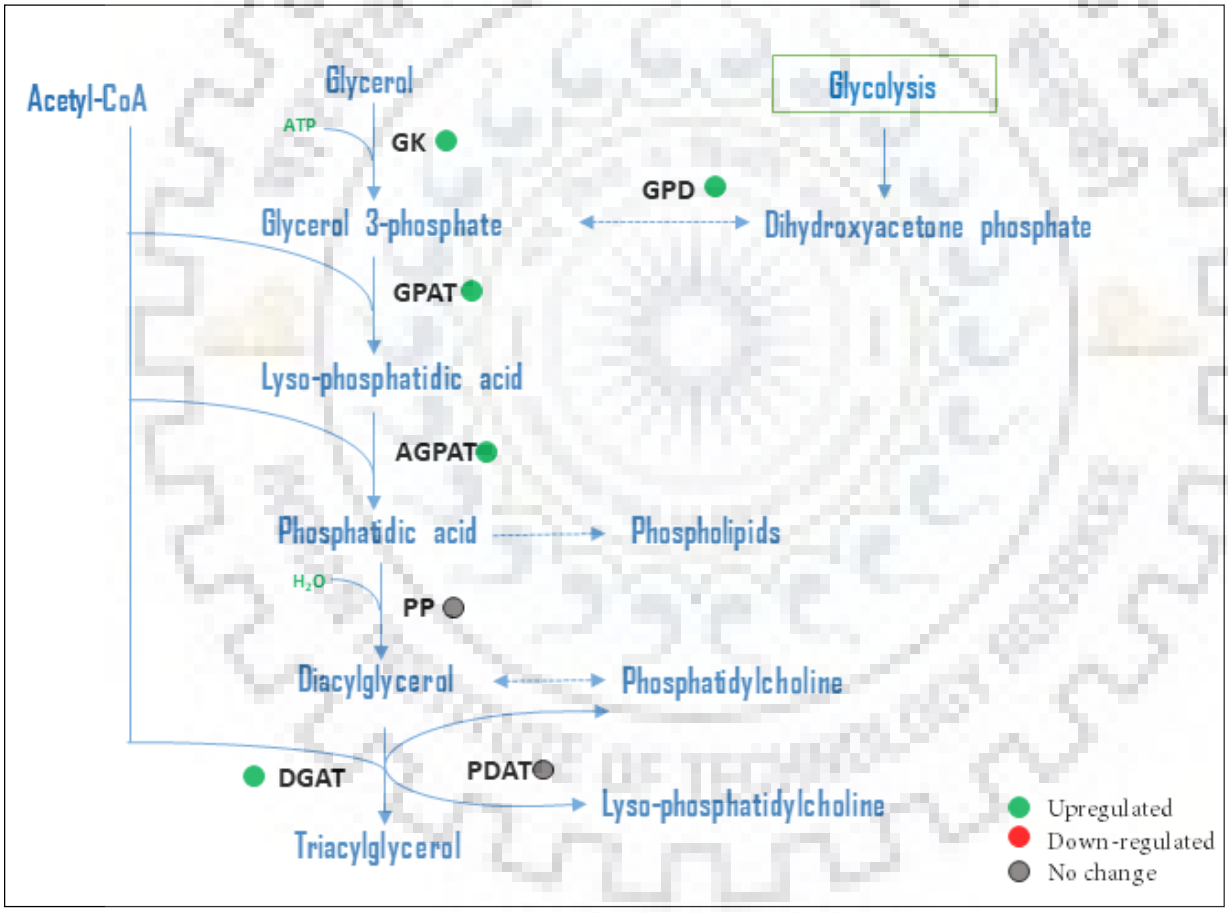

Fig. 5.11 Expression profile of genes related to triacylglycerol biosynthesis. "AGPAT, 1-acyl-sn-glycerol-3-phosphate O-acyltransferase; DGAT, diacylglycerol O-acyltransferase; GK, glycerol kinase; GPAT, glycerol-3-phosphate O-acyltransferase; PP, phosphatidate phosphatase and PDAT, phospholipid diacylglycerol acyltransferase".

5.3.3.2 Differential gene expression related to Starch synthesis and β-oxidation under nitrogen limitation

Our transcriptome analysis showed while the gene encoding starch synthase (SS) was upregulated under nitrogen limited condition, many genes associated with the starch synthesis mainly PGM and AGPase were down-regulated as shown in Fig. 5.12. Thus, indicating that the starch biosynthesis pathway might be repressed, resulting in overall low starch contents and microalgae preferred to synthesize lipids rather than starch under N-limitations. However, the genes associated with the starch catabolism, specifically α-amylase that hydrolyzes starch to glucose, was down-regulated suggesting that the microalgal cells under N-limitation maintained starch levels by repressing starch degradation and these findings are in agreement with the earlier report of *Chlorella sorokiniana* (Li et al., 2016). Moreover, our transcriptome data revealed that the genes associated with the glycolysis, specifically the three subunits of the pyruvate dehydrogenase complex, which convert the glucose to acetyl- CoA were up-regulated under nitrogen-limited conditions. Glycolysis generates pyruvate and other high energy compounds, which are essential for fatty acid biosynthesis (Plaxton, 1996).

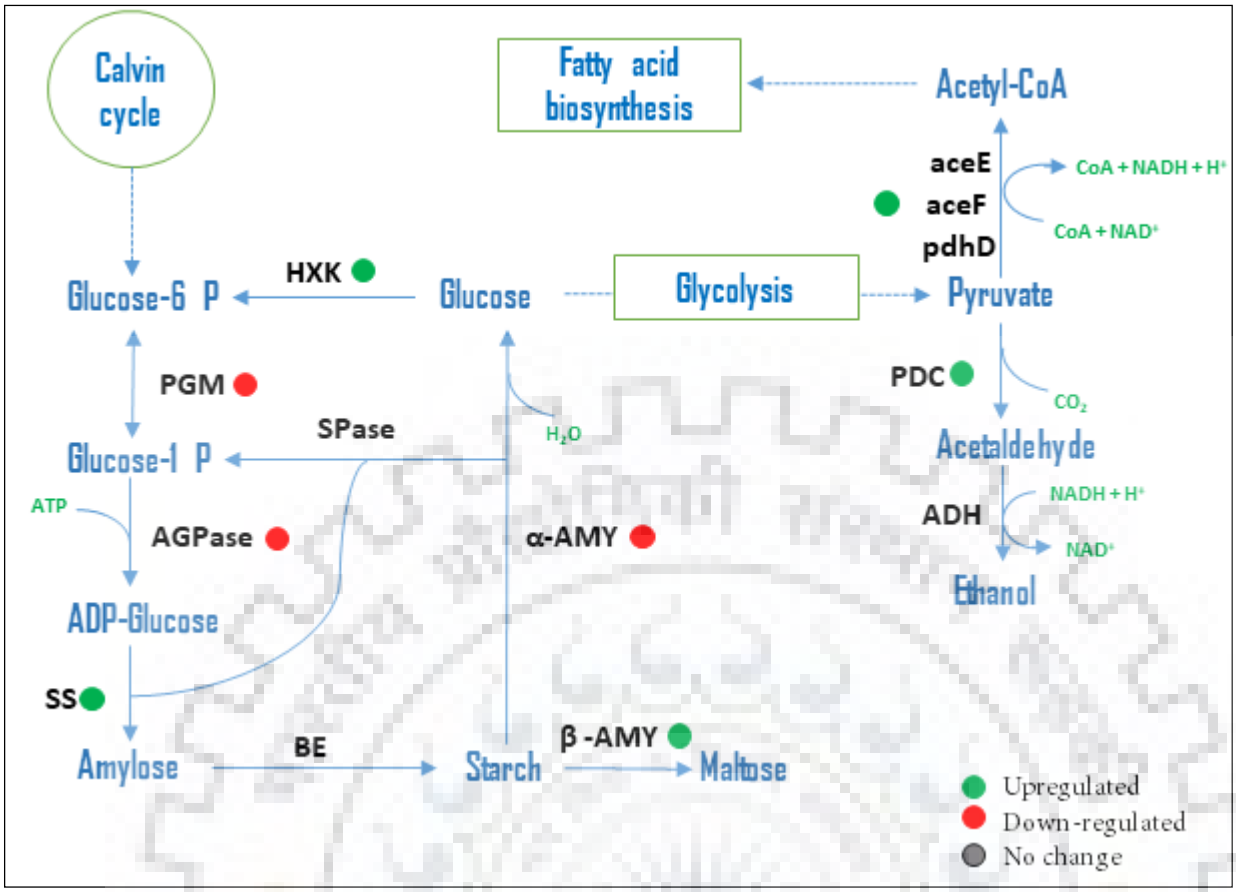

Fig. 5.12. Expression profile of genes related to starch biosynthesis. "aceE, pyruvate dehydrogenase; aceF, pyruvate dehydrogenase; ADH, alcohol dehydrogenase; AGPase, ADP-glucose pyrophosphorylase; α-AMY, α-amylase; BE, α-1,4-glucan branching enzyme; β-AMY, β-amylase; HXK, hexokinase; PDC, pyruvate decarboxylase; pdhD, dihydrolipoamide dehydrogenase; SS, starch synthase and SPase, starch phosphorylase".

Furthermore, we found the down-regulation of the β-oxidation pathway (ACox1 and ACAT) in nitrogen limited conditions (Fig 5.13), indicating that the fatty acid oxidation might be inhibited to enhanced the TAG pool under the stress conditions. This result was also reported in *Neochloris oleoabundans* (Rismani-Yazdi et al., 2012).

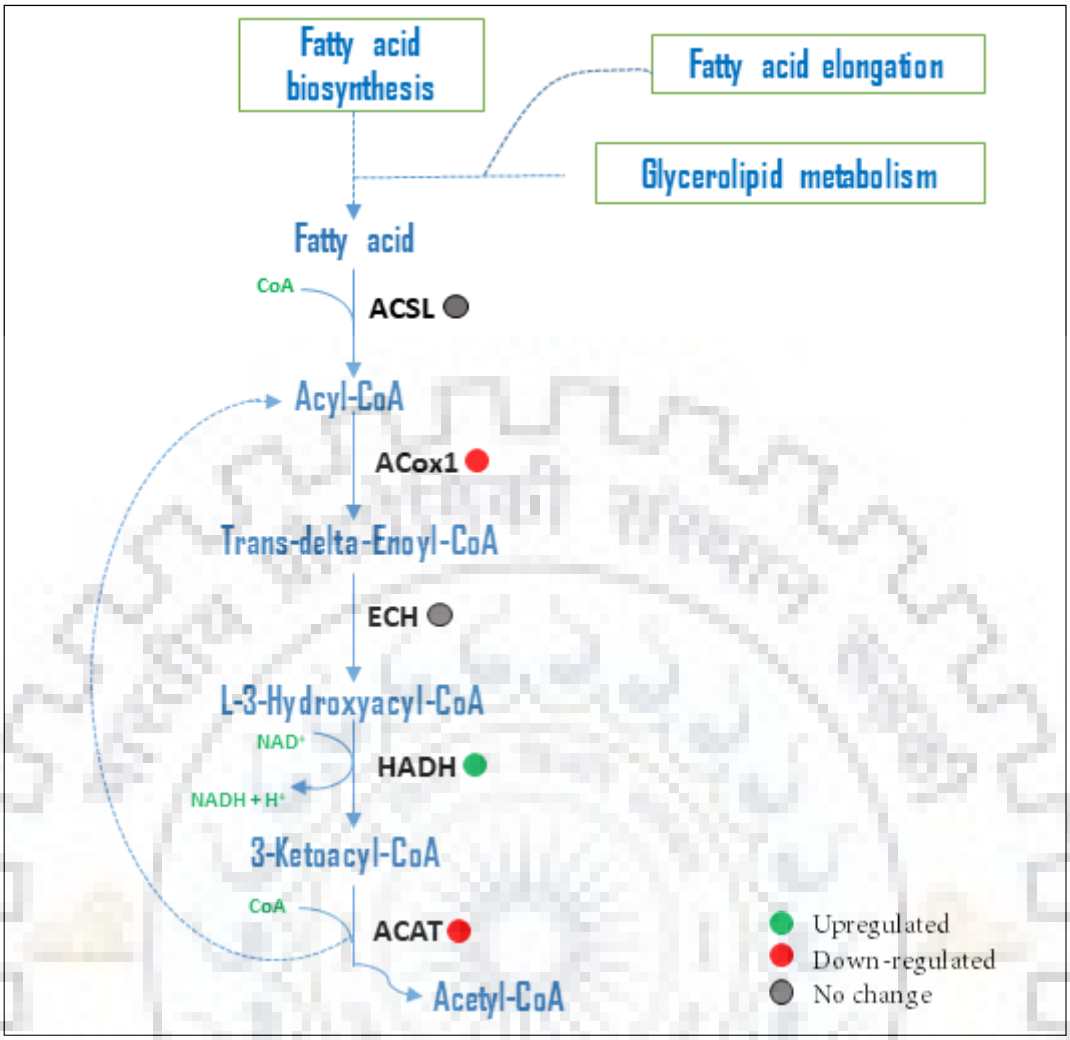

Fig. 5.13. Expression profile of genes related to β-oxidation. "ACS, acyl-CoA synthetase; ACOX1, acyl-CoA oxidase; ACAT, acetyl-CoA-acetyltransferase; ECH, enoyl-CoA hydratase and HADH, 3-hydroxy acyl-CoA dehydrogenase".

5.3.4 Transcription Factor Analysis

Identification of the abundant transcription factor families was carried out using blastx analysis. Transcription factors play essential roles in response to stress conditions by modulating the gene expression. After searched against all the transcription factor database of PlantTFDB, 2159 transcripts were observed to have homologous sequences and were consigned into 31 families (Fig 5.14). The most abundant transcription factor families were C3H family, followed by the bHLH transcription factor family in microalgae *Desmodesmus* sp. JS07. C3H transcription factors were reported to play a significant role during embryogenesis in Arabidopsis (Yadegari et al., 1994).

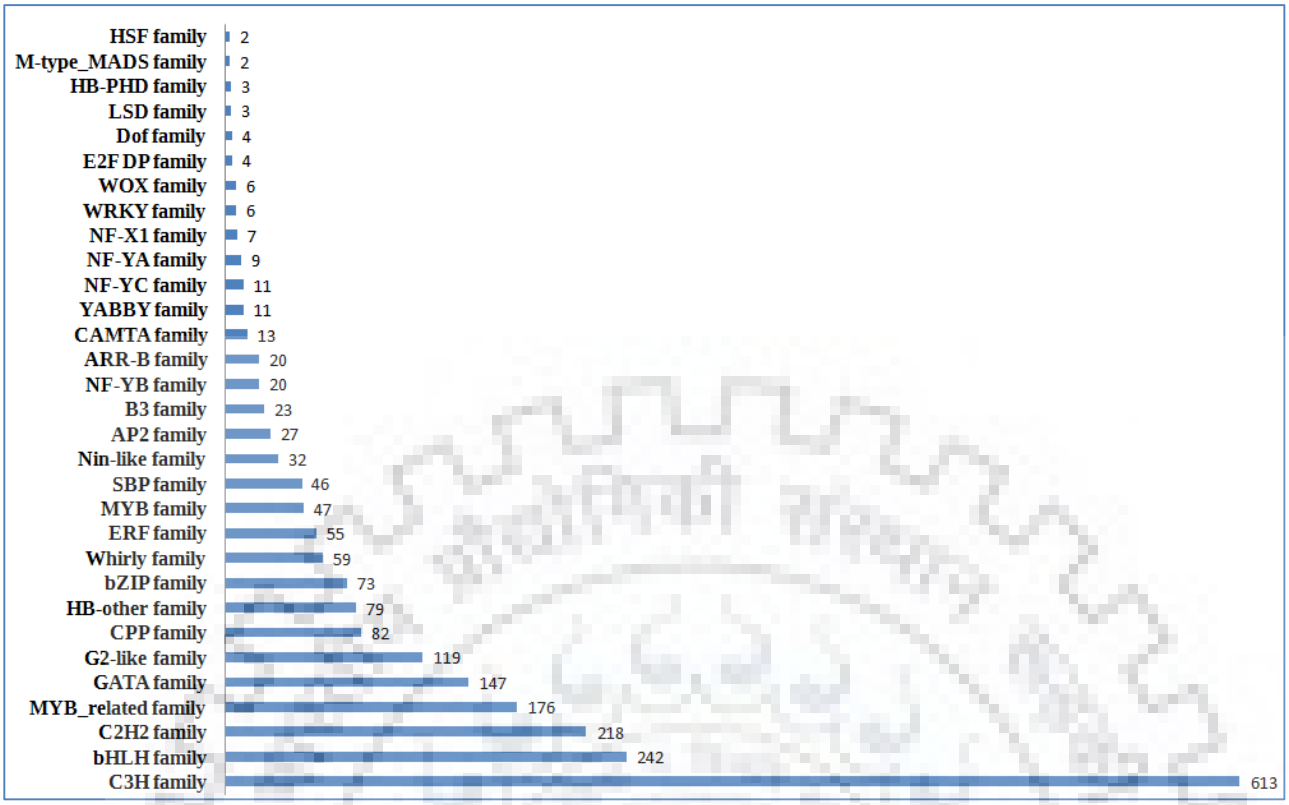

Fig. 5.14. The transcription factor family distribution in *Desmodesmus* sp. JS07

Besides, the differential expression of transcription factors was also studied, and it was observed that 82 transcripts assigned to 31 families of different transcription factors were found to be differentially expressed. Among them, 43 transcripts were up regulated while 39 were down-regulated in response to nitrogen limitation. So far, it has been identified that bHLH family transcription factors were involved in regulating lipid biosynthesis in plants (Courchesne et al., 2009). In the present work, bHLH34 transcription factor was observed to be upregulated in the nitrogen-limited condition that denotes the importance of the bHLH family. Likewise, most of the transcription factor families such as MYB related, SBP, and C3H family were also observed to be up-regulated in *Chlamydomonas reinhardtii* under nitrogen starvation (Ibáñez-Salazar et al., 2014). Therefore, the regulation of these transcription factors would be a promising strategy to enhance lipid content in microalgae.

5.4. Conclusion

The transcriptome and differential gene expression of *Desmodesmus* sp. JS07 under nitrogen-limited and normal conditions facilitated the investigation of a broad diversity of genes and pathways that encompass the metabolic responses associated with lipid accumulation. In this study, RNA-seq techniques were used to analyze the differential gene expression profile of

Desmodesmus sp. JS07 that revealed the up-regulation of potential genes related to fatty acid and TAG biosynthesis. Further, the down-regulation of genes associated with starch biosynthesis providing an extra pool of fatty acids for TAG synthesis under nitrogen-limited conditions. Transcriptome analysis not only provides the datasets of *Desmodesmus* sp. JS07, but also biological insights into the expression of genes related to lipid accumulation. These identified gene sequences, including the transcription factors during enhanced TAG accumulation under N-limitation, could be leveraged in future metabolic modification approaches in microalgae that led to sustainable biofuel production.

Part a: Heterologous expression of BnDGAT in *Desmodesmus* sp. JS07

6a.1. Introduction

Nowadays, there has been an increasing interest in exploring microalgae for the production of biodiesel as they have higher growth rate, rely on photosynthesis, absorb a large amount of CO_2 and occupy less land (Lu et al., 2017). Equivalent to most plants, microalgae accumulate lipids in the form of triacylglycerol (TAG), a precursor for biodiesel production (Mubarak et al., 2014). Nonetheless, the commercially viable production of these has been restricted as the TAG yields from the algal strains presently used for the biodiesel production are far less than the theoretical maximum (Chisti, 2007), and efforts have been made for achieving an increased yield of the TAG. The understanding of the regulatory mechanism and pathways involved in lipid synthesis would facilitate the genetic manipulation of microalgae for the enhanced level of the TAG biosynthesis.

The lipid biosynthesis in microalgae has been reported to be mediated mainly via two pathways, fatty acid and TAG synthesis that occurs in the chloroplast and the endoplasmic reticulum respectively (Wei et al., 2017). The later pathway starts from glycerol-3-phosphate and four enzymes are involved in the synthesis of TAG comprising of glycerol-3-phosphate dehydrogenase (GPD), lysophosphatidic acyltransferase (LPAAT), glycerol-3-phosphate acyltransferase (GPAT) and diacylglycerol acyltransferase (DGAT) (Griffiths and Harrison, 2009). The last step mediated by DGAT employs transfer of acyl moiety from acyl-CoA to the sn-3 position of DAG for TAG assembly. DGAT is believed to play an important role in TAG biosynthesis as it catalyzes the committed step of the Kennedy pathway. Therefore, efforts have been focused on DGAT and its overexpression in plant and algae for enhanced TAG accumulation.

Nowadays, modulated overexpression of genes related to the Kennedy pathway looks to be a viable and productive approach for achieving higher TAG accumulation in algae. In plants, DGAT was observed as one of pivotal enzyme and has been attempted for increasing its expression in *Nicotiana tabacum, Arabidopsis thaliana* and *Brassica napus* that led into enhanced TAG levels (Andrianov et al., 2010; Sanjaya et al., 2013; Zou et al., 1997). Not much

information for genetic transformation of this enzyme is available in microalgal strains up to now. Recently, the overexpression of DGAT1 in microalga, *Nannochloropsis oceanica* regulates TAG biosynthesis and its composition (Wei et al., 2017). Similarly, an augmented lipid production in green microalga *Chlamydomonas reinharditii* was observed by the introduction of *Brassica napus* DGAT2 (Ahmad et al., 2015). Moreover, Wagner et al., 2010 had also detected three putative type-2 DGAT genes in the microalga *Ostreococcus tauri* and transformed OtDGAT2A and B into *Saccharomyces cerevisiae* that led into improved TAG accumulation.

Advances in the genomics of microalgae have enabled into approaches for molecular modification of TAG biosynthesis cascade. *De novo* transcriptome analysis of microalgae *Desmodesmus* sp. JS07 grown under nitrogen-limited conditions in our laboratory revealed the upregulation of the genes associated with the TAG biosynthesis, including DGAT1 and DGAT2. Thus to evaluate the potential impact of DGAT2 in the regulation of lipid accumulation, we had attempted to transform the *Desmodesmus* sp. JS07 with the heterologous construct containing type-2 DGAT gene from *Brassica napus* for achieving the enhanced levels of DGAT2 expression. Molecular analysis of the transformants harboring BnDGAT2 was authenticated by PCR and eGFP expression. Impact of heterologous expression of BnDGAT2 on lipid accumulation and fatty acid profile was analyzed.

Materials and Methods

6a.2.1. Microalgae strain and culture conditions

The microalgae *Desmodesmus* sp. JS07 was used in this study. The strain was maintained in BG11 media at 25 ± 2^0C under continuous illumination from white fluorescent lamps at 200 μEm^{-2} s^{-1} at 150 rpm. IN this study, the strain was grown in TAP (Tris-acetate phosphate) medium comprising: Tris (hydroxymethyl) amino methane (2.42 g/L) (pH 7.0), NH_4Cl (375 mg/L), K_2HPO_4 (108 mg/L), $MgSO_4.7H_20$ (100 mg/L), KH_2PO_4 (54 mg/L), $CaCl_2.2H_2O$ (50 mg/L), glacial acetic acid (1 mL/L) and trace metal solutions (1 mL/L). Trace metals stock solution was prepared by using: EDTA disodium salt (50 g/L), $ZnSO_4.7H_2O$ (22 g/L), KOH (17 g/L), H_3BO_3 (11.4 g/L), $MnCl_2.4H_2O$ (5.06 g/L), $CoCl_2.6H_2O$ (1.61 g/L), $Cu.SO_4.5H_2O$ (1.57 g/L) and $(NH_4)6Mo_7O_{24}.4H_2O$ (1.10 g/L).

6a.2.2 Construct for overexpression of BnDGAT in *Desmodesmus* sp. JS07

The pAlgae-DGAT-eGFP construct (Fig 1) of size 7283 bp was a kind gift from ICGEB, New Delhi, India. The cassette containing 'BnDGAT2-6XHISKDEL-NOS-PolyA-35Sde-eGFP-

ocspolyA' fragment was cloned in the pCHLAMY_1 vector (4283 bp) as defined by Ahmad et al., 2015. It contained the DGAT2 (diacylglycerol acyl transferase) gene from *Brassica napus* fused with '6XHIS and KDEL-NOSPolyA sequences'. Hsp70-RbcS2 promoter and 35Sde regulated the expression of BnDGAT2 and eGFP reporter gene respectively. It had hygromycin resistance gene (Aph7) with β-tubulin promoter as a selectable marker for algae. The construct was maintained into DH5α cells and were selected on LB plates consisting 100µg/ml ampicillin.

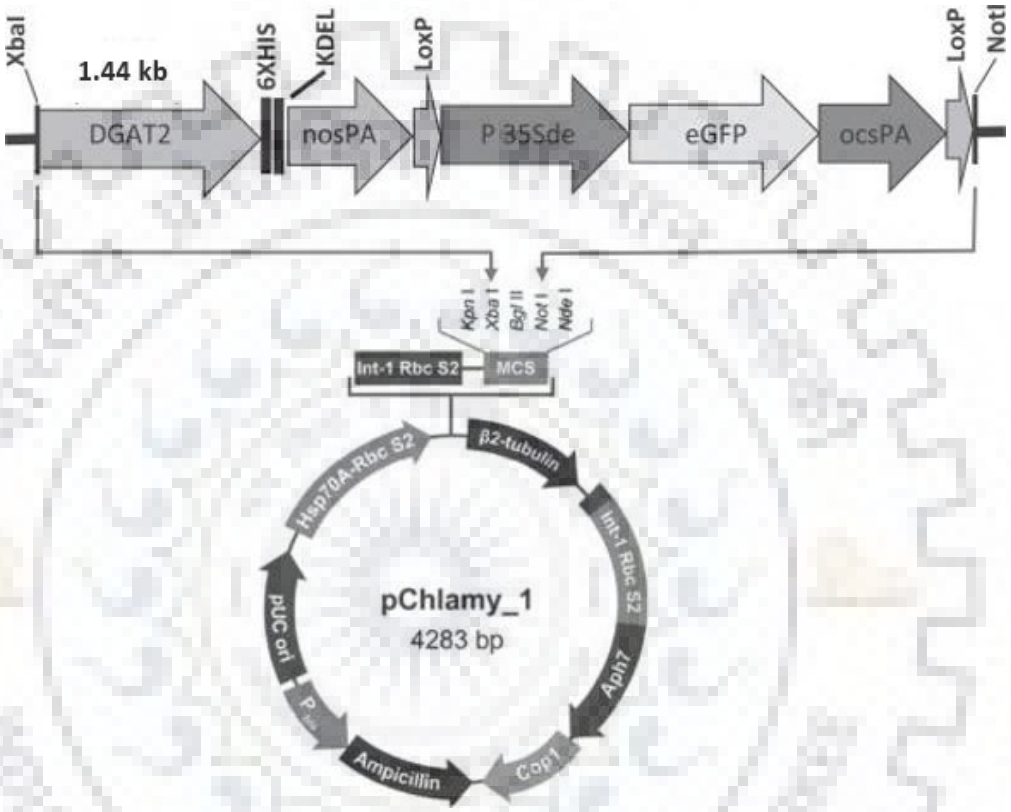

Fig. 6a.1 pAlgae-DGAT-eGFP construct

6a.2.3. Minimal inhibitory concentration (MIC) of antibiotic on *Desmodesmus* sp. JS07

The minimal inhibitory concentration of hygromycin B on microalgae *Desmodesmus* sp. JS07 was enumerated. Microalgal cells (1×10^8) were grown on TAP agar plates supplemented with hygromycin B to the concentrations ranging from 0 - 250 µg/ml. Cells were incubated for twenty days and the concentration above which no growth of strain was observed, was selected as a minimal inhibitory concentration and used for the selection of transformants.

6a.2.4. Microalgal transformation

Desmodesmus sp. JS07 cells in the exponential phase (OD_{750}=0.4-0.6) were collected by centrifugation at 3000 rpm for 15min at 4°C. Pellet was washed with TAP medium having 40

mM sucrose solution and re-suspended in the same medium to a final concentration of 10^8 cells/ml. 250µl this suspension was transferred to a 4 mm electro-cuvette. 4µ g of the linearized 'pAlgae-DGAT-eGFP' construct was then added to the suspension and were kept on ice for 20min. Electroporation was performed using a GenePulser (Bio-Rad, USA) set at the 2KV voltage and for 4ms. The electroporated cells were recovered in the dark for 15 min on ice and transferred into 10ml fresh TAP medium having 40 mM sucrose solution. The cells were incubated in the dark for 24hr at 25ºC with continuous agitation at 130 rpm before plating on the selective media. The plates were incubated under continuous light for 20-25 days until the green colonies appeared on the TAP media with 150 µg/ml hygromycin.

6a.2.5. Analysis of transformation

Transformed and untransformed *Desmodesmus* sp. JS07 cells in the exponential phase were collected, and genomic DNA was extracted by the DNeasy plant mini kit (Qiagen GmbH, Hilden, Germany) The BnDGAT2 gene integration in the transformed cell lines were confirmed by PCR using the *B. napus* DGAT2 DNA sequence-specific primers (F-5´GATTCTGCCTTCTTATCAGGTGACAC3´ and R-5´CGAACCATCCATTTGTGAACAGG3´). PCR was performed with: initial denaturation for 2 min at 95 °C followed by denaturation for 30 s at 95 °C, annealing for 30 s at 58 °C and extension for 1 min at 72 °C for 30 cycles, then the final extension for 10 min at 72 °C. The PCR product was examined on a 1% agarose gel.

6a.2.6. Evaluation of GFP expression

Transformed *Desmodesmus* sp. JS07 cells were subjected for evaluation for GFP expression using fluorescence microscope (EVOS-FL, Advance Microscopy Group, AMG, USA) with an excitation filter at 480 nm and emission at 527 nm.

6a.2.7. Protein extraction

Transformed and untransformed *Desmodesmus* sp. JS07 cells (50 ml) at exponential phase, were harvested by centrifugation for (8000 rpm, 10min). The pellet was resuspended in lysis buffer containing 20mM Tris-HCl, pH, 7.4, 1mM EDTA, 200mM NaCl, and 10 mM β-mercaptoethanol. Cells were subjected to three-lysis cycle (82.8 kPa, 4 °C) in a French pressure cell. The cell-free extract was obtained by centrifugation (8000 rpm, 10min) at 4 °C, and protein concentration was determined using the Bradford method (Thermo Fisher Scientific India Pvt.

Ltd., Mumbai, India). Proteins were electrophoresed in 12.5% polyacrylamide gels and visualized by staining with Coomassie Brilliant Blue R- 250.

6a.2.8. Western blot analysis

Crude proteins (about 20 μg) from the transformed and untransformed cells were resolved by SDS-PAGE (Mini protein Tetra cell Bio-Rad) and electrophoretically transferred to Hybond-C membranes (GE Healthcare) by applying 100 V for 75 min. The protein was identified by western blot using the primary antibody: purified monoclonal mouse Anti-His antibodies (Sigma, St. Louis, MO) (1:15000 dilutions) followed by secondary antibodies (Sigma) (1:1500 dilutions), coupled to Horse Radish Peroxidase (HRP). Western blots were developed using ECL western blotting detection reagent (Pierce) as per the manufacturer's instructions.

6a.2.9. Visualization of lipid globules by Nile Red fluorescence

The distribution of lipid globules in microalgal cells was detected by fluorescence microscopy (60X) using Nile Red. The Nile Red staining was performed as described in section 2.2.3.2.

6a.2.10. Lipid extraction and quantification

The microalgal biomass was harvested after 15 days of cultivation (late log phase) by centrifugation and lyophilized. The extraction of lipids from the lyophilized biomass (100mg) was performed by using Bligh and Dyer's method as described in section 2.2.3.3.

6a.2.11.Fatty acid methyl esters (FAMEs) profiling

For fatty acid methyl esters (FAMEs) analysis, transesterification of the total lipids (~100mg) was performed using 1 mL of 2% (v/v) sulphuric acid in methanol. Afterwards, the samples were incubated at 60^{o}C for 3hr and FAMEs were extracted using hexane (1 mL) and then vortexing for 5 min. 500 μL of this hexane containing FAMEs was then used for GC-MS analysis as described in section 2.2.3.5.

6a.3. Results and discussion

6a.3.1 Selective marker for genetic engineering of *Desmodesmus* sp. JS07

The minimal inhibitory concentration (MIC) of Hygromycin B (HygB) for *Desmodesmus* sp. JS07 on TAP agar plate medium (0- 250μg/ml) was detected. For that, plates containing approx. 10^8 *Desmodesmus* sp. JS07 cells were incubated at 25 °C and monitored daily. As shown in Fig

6a.2, there was no growth observed for *Desmodesmus* sp. JS07 at 150 µg/ml of hygromycin. Thus, HygB at the concentration of 150 µg/mL was used for the selection of transformants.

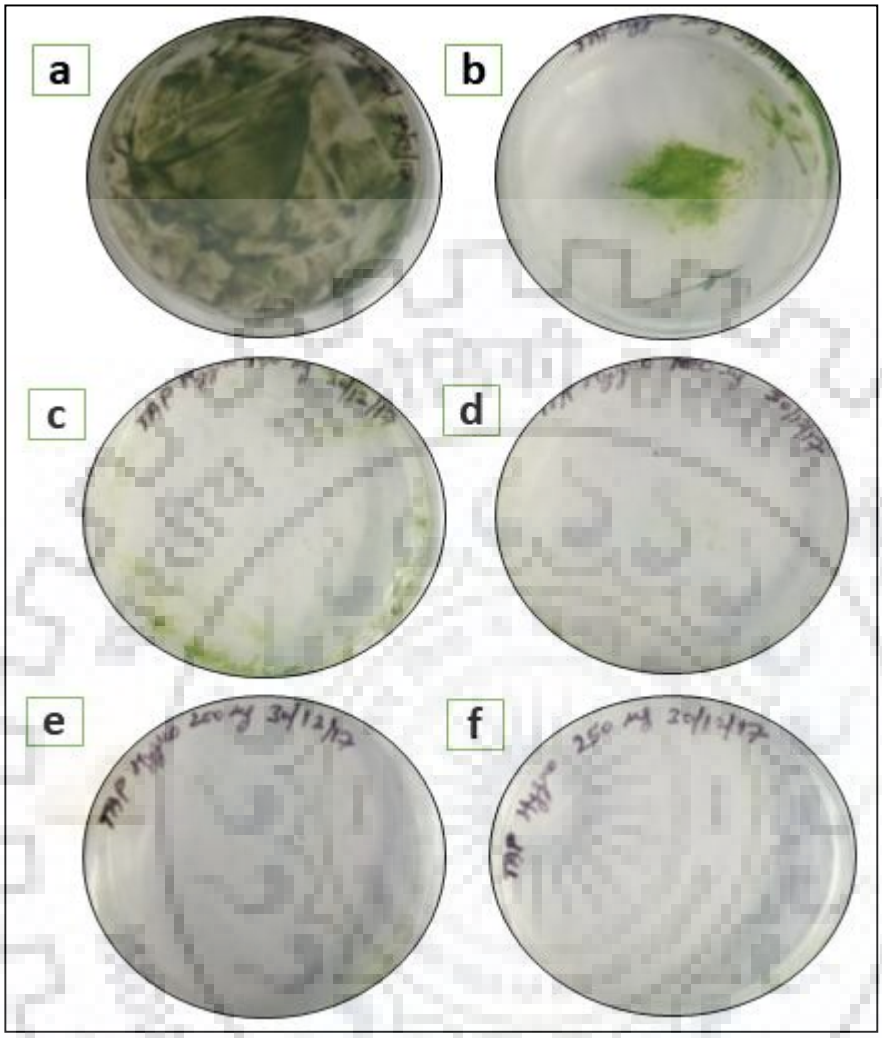

Fig 6a.2. Growth of *Desmodesmus* sp. JS07 at a varying concentration of hygromycin on the in TAP medium; a cell growth without antibiotic; b-f, cell growth at 50, 100,150,200 and 250 µg/mL Hyg-B respectively.

6a.3.2 Transformation of microalgae

The microalga *Desmodesmus* sp. JS07 was transformed with the construct pAlgae-DGAT-eGFP via electroporation. Initially to derive a viable transformation system for *Desmodesmus* sp. JS07, three different parameters, i.e. plasmid amount, pulse time, and pulse voltage were optimized. The transformation efficiency of 130 colonies/ 10^6 cells was detected using 4 µg of plasmid DNA with 1ml of *Desmodesmus* sp. JS07 cells. However, the transformation efficiency showed no further increase with the increase in concentration of plasmid DNA above 4 µg. Higher transformation efficiency was observed at the pulse time of 4 ms with an optimal voltage of 2kV.

6a.3.3. Selection of *Desmodesmus* sp. JS07 transformants

Using the derived parameters, *Desmodesmus* sp. JS07 cells were transformed with *Bn*DGAT-eGFP construct, and the transformed colonies harboring the hygromycin resistant gene (aph7) were screened on hygromycin-supplemented TAP medium (150µg/ml). The hygromycin resistant *Desmodesmus* sp. JS07 cell became visible after 15-18 days of incubation, whereas the hygromycin sensitive cells did not survive after 7-8 days of incubation on the selective TAP-agar medium, (Fig 6a.3). Moreover, the transformed cells harboring BnDGAT-eGFP construct grew well in the liquid TAP medium supplemented with 100 µg/ml hygromycin. Further, positive transformants were then grown at intervals of selective and non-selective TAP media for more than two months to obtain stable transgenic of *Desmodesmus* sp. JS07. Afterwards, 15 colonies were selected on hygromycin-supplemented plates and subjected to PCR. Subsequently, five independent transformed cell lines were evaluated for their genetic stability and the stable positive transformants thus obtained were used for further studies.

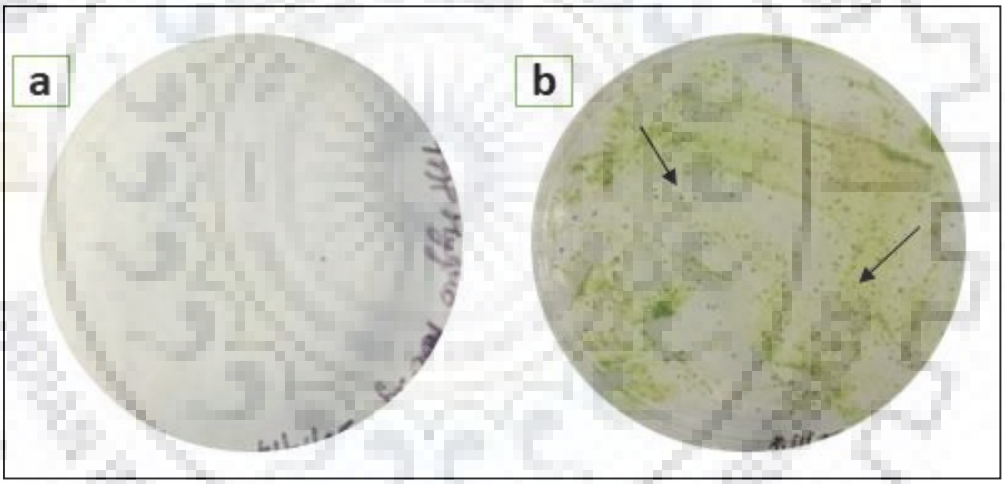

Fig. 6a.3 Hygromycin selection of putative *Desmodesmus* sp. JS07 transformants; a, wild type cells and b, transformants at 150 µg/mL Hyg-B

6a.3.4 Evaluation of transgene integration through PCR

Transformed *Desmodesmus* sp. JS07 cells were analyzed for transgene integration through PCR using a *Brassica napus* DGAT2-gene-specific primer. The genomic DNA was extracted from the transformed *Desmodesmus* sp. JS07 cell lines (T1–T4). PCR amplification was performed on the genomic DNA, yielding about 600 bp products in transformed cells (T1-T4) whereas no amplicon was detected in the wild type, as shown in Fig. 4. Further, the positive transformants of *Desmodesmus* sp. JS07 were analyzed for the GFP expression and lipid accumulation.

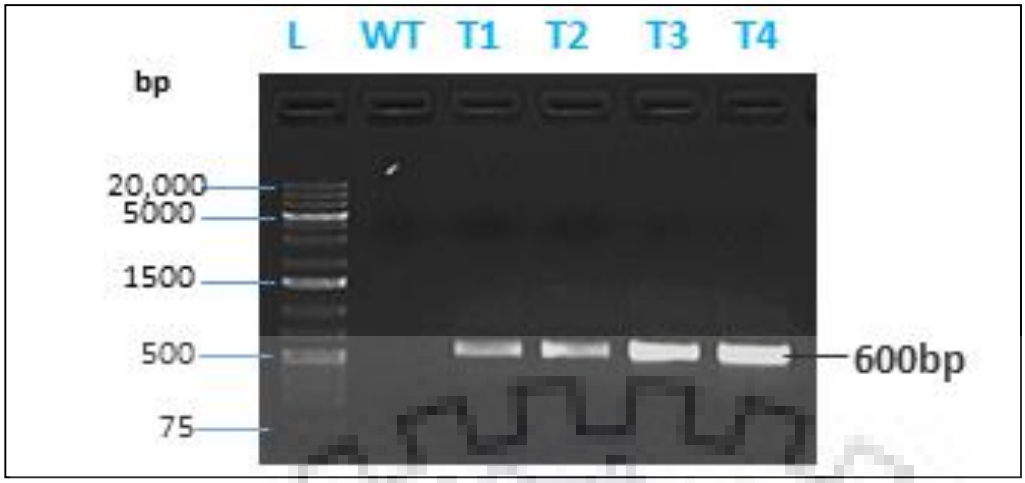

Fig. 6a.4 PCR analysis for confirming the transgene integration in the *Desmodesmus* sp. JS01 transformants (T1-T4)

6a.3.5 Evaluation of GFP expression by fluorescence microscopy

Gene transfer was further confirmed by selecting the transformed *Desmodesmus* sp. JS07 and subjected to fluorescence microscopy for eGFP (Green fluorescent protein) evaluation. As shown in Fig.6a.5, a boosted GFP expression was detected in the transformed *Desmodesmus* sp. JS07 (T4 lines) whereas wild type *Desmodesmus* sp. JS07 cells had shown red color due to chlorophyll auto-fluorescence. eGFP gene expression was modulated by the CaMV35S promoter to visually recognize the transformed *Desmodesmus* sp. JS07 cell lines. This has demonstrated that the eGFP gene had successfully expressed and fluorescence from GFP enabled in the visualization of the transformants.

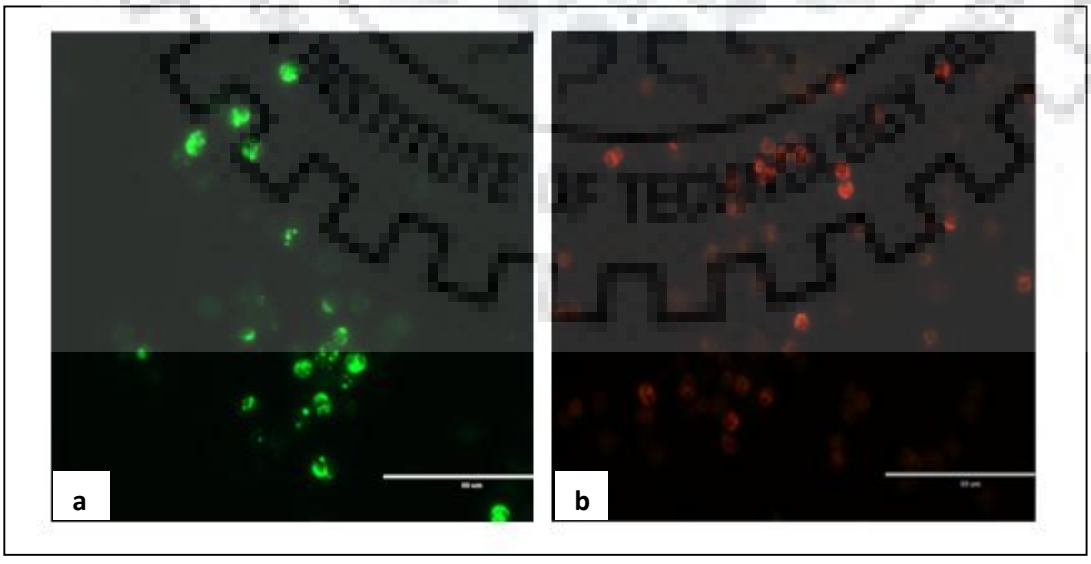

Fig 6a.5. Fluorescence microscopy of transformed (a) and wild type (b) *Desmodesmus* sp. JS07 cells at 60X.

6a.3.7 BnDGAT2 expression in *Desmodesmus* sp. JS07 with

Expression of the BnDGAT2 driven by HSP70A-RBCS2 promoter in transformed *Desmodesmus* sp. JS07 cells were analyzed by SDS-PAGE, Coomassie blue staining, and Western blots. A 39 kDa protein band had detected in the transformed cell lines (T1-T4) while the same did not appear in the wild type cells. Further, the protein samples from the wild type and transformed (T3 and T4) cell lines were transferred to the membrane followed by hybridization with 6XHIS monoclonal antibodies indicated the expression of the DGAT2 in the transformed cells.

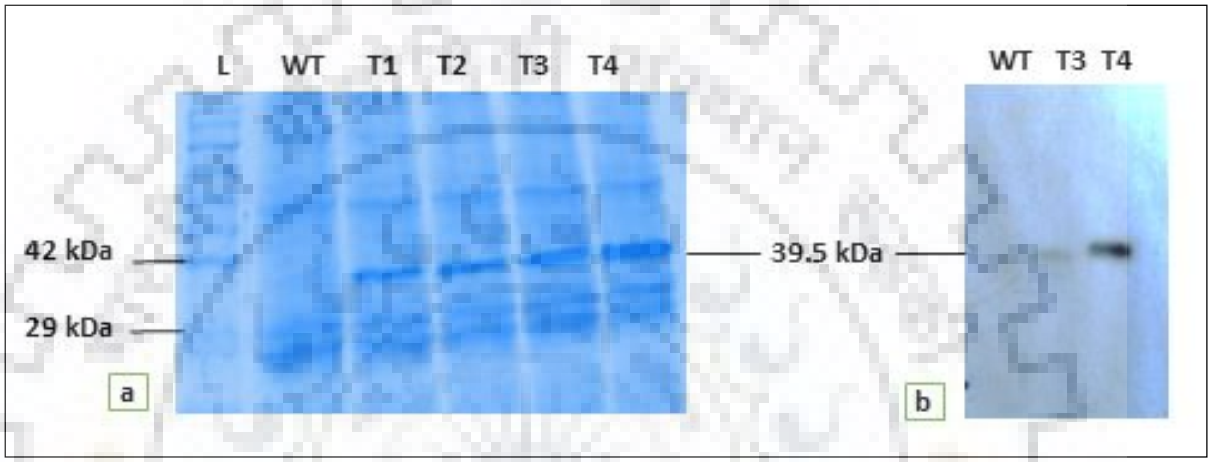

Fig. 6a.6 Evaluation of BnDGAT2 expression; a Coomassie blue gel showing ~39.5 kDa protein in T1-T4 transformants; b, western blot analysis is showing ~39.5 kDa band in T3 & T4 transformants of *Desmodesmus* sp. JS07.

6a.3.8 Analysis of lipid by Nile red staining

Neutral lipid accumulation was visually confirmed in the transformed (T4 cell lines) and wild type *Desmodesmus* sp. JS07 by Nile red fluorescent dye analysis. The overexpression of BnDGAT2 in *Desmodesmus* sp. JS07 revealed an increased in both the size and number of lipid bodies whereas the wild type cells showed a smaller number of lipid droplets (Fig. 6a.7)

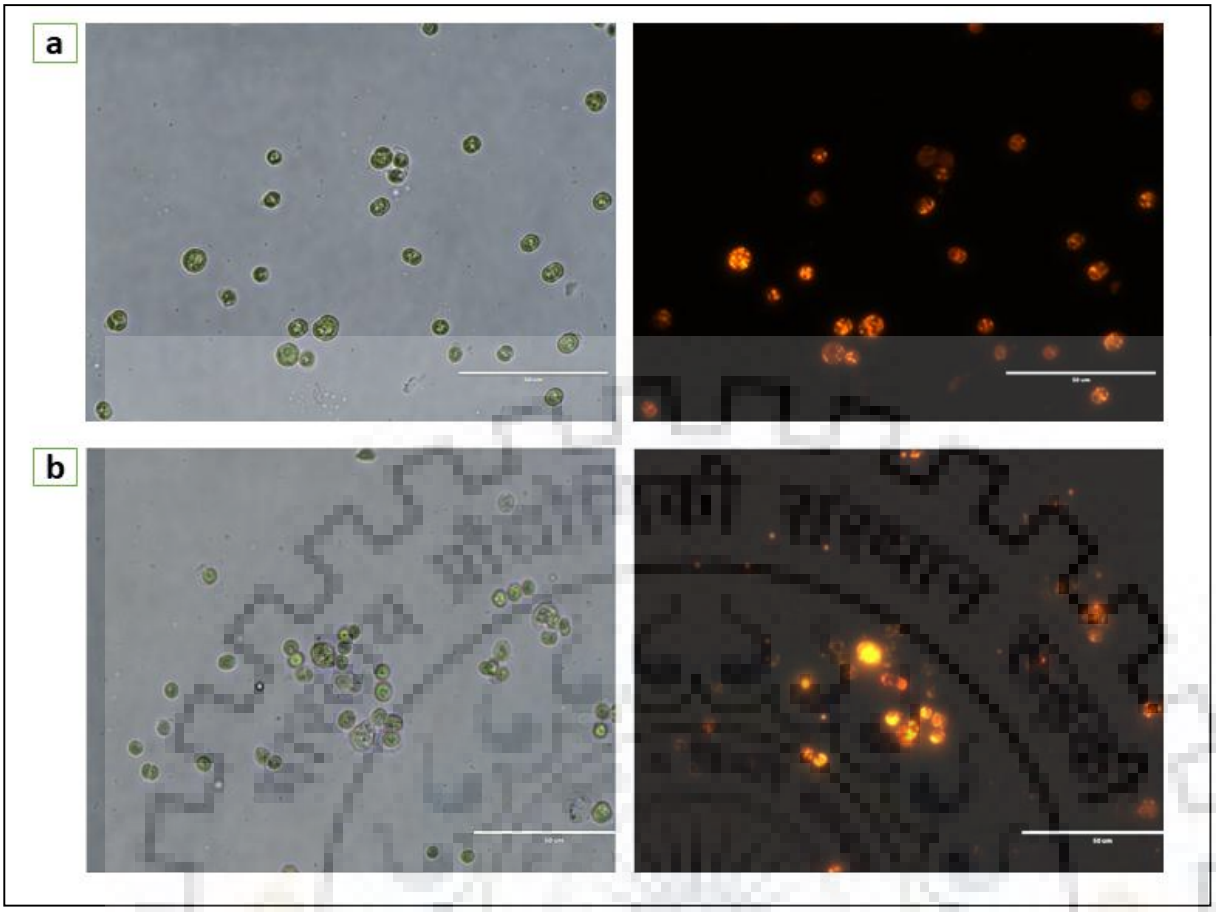

Fig. 6a.7 Fluorescence microscopy of a, wild type and b, transformed *Desmodesmus* sp. JS07 cells at 60X to visualise lipid globules.

6a.3.9 Analysis of biomass, lipid content and productivity in transformed *Desmodesmus* sp. JS07

To evaluate the expression of BnDGAT2 gene encoding a putative acyl-CoA diacylglycerol acyltransferase gene on triacylglycerol (TAG) biosynthesis, pAlgae-DGAT-eGFP construct was prepared and overexpressed in *Desmodesmus* sp. JS07. The transformed *Desmodesmus* sp. JS07 was cultured in TAP medium, and biomass, and lipid content were then analyzed. Results showed (Table 6a.1) that the transformed *Desmodesmus* sp. JS07 (0.82 gm/L) exhibited similar biomass to that of the wild type cells (0.91 gm/L) on the dry weight basis as observed on the fourteenth day. Further, the lipid content was estimated from the dry biomass of the transformed and untransformed microalga. As shown in Table 1, lipid content and lipid productivity of the transformed *Desmodesmus* sp. JS07 exhibited an increase to 24.91±2.81 % and 33.05±1.44 mg/L/d respectively, which was 1.24 and 1.22 fold higher than those obtained for the wild type *Desmodesmus* sp. JS07 respectively. This is the first report to show the heterologous expression of *Brassica napus* DGAT2 gene in *Desmodesmus* sp. JS07 that led to a significant increase in

lipid accumulation. A substantial increase in the lipid accumulation of *Chlamydomonas reinhardtii* with BnDGAT2 expression was also observed by Ahmad et al., 2015.

Table 6a.1. Estimation of biomass and lipid content in transformed *Desmodesmus sp*. JS07

Organism	**Biomass Productivity (mg/L/day)**	**Lipid content (%)**	**Lipid Productivity (mg/L/day)**
Wild type *Desmodesmus sp.* JS07	134.42±3.34	20.04±1.11	26.93±1.39
Transformed *Desmodesmus sp*. JS07	132.71±4.07	24.91±2.81	33.05±1.44

6a.3.10 Fatty acid methyl ester (FAME) profiling

The FAME profiling of transformed *Desmodesmus* sp. JS07 was determined and compared with the wild type. The results had shown a noteworthy alteration in the FAME composition of transformed *Desmodesmus* sp. JS07. The total saturated fatty acid content (mainly palmitic acid (C16:0) and stearic acid (C18:0) had reduced in the transformed cells as compared to the wild type cells (Fig. 5). However, the monounsaturated fatty acids (MUFA) mainly oleic acid (C18:1) and palmitoleic acid (C16:1) and polyunsaturated fatty acids (PUFA) mainly a-linolenic fatty acid had notably enhanced in the transformed *Desmodesmus* sp. JS07. Similarly Wei et al., 2017 had observed the significant rise in the relative contents of C16:1 and C18:1 in microalga *C. reinhardtii* by heterologous expression of type-I diacylglycerol acyltransferase genes from *N. oceanica* (NoDGAT1A).

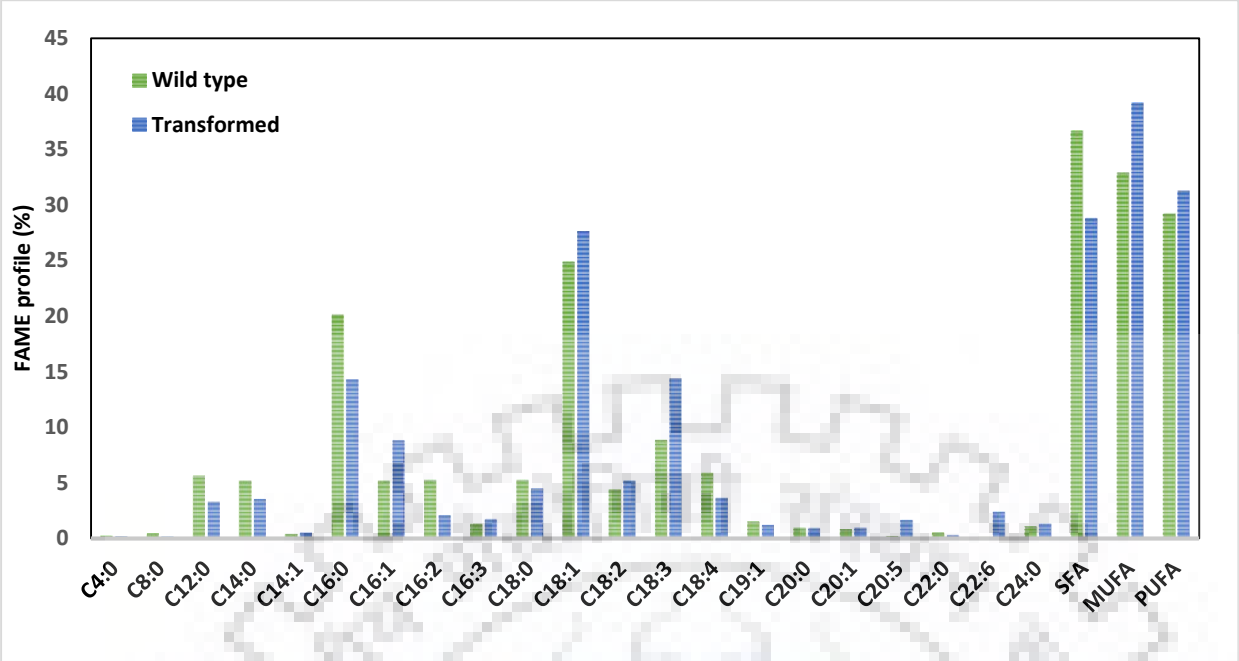

Fig. 6a.8 Fatty acid profile of wild type and transformed *Desmodesmus sp*. JS07

6a.4. Conclusion

The *Brassica napus* BnDGAT2 was transformed in the microalgae *Desmodesmus sp.* JS07 using electroporation. Major parameters for transformation using electroporation were defined. The transformants displayed similar growth rate and had enhanced lipid content compared to the wild type strain; thus, without compromising the biomass yield for this strain. Further, the lipid composition analysis had shown a higher amount of monounsaturated and polyunsaturated fatty acids and a lesser amount of saturated fatty acids. The unsaturated fatty acids as observed increased the cetane number and heat of combustion while saturated fatty acids had increased the thermal efficiency and NOX emission. Thus, the parameters defined for the transformation of *Desmodesmus sp.* JS07 may yield into further molecular modifications of this strain along with systematic functional genomics studies to understand the molecular cascade regulating lipid accumulation in the microalgal strain.

Part b: Homologous expression of CvGPD1 in *Desmodesmus* sp. JS07

6b. Introduction

Renewable energy is one of the most viable alternatives to address energy security, carbon emission, and increased fuel consumption challenges that had resulted in global warming and increasing fossil fuel costing concerns. These issues have encouraged interest in exploring alternative sources, and oleaginous microalgae appear to be one of the promising sources for renewable energy.

GPD is one of the pivotal enzymes in lipid metabolism for glycerolipid synthesis, as it catalyzes the reduction of dihydroxyacetone phosphate (DHAP) to glycerol-3-phosphate (G3P). Sequentially G3P obtained can be used as a precursor for glycerolipid synthesis (Ghoshal et al., 2002; Herrera-Valencia et al., 2012). Genes encoding GPD have been characterized and cloned from algae and a few plant species (He et al., 2009). The increased and modulated expression of the GPDH gene from *Saccharomyces cerevisiae* in *Brassica napus* led into the increased flux for glycerol-3-phosphate in the developing seeds which improved the lipid content by 40% in the mature seeds of this plant (Vigeolas et al., 2007).

Further, the development in protein engineering has enabled in modifying proteins for achieving increased turnover number and stability (Long et al., 2016). Irrespective of the contribution of protein engineering in producing novel proteins with desired properties, it can also serve as a potential tool for exploring the structure-function relationships (Sudhir et al., 2016). Thus, the substitution of amino acids onto defined sites may yield into modified properties with improved characteristics. To engineer the protein for improved activity and stability for commercial applications includes various strategies comprising site-directed mutagenesis directed evolution, random point mutations, and chain extension (Kotzia and Labrou, 2009; Sidhu and Kossiakoff, 2007; Vidya et al., 2014)

Thus, this study has aimed to clone and transform the Glycerol 3 phosphate dehydrogenase gene of *Chlorella variabilis* to *Desmodesmus* sp. JS07 and to analyses the impact of its expression on lipid content. Further, the CvGPD1 gene was mutagenized and sub cloned in the pET-28a (+) to elucidate its impact on enzyme activity and stability. The construct(s) with improved qualities was transformed into *Desmodesmus sp.* JS07 and the lipid content after that was analyzed. Subsequently, bioinformatics tools were employed to investigate structural changes responsible for the improved characteristics of the mutant.

6b.2. Materials and Methods

6b.2.2 Synthesis and cloning of the gene

The expression vector pCHLAMY_1 (4283 bp) was procured from ICGEB, Delhi, India. The vector contained Hsp70-RbcS2 and b-tubulin promoter for the expression of the GPD1 gene from *Chlorella variabilis* and hygromycin resistance gene (aph7) (selectable marker), respectively. The *Cv*GPD1 (Accession no. XM_005847581.1) gene fused with 6XHIS tag and terminator sequence NOSPolyA was chemically synthesized (BioBasic Inc. Markham, Ontario, Canada) and cloned at Kpn1 and Nde1 restriction sites in the pCHLAMY_1 vector. The recombinant plasmid was then transformed into *E.coli* DH5α cells. Selection of the positive clones was done on LB plates containing 100 µg/mL ampicillin.

6b.2.3 Site-directed Mutagenesis

The final construct (*Cv*GPD1:pCHLAMY_1) was used as a template for the site-directed mutagenesis. Using the overlap-extension PCR method (Ge and Rudolph, 1997), site-directed mutagenesis of *Cv*GPD1 gene was done to generate two mutant versions of wild type *Cv*GPD1 namely, M1 (CvGPD1Ile^{551}His) and M2 (CvGPD1Gly^{557}Ser) using primer pairs F1,F2,F3 and F4 for M1 and F1,F2,F5 and F6 for M2 listed in Table 1. The DNA sequencing was done to determine the introduction of the desired mutations in the gene.

Table 6b.1 List of primer set used for site-directed mutagenesis

Primer Name	**Primer Sequence**
F1	5´ GACACGGTACCGATGCGGAAGGTTG 3´
F2	5´ AGCAGGTGGCGTGCAGGTCTGCCACGCCGCACG 3´
F3	5´ GGCAGACCTGCACGCCACCTGCTACGGCGGGCG 3´
F4	5´ GACACCATATGCCCGATCTAGTAAC 3´
F5	5´ GCGGTTGCGCGAGCCGTAGCAGGTGGCAATCA 3´
F6	5´ CTGCTACGGCTCGCGCAACCGCCTGGTGGCGC 3´

6b.2.4 Sub cloning in the bacterial expression vector

The wild type (WT-*Cv*GPD1) and mutants (M1-*Cv*GPD1Ile^{551}-His and M2- *Cv*GPD1Gly^{557}-Ser) were subcloned in pET28a (+) bacterial expression vector to evaluate the protein expression and enzyme activity. Sub cloning was accomplished after PCR amplification using a specific primer

set (FP 5´-ACTCCTGCGGTGGAGGCAGGTGGGGCA-3´ RP 5´-CCTGCCTCCACCGCAGGAGGTCCTGGA-3´). The primers were designed according to the GPD1 gene of *Chlorella variabilis* (Accession no. XM_005847581.1) available in the National Center for Biotechnology Information (NCBI) Web site. The forward and reverse primer contained NdeI and BamHI restriction site, respectively. PCR amplification was performed in a reaction volume of 50 uL consisting of 8 µL of pCHLAMY_1 plasmid DNA (5 ng/µl), 10 µL of 5X Phusion HF Buffer, 1 µL each of the forward and reverse primer, 1.5 µl of $MgCl_2$ (3.5 mM), 1 µl of dNTPs (10 mM), 0.25 µl of Phusion polymerase and 31.25 µL of nuclease-free water. PCR conditions were as follow 1 cycle at 98˚C for 30 sec, 30 cycles each at 98˚C for 15 sec, 72˚C for 30 sec and 72˚C for 1 min and a final extension at 72◦C for 5 min. Amplified products were subjected for agarose gel electrophoresis (1% agarose in 1X TAE buffer). The resulting PCR amplicon and plasmid pET28a (+) were digested with NdeI and BamHI. The digest was electrophoresed on agarose gels and purified using a Gel Purification kit (Favorgen). The purified PCR product was then ligated into the linearized pET28a (+) vector. The ligation product was then subjected to transformation in E.coli DH5α. Furthermore, LB agar supplemented with kanamycin (50 µg/mL) was used for the selection of transformants.

6b.2.5 Evaluation of protein expression

The recombinant plasmids (WT, M1, and M2) were isolated from the cloning host *E.coli* DH5α using Plasmid purification kit (Qiagen) and transformed into the expression host *E. coli* BL21 (DE3) cells. The cells harboring recombinant pET-28a (+)/WTGPD1, M1 and M2 were allowed to grow in 5 mL of Kanamycin (50 µg/mL) supplemented LB broth at 37^0 C, overnight. The secondary culture was inoculated with the overnight grew culture in 100 mL of kanamycin (50µg/mL) supplemented LB broth at 37^0 C, 200 rpm (New Brunswick Incubator Shaker, USA) until an optical density of 0.6 was reached. After achieving the desired O.D., IPTG (1mM) was added for protein induction, and the culture was kept under shaking condition at 37˚C. After 6 h of post-induction period, cells were harvested (6000 rpm, 10 min) at 4^0 C and resuspended in 20 mL of lysis buffer (50 mM NaH_2PO_4, 10 mM imidazole, 300 mM NaCl [pH 8.0]) supplemented with lysozyme (1 mg/mL) and incubated for 30 min on ice. Cell disruption was carried out via sonication (Helix Biotech) on ice for 5 min (5 sec ON and 10 sec OFF) followed by centrifugation at 12000 rpm for 20 min, 4^0 C. The analysis of the crude extract and its molecular mass determination was done by SDS-PAGE.

6b.2.6 Western blot analysis

Recombinant proteins (WT, M1, M2) carrying N-terminal His tags were subjected to western blot analysis as described in section 6a.2.8.

6b.2.7 Enzyme activity

The GPDH activity was determined using a Glycerol-3-Phosphate Dehydrogenase (GPDH) Assay kit (Sigma Aldrich). The determination of enzyme activities of recombinant proteins was done using an NADH calibration curve. One unit of GPDH is the amount of enzyme that generates 1.0 mmole of NADH per minute at pH eight at 37 °C.

6b.2.8 Protein Structure by Homology Modeling

SWISS-MODEL workspace (http://swissmodel.expasy.org) was used for the prediction of the three-dimensional structure of the GPD1 and its mutants. Further, Jmol program version 12.0 (http://www.jmol.org) was used for visualizing and editing of the predicted 3D models.

2.9 Microalgal transformation via electroporation

Desmodesmus sp. JS07 cells in the exponential phase (OD_{750}=0.4-0.6) were collected by centrifugation at 3000 rpm for 15min at 4^{o}C and transformed with 5µ g of the linearized 'pAlgae-CvGPD1' and pAlgae-CvGPD1Ile551-His' as described in section 6a.2.4.

6b.2.10 Molecular analysis of transformant by PCR

Transformed and untransformed *Desmodesmus* sp. JS07 cells in the exponential phase were collected, and genomic DNA was extracted by the DNeasy plant mini kit (Qiagen GmbH, Hilden, Germany) The CvGPD1 and CvGPD1Ile^{551}His gene integration in the transformed cell lines were confirmed by PCR using the *aph7* DNA sequence-specific primers (forward primer 5´-GATTCTGCCTTCTTATCAGGTGACAC-3´ and reverse primer 5´-CGAACCATCCATTTGTGAACAGG-3´). PCR conditions were followed as discussed in section 6a.2.5.

6b.2.11 Lipid extraction and quantification

The microalgal biomass was harvested after 15 days of cultivation (late log phase) by centrifugation and lyophilized. The extraction of lipids from the lyophilized biomass (100mg) was performed by using Bligh and Dyer's method as described in section 2.2.3.3.

6b.2.12 Fatty acid methyl esters (FAMEs) profiling

For fatty acid methyl esters (FAMEs) analysis, total lipids (~100mg) were transesterified using 1 mL of 2% (v/v) sulphuric acid in methanol. Afterwards, the samples were incubated at 60^{o}C for 3hr, and the extraction of FAMEs was done using hexane (1 mL) followed by vortexing for 5 min. The GC-MS analysis of 500 µL of the hexane containing FAMEs was then carried out as described in section 2.2.3.5.

6b.3. Results and Discussion

6b.3.1 Cloning of GPD1

The synthesized *Cv*GPD1 gene construct was cloned at Kpn1 and Nde1 restriction sites in the pCHLAMY_1 vector. The cloning was confirmed by double digestion with the restriction enzymes (Fig. 6b.1) and sequencing of the recombinant plasmid.

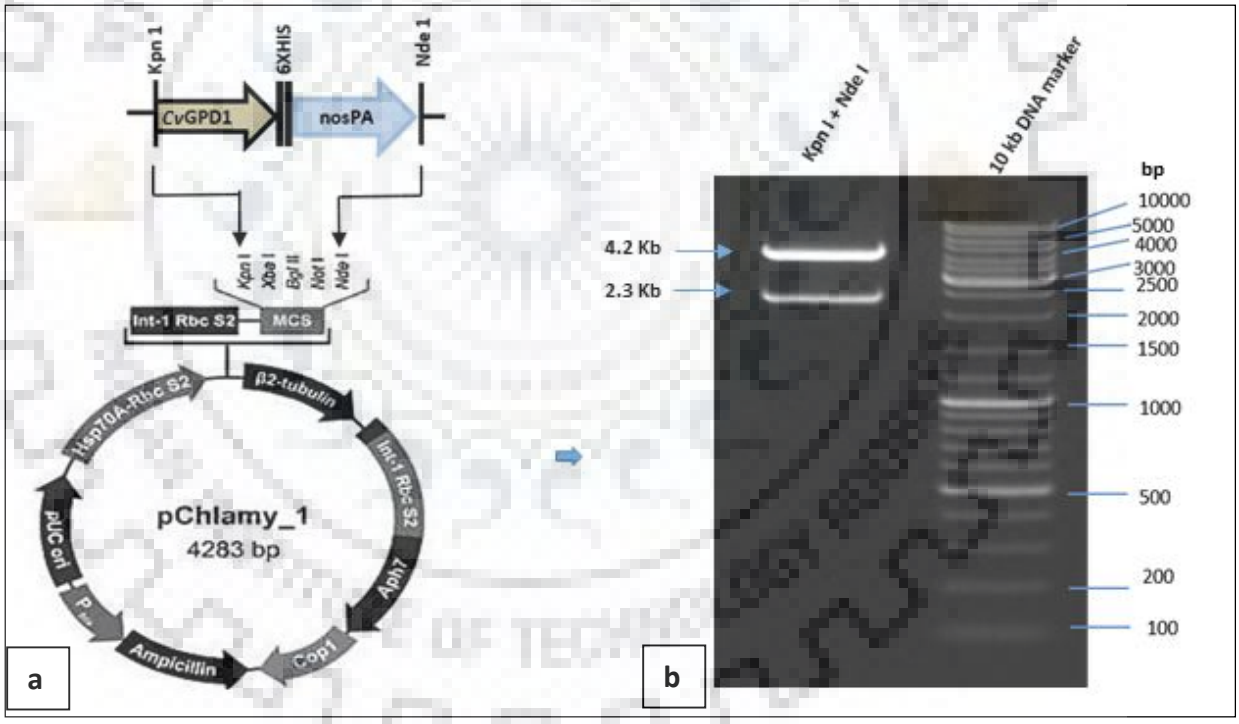

Fig. 6b.1 Cloning of Glycerol 3 phosphate dehydrogenase of *Chlorella variabilis* in pChlamy_1 vector; a, representation of pAlgae-CvGPD1 construct; b, Restriction digestion profile of recombinant pCHLAMY_1:CvGPD1 with KpnI/NdeI showing expected Size: 4.2 Kb (pChlamy_1) + 2.3 Kb (CvGPD1).

6b.3.2 Site-directed mutagenesis

6b.3.2.1 Ile^{551}His (ATT-CAC)

The CvGPD1 gene was subjected to mutagenesis in order to get a variant with increased catalytic activity. In order to elucidate the target residues for mutagenesis BLASTp analysis of *Chlorella variabilis* GPD1 with the PDB database was performed, that had denoted its maximum similarity with *Homo sapien* GPD1 protein and *Thermotoga maritima* GPD1 protein. As per the protein structure analysis of human GPD1 by Ou et al., 2006, it was denoted that Thr^{264} is involved in H-bonding with Lys^{204} that provides a proton to DHAP to form G3P. Since Thr^{264} and Lys^{204} were highly conserved in this enzyme, and therefore these residues were not taken into consideration. Further, on the detailed structural analysis of *Homo sapien* GPD1 protein, a hydrophobic amino acid residue Ile^{267} was found nearby Thr^{264} and Lys^{204} that involved in the hydrogen bonding with Lys^{204}. Moreover, Isoleucine was also replaced by histidine in *Thermotoga maritima* GPD1 protein sequence at one position. Thus, replacing Ile with His (Ile^{551}His) in *Chlorella variabilis* GPD1 may impact the deprotonation activity of Lys^{204}, thereby improving the catalytic activity of the enzyme.

6b.3.2.1 Gly^{557}Ser (GGG-TCG)

Further, sequence alignment between *Homo sapien* GPD1 and *Leishmania mexicana* GPDH had shown a higher degree of structural homology Ou et al., 2006. The structural analysis of GPDH from *Leishmania mexicana* elucidated that Ser273 acts as a hydrogen bond donor during catalysis reaction (Choe et al., 2003). Serine is also present at the same position in the GPD1 crystal structure of *Thermotoga maritima*. However, in *Chlorella variabilis*, Gly is present in place of Ser at the corresponding position, and that may be not involved and contribute to the catalytic activity. Therefore, replacing Gly with Ser (Gly^{557}Ser) in *Chlorella variabilis* GPDH may probably lead to the increased catalytic activity of the enzyme. Fig 6b.2 represents the multiple alignments of the wild type sequence with mutant 1 and 2 confirming the successful site-directed mutagenesis in Mutant 1 and 2.

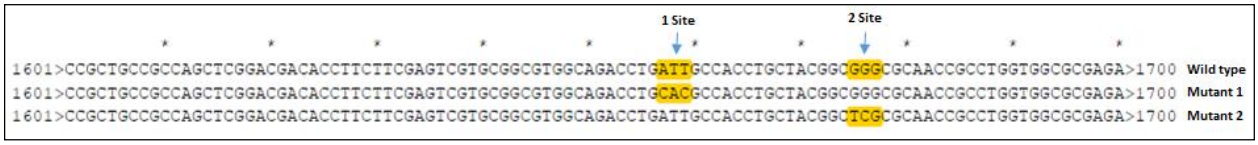

Fig. 6b.2 Multiple sequence alignment of the wild type CvGPD1 gene with Mutant 1 (CvGPD1Ile^{551}His; ATT-CAC) and Mutant 2 (CvGPD1Gly^{557}Ser; GGG-TCG) confirming the side directed mutagenesis.

6b.3.3 Sub cloning in the bacterial expression vector

The 2 Kb gene fragment was amplified and cloned in pET28a(+) vector with six His-Tag at the N-terminus of the recombinant protein. The insert in the recombinant vector was verified by double digestion with NdeI and BamHI. (Fig. 6b.3). Further, the recombinant plasmid was sequenced to confirm the correct frame of the nucleotide sequence.

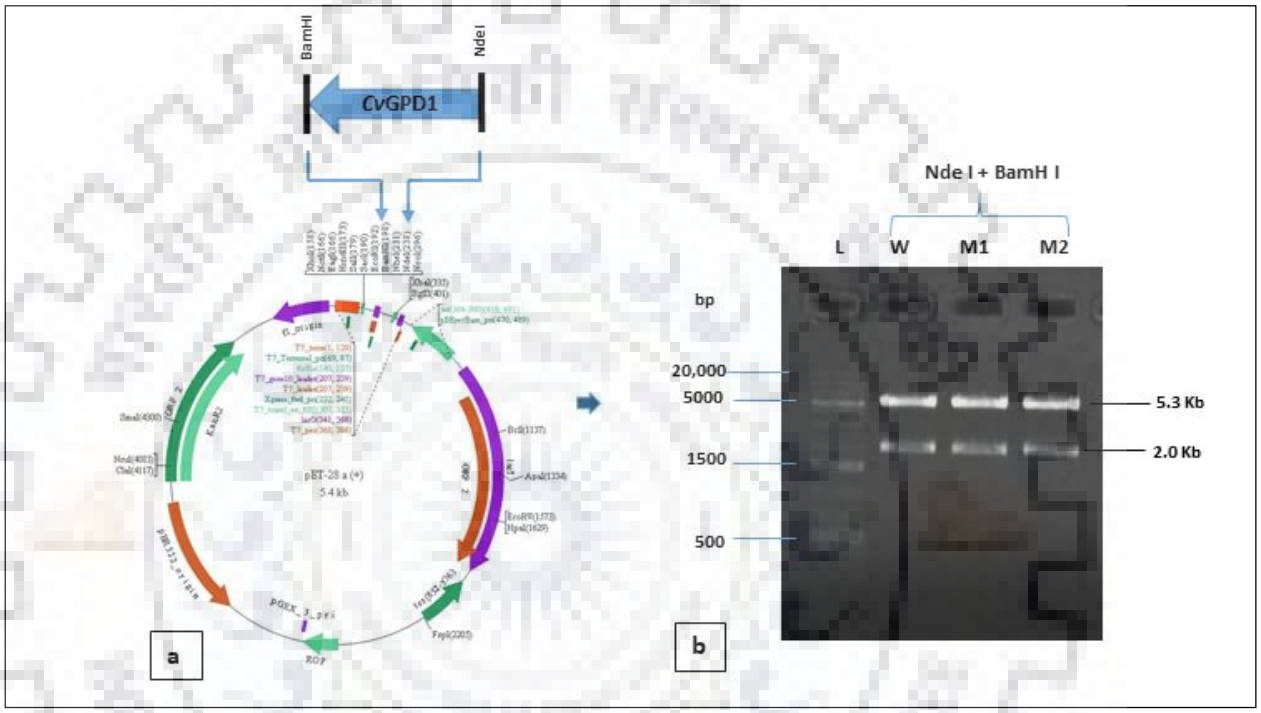

Fig. 6b.3 Cloning of Glycerol 3 phosphate dehydrogenase of *Chlorella variabilis* in pET-28a vector; a, representation of pET-28a-CvGPD1 construct; b, Restriction digestion profile of recombinant pCHLAMY_1:CvGPD1 with NdeI/BamHI showing expected Size: 5.3 Kb (pET-28a) + 2.0 Kb (CvGPD1).

6b.3.4 Protein expression, purification and enzyme activity

For heterologous expression in bacteria, *Cv*GPD1 and the mutants M1 (CvGPD1Ile^{551}His) and M2 (CvGPD1Gly^{557}Ser) expression plasmids were constructed, and expression was analyzed in *E.coli* BL21 (DE3) host strain. Following IPTG induction (1mM, 6 h), the expression product containing His-tag was analyzed using SDS-PAGE followed by Coomassie Blue staining and western blot analysis, that had indicated a predominant band with an apparent molecular mass of 75 kDa in wild type pET-28a: CvGPD1 and its mutant M1 and M2.

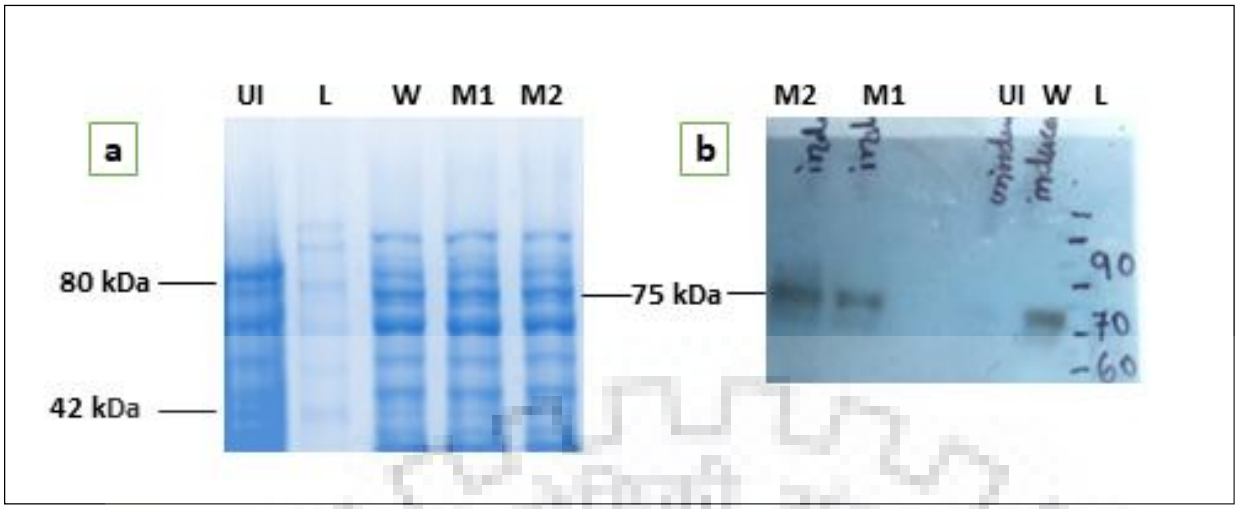

Fig. 6b.4 Evaluation of pET-28a:CvGPD1 and its mutant M1 (CvGPD1Ile^{551}His) and M2 (CvGPD1Gly^{557}Ser) expression in bacterial expression system; a, Coomassie blue gel showing ~75 kDa protein in wild type (W), mutant 1 (M1) and mutant 2 (M2); b, western blot analysis showing ~75 kDa band in wild type (W), mutant 1(M1) and mutant 2 (M2) of *Desmodesmus* sp. JS07.

The crude wild type and mutant enzymes were incubated under assay conditions, and the amount of NADH liberated was estimated. GPD1 assay of mutants and wild enzymes revealed that the wild type enzyme had an increased enzyme activity of 8.1 ± 0.54 U/ml whereas the M1 (Ile^{551}His) at had an enzyme activity of 12.32 ± 0.76 U/ml whereas M2 (Gly^{557}Ser) did not show any increase in activity. The mutant Ile^{551}His, exhibiting higher catalytic activity may be because of increased turnover of the mutagenized enzyme.

Table 6b.2. Enzyme activity of pET28a:CvGPD1 construct and its mutants M1 and M2

Constructs	GPD1 Activity (mU/ml)
CvGPD1 (W)	8.1 ± 0.54
CvGPD1Ile^{551}His (M1)	12.32 ± 0.76
CvGPD1Gly^{557}Ser (M2)	6.88 ± 0.33

6b.3.5 Computational analysis

The high-resolution crystal structure of Homo Sapiens GPD1 protein (GPD1, EC 1.1.1.8) decoded the structure-function relationship of GPD1. The three-dimensional structure prediction for the GPD1 of the three CvGPD1 and two mutants were obtained by homology modeling, employing Homo sapiens GPD1 crystal structure as a template. Assessment of the structure

quality was done with the help of PROCHECK, 14 that showed 92.3% of the residues placed in the most favorable region of the Ramachandran plot (Fig. 6b.5). The rest 7.7% residues were found to be in additionally allowed regions with no residues in the generously allowed or disallowed regions.

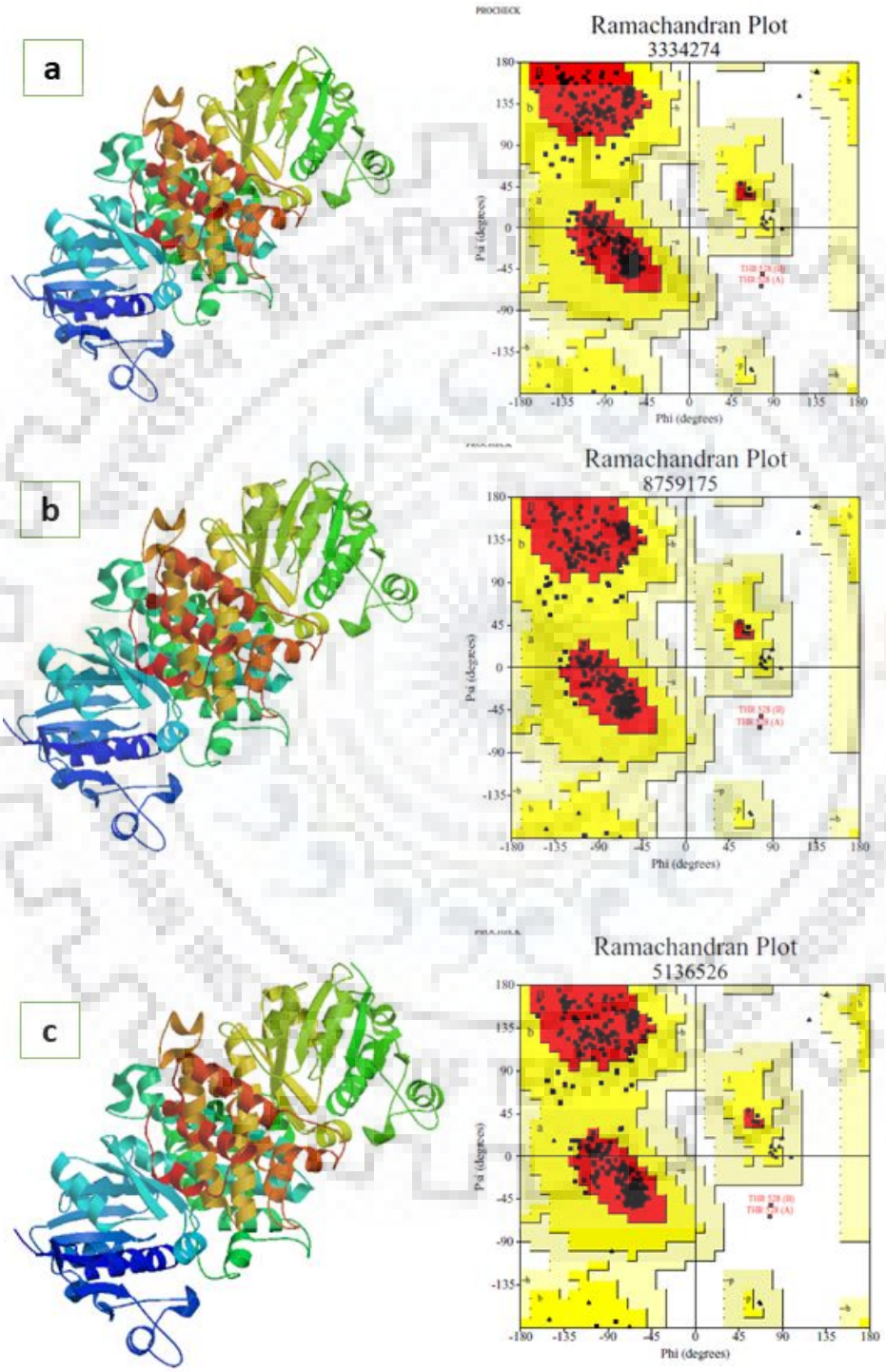

Fig.6b.5 Structural representation of wild type and mutants with corresponding Ramachandran plot. **a,** CvGPD1; **b**, CvGPD1Ile^{551}His; **c**, CvGPD1Gly^{557}Ser. The colour indicates the progression from N (blue) to C (green) terminus.

Further, to have a deeper insight into the structural basis of catalytic activity of mutants in comparison to the wild type Homo sapiens GPD1 structure was analyzed, and it was observed that in human GPD1 structure, the GPD1/DHAP/NAD^+ ternary complex enables us to delineate the putative active site. Eight amino acid residues (Lys^{120}, Lys^{204}, Asp^{260}, Arg^{269}, Asn^{270}, Ile^{152}, Asn^{205}, Thr^{264}) directly associates with the substrate, however only five residues of these (Lys^{120}, Lys^{204}, Asp^{260}, Arg^{269}, Asn^{270}) are fully conserved in all GPDs sequenced thus far; Asn^{205} and Thr^{264} are identical in 23 GPDs along with the *Chlorella variabilis* GPD but are replaced with aspartate in rabbit GPD and serine in *Saccharomyces pombe*. Analysis of the *C. variabilis* GPD1 structure showed that ILE^{152} as in human GPD1 lay at 551 positions in *C. variabilis* and involved a hydrogen bond interaction network. Replacing Ile at 551 positions with His might result in the formation of extra hydrogen bonds or salt bridges with active site residues, suggesting a smaller accessible surface of the binding pocket and the loop closure is an absolute prerequisite for substrate turnover. Moreover, on superimposing the wild type structure with CvGPD1Ile^{551}His structure, it was observed that Ile was present on the helix region and on replacing it with His, there is no change in the structure occurred. Therefore, changes in the side-chain conformation due to the extra bonding might be responsible for the difference in the enzymatic activity of Ile551His and wild type when they function in a bacterial expression system. Whereas, analysis of the Gly^{557}Ser structure showed that Gly^{557} lies at the external surface of CvGPD1 enzyme at helix region and replacing it with serine causes the structure deformations as Ser moved to the turns (Fig. 6b.6) and might led to opening of the binding pockets of the structure which thereby hinder the substrate binding at the active site . Hence, no increase in activity was also found for this mutant.

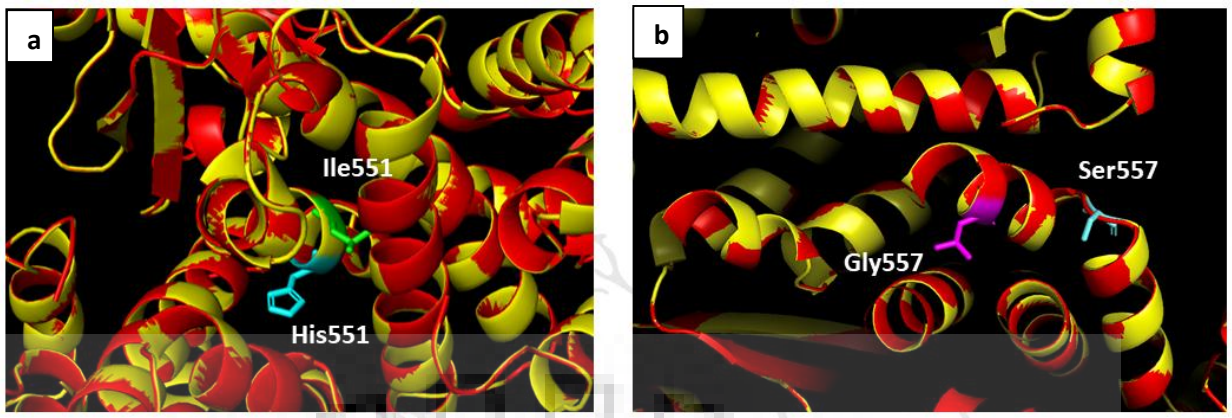

Fig. 6b.6 Three dimensional structural superimpositions of a, wild type with mutant 1 (CvGPD1Ile^{551}His) and b, wild type with mutant 2 (CvGPD1Gly^{557}Ser)

6b.3.6 Transformation of microalgae

The microalga *Desmodesmus* sp. JS07 was transformed with the construct 'pAlgae-CvGPD1' and 'pAlgae-CvGPD1Ile^{551}His' via electroporation. The transformation efficiency of 120 colonies/ 10^6 cells and 90 colonies/ 10^6 cells were observed with 5 µg of plasmid DNA of CvGPD1 and CvGPD1Ile^{551}His respectively combined into 1ml of *Desmodesmus* sp. JS07 cells independently.

6b.3.7 Selection of *Desmodesmus* sp. JS07 transformants

Using the derived parameters, *Desmodesmus* sp. JS07 cells were transformed with CvGPD1 and CvGPD1Ile^{551}His construct. Transformed colonies harboring the hygromycin resistant gene (aph7) were screened on hygromycin-supplemented TAP medium (150µg/ml). The hygromycin resistant *Desmodesmus* sp. JS07 cell became visible after 25 days of incubation, whereas the wild type cells did not survive on the selective TAP-agar medium, (Fig 6b.7c & 6b.8c). Positive transformants were then grown at intervals of selective and non-selective TAP media for more than one months to obtain stable transgenic of *Desmodesmus* sp. JS07. Afterwards, 10 colonies harboring CvGPD1 and CvGPD1Ile^{551}His construct each was selected on hygromycin-supplemented plates and subjected to PCR. Further, three independent transformed cell lines harboring CvGPD1 and five from transformed cell lines harboring CvGPD1Ile^{551}His construct were evaluated for their genetic stability and were used for further studies.

6b.3.8 Evaluation of transgene integration through PCR

Transformed *Desmodesmus* sp. JS07 cells were analyzed for transgene integration by PCR using a *hygromycin*-gene (aph7) specific primer. The genomic DNA was isolated independently from

the transformed *Desmodesmus* sp. JS07 cell lines harboring CvGPD1 and CvGPD1Ile^{551}His construct. PCR amplification was performed on the genomic DNA, yielding about 500 bp products in transformed cells, whereas no amplicon was observed in the wild type, as shown in Fig. 7d and 8d. Further, the positive transformants of *Desmodesmus* sp. JS07 harboring CvGPD1 and CvGPD1Ile^{551}His constructs were analyzed for biomass and lipid content.

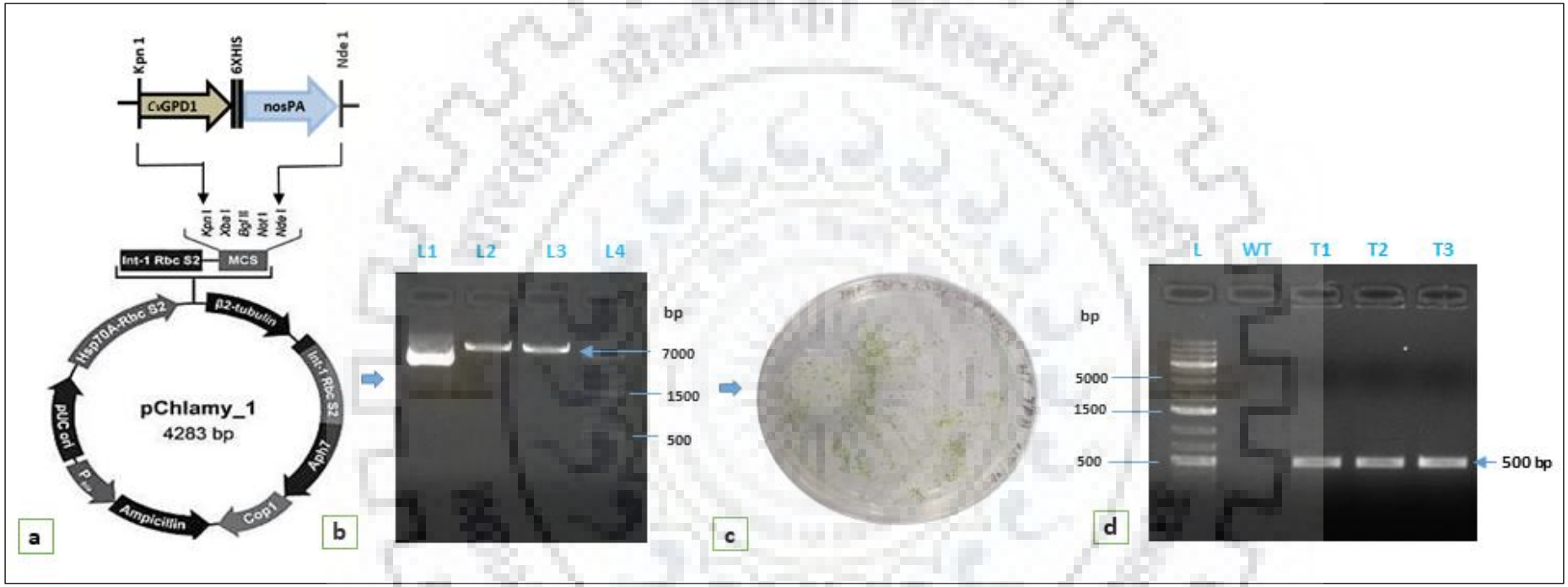

Fig.6b.7 Transformation of pAlgae-CvGPD1' in *Desmodesmus* sp. JS07; **a**, representation of pAlgae-CvGPD1 construct; **b,** Linearization of pAlgae-CvGPD1 plasmid showing approx. 7 Kb band (L1, Uncut vector; L2, 1Kb plus DNA Ladder; L3 & L4, linearized vector, size approx. 7 Kb); **c**, Hygromycin selection of putative *Desmodesmus* sp. JS07 is harboring CvGPD1 construct; **d,** Hyg-gene-specific PCR amplification from genomic DNA of a few hygromycin-resistant colonies of *Desmodesmus* sp. JS07 harboring CvGPD1 construct showing 500bp band in T1-T3 lines.

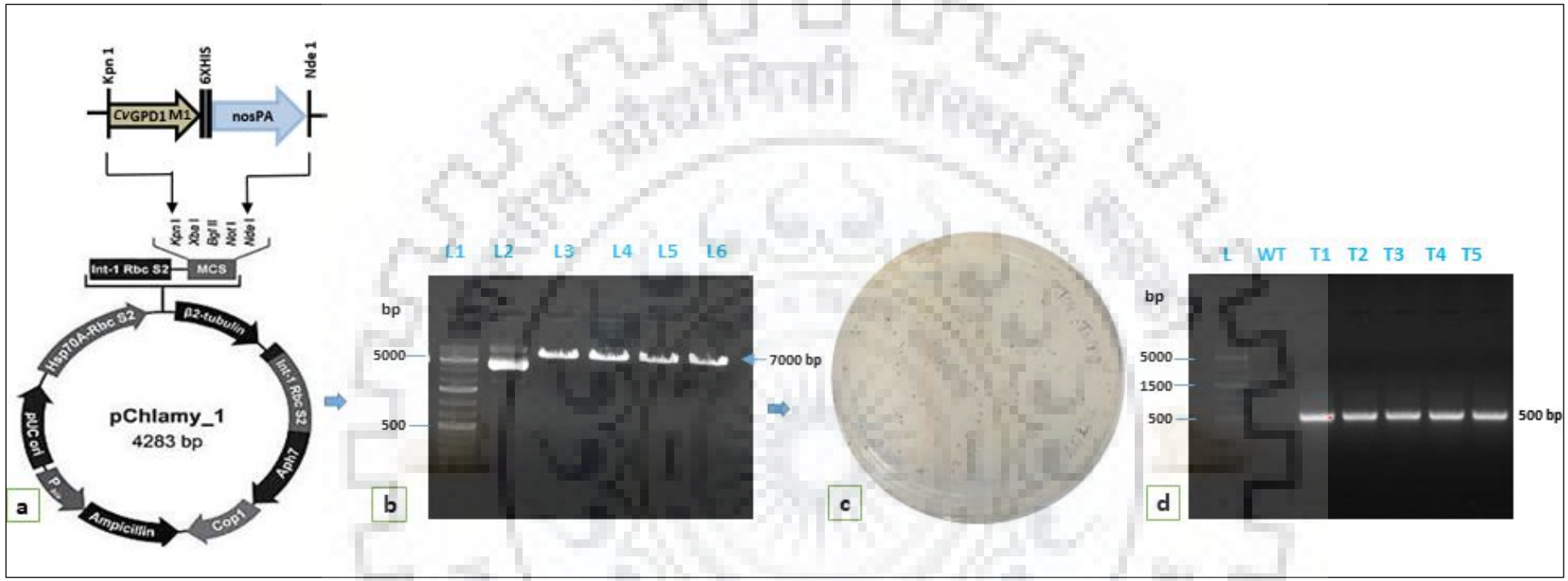

Fig. 6b.8 Transformation of pAlgae-CvGPD1Ile^{551}His in *Desmodesmus* sp. JS07; **a,** representation of pAlgae-CvGPD1Ile^{551}His construct; **b**, Linearization of pAlgae-CvGPD1Ile^{551}His plasmid showing approx. 7 Kb band (L1, Uncut vector; L2, 1Kb plus DNA Ladder; L3 - L6, linearized vector, size approx. 7 Kb); **c**, Hygromycin selection of putative *Desmodesmus* sp. JS07 is harboring CvGPD1 construct; **d,** Hyg-gene-specific PCR amplification from genomic DNA of a few hygromycin-resistant colonies of *Desmodesmus* sp. JS07 harboring CvGPD1Ile^{551}His construct showing 500bp band in T1-T5 lines.

6b.3.9 Analysis of biomass, lipid content, and productivity in transformed *Desmodesmus* sp. JS07

To evaluate the impact of CvGPD1 and CvGPD1Ile^{551}His gene encoding a putative glycerol-3-phosphate dehydrogenase gene and its mutant respectively on triacylglycerol (TAG) biosynthesis, pAlgae-CvGPD1' and 'pAlgae-*Cv*GPD1Ile^{551}His' constructs were prepared and transformed to *Desmodesmus* sp. JS07. The transformed non-transformed *Desmodesmus* sp. JS07 were cultured in TAP medium, and biomass, and lipid yield were then analyzed. Results showed (Table 6b.3) that the biomass productivity among three strains, i.e. wild type, transformed *Desmodesmus* with CvGPD1 and CvGPD1Ile^{551}His, were similar. However, as shown in Table 1, lipid content and lipid productivity of the transformed *Desmodesmus* sp. JS07 harboring CvGPD1Ile^{551}His' exhibited an increase up to 31.01±2.81 % and 40.99±1.34 mg/L/d respectively that was 1.62 and 1.66 fold higher than those obtained for the wild type *Desmodesmus* sp. JS07 respectively. While *Desmodesmus* sp. JS07 transformed with CvGPD1 showed an increase of 1.25 and 1.3 fold in lipid content and productivity respectively than wild type. Thus denoting *Desmodesmus* sp. JS07 transformed with CvGPD1Ile^{551}His construct might be a potential candidate for biofuel production. Currently, GPD, GPAT, LPAAT, and DGAT are considered as the key enzymes of TAG biosynthesis and play an important role in lipid production (Lv et al., 2013). Introduction and overexpression of these genes in microalgae lead to an enhanced lipid content (Fukuda et al., 2018; Wei et al., 2017). Therefore, our approach of overexpression of CvGPD1 and modified CvGPD1 into *Desmodesmus* sp. JS07 had led into enhanced lipid production, and therefore this strategy may contribute significantly in modulating microalgae with higher lipid content and thereby would add towards decreasing the cost of biodiesel production.

Table 6b.3. Estimation of biomass and lipid content in transformed *Desmodesmus sp*. JS07

***Desmodesmus* sp. JS07**	**Biomass Productivity (mg/L/day)**	**Lipid content (%)**	**Lipid Productivity (mg/L/day)**
Wild type	129.11 ± 1.42	19.08 ± 3.32	24.63±1.89
Transformed with *Cv*GPD1	134.02 ± 2.05	23.91 ± 2.81	32.04 ± 0.84
Transformed with *Cv*GPD1Ile^{551}His (M1)	132.21 ± 1.05	31.01 ± 2.81	40.99 ± 1.34

6b.3.10 Fatty acid methyl ester (FAME) profiling

The fatty acid methyl ester profiling of *Desmodesmus* sp. JS07 harboring CvGPD1 and CvGPD1Ile^{551}His were determined and compared with wild type cells. The results showed (Fig. 9) that with overexpression of CvGPD1 and CvGPD1Ile^{551}His, the total fatty acid content had increased due to the increased levels of different fatty acids. For instance, mono unsaturated fatty acid primarily C18:1 had increased to 28.87 % and 31.22% in CvGPD1 and CvGPD1Ile^{551}His transformed *Desmodesmus* sp. JS07 respectively compared to wild type (24.89%). The overexpression of CvGPD1 and CvGPD1Ile^{551}His led into the increased levels of saturated fatty acids mainly C16:0 and C18:0 whereas the polyunsaturated fatty acids C18:3 and C18:4 had decreased as compared to the wild type. Similarly, Lu et al., 2017 had shown that the overexpression of GPD1 in green microalga *Chlamydomonas reinhardtii* lead into increased levels of saturated and monounsaturated fatty acids. Our results are also in agreement with the earlier observations of Mentewab and Stewart, 2005. Thus, it is evident that the introduction of CvGPD1 and CvGPD1Ile^{551}His in microalgae *Desmodesmus* sp. JS07 can significantly improve the lipid content, in particular enhancing the levels of saturated and monounsaturated fatty acids mainly C16:0 and C18:1, which make genetically modified *Desmodesmus* sp. JS07 as a potential strain yielding into higher lipid content and thereby enabling in cutting the cost for biodiesel production.

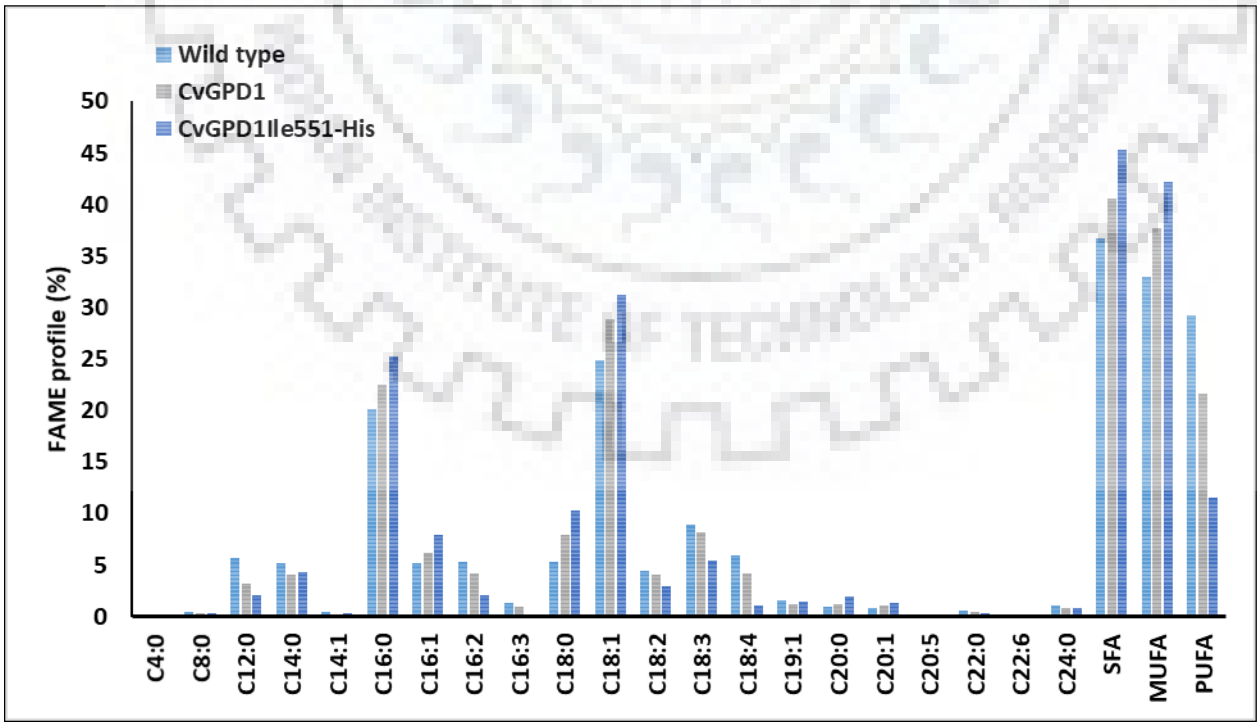

Fig. 6b.**9** Fatty acid profile of wild type and CvGPD1 and CvGPD1Ile^{551}His transformed *Desmodesmus sp*. JS07.

6b.4. Conclusion

The CvGPD1 gene was cloned in pChlamy_1 vector followed by mutagenesis of the GPD1 gene at $Ile^{551}His$ and $Gly^{557}Ser$ sites. The gene fragment was 2.1kb and encoded 699 amino acids protein sequence with an estimated molecular weight of 76.6 kDa. The prokaryotic expression vectors pET-28a-GPD1, pET-28a-GPD1$Ile^{551}His$, and pET-28a-GPD1$Gly^{557}Ser$ were constructed and transformed into *E. coli* to assess the catalytic activity of the wild type and mutagenized enzymes. The structural analysis of the G-3-P binding sites had indicated that the increased enzymatic activity might have been due to the enlarged accessible surface of the phosphate group-binding pocket following Ile551 mutation to His. Thus, this increased activity may significantly contribute to higher lipid accumulation in the microalgae. Further, to analyze the impact of CvGPD1 and CvGPD1$Ile^{551}His$ on TAG synthesis, these constructs were transformed into *Desmodesmus* sp. JS07. The observations following transformation had shown higher lipid accumulation up to 31.22% in *Desmodesmus* sp. JS07 harboring CvGPD1$Ile^{551}His$, with a significant increase in monounsaturated and saturated fatty acid. Thus, overexpression of this gene has modified the algal strain with enhanced lipid accumulation that may add towards achieving a further decrease in the cost biodiesel production.

- The variations in petroleum fuel costs, depleting fossil fuel reserves and reliance on foreign petroleum resources has rejuvenated enormous interest in a variety of renewable biofuels.
- Biodiesel is deemed as a good alternative to overcome the problem of depleting oil reserves since it appears to have a competitive performance to that of the petroleum fuel.
- Microalgae are especially promising as a source of fuel due to the environmental and ecological considerations as they rely on carbon dioxide and can be cultivated on marginal land, using waste or salt water.
- However, biodiesel production from algae is unlikely to be feasible since the yields obtained are currently uneconomical in the available strains and production processes.
- The present work highlights the strategies that could be viable and promising for increased lipid accumulation for sustainable production of biofuel from microalgae.
- Nutrient limitation is one of the most effective approaches in inducing oil accumulation in microalgae. Among the microalgal strains, Desmodesmus sp. JS07 fulfils the major requirements for lipid production, including high lipid content, and productivity under 25%N.
- Phytohormones are the potential biochemical modulators for cell growth and lipid accumulation in microalgae and their synergistic impact had led into a notable increase in the biomass and lipid contents.
- Lipidome profiling deciphered an increase in the levels of TAGs with a concurrent decrease in the number of polar lipids PG, PC, PE and PI, denoting a remodeling of the intracellular lipid pools for enhanced TAG accumulation under nitrogen limited conditions.
- Majority of the newly synthesized TAGs were enriched in C16:0, C18:0 and C18:1 fatty acids that apparently is preferable for improved biofuel properties; conclusively rendering Desmodesmus sp. JS07 a pivotal strain for biofuel production.

- *De novo* transcriptome analysis was used to compare the differential gene expression profile of *Desmodesmus* sp. JS07 that revealed the up-regulation of fatty acid and TAG biosynthesis associated genes.

- Targeting and modifying the key regulatory enzymes of the lipid biosynthetic cascade led into the increased lipid content by 1.6 fold in the CvGPD1IH transformed Desmodesmus sp. JS07 as compared to wild type.

- So, thus the synergistic impact of phytohormones and implying the molecular modification approaches have resulted into increased biomass and lipid content for commercial exploitation of microalgal resources for the production of biodiesel, a clean and renewable fuel.

- Co-expression of BnDGAT2 and CvGPD1 constructs may be performed to further improve the lipid content and profile of algal strains.
- The lipid accumulation can be further analyzed following phytohormones treatment to the transformed algal strain.
- Approaches involving the molecular modification of algal cells gene encoding for the transcription factors may be analyzed.
- Analysis of lipid accumulation following scale up of the process using photo bioreactors.

1. Abou-Shanab, R.A.I., Matter, I.A., Kim, S.-N., Oh, Y.-K., Choi, J., Jeon, B.-H., 2011. Characterization and identification of lipid-producing microalgae species isolated from a freshwater lake. Biomass and Bioenergy 35, 3079–3085.
2. Ahlgren, G., Hyenstrand, P., 2003. Nitrogen limitation effects of different nitrogen sources on nutritional quality of two freshwater organisms, *Scenedesmus quadricauda* (chlorophyceae) and *Synechococcus* sp. (cyanophyceae). J. Phycol. 39, 906–917.
3. Ahmad, I., Sharma, A.K., Daniell, H., Kumar, S., 2015. Altered lipid composition and enhanced lipid production in green microalga by introduction of *Brassica* diacylglycerol acyltransferase 2. Plant Biotechnol. J. 13, 540–550.
4. Allen, James W., DiRusso, C.C., Black, P.N., 2015. Triacylglycerol synthesis during nitrogen stress involves the prokaryotic lipid synthesis pathway and acyl chain remodeling in the microalgae *Coccomyxa subellipsoidea*. Algal Res. 10, 110–120.
5. Alptekin, E., Canakci, M., 2008. Determination of the density and the viscosities of biodiesel-diesel fuel blends. Renew. Energy 33, 2623–2630.
6. Amaro, H.M., Guedes, A.C., Malcata, F.X., 2011. Advances and perspectives in using microalgae to produce biodiesel. Appl. Energy 88, 3402–3410.
7. An, H., Yang, W.M., Maghbouli, A., Li, J., Chou, S.K., Chua, K.J., 2013. Performance, combustion and emission characteristics of biodiesel derived from waste cooking oils. Appl. Energy 112, 493–499.
8. Andrianov, V., Borisjuk, N., Pogrebnyak, N., Brinker, A., Dixon, J., Spitsin, S., Flynn, J., Matyszczuk, P., Andryszak, K., Laurelli, M., Golovkin, M., Koprowski, H., 2010. Tobacco as a production platform for biofuel: overexpression of *Arabidopsis* DGAT and LEC2 genes increases accumulation and shifts the composition of lipids in green biomass. Plant Biotechnol. J. 8, 277–287.
9. Antunes, W.M., de Oliveira Veloso, C. and Henriques, C.A. 2008. Transesterification of soybean oil with methanol catalyzed by basic solids. Catalysis Today, 133, pp.548-554.
10. Aravantinou, A.F., Theodorakopoulos, M.A., Manariotis, I.D., 2013. Selection of microalgae for wastewater treatment and potential lipids production. Bioresour. Technol. 147, 130–134.

11. Armbrust, E.V., Berges, J.A., Bowler, C., Green, B.R., Martinez, D., Putnam, N.H., Zhou, S., Allen, A.E., Apt, K.E., Bechner, M., Brzezinski, M.A., Chaal, B.K., Chiovitti, A., Davis, A.K., Demarest, M.S., Detter, J.C., Glavina, T., Goodstein, D., Hadi, M.Z., Hellsten, U., Hildebrand, M., Jenkins, B.D., Lau, W.W.Y., Lane, T.W., Larimer, F.W., Lippmeier, J.C., Lucas, S., Montsant, A., Obornik, M., Parker, M.S., Palenik, B., Pazour, G.J., Richardson, P.M., Rynearson, T.A., Saito, M.A., Schwartz, D.C., Thamatrakoln, K., Valentin, K., Vardi, A., Wilkerson, F.P., Rokhsar, D.S., 2004. The Genome of the Diatom. Science (80). 306, 79–86.

12. Bajguz, A., Piotrowska-Niczyporuk, A., 2013. Synergistic effect of auxins and brassinosteroids on the growth and regulation of metabolite content in the green alga *Chlorella vulgaris* (Trebouxiophyceae). Plant Physiol. Biochem. 71, 290–297.

13. Barelli, H., Antonny, B., 2016. Lipid unsaturation and organelle dynamics. Curr. Opin. Cell Biol. 41, 25–32.

14. Beer, L.L., Boyd, E.S., Peters, J.W., Posewitz, M.C., 2009. Engineering algae for biohydrogen and biofuel production. Curr. Opin. Biotechnol. 20, 264–271.

15. Bellou, S., Baeshen, M.N., Elazzazy, A.M., Aggeli, D., Sayegh, F., Aggelis, G., 2014. Microalgal lipids biochemistry and biotechnological perspectives. Biotechnol. Adv. 32, 1476–1493.

16. Benning, C., 2008. A role for lipid trafficking in chloroplast biogenesis. Prog. Lipid Res. 47, 381–389.

17. Bligh, E.G., Dyer, W.J., 1959. Extraction of Lipids in Solution by the Method of Bligh & Dyer. Can. J. Biochem. Physiol. 2, 911–917.

18. Bohutskyi, P., Liu, K., Nasr, L.K., Byers, N., Rosenberg, J.N., Oyler, G.A., Betenbaugh, M.J., Bouwer, E.J., 2015. Bioprospecting of microalgae for integrated biomass production and phytoremediation of unsterilized wastewater and anaerobic digestion centrate. Appl. Microbiol. Biotechnol. 99, 6139–6154.

19. Bowler, C., Allen, A.E., Badger, J.H., Grimwood, J., Jabbari, K., Kuo, A., Maheswari, U., Martens, C., Maumus, F., Otillar, R.P., Rayko, E., Salamov, A., Vandepoele, K., Beszteri, B., Gruber, A., Heijde, M., Katinka, M., Mock, T., Valentin, K., Verret, F., Berges, J.A., Brownlee, C., Cadoret, J.-P., Chiovitti, A., Choi, C.J., Coesel, S., De Martino, A., Detter, J.C., Durkin, C., Falciatore, A., Fournet, J., Haruta, M., Huysman, M.J.J., Jenkins, B.D., Jiroutova, K., Jorgensen, R.E., Joubert, Y., Kaplan, A., Kröger, N., Kroth, P.G., La Roche, J., Lindquist, E., Lommer, M., Martin–Jézéquel, V., Lopez, P.J., Lucas, S., Mangogna, M., McGinnis, K., Medlin, L.K., Montsant, A., Secq, M.-

P.O., Napoli, C., Obornik, M., Parker, M.S., Petit, J.-L., Porcel, B.M., Poulsen, N., Robison, M., Rychlewski, L., Rynearson, T.A., Schmutz, J., Shapiro, H., Siaut, M., Stanley, M., Sussman, M.R., Taylor, A.R., Vardi, A., von Dassow, P., Vyverman, W., Willis, A., Wyrwicz, L.S., Rokhsar, D.S., Weissenbach, J., Armbrust, E.V., Green, B.R., Van de Peer, Y., Grigoriev, I. V., 2008. The *Phaeodactylum* genome reveals the evolutionary history of diatom genomes. Nature 456, 239–244.

20. Boyle, N.R., Page, M.D., Liu, B., Blaby, I.K., Casero, D., Kropat, J., Cokus, S.J., Hong-Hermesdorf, A., Shaw, J., Karpowicz, S.J., Gallaher, S.D., Johnson, S., Benning, C., Pellegrini, M., Grossman, A., Merchant, S.S., 2012. Three acyltransferases and nitrogen-responsive regulator are implicated in nitrogen starvation-induced triacylglycerol accumulation in *Chlamydomonas*. J. Biol. Chem. 287, 15811–25.
21. Bradley, P.M., Cheney, D.P., 1990. Some effects of plant growth regulators on tissue cultures of the marine red alga *Agardhiella subulata* (Gigartinales, Rhodophyta). Hydrobiologia 204–205, 353–360.
22. Breuer, G., Lamers, P.P., Martens, D.E., Draaisma, R.B., Wijffels, R.H., 2012. The impact of nitrogen starvation on the dynamics of triacylglycerol accumulation in nine microalgae strains. Bioresour. Technol. 124, 217–226.
23. C, J.A., S, A.L., 2013. Isolation and Characterization of Freshwater Microalgae Species from Marikina River Palma, Juvy Ann C. and Tayo, Anne Laurene S. Institute of Biology, College of Science, University of the Philippines Diliman.
24. Callaway, J.C. 2004. Hempseed as a nutritional resource: an overview. Euphytica, 140(1-2), pp.65-72.
25. Challagulla, V., Fabbro, L., Nayar, S., 2015. Biomass, lipid productivity and fatty acid composition of fresh water microalga *Rhopalosolen saccatus* cultivated under phosphorous limited conditions. Algal Res. 8, 69–75.
26. Chauhan, B.S., Kumar, N., Cho, H.M., Lim, H.C., 2013. A study on the performance and emission of a diesel engine fueled with *Karanja* biodiesel and its blends. Energy 56, 1–7.
27. Chen, L., Liu, T., Zhang, W., Chen, X. and Wang, J. 2012. Biodiesel production from algae oil high in free fatty acids by two-step catalytic conversion. Bioresource technology, 111, pp.208-214.
28. Cheng, J.-S., Niu, Y.-H., Lu, S.-H., Yuan, Y.-J., 2012. Metabolome analysis reveals ethanolamine as potential marker for improving lipid accumulation of model photosynthetic organisms. J. Chem. Technol. Biotechnol. 87, 1409–1418.

29. Chiranjeevi, P., Venkata Mohan, S., 2016. Optimizing the Critical Factors for Lipid Productivity during Stress Phased Heterotrophic Microalgae Cultivation. Front. Energy Res. 4, 1–10.
30. Chisti, Y., 2007. Biodiesel from microalgae. Biotechnol. Adv. 25, 294–306.
31. Cho, K., Kim, K.-N., Lim, N.-L., Kim, M.-S., Ha, J.-C., Ho Shin, H., Kim, M.-K., Roh, W., Kim, D., Oda, T., 2015. Enhanced biomass and lipid production by supplement of myo-inositol with oceanic microalga *Dunaliella salina*. Biomass and Bioenergy 72, 1–7.
32. Cobos, M., Paredes, J.D., Maddox, J.D., Vargas-Arana, G., Flores, L., Aguilar, C.P., Marapara, J.L., Castro, J.C., 2017. Isolation and characterization of native microalgae from the Peruvian Amazon with potential for biodiesel production. Energies 10, 1–16.
33. Courchesne, N.M.D., Parisien, A., Wang, B., Lan, C.Q., 2009. Enhancement of lipid production using biochemical, genetic and transcription factor engineering approaches. J. Biotechnol. 141, 31–41.
34. Dao, G.H., Wu, G.X., Wang, X.X., Zhuang, L.L., Zhang, T.Y., Hu, H.Y., 2018. Enhanced growth and fatty acid accumulation of microalgae *Scenedesmus* sp. LX1 by two types of auxin. Bioresour. Technol. 247, 561–567.
35. Darwish, E., Testerink, C., Khalil, M., El-Shihy, O., Munnik, T., 2009. Phospholipid Signaling Responses in Salt-Stressed Rice Leaves. Plant Cell Physiol. 50, 986–997.
36. Dayananda, C., Sarada, R., Bhattacharya, S., Ravishankar, G.A., 2005. Effect of media and culture conditions on growth and hydrocarbon production by *Botryococcus braunii*. Process Biochem. 40, 3125–3131.
37. De Bhowmick, G., Koduru, L., Sen, R., 2015. Metabolic pathway engineering towards enhancing microalgal lipid biosynthesis for biofuel application—A review. Renew. Sustain. Energy Rev. 50, 1239–1253.
38. Demirbas, A., Fatih Demirbas, M., 2011. Importance of algae oil as a source of biodiesel. Energy Convers. Manag. 52, 163–170.
39. Demirbas, M.F., 2011. Biofuels from algae for sustainable development. Appl. Energy 88, 3473–3480.
40. Deng, X., Cai, J., Fei, X., 2013. Effect of the expression and knockdown of citrate synthase gene on carbon flux during triacylglycerol biosynthesis by green algae *Chlamydomonas reinhardtii*. BMC Biochem. 14, 38.
41. Driver, T., Bajhaiya, A., Pittman, J.K., 2014. Potential of Bioenergy Production from Microalgae. Curr. Sustain. Energy Reports 94–103.

42. Eze, S.O., Ngadi, M.O., Alakali, J.S. and Odinaka, C.J. 2013. Quality assessment of biodiesel produced from after fry waste palm kernel oil (pko). Journal of Natural and Applied Sciences, 1(1), pp.38-46.

43. Fan, J., Andre, C., Xu, C., 2011. A chloroplast pathway for the de novo biosynthesis of triacylglycerol in *Chlamydomonas reinhardtii*. FEBS Lett. 585, 1985–1991.

44. Fan, J., Cui, Y., Wan, M., Wang, W., Li, Y., 2014. Lipid accumulation and biosynthesis genes response of the oleaginous *Chlorella pyrenoidosa* under three nutrition stressors. Biotechnol. Biofuels 7, 17.

45. Fukuda, S., Hirasawa, E., Takemura, T., Takahashi, S., Chokshi, K., Pancha, I., Tanaka, K., Imamura, S., 2018. Accelerated triacylglycerol production without growth inhibition by overexpression of a glycerol-3-phosphate acyltransferase in the unicellular red alga *Cyanidioschyzon merolae*. Sci. Rep. 8, 1–12.

46. Ghoshal, D., Mach, D., Agarwal, M., Goyal, Archana, Goyal, Arun, 2002. Osmoregulatory Isoform of Dihydroxyacetone Phosphate Reductase from Dunaliella tertiolecta: Purification and Characterization. Protein Expr. Purif. 24, 404–411.

47. Goncalves, E.C., Koh, J., Zhu, N., Yoo, M.J., Chen, S., Matsuo, T., Johnson, J. V., Rathinasabapathi, B., 2016. Nitrogen starvation-induced accumulation of triacylglycerol in the green algae: Evidence for a role for ROC40, a transcription factor involved in circadian rhythm. Plant J. 85, 743–757.

48. Govender, T., Ramanna, L., Rawat, I., Bux, F., 2012. BODIPY staining, an alternative to the Nile Red fluorescence method for the evaluation of intracellular lipids in microalgae. Bioresour. Technol. 114, 507–511.

49. Griffiths, M.J., Harrison, S.T.L., 2009. Lipid productivity as a key characteristic for choosing algal species for biodiesel production. J. Appl. Phycol. 21, 493–507.

50. Griffiths, M.J., van Hille, R.P., Harrison, S.T.L., 2012. Lipid productivity, settling potential and fatty acid profile of 11 microalgal species grown under nitrogen replete and limited conditions. J. Appl. Phycol. 24, 989–1001.

51. Guschina, I.A., Everard, J.D., Kinney, A.J., Quant, P.A., Harwood, J.L., 2014. Studies on the regulation of lipid biosynthesis in plants: application of control analysis to soybean. Biochim. Biophys. Acta - Biomembr. 1838, 1488–1500.

52. Guschina, I.A., Harwood, J.L., 2009. Algal lipids and effect of the environment on their biochemistry, in: Lipids in Aquatic Ecosystems. Springer New York, New York, NY, pp. 1–24.

53. Gwak, Y., Hwang, Y., Wang, B., Kim, M., Jeong, J., Lee, C., Hu, Q., 2014. Comparative analyses of lipidomes and transcriptomes reveal a concerted action of multiple defensive systems against photooxidative stress in Haematococcus pluvialis.

54. He, H., Rodgers, R.P., Marshall, A.G., Hsu, C.S., 2011. Algae polar lipids characterized by online liquid chromatography coupled with hybrid linear quadrupole ion trap/Fourier transform ion cyclotron resonance mass spectrometry. Energy and Fuels 25, 4770–4775.

55. He, Y., Meng, X., Fan, Q., Sun, X., Xu, Z., Song, R., 2009. Cloning and characterization of two novel chloroplastic glycerol-3-phosphate dehydrogenases from *Dunaliella viridis*. Plant Mol. Biol. 71, 193–205.

56. Herrera-Valencia, V.A., Macario-González, L.A., Casais-Molina, M.L., Beltran-Aguilar, A.G., Peraza-Echeverría, S., 2012. In Silico Cloning and Characterization of the Glycerol-3-Phosphate Dehydrogenase (GPDH) Gene Family in the Green Microalga *Chlamydomonas reinhardtii*. Curr. Microbiol. 64, 477–485.

57. Huang, G., Chen, F., Wei, D., Zhang, X., Chen, G., 2010. Biodiesel production by microalgal biotechnology. Appl. Energy 87, 38–46.

58. Huang, W., Ye, J., Zhang, J., Lin, Y., He, M., Huang, J., 2016. Transcriptome analysis of *Chlorella zofingiensis* to identify genes and their expressions involved in astaxanthin and triacylglycerol biosynthesis. Algal Res. 17, 236–243.

59. Huang, Y., Cheng, J., Lu, H., He, Y., Zhou, J., Cen, K., 2017. Transcriptome and key genes expression related to carbon fixation pathways in *Chlorella* PY-ZU1 cells and their growth under high concentrations of CO 2. Biotechnol. Biofuels 10, 1–10.

60. Huerlimann, R., de Nys, R., Heimann, K., 2010. Growth, lipid content, productivity, and fatty acid composition of tropical microalgae for scale-up production. Biotechnol. Bioeng. 107, 245–257.

61. Hunt, R.W., Chinnasamy, S., Bhatnagar, A., Das, K.C., 2010. Effect of Biochemical Stimulants on Biomass Productivity and Metabolite Content of the Microalga, *Chlorella sorokiniana*. Appl. Biochem. Biotechnol. 162, 2400–2414.

62. Ibáñez-Salazar, A., Rosales-Mendoza, S., Rocha-Uribe, A., Ramírez-Alonso, J.I., Lara-Hernández, I., Hernández-Torres, A., Paz-Maldonado, L.M.T., Silva-Ramírez, A.S., Bañuelos-Hernández, B., Martínez-Salgado, J.L., Soria-Guerra, R.E., 2014. Over-expression of Dof-type transcription factor increases lipid production in Chlamydomonas reinhardtii. J. Biotechnol. 184, 27–38.

63. Ikaran, Z., Suárez-Alvarez, S., Urreta, I., Castañón, S., 2015. The effect of nitrogen limitation on the physiology and metabolism of *Chlorella vulgaris* var L3. Algal Res. 10, 134–144.

64. Iwai, M., Ikeda, K., Shimojima, M., Ohta, H., 2014. Enhancement of extraplastidic oil synthesis in *Chlamydomonas reinhardtii* using a type-2 diacylglycerol acyltransferase with a phosphorus starvation-inducible promoter. Plant Biotechnol. J. 12, 808–819.

65. Jouhet, J., Maréchal, E., Block, M.A., 2007. Glycerolipid transfer for the building of membranes in plant cells. Prog. Lipid Res. 46, 37–55.

66. Joyard, J., Ferro, M., Masselon, C., Seigneurin-Berny, D., Salvi, D., Garin, J., Rolland, N., 2010. Chloroplast proteomics highlights the subcellular compartmentation of lipid metabolism. Prog. Lipid Res. 49, 128–158.

67. Jusoh, M., Loh, S.H., Chuah, T.S., Aziz, A., Cha, T.S., 2015. Elucidating the role of jasmonic acid in oil accumulation, fatty acid composition and gene expression in *Chlorella vulgaris* (Trebouxiophyceae) during early stationary growth phase. Algal Res. 9, 14–20.

68. Kheira, A.A.A. and Atta, N.M. 2009. Response of Jatropha curcas L. to water deficits: Yield, water use efficiency and oilseed characteristics. Biomass and Bioenergy, 33(10), pp.1343-1350.

69. Klok, A.J., Lamers, P.P., Martens, D.E., Draaisma, R.B., Wijffels, R.H., 2014. Edible oils from microalgae: Insights in TAG accumulation. Trends Biotechnol. 32, 521–528.

70. Knothe, G., 2012. Fuel Properties of Highly Polyunsaturated Fatty Acid Methyl Esters. Prediction of Fuel Properties of Algal Biodiesel. Energy & Fuels 26, 5265–5273.

71. Koid, A.E., Liu, Z., Terrado, R., Jones, A.C., Caron, D.A., Heidelberg, K.B., 2014. Comparative transcriptome analysis of four prymnesiophyte algae. PLoS One 9.

72. Kotzia, G.A., Labrou, N.E., 2009. Engineering thermal stability of l-asparaginase by in vitro directed evolution. FEBS J. 276, 1750–1761.

73. Kulay, L.A. and Silva, G.A. 2005. September. Comparative screening LCA of agricultural stages of soy and castor beans. In 2nd international conference on life cycle management–LCM2005 (pp. 5-7).

74. Kwak, H.S., Kim, J.Y.H., Woo, H.M., Jin, E., Min, B.K., Sim, S.J., 2016. Synergistic effect of multiple stress conditions for improving microalgal lipid production. Algal Res. 19, 215–224.

75. Lam, M.K., Lee, K.T., 2012. Microalgae biofuels: A critical review of issues, problems and the way forward. Biotechnol. Adv. 30, 673–690.

76. Lang, I., Hodac, L., Friedl, T., Feussner, I., 2011. Fatty acid profiles and their distribution patterns in microalgae: a comprehensive analysis of more than 2000 strains from the SAG culture collection. BMC Plant Biol. 11, 124.

77. Lawton, R.J., de Nys, R., Magnusson, M.E., Paul, N.A., 2015. The effect of salinity on the biomass productivity, protein and lipid composition of a freshwater macroalga. Algal Res. 12, 213–220.

78. Lee, Y.J., Leverence, R.C., Smith, E.A., Valenstein, J.S., Kandel, K., Trewyn, B.G., 2013. High-throughput analysis of algal crude oils using high resolution mass spectrometry. Lipids 48, 297–305.

79. Lei, A., Chen, H., Shen, G., Hu, Z., Chen, L., Wang, J., 2012. Expression of fatty acid synthesis genes and fatty acid accumulation in *Haematococcus pluvialis* under different stressors. Biotechnol. Biofuels 5, 18.

80. Li, J., Han, D., Wang, D., Ning, K., Jia, J., Wei, L., Jing, X., Huang, S., Chen, J., Li, Y., Hu, Q., Xu, J., 2014. Choreography of Transcriptomes and Lipidomes of *Nannochloropsis* Reveals the Mechanisms of Oil Synthesis in Microalgae 26, 1645–1665.

81. Li, J., Niu, X., Pei, G., Sui, X., Zhang, X., Chen, L., Zhang, W., 2015. Identification and metabolomic analysis of chemical modulators for lipid accumulation in *Crypthecodinium cohnii*. Bioresour. Technol. 191, 362–368.

82. Li, L., Zhang, G., Wang, Q., 2016. De novo transcriptomic analysis of *Chlorella sorokiniana* reveals differential genes expression in photosynthetic carbon fixation and lipid production. BMC Microbiol. 16, 1–12.

83. Li, Y., Fei, X., Deng, X., 2012. Novel molecular insights into nitrogen starvation-induced triacylglycerols accumulation revealed by differential gene expression analysis in green algae *Micractinium pusillum*. Biomass and Bioenergy 42, 199–211.

84. Lian, M., Huang, H., Ren, L., Ji, X., Zhu, J., Jin, L., 2010. Increase of Docosahexaenoic Acid Production by *Schizochytrium sp*. Through Mutagenesis and Enzyme Assay. Appl. Biochem. Biotechnol. 162, 935–941.

85. Li-Beisson, Y., Beisson, F., Riekhof, W., 2015. Metabolism of acyl-lipids in *Chlamydomonas reinhardtii*. Plant J. 82, 504–522.

86. Liu, J., Qiu, W., Song, Y., 2016. Stimulatory effect of auxins on the growth and lipid productivity of *Chlorella pyrenoidosa* and *Scenedesmus quadricauda*. Algal Res. 18, 273–280.

87. Liu, Q., Siloto, R.M.P., Lehner, R., Stone, S.J., Weselake, R.J., 2012. Acyl-CoA:diacylglycerol acyltransferase: Molecular biology, biochemistry and biotechnology. Prog. Lipid Res. 51, 350–377.

88. Long, S., Zhang, X., Rao, Z., Chen, K., Xu, M., Yang, T., Yang, S., 2016. Amino acid residues adjacent to the catalytic cavity of tetramer l-asparaginase II contribute significantly to its catalytic efficiency and thermostability. Enzyme Microb. Technol. 82, 15–22.

89. López García de Lomana, A., Schäuble, S., Valenzuela, J., Imam, S., Carter, W., Bilgin, D.D., Yohn, C.B., Turkarslan, S., Reiss, D.J., Orellana, M. V., Price, N.D., Baliga, N.S., 2015. Transcriptional program for nitrogen starvation-induced lipid accumulation in *Chlamydomonas reinhardtii*. Biotechnol. Biofuels 8, 207.

90. Lu, J., Li, Y., Wang, C., Hu, Z., Deng, X., Li, H., 2017. Effect of overexpression of LPAAT and GPD1 on lipid synthesis and composition in green microalga *Chlamydomonas reinhardtii*. J. Appl. Phycol. 30, 1711–1719.

91. Lu, S., Wang, J., Ma, Q., Yang, J., Li, X., Yuan, Y.-J., 2013. Phospholipid Metabolism in an Industry Microalga *Chlorella sorokiniana*: The Impact of Inoculum Sizes. PLoS One 8, e70827.

92. Lu, Y., Xu, J., 2015. Phytohormones in microalgae: A new opportunity for microalgal biotechnology. Trends Plant Sci. 20, 273–282.

93. Lv, H., Qu, G., Qi, X., Lu, L., Tian, C., Ma, Y., 2013. Transcriptome analysis of *Chlamydomonas reinhardtii* during the process of lipid accumulation. Genomics 101, 229–237.

94. Malcata, F.X., 2011. Microalgae and biofuels: A promising partnership. Trends Biotechnol. 29, 542–549.

95. Mandotra, S.K., Kumar, P., Suseela, M.R., Nayaka, S., Ramteke, P.W., 2016. Evaluation of fatty acid profile and biodiesel properties of microalga *Scenedesmus abundans* under the influence of phosphorus, pH and light intensities. Bioresour. Technol. 201, 222–229.

96. Martin, G.J.O., Hill, D.R.A., Olmstead, I.L.D., Bergamin, A., Shears, M.J., Dias, D.A., Kentish, S.E., Scales, P.J., Botte, C.Y., 2014. Lipid Profile Remodeling in Response to Nitrogen Deprivation in the Microalgae *Chlorella* sp. (Trebouxiophyceae) and *Nannochloropsis* sp . 9.

97. Mata, T.M., Martins, A.A., Caetano, N.S., 2010. Microalgae for biodiesel production and other applications: A review. Renew. Sustain. Energy Rev. 14, 217–232.

98. Mentewab, A., Stewart, C.N., 2005. Overexpression of an *Arabidopsis thaliana* ABC transporter confers kanamycin resistance to transgenic plants. Nat. Biotechnol. 23, 1177–1180.

99. Merchant, S.S., Prochnik, S.E., Vallon, O., Harris, E.H., Karpowicz, S.J., Witman, G.B., Terry, A., Salamov, A., Fritz-Laylin, L.K., Maréchal-Drouard, L., Marshall, W.F., Qu, L.-H., Nelson, D.R., Sanderfoot, A.A., Spalding, M.H., Kapitonov, V. V., Ren, Q., Ferris, P., Lindquist, E., Shapiro, H., Lucas, S.M., Grimwood, J., Schmutz, J., Cardol, P., Cerutti, H., Chanfreau, G., Chen, C.-L., Cognat, V., Croft, M.T., Dent, R., Dutcher, S., Fernández, E., Fukuzawa, H., González-Ballester, D., González-Halphen, D., Hallmann, A., Hanikenne, M., Hippler, M., Inwood, W., Jabbari, K., Kalanon, M., Kuras, R., Lefebvre, P.A., Lemaire, S.D., Lobanov, A. V., Lohr, M., Manuell, A., Meier, I., Mets, L., Mittag, M., Mittelmeier, T., Moroney, J. V., Moseley, J., Napoli, C., Nedelcu, A.M., Niyogi, K., Novoselov, S. V., Paulsen, I.T., Pazour, G., Purton, S., Ral, J.-P., Riaño-Pachón, D.M., Riekhof, W., Rymarquis, L., Schroda, M., Stern, D., Umen, J., Willows, R., Wilson, N., Zimmer, S.L., Allmer, J., Balk, J., Bisova, K., Chen, C.-J., Elias, M., Gendler, K., Hauser, C., Lamb, M.R., Ledford, H., Long, J.C., Minagawa, J., Page, M.D., Pan, J., Pootakham, W., Roje, S., Rose, A., Stahlberg, E., Terauchi, A.M., Yang, P., Ball, S., Bowler, C., Dieckmann, C.L., Gladyshev, V.N., Green, P., Jorgensen, R., Mayfield, S., Mueller-Roeber, B., Rajamani, S., Sayre, R.T., Brokstein, P., Dubchak, I., Goodstein, D., Hornick, L., Huang, Y.W., Jhaveri, J., Luo, Y., Martínez, D., Ngau, W.C.A., Otillar, B., Poliakov, A., Porter, A., Szajkowski, L., Werner, G., Zhou, K., Grigoriev, I. V., Rokhsar, D.S., Grossman, A.R., 2007. The *Chlamydomonas* Genome Reveals the Evolution of Key Animal and Plant Functions. Science (80). 318, 245–250.

100. Miller, R., Wu, G., Deshpande, R.R., Vieler, A., Gärtner, K., Li, X., Moellering, E.R., Zäuner, S., Cornish, A.J., Liu, B., Bullard, B., Sears, B.B., Kuo, M.-H., Hegg, E.L., Shachar-Hill, Y., Shiu, S.-H., Benning, C., 2010. Changes in transcript abundance in *Chlamydomonas reinhardtii* following nitrogen deprivation predict diversion of metabolism. Plant Physiol. 154, 1737–1752.

101. Mostafa, S.S.M., El-Gendy, N.S., 2017. Evaluation of fuel properties for microalgae *Spirulina platensis* bio-diesel and its blends with Egyptian petro-diesel. Arab. J. Chem. 10, S2040–S2050.

102. Mubarak, M., Shaija, A., Suchithra, T.V., 2014. A review on the extraction of lipid from microalgae for biodiesel production. Algal Res. 7, 117–123.

103. Mühlroth, A., Li, K., Røkke, G., Winge, P., Olsen, Y., Hohmann-Marriott, M., Vadstein, O., Bones, A., 2013. Pathways of Lipid Metabolism in Marine Algae, Co-Expression Network, Bottlenecks and Candidate Genes for Enhanced Production of EPA and DHA in Species of *Chromista*. Mar. Drugs 11, 4662–4697.

104. Mutanda, T., Ramesh, D., Karthikeyan, S., Kumari, S., Anandraj, A., Bux, F., 2011. Bioprospecting for hyper-lipid producing microalgal strains for sustainable biofuel production. Bioresour. Technol. 102, 57–70.

105. Nascimento, I.A., Marques, S.S.I., Cabanelas, I.T.D., Pereira, S.A., Druzian, J.I., de Souza, C.O., Vich, D.V., de Carvalho, G.C., Nascimento, M.A., 2013. Screening Microalgae Strains for Biodiesel Production: Lipid Productivity and Estimation of Fuel Quality Based on Fatty Acids Profiles as Selective Criteria. Bioenergy Res. 6, 1–13.

106. Nedbalová, L., Procházková, L., Sigler, K., 2014. Phytochemistry Lipidomic profiling of snow algae by ESI-MS and silver-LC / APCI-MS 100, 34–42.

107. Neto, C.J.D., Sydney, E.B., de Souza Vandenberghe, L.P., Soccol, C.R., 2016. Microbial Oil for Biodiesel Production. Springer, Cham, pp. 387–406.

108. Nielsen, D.C. 2008, January. Oilseed productivity under varying water availability. In Proceedings of 20th annual central plains irrigation conference and exposition (pp. 30-33).

109. Ohlrogge, J., Browse, J., 1995. Lipid biosynthesis. Plant Cell 7, 957–70.

110. Ördög, V., Stirk, W.A., Bálint, P., Aremu, A.O., Okem, A., Lovász, C., Molnár, Z., van Staden, J., 2016. Effect of temperature and nitrogen concentration on lipid productivity and fatty acid composition in three *Chlorella* strains. Algal Res. 16, 141–149.

111. Park, J., Na, S., Lee, Y., Lee, S., Park, S., Jeon, N., 2013. Measurement of Lipid Droplet Accumulation Kinetics in *Chlamydomonas reinhardtii* Using Seoul-Fluor. Energies 6, 5703–5716.

112. Park, W.K., Yoo, G., Moon, M., Kim, C.W., Choi, Y.E., Yang, J.W., 2013. Phytohormone supplementation significantly increases growth of *Chlamydomonas reinhardtii* cultivated for biodiesel production. Appl. Biochem. Biotechnol. 171, 1128–1142.

113. Parsaeimehr, A., Mancera-Andrade, E.I., Robledo-Padilla, F., Iqbal, H.M.N., Parra-Saldivar, R., 2017. A chemical approach to manipulate the algal growth, lipid content and high-value alpha-linolenic acid for biodiesel production. Algal Res. 26, 312–322.

114. Parsaeimehr, A., Sun, Z., Dou, X., Chen, Y.-F., 2015. Simultaneous improvement in production of microalgal biodiesel and high-value alpha-linolenic acid by a single regulator acetylcholine. Biotechnol. Biofuels 8, 11.

115. Pasquet, V., Ulmann, L., Mimouni, V., Guihéneuf, F., Jacquette, B., Morant-Manceau, A., Tremblin, G., 2014. Fatty acids profile and temperature in the cultured marine diatom *Odontella aurita*. J. Appl. Phycol. 26, 2265–2271.

116. Patel, V., Berthold, D., Puranik, P., Gantar, M., 2015. Screening of cyanobacteria and microalgae for their ability to synthesize silver nanoparticles with antibacterial activity. Biotechnol. Reports 5, 112–119.

117. Pinzi, S., Garcia, I.L., Lopez-Gimenez, F.J., Luque de Castro, M.D., Dorado, G., Dorado, M.P., 2009. The Ideal Vegetable Oil-based Biodiesel Composition: A Review of Social, Economical and Technical Implications. Energy & Fuels 23, 2325–2341.

118. Piotrowska, A., Czerpak, R., 2009. Cellular response of light/dark-grown green alga *Chlorella vulgaris* Beijerinck (Chlorophyceae) to exogenous adenine- and phenylurea-type cytokinins. Acta Physiol. Plant. 31, 573–585.

119. Piotrowska-Niczyporuk, A., Bajguz, A., 2014. The effect of natural and synthetic auxins on the growth, metabolite content and antioxidant response of green alga *Chlorella vulgaris* (Trebouxiophyceae). Plant Growth Regul. 73, 57–66.

120. Plaxton, W.C., 1996. The organization and regulation of plant glycolysis. Annu. Rev. Plant Physiol. Plant Mol. Biol. 47, 185–214.

121. Quinn, J.C., Davis, R., 2015. The potentials and challenges of algae based biofuels: A review of the techno-economic, life cycle, and resource assessment modeling. Bioresour. Technol. 184, 444–452.

122. Rai, A., Saito, K., 2016. Omics data input for metabolic modeling. Curr. Opin. Biotechnol. 37, 127–134.

123. Rashid, U. and Anwar, F. 2008. Production of biodiesel through optimized alkaline-catalyzed transesterification of rapeseed oil. Fuel, 87(3), pp.265-273.

124. Rawat, I., Ranjith Kumar, R., Mutanda, T., Bux, F., 2013. Biodiesel from microalgae: A critical evaluation from laboratory to large scale production. Appl. Energy 103, 444–467.

125. Ren, L., Hu, X., Zhao, X., Chen, S., Wu, Y., Li, D., Yu, Y., Geng, L., Ji, X., Huang, H., 2017. Transcriptomic Analysis of the Regulation of Lipid Fraction Migration and Fatty Acid Biosynthesis in *Schizochytrium* sp. Sci. Rep. 7, 1–10. https://doi.org/10.1038/s41598-017-03382-9

126. Renuka, N., Guldhe, A., Singh, P., Ansari, F.A., Rawat, I., Bux, F., 2017. Evaluating the potential of cytokinins for biomass and lipid enhancement in microalga *Acutodesmus obliquus* under nitrogen stress. Energy Convers. Manag. 140, 14–23.

127. Rismani-Yazdi, H., Haznedaroglu, B.Z., Hsin, C., Peccia, J., 2012. Transcriptomic analysis of the oleaginous microalga *Neochloris oleoabundans* reveals metabolic insights into triacylglyceride accumulation. Biotechnol. Biofuels 5, 1.

128. Ruangsomboon, S., 2015. Effects of different media and nitrogen sources and levels on growth and lipid of green microalga *Botryococcus braunii* KMITL and its biodiesel properties based on fatty acid composition. Bioresour. Technol. 191, 377–384.

129. Rubio, V., Bustos, R., Irigoyen, M.L., Cardona-López, X., Rojas-Triana, M., Paz-Ares, J., 2009. Plant hormones and nutrient signaling. Plant Mol. Biol. 69, 361–373.

130. Sakthivel, R., Elumalai, S., Arif, M., 2011. Microalgae lipid research, past, present: a critical review for biodiesel production, in the future. J. Exp. Sci. 2, 29–49.

131. Salama, E.S., Jeon, B.H., Chang, S.W., Lee, S. hun, Roh, H.S., Yang, I.S., Kurade, M.B., El-Dalatony, M.M., Kim, D.H., Kim, K.H., Kim, S., 2017. Interactive effect of indole-3-acetic acid and diethyl aminoethyl hexanoate on the growth and fatty acid content of some microalgae for biodiesel production. J. Clean. Prod. 168, 1017–1024.

132. Salama, E.S., Kabra, A.N., Ji, M.K., Kim, J.R., Min, B., Jeon, B.H., 2014. Enhancement of microalgae growth and fatty acid content under the influence of phytohormones. Bioresour. Technol. 172, 97–103.

133. Sanjaya, Miller, R., Durrett, T.P., Kosma, D.K., Lydic, T.A., Muthan, B., Koo, A.J.K., Bukhman, Y. V, Reid, G.E., Howe, G.A., Ohlrogge, J., Benning, C., 2013. Altered lipid composition and enhanced nutritional value of *Arabidopsis* leaves following introduction of an algal diacylglycerol acyltransferase 2. Plant Cell 25, 677–93.

134. Sarkar, D., Shimizu, K., 2015. An overview on biofuel and biochemical production by photosynthetic microorganisms with understanding of the metabolism and by metabolic engineering together with efficient cultivation and downstream processing. Bioresour. Bioprocess. 2, 17.

135. Schwarz, D., Orf, I., Kopka, J., Hagemann, M., 2013. Recent Applications of Metabolomics toward Cyanobacteria. Metabolites 3, 72–100.

136. Scibilia, L., Girolomoni, L., Berteotti, S., Alboresi, A., Ballottari, M., 2015. Photosynthetic response to nitrogen starvation and high light in *Haematococcus pluvialis*. Algal Res. 12, 170–181.

137. Sharma, D.K., Gautam, K., Jueppner, J., Giavalisco, P., Rihko-Struckmann, L., Pareek, A., Sundmacher, K., 2015. UPLC-MS analysis of *Chlamydomonas reinhardtii* and *Scenedesmus obliquus* lipid extracts and their possible metabolic roles. J. Appl. Phycol. 27, 1149–1159.

138. Sharma, K.K., Schuhmann, H., Schenk, P.M., 2012. High lipid induction in microalgae for biodiesel production. Energies 5, 1532–1553.

139. Sibi, G., Shetty, V., Mokashi, K., 2015. Enhanced lipid productivity approaches in microalgae as an alternate for fossil fuels – A review. J. Energy Inst. 1–5.

140. Sidhu, S.S., Kossiakoff, A.A., 2007. Exploring and designing protein function with restricted diversity. Curr. Opin. Chem. Biol. 11, 347–354.

141. Simionato, D., Block, M.A., La Rocca, N., Jouhet, J., Maréchal, E., Finazzi, G., Morosinotto, T., 2013. The response of *Nannochloropsis gaditana* to nitrogen starvation includes de novo biosynthesis of triacylglycerols, a decrease of chloroplast galactolipids, and reorganization of the photosynthetic apparatus. Eukaryot. Cell 12, 665–76.

142. Singh, A., Nigam, P.S., Murphy, J.D., 2011. Renewable fuels from algae: An answer to debatable land based fuels. Bioresour. Technol. 102, 10–16.

143. Singh, B., Guldhe, A., Rawat, I., Bux, F., 2014. Towards a sustainable approach for development of biodiesel from plant and microalgae. Renew. Sustain. Energy Rev. 29, 216–245.

144. Soni, N.K., Varma, A.K., Mondal, P., Srivastava, M.N., 2013. Production of Bio-oil from Native Algae of Solani Aquaduct Roorkee. Green 3, 225–234.

145. Storms, Z.J., Cameron, E., De, H., Siegler, H., Mccaffrey, W.C., 2014. A Simple and Rapid Protocol for Measuring Neutral Lipids in Algal Cells Using Fluorescence 1. Isolation of Dry Algal Biomass to be Used as Standards for Fluorescence Readings 2. Gravimetric Quantification of Neutral Lipids by Hexane Extraction (Adapted 1–7).

146. Subramaniam, R., Dufreche, S., Zappi, M., Bajpai, R., 2010. Microbial lipids from renewable resources: production and characterization. J. Ind. Microbiol. Biotechnol. 37, 1271–1287.

147. Sudhir, A.P., Agarwaal, V. V, Dave, B.R., Patel, D.H., Subramanian, R.B., 2016. Enhanced catalysis of L-asparaginase from *Bacillus licheniformis* by a rational redesign. Enzyme Microb. Technol. 86, 1–6.

148. Tabatabaei, M., Tohidfar, M., Jouzani, G.S., Safarnejad, M., Pazouki, M., 2011. Biodiesel production from genetically engineered microalgae: Future of bioenergy in Iran. Renew. Sustain. Energy Rev. 15, 1918–1927.

149. Tai, M., Stephanopoulos, G., 2013. Engineering the push and pull of lipid biosynthesis in oleaginous yeast *Yarrowia lipolytica* for biofuel production. Metab. Eng. 15, 1–9.

150. Takagi, M., Yoshida, T., 2006. Effect of Salt Concentration on Intracellular Accumulation of Lipids and Triacylglyceride in Marine Microalgae *Dunaliella* Cells 101, 223–226.

151. Talebi, A.F., Tohidfar, M., Mousavi Derazmahalleh, S.M., Sulaiman, A., Baharuddin, A.S., Tabatabaei, M., 2015. Biochemical Modulation of Lipid Pathway in Microalgae *Dunaliella* sp. for Biodiesel Production. Biomed Res. Int. 2015, 597198.

152. Tarakhovskaya, E.R., Maslov, Y.I., Shishova, M.F., 2007. Phytohormones in algae. Russ. J. Plant Physiol. 54, 163–170.

153. Tate, J.J., Gutierrez-Wing, M.T., Rusch, K.A., Benton, M.G., 2013. The Effects of Plant Growth Substances and Mixed Cultures on Growth and Metabolite Production of Green Algae *Chlorella* sp.: A Review. J. Plant Growth Regul. 32, 417–428.

154. Tevatia, R., Allen, J., Blum, P., Demirel, Y., Black, P., 2014. Modeling of rhythmic behavior in neutral lipid production due to continuous supply of limited nitrogen: Mutual growth and lipid accumulation in microalgae. Bioresour. Technol. 170, 152–159.

155. Tian, B., Wang, Y., Zhu, Y., Lu, X., Huang, K., Shao, N., Beck, C.F., 2006. Synthesis of the photorespiratory key enzyme serine: glyoxylate aminotransferase in *C. reinhardtii* is modulated by the light regime and cytokinin. Physiol. Plant. 127, 571–582.

156. Trentacoste, E.M., Shrestha, R.P., Smith, S.R., Glé, C., Hartmann, A.C., Hildebrand, M., Gerwick, W.H., 2013. Metabolic engineering of lipid catabolism increases microalgal lipid accumulation without compromising growth. Proc. Natl. Acad. Sci. U. S. A. 110, 19748–53.

157. Valdez-ojeda, R., González-muñoz, M., Us-vázquez, R., Narváez-zapata, J., Chavarria-hernandez, J.C., López-adrián, S., Barahona-pérez, F., Toledano-thompson, T., Garduño-solórzano, G., María, R., Medrano, E., 2015. Characterization of five fresh water microalgae with potential for biodiesel production 7, 33–44.

158. Vance, B.D., 1987. Phytohormone effects on cell division in *Chlorella pyrenoidosa* chick (TX-7-11-05) (chlorellaceae). J. Plant Growth Regul. 5, 169–173.

159. Vidya, J., Ushasree, M.V., Pandey, A., 2014. Enzyme and Microbial Technology Effect of surface charge alteration on stability of l -asparaginase II from *Escherichia* sp. Enzyme Microb. Technol. 56, 15–19.

160. Vigeolas, H., Waldeck, P., Zank, T., Geigenberger, P., 2007. Increasing seed oil content in oil-seed rape (*Brassica napus* L.) by over-expression of a yeast glycerol-3-phosphate dehydrogenase under the control of a seed-specific promoter. Plant Biotechnol. J. 5, 431–441.

161. Vítová, M., Goecke, F., Sigler, K., 2016. Lipidomic analysis of the extremophilic red alga *Galdieria sulphuraria* in response to changes in pH 13, 218–226.

162. Vollmann, J., Moritz, T., Kargl, C., Baumgartner, S. and Wagentristl, H. 2007. Agronomic evaluation of camelina genotypes selected for seed quality characteristics. Industrial Crops and Products, 26(3), pp.270-277.

163. Wagner, M., Hoppe, K., Czabany, T., Heilmann, M., Daum, G., Feussner, I., Fulda, M., 2010. Identification and characterization of an acyl-CoA: Diacylglycerol acyltransferase 2 (DGAT2) gene from the microalga O. tauri. Plant Physiol. Biochem. 48, 407–416.

164. Wei, H., Shi, Y., Ma, X., Pan, Y., Hu, H., Li, Y., Luo, M., Gerken, H., Liu, J., 2017. A type-I diacylglycerol acyltransferase modulates triacylglycerol biosynthesis and fatty acid composition in the oleaginous microalga, *Nannochloropsis oceanica*. Biotechnol. Biofuels 10, 1–18.

165. Werner, T., Motyka, V., Strnad, M., Schmülling, T., 2001. Regulation of plant growth by cytokinin. Proc. Natl. Acad. Sci. U. S. A. 98, 10487–92.

166. Wijffels, R.H., Barbosa, M.J., 2010. An Outlook on Microalgal Biofuels. Science (80). 329, 796–799.

167. Work, V.H., Radakovits, R., Jinkerson, R.E., Meuser, J.E., Elliott, L.G., Vinyard, D.J., Laurens, L.M.L., Dismukes, G.C., Posewitz, M.C., 2010. Increased lipid accumulation in the *Chlamydomonas reinhardtii* sta7-10 starchless isoamylase mutant and increased carbohydrate synthesis in complemented strains. Eukaryot. Cell 9, 1251–61.

168. Xu, X.-Q., Beardall, J., 1997. Effect of salinity on fatty acid composition of a green microalga from an antarctic hypersaline lake. Phytochemistry 45, 655–658.

169. Yadegari, R., Paiva, Gr., Laux, T., Koltunow, A.M., Apuya, N., Zimmerman, J.L., Fischer, R.L., Harada, J.J., Goldberg, R.B., 1994. Cell Differentiation and Morphogenesis Are Uncoupled in *Arabidopsis* raspberry Embryos. PLANT CELL ONLINE 6, 1713–1729.

170. Yang, Z.-K., Ma, Y.-H., Zheng, J.-W., Yang, W.-D., Liu, J.-S., Li, H.-Y., 2014. Proteomics to reveal metabolic network shifts towards lipid accumulation following nitrogen deprivation in the diatom *Phaeodactylum tricornutum*. J. Appl. Phycol. 26, 73–82.

171. Yao, L., Qi, F., Tan, X., Lu, X., 2014. Improved production of fatty alcohols in cyanobacteria by metabolic engineering. Biotechnol. Biofuels 7, 94.

172. Yao, Y., Lu, Y., Peng, K.-T., Huang, T., Niu, Y.-F., Xie, W.-H., Yang, W.-D., Liu, J.-S., Li, H.-Y., 2014. Glycerol and neutral lipid production in the oleaginous marine diatom *Phaeodactylum tricornutum* promoted by overexpression of glycerol-3-phosphate dehydrogenase. Biotechnol. Biofuels 7, 110.

173. Yewalkar-Kulkarni, S., Gera, G., Nene, S., Pandare, K., Kulkarni, B., Kamble, S., 2017. Exploiting Phosphate-Starved cells of *Scenedesmus* sp. for the Treatment of Raw Sewage. Indian J. Microbiol. 57, 241.

174. Yilancioglu, K., Cokol, M., Pastirmaci, I., Erman, B., Cetiner, S., 2014. Oxidative Stress Is a Mediator for Increased Lipid Accumulation in a Newly Isolated *Dunaliella salina* Strain. PLoS One 9, e91957.

175. Yin, H.C., 1937. Effect of Auxin on *Chlorella Vulgaris*. Proc. Natl. Acad. Sci. U. S. A. 23, 174–6.

176. Yu, Z., Pei, H., Jiang, L., Hou, Q., Nie, C., Zhang, L., 2018. Phytohormone addition coupled with nitrogen depletion almost tripled the lipid productivities in two algae. Bioresour. Technol. 247, 904–914.

177. Yu, Z., Song, M., Pei, H., Jiang, L., Hou, Q., Nie, C., Zhang, L., 2017. The effects of combined agricultural phytohormones on the growth, carbon partitioning and cell morphology of two screened algae. Bioresour. Technol. 239, 87–96.

178. Zhang, J., Hao, Q., Bai, L., Xu, J., Yin, W., Song, L., Xu, L., Guo, X., Fan, C., Chen, Y., Ruan, J., Hao, S., Li, Y., Wang, R., Hu, Z., 2014. Overexpression of the soybean transcription factor GmDof4 significantly enhances the lipid content of *Chlorella ellipsoidea*. Biotechnol. Biofuels 7, 128.

179. Zhang, Y.M., Chen, H., He, C.L., Wang, Q., 2013. Nitrogen Starvation Induced Oxidative Stress in an Oil-Producing Green Alga *Chlorella sorokiniana* C3. PLoS One 8, 1–12.

180. Zheng, M., Tian, J., Yang, G., Zheng, L., Chen, G., Chen, J., Wang, B., 2013. Transcriptome sequencing, annotation and expression analysis of *Nannochloropsis* sp. at different growth phases. Gene 523, 117–121.

181. Zou, J., Katavic, V., Giblin, E.M., Barton, D.L., MacKenzie, S.L., Keller, W.A., Hu, X., Taylor, D.C., 1997. Modification of Seed Oil Content and Acyl Composition in the Brassicaceae by Expression of a Yeast sn-2 Acyltransferase Gene. PLANT CELL ONLINE 9, 909–923.